Charles University

First Faculty of Medicine

Branch of study: Molecular and Cell Biology, Genetics and Virology

Ondřej Vít

Proteomic analysis of soluble and transmembrane proteins in human lymphoma cells

Doctoral Thesis

Supervisor: Doc. RNDr. Jiří Petrák, Ph.D.

Prague, 2017

Declaration:

I hereby declare that I completed this doctoral thesis independently and I have properly cited all the resources and literature. I also declare that I did not use this thesis to acquire the same or another academic degree.

I agree with prolonged saving of an electronic version of my work in the system database Theses.cz interuniversity project for the systematic control of the similarity of theses.

Prague, January 24, 2017

Ondřej Vít

Identification record:

VÍT, Ondřej. *Proteomic analysis of soluble and transmembrane proteins in human lymphoma cell. [Proteomická analýza solubilních a transmembránových proteinů buněk lymfomu.]* Prague, 2017. 169 pages including 5 appendices. Doctoral thesis (Ph.D.), Charles University, First Faculty of Medicine, BIOCEV. Supervisor: Doc. RNDr. Jiří Petrák, Ph.D.

Acknowledgements:

I would like to express my gratitude to everyone, who helped me finish this work, especially to my supervisor, Doc. Jiří Petrák, for his guidance, support and patience, to Dr. Petr Man and his collaborators and students for their help. I also thank my labmates and colleagues from the Institute of Pathological Physiology and from BIOCEV, to my family and friends, most of all to my wife Eva, who gave me all of her love and support.

Abstract

In the works presented here, we studied molecular changes associated with drug resistance in human mantle cell lymphoma (MCL) cells using proteomics. Our analyses allowed us to identify causal and/or secondary changes in protein expression associated with the development of resistance to the experimental drug TRAIL and the clinically used antimetabolites cytarabine and fludarabine. Resistance of MCL cells to the recombinant proapoptotic cytokine TRAIL was associated with downregulation of key enzymes of purine metabolism. This pathway potentially represents a molecular “weakness”, which could be used as a therapeutic target for selective elimination of such resistant cells.

Resistance to the pyrimidine analog drug cytarabine was associated with cross-resistance to other antinucleosides. Proteomic and transcriptomic analyses showed pronounced downregulation of deoxycytidine kinase (dCK), which activates both purine and pyrimidine antinucleosides. This change explains the cross-resistance and is the causal mechanism of resistance to cytarabine. Our observations suggest that MCL patients, who do not respond to cytarabine-based therapy, should be treated with non-nucleoside drugs.

MCL cells resistant to purine-derived antinucleoside fludarabine were cross-resistant to all tested antinucleosides and also to ibrutinib, inhibitor of Bruton tyrosine kinase (BTK). Our proteomic analysis using a metabolic labeling approach (SILAC) showed marked downregulation of dCK and BTK among the differentially expressed proteins. Further, we detected upregulation of the anti-apoptotic protein Bcl-2, and demonstrated increased sensitivity of fludarabine-resistant MCL cells to the Bcl-2 inhibitor ABT199.

These “proof of concept” studies demonstrated the potential of proteomic analysis for personalized therapy of resistant malignancies. Proteomics, however, still has its limitations: the second section of this thesis deals with integral membrane proteins (IMPs). IMPs are underrepresented in conventional proteomic analyses, primarily due to their amphipathy, low digestibility with trypsin, and low expression levels. These properties call for specific approaches. We introduced an improved and simplified method for IMP analysis that targets transmembrane segments of IMPs. We used this method to characterize the membrane proteome of a MCL cell line. We identified over 800 IMPs including several so-called “missing proteins”, that had not previously been observed on the protein level.

Key words: proteomics, mantle cell lymphoma, drug resistance, drug targets, integral membrane proteins, mass spectrometry

Abstrakt

V prezentovaných pracích jsme se s využitím proteomiky zabývali molekulárními změnami v buňkách lymfomu z buněk plášťové zóny (mantle cell lymphoma, MCL), souvisejícími s vznikem lékové rezistence. Identifikovali jsme tak kauzální a/nebo sekundární změny v proteinové expresi, spojené s rozvojem rezistence vůči experimentální molekule TRAIL a klinicky používaným antimetabolitům cytarabinu a fludarabinu. Odvozené buňky MCL rezistentní vůči proapoptotickému cytokinu TRAIL se vyznačovaly sníženou expresí klíčových enzymů metabolismu purinů. Tuto metabolickou dráhu tak lze považovat za „slabinu“, kterou by bylo možné využít coby terapeutický cíl k selektivní eliminaci takovýchto rezistentních buněk.

Rezistence vůči pyrimidinovému analogu cytarabinu se projevila křížovou rezistencí k dalším antinukleosidům. Proteomická a transkriptomická analýza ukázaly výrazně sníženou expresi deoxycytidin kinázy (dCK), jež je nutná k aktivaci purinových i pyrimidinových antinukleosidů. Tato změna vysvětluje křížovou rezistenci a je kauzálním mechanizmem rezistence vůči cytarabinu. Naše výsledky naznačují, že pacienti s MCL, u nichž selhala léčba založená na cytarabinu, by neměli být léčeni antinukleosidovými léčivy.

Buňky MCL rezistentní vůči purinovému antinukleosidu fludarabinu vykazovaly křížovou rezistenci vůči všem testovaným antinukleosidům a také ibrutinibu, inhibitoru Brutonovy tyrozinkinázy (BTK). Naše proteomická analýza provedená pomocí metabolického značení (SILAC) ukázala mimo jiné výrazně sníženou expresi dCK a BTK. Rovněž jsme detekovali zvýšenou expresi anti-apoptotického proteinu Bcl-2, a doložili zvýšenou citlivost těchto rezistentních buněk MCL k inhibitoru Bcl-2, ABT199. Tyto práce dokládají, že proteomika má potenciál pro určování vhodné terapie rezistentních nádorových onemocnění.

Proteomika má však stale určitá omezení, z nichž zásadní je nekompatibilita s integrálními membránovými proteiny (IMP). Tomuto tématu se věnuji v druhé části dizertační práce. IMP jsou v běžných proteomických analýzách neúměrně málo zastoupeny, především vlivem jejich amfipatie, nízké štěpitelnosti trypsinem a nízkých hladin exprese. Kvůli těmto vlastnostem jsou k analýze IMP potřeba specifické postupy. V naší metodologické práci jsme představili vylepšenou a zjednodušenou metodu pro analýzu IMP, cílící na transmemránové úseky IMP. Touto metodou jsme charakterizovali membránový proteom buněčné linie MCL. Identifikovali jsme více než 800 IMP včetně několika tzv. „missing proteins“, které dosud nebyly detekovány na proteinové úrovni.

Klíčová slova: proteomika, lymfom z buněk plášťové zóny, léková rezistence, cíle léčiv, integrální membránové proteiny, hmotnostní spektrometrie.

List of abbreviations

2-DE	two-dimensional electrophoresis
APRT	adenine phosphoribosyltransferase
BCR	B-cell receptor
BTK	Bruton tyrosine kinase
CSC	cell surface capture
dCK	deoxycytidine kinase
FA	formic acid
FASP	filter-aided sample preparation
FDR	false discovery rate
hppK	high pH, proteinase K
hpTC	high pH, trypsin, CNBr
IEF	isoelectric focusing
IMPs	integral membrane proteins
IMPDH2	inosine-5'-monophosphate dehydrogenase 2
IPG	immobilized pH gradient
iTRAQ	isobaric tags for relative and absolute quantitation
LC	liquid chromatography
MALDI	matrix-assisted laser desorption/ionization
MCL	mantle cell lymphoma
MS	mass spectrometry
MS/MS	tandem mass spectrometry
PMF	peptide mass fingerprinting
PNP	purine nucleoside phosphorylase
PSAT-1	phosphoserine aminotransferase 1
RP-LC	reversed-phase liquid chromatography
SDC	sodium deoxycholate
SDS	sodium dodecyl sulfate
SILAC	stable isotope labeling with amino acids in cell culture
SPEG	solid phase extraction of formerly N-glycosylated glycoproteins
TRAIL	tumor necrosis factor-related apoptosis-inducing ligand

Contents

1 Introduction

Proteins are the primary effector molecules of living entities – they execute most biological tasks on the molecular level. Regulation of protein synthesis as well as protein degradation, or chemical (post-translational) modifications of proteins are essential for customizing the needs of the cell, tissue or the entire organism. These aspects can also play a distinct role in diseases. Changes in protein expression happen in response to a disease, and conversely, deregulation of protein expression caused e.g. by a genetic factor may be one of the effectors of a disease. From the medical point of view, deregulation of protein expression in relation to a disease can also become diagnostic or prognostic factor (a biomarker). The detection of altered protein expression in a clinical sample can indicate the onset of an illness or enable the specification of a type of disease. In other cases, a differentially expressed protein may become a therapeutic target, when its altered expression enables a more efficient action of a drug. Quantitative proteomics, a set of methods for large-scale analysis of changes in protein expression, can provide information about such changes of protein expression.

This dissertation thesis presents four studies, focusing on two separate but related issues. For this reason, the thesis is divided into two sections. The first section presents three studies on drug resistance in mantle cell lymphoma that we performed with the use of quantitative proteomics. In these works, our goal was either to elucidate the mechanisms of drug resistance in lymphoma cells, and/or to obtain information on specific alterations in these resistant cells that would enable us to propose new therapeutic targets for their selective elimination.

The second section deals specifically with integral membrane proteins. Because of their physical and chemical properties and low expression levels, integral membrane proteins represent technological challenge for proteomics and require specific analytical strategies. In this section, I summarize the recent advances in the proteomics analysis of integral membrane proteins and present our new approach for the analysis of integral membrane proteins. We applied our method to inventarize the membrane proteome of mantle cell lymphoma cells.

2 Literature review

2.1 Proteome and proteomics

The word “proteome” originates from a combination of the words “genome” and “protein.” It was coined by Marc Wilkins in the early 1990s (Wasinger *et al.*, 1995, Wilkins, 2009) as a parallel to the term “genome,” and denotes the entire set of proteins in a given cell type, tissue, or organism at a given time. It includes all “variants” of proteins resulting from alternative splicing and posttranslational modifications. In a wider sense, proteome is also characterized by its dynamic features, such as protein metabolic turnover, the localization of proteins and protein-protein interactions.

Proteomics is the study of the proteome: it attempts to describe the quantitative or qualitative state of proteome(s). Expression or **quantitative proteomics** seeks to quantitatively assess proteomes and their changes under different physiological or pathological conditions. Such analyses allow the identification of molecular mechanisms that participate in various biological processes, including molecular mechanisms of human diseases. **In our work, we employed different methods of quantitative proteomics to examine the global changes of protein expression in lymphoma cells responsible for or associated with the development of resistance to certain anti-cancer drugs.**

The current technological foundations of proteomics are primarily the methods for separation of proteins and peptides, namely liquid chromatography (LC) and electrophoresis, combined with mass spectrometry (MS), which enables protein identification and quantification. At its onset, proteomic research was based mainly on two-dimensional electrophoresis (2-DE) of intact proteins in combination with MS for their identification. This can be described as **the “classical” approach**. Inherent limitations of the “classical” approach, plus the demand for more powerful and robust methods and improvements of MS instrumentation, led to the development of **the “shotgun” approach.** This strategy was inspired by the genomic “shotgun” approach, i.e. fragmenting the genome into overlapping molecules for their sequencing and subsequent rearrangement into integrated sequence information. The proteomic “shotgun” approach is typically based on sequence-specific proteolysis of the sample, liquid chromatography (LC) separation of the resulting complex mixture of peptides and tandem MS (MS/MS) analysis, which allows the identification of the proteins (see chapter 2.1.2). While the importance of the 2-DE-based “classical” proteomic strategy has gradually declined, the “shotgun” proteomic approach has

undergone enormous technological progress and is currently the principal strategy for proteomic research.

After the determination of the complete sequence of human genome by the Human Genome Project in 2004, it was shown that the total number of protein coding genes is approximately 20,000, much less than previously assumed (Clamp *et al.*, 2007). In an analogy, the Human Proteome Project was established to describe the whole proteome in various types of human cells, tissues or body fluids (Kaiser 2002, Omenn *et al.*, 2005). Soon, it became evident that the project had much larger proportions and complexity. Since protein expression includes many variables, namely alternative splicing, RNA editing and post-translational processing and modifications, the total number of proteins in proteomes (esp. in eukaryotes) is much larger than the number of genes. A single gene can give rise to several polypeptides of different structure and function. The different molecular variants that stem from alternative splicing of RNA transcripts and post-translational modifications, in which the protein product of a single gene exist, are most commonly called "**proteoforms**" (Smith & Kelleher, 2013) or protein species (Jungblut *et al.*, 2008). It has been estimated that the human proteome may contain 100,000 (Gstaiger & Aebersold, 2009), 250,000 (Kelleher, 2012), and even over million (Jensen, 2004) proteoforms depending on the definition.

The multiple levels of regulation of protein expression also explain the low correlation between expression levels of proteins and their respective mRNAs (Schwanhäusser *et al.*, 2011, Wu *et al.*, 2013). Large-scale transcriptomic analyses, which are based on amplification and sequencing of nucleic acids, are reliable and extremely sensitive methods. This is a major reason why they have become the methods of choice in biomedical research. The molecules that execute most of the molecular biochemical processes, which add up to the final phenotype of an organism, are, however, proteins. Because of the discrepancy between mRNA and protein expression, proteomic analyses may therefore provide more precise information about biological processes than a transcriptomic analysis.

Proteins cannot be amplified, and their studies have to rely on their available amounts in the sample. This is further complicated by the extreme variability of protein copy numbers, which can vary between single molecules and 10^7 copies in a typical cell (Beck *et al.*, 2011), or even up to over ten orders of magnitude, as is estimated in human serum (Anderson *et al.*, 2004). The high dynamic range of protein concentrations exceeds the dynamic range of most analytical techniques and complicates proteome analysis. Identification of low abundant proteins in complex samples is

hindered by the presence of highly abundant proteins and their incomparably higher MS signal intensities. Various immunoafinity-depletion systems as well as antibody-free methods have been developed to address this problem in blood plasma and other body fluids (Pernemalm & Lehtiö, 2014).

Despite the recent technological progress in MS instrumentation, which has enabled the identification of thousands of proteins in a single experiment, detection of less abundant proteins is still a limiting factor in proteomics and may lead to the loss of valuable information. Some protein groups, such as integral membrane proteins, require special approaches due to their physico-chemical properties, as will be discussed in Section II of this thesis (chapter 4).

2.1.1 The technological basis of proteomics

Current proteomic methods are based on the combination of electrophoretic or chromatographic separation and mass spectrometry. Since mass spectrometry is the central technology and is common to both the "classical" and the "shot-gun" strategies, I will firstly briefly introduce the basic principles of MS.

MS is an analytical technique that allows precise determination of the molecular mass of chemical substances. The essential prerequisite of the measurement is ionization of the analyte, which in the case of proteomics is done by soft ionization techniques, most frequently electrospray ionization (ESI, Fenn *et al.*, 1989) or matrix-assisted laser desorption/ionization (MALDI, Karas *et al.*, 1985). The ions are then accelerated by an electric field to a mass analyzer, where they partition according to their mass to charge (*m/z*) ratio. The most widely used mass analyzers in proteomics are the time of flight (TOF) analyzer (Weickhardt *et al.*, 1996), ion cyclotron resonance (Marshall *et al.*, 1998), quadrupole ion trap (March, 2000), linear quadrupole ion trap (Schwartz *et al.*, 2002) and most recently the orbitrap mass analyzer (Hu *et al.*, 2005). The partitioned ions are then recorded by a detector and the resulting mass spectrum displays the *m/*z values plotted against signal intensity.

To be compatible with high-resolution MS analysis, proteins are usually enzymatically or chemically cleaved into smaller fragments, peptides. The masses (*m/z* ratios) of the peptides or peptide fragments, generated inside the mass spectrometer, are then compared with the theoretical masses of the peptides derived from *in silico* cleavage of all protein sequences present in the gene and protein databases. Matching of experimental and theoretical masses thus enables peptide and protein identification. The correlation between the theoretical *m/z* values and the values

observed in spectra is statistically evaluated and marked with a score to indicate the significance of the identification. Two basic methods for protein identification in MS are **peptide mass fingerprinting and tandem MS (MS/MS)**.

2.1.1.1 The "classical" proteomic approach

In this rather historical approach, complex protein mixtures are separated by two-dimensional electrophoresis (2-DE), which combines isoelectric focusing (IEF) of proteins with SDS-polyacrylamide gel electrophoresis (SDS-PAGE). IEF separates proteins based on their isoelectric point (pI) in gels with immobilized pH gradients (IPG). The IPG gel strip is then fixed on a SDS-polyacrylamide gel and the focused proteins are separated by SDS-PAGE. 2-DE results in separation of proteins in the electrophoretic gels into spots, which can be visualized by staining. Typically, up to 1,500 spots can be detected on the gels using Coomassie Brilliant Blue, silver nitrate or fluorescent staining (Görg *et al.*, 2004). Series of gel replicates are subjected to densitometric image analysis, and only those protein spots with altered density are selected for protein identification by MS. One spot optimally contains a single protein (proteoform), which can be in-gel digested with a specific endoprotease. The peptides are then extracted and identified by MS using **peptide mass fingerprinting (PMF)** (Pappin *et al*., 1993).

PMF is one of the two principal methods of protein identification using MS, and is typically used in the "classical" proteomic approach. Proteins are digested with a sequence-specific protease, most frequently with trypsin, which cleaves a peptide bond following the basic amino acids arginine and lysine (except if the following amino acid is proline). The resulting peptide mixture is analyzed by MS. The mass spectrum of several peptides from one protein is characteristic for a particular protein, hence the fingerprint analogy. The *m/z* values of the peptides are compared with theoretical masses of tryptic peptides resulting from "*in silico*" digest of all proteins, open reading frames or genes present in the inquired database. If a statistically significant match is found, the protein is considered identified.

The "classical approach" of using 2-DE along with PMF has been used as a central technology of proteomics since its onset. This methodology has certain limitations (see chapter 2.1.3), but despite them, it prevailed in proteomics as a main strategy until new technologies required for the "shotgun" proteomic approach reached the necessary performance and became accessible for research laboratories.

2.1.1.2 The "shotgun" proteomic approach

In "shotgun" proteomics, the proteins are digested with a sequence-specific endoprotease. The resulting complex peptide sample is then separated, most often by chromatographic methods, usually reversed-phase (RP) liquid chromatography (LC) prior to MS analysis (LC-MS).

The currently used RP-LC columns have most commonly µl or nl per minute flow rates (hence micro- and nano-LC), inner diameters of less than 1 or 0.1 mm (in micro and nano-LC, respectively) and are operated at high pressures. The use of such columns ensures the separation of peptides with high resolution. The resolving power can be further enhanced when two successive orthogonal chromatographic separations are used (2-D LC) (Wilson *et al.*, 2015). Effective separation is often attained by combining different types of LC, e.g. ion exchange chromatography (separation based on peptide charge) with RP-LC (separation based on peptide hydrophobicity) or high pH RP-LC with standard low pH RP-LC (difference in charge under high and low pH influences separation selectivity, Yang *et al.*, 2012).

The peptides are typically eluted from RP continually into the electrospray of a mass spectrometer and peptides are identified using **tandem mass spectrometry (MS/MS)**. Masses of the intact peptides are measured in the first MS. From the resulting spectra, peptides are selected as precursors for further measurement, for which they undergo some form of molecule fragmentation. This can be, for example, collision-induced dissociation, which involves collisions of the gas-phase peptides with inert gas molecules, electron capture dissociation or electron transfer dissociation, which uses the direct introduction of low-energy electrons to trapped gas-phase ions (Brodbelt, 2016).

The fragmentation occurs randomly, preferentially on the peptide backbone. The resulting peptide fragmentation spectrum contains peptide ion peaks with *m/z* values, which are again, as in PMF, compared with theoretical mass values, this time of all possible peptide fragments. The identification of proteins is based on obtaining information about peptide sequences from peptide fragmentation spectra (peptide-spectrum matches, PSMs). This is done by one of several available database search engines, such as Sequest (Eng *et al.*, 1994), Mascot (Perkins *et al.*, 1999) or others. Then the identified peptide sequences are assembled into a set of confident proteins, a process called protein inference (Huang *et al.*, 2012). Finally, it is necessary to assess the reliability of these identifications by estimating collective false discovery rates (FDR) or by determining correctness probabilities for each PSM (Nesvizhskii, 2010).

Current MS/MS instrumentation is capable of identifying over 10,000 proteins in a single experiment (Beck *et al.*, 2011, Nagaraj *et al.*, 2011) depending on the fractionation complexity. Compared with the "classical" proteomic approach, the whole process requires less manual effort and allows deeper proteome coverage.

2.1.2 Quantification in proteomics

The mission of expression proteomics is the evaluation of changes in proteomes resulting from various influences on the organism, tissue or cells under study. The goal is to identify proteins that are differentially expressed, i.e. to assess the relative quantity of individual proteins in the two or more samples.

Quantification in the classical 2-DE proteomic approach is based on comparison of optical densities of the visualized protein spots with image analysis software. The protein identity is then revealed after cutting out the spots, in-gel protein digestion, extraction of peptides and their MS or MS/MS analysis.

To detect the relative protein abundances in the "shotgun" proteomic approach, quantitative MS technologies have been developed. There are currently two major approaches for MS-based quantitative proteomics: **differential isotopic labeling** and **label-free quantification**.

MS is not a quantitative method *per se*. Ion signal intensities do not directly determine the abundance of the detected peptide, because they are dependent on other factors than just the amount of the ionized peptides. Other components of the sample (other peptides) compete for charge during ionization and cause ion suppression. Comparing MS/MS spectra resulting from two or more different samples was not considered reliable nor feasible in the past (later, however, it was proven to be practicable under specific conditions, see chapter 2.1.2.3).

Isotopic labeling methods make use of the fact that MS allows discrimination between chemically identical substances with different isotope composition in a single mass spectrum. Protein or peptide samples differentially labeled with molecules containing stable isotopes (primarily ^{13}C, ^{15}N and ^{18}O) can therefore be mixed and analyzed as a single sample. The presence of "heavy" isotopes introduces mass shift and therefore enables discrimination of the samples, and the ratio of signal intensities enables the relative quantification for peptides.

The stable isotope labels are most commonly introduced either by chemical or metabolic labeling. Less common enzymatic labeling is based on trypsin digestion in $H_2{}^{18}O$, which leads to incorporation of ^{18}O into one of the samples (Yao *et al.*, 2001).

2.1.2.1 Chemical isotope labeling

For **chemical isotope labeling**, the samples to be compared can each be labeled with one of the multiple versions of isotope-labeled tagging reagents. The labeling is made possible through a reactive group that forms a covalent bond by reacting with either cysteine SH groups, or more frequently, with primary amine groups, as is done with isobaric mass tags such as isobaric tags for relative and absolute quantitation, (iTRAQ, Ross *et al.*, 2004) and tandem mass tags (TMT, Thompson *et al.*, 2003).

The iTRAQ label consists of 1) a N-hydroxysuccinimide reactive group that allows the formation of a covalent bond with primary amine groups (cysteine labeling TMT tags are also available); 2) a reporter group with differing masses in each set of tags, which is cleaved during the peptide fragmentation and provides the resulting intensity ratio in the MS/MS spectra, and 3) a balance group (see Figure 1.1 A) The total mass of the reporter and balance components of the molecule are kept constant using differential isotopic enrichment with ^{13}C, ^{15}N, and ^{18}O atoms (see Figure 1.1 B). The TMT labels have analogous components as in the iTRAQ molecule and use the same principle (see Figure 1.1 C).

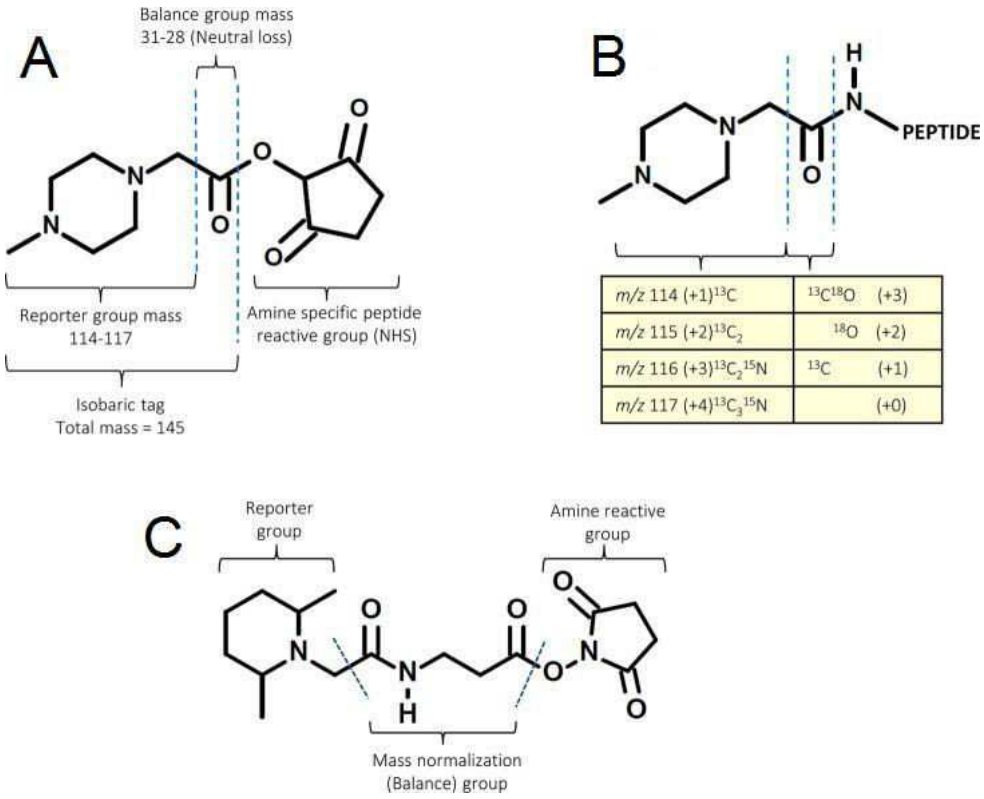

Figure 1.1. *The components of the iTRAQ and TMT label.* ***A.*** *The structure of a iTRAQ label molecule.* ***B.*** *The isotopic composition of the reporter and balance components of the molecule.* ***C.*** *Chemical structure of a TMT reagent with analogous components as in the iTRAQ molecule (Taken from Rauniyar & Yates, 2014).*

The tag forms amide linkages to peptide amines, and this linkage fragments in a similar way as backbone peptide bonds. During fragmentation, the balance moiety is lost (neutral loss), while charge is retained by the reporter group fragment. This means that the peptides from differentially labeled samples have identical mass, but can be distinguished following fragmentation by the isotope encoded reporter ions in the low mass range region of the MS/MS spectra. The relative intensities of these reporter ions are the basis for quantification (see Figure 1.2). This principle also means that the complexity of peptide mass spectra is not increased compared to unlabeled sample. (Bantscheff *et al.*, 2012)

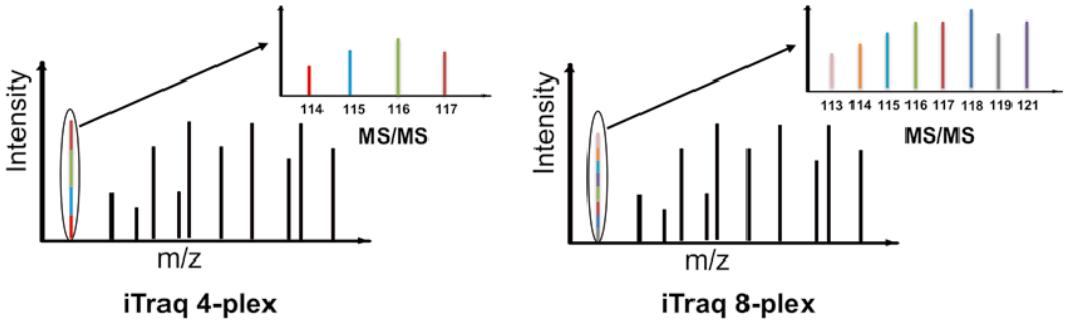

Figure 1.2. *During MS/MS of an iTRAQ-labeled sample, the reporter ions of differential masses are released from a peptide to give sample-specific quantitation of a particular peptide (Taken from Aggarwal & Yadav, 2016).*

As opposed to metabolic labeling methods, which require growing cells, the use of the chemical labeling methods is virtually unlimited: it can be used for proteomic quantification in clinical samples such as body fluids or frozen tissue samples. A major advantage of chemical labeling methods is their suitability to multiplexing: iTRAQ and TMT labels are available in up to 8-plex and 10-plex sets of tags, respectively.

2.1.2.2 Metabolic isotope labeling

Stable isotope labeling with amino acids in cell culture (SILAC, Ong *et al.*, 2002) is the most common metabolic labeling approach for mammalian cells in proteomics. In this method, the cells are grown in culture media containing either standard or isotopically labeled amino acids (“light” and “heavy” medium), which are introduced into the newly synthesized proteins. The amino acids selected for isotopic labeling should be essential for the cultured cells, so that the culture medium is the only source of that particular amino acid for the growing cells (Ong & Mann, 2006). $^{13}C_6$,$^{15}N_4$ arginine and $^{13}C_6$,$^{15}N_2$ lysine are the most typically used amino acids, and ensure that

most of the peptides following tryptic digestion of the protein sample contain at least one labeled amino acid. The “heavy” labeled peptides can be distinguished from the “light” peptides in the MS spectra due to a defined mass shift. Comparing the intensities of the “light” and “heavy” precursor ions allows relative quantification, while identification is done by MS/MS.

The harvested “heavy” and “light” cells can then be immediately mixed, which is a major advantage of the method. Systematic errors arising from sample handling are thus mostly eliminated, as opposed to other quantitative proteomic methods, where samples are processed separately during a significant part of the workflow.

The typical arrangement of SILAC allows comparison of two samples, “heavy” and “light.” To compare three samples, “triple SILAC” is routinely performed with the use of alternatively isotopically labeled amino acids (typically $^{13}C_6$ arginine and $^{13}C_6$ or $^{2}H_4$ lysine, Van Damme *et al.*, 2009, Hoedt *et al.*, 2014). The Neutron encoding (NeuCode) approach was recently introduced, which enabled 18-plex SILAC-based quantification using six lysine isotopologues (Merrill *et al.*, 2014). The use of deuterium labeled amino acids in the multiplexed methods is, however, problematic, as this may lead to shifts in retention time in RP-LC (Zhang *et al.*, 2001), which may hamper accurate quantification.

As SILAC is limited to cells or organisms that can be metabolically labeled, it is not generally applicable to human tissues and body fluids. To overcome this a method called super-SILAC was introduced. It uses a mix of multiple “heavy” SILAC labeled cell lines representative of a particular tissue. The “heavy” labeled cell mixture can be combined with the samples of interest, acting as the “heavy” sample. The method was originally introduced for a quantitative analysis of human breast and brain tumor tissues (Geiger *et al.*, 2010)

2.1.2.3 Label-free quantification

The development of quantitative “shotgun” proteomic approaches in the previous decade was primarily focused on isotope labeling methods. These methods proved to be accurate and reliable. The price of the isotopic labels is very high, however, and the chemical labeling introduces multiple time-consuming steps into the protocol. In addition, metabolic labeling increases sample complexity, which may reduce the sensitivity of the method.

Label-free quantification was considered problematic for a long period of time. MS ion intensities, when compared between multiple measurements do not generally provide quantitative information. This is because the intensities of peptide ions are influenced by other factors than

only peptide abundance, primarily by ion suppression caused by the presence of other peptides in the sample competing for charge during ionization. It was eventually observed, however, that peptide precursor ion intensities, or the number of precursor ion spectra selected for MS/MS can be used for protein quantification, given that conditions remain strictly identical between separate LC-MS analyses.

Quantification based on peptide **precursor ion intensities** relies on a correlation between areas under curve of the matched peptides in the MS spectra and the abundance of identified peptides (and therefore also proteins) in the original sample. It involves the integrated measurement of chromatographic peak areas for all peptides in LC-MS runs (Gstaiger & Aebersold, 2009).

Spectral counting is based on the assumption that abundance of the peptide in the sample can be correlated with the rate at which a peptide precursor ion is selected for MS/MS fragmentation in a mass spectrometer (MacCoss *et al.*, 2003). For relative protein quantification, the spectral counts are averaged into a protein abundance index.

The relative quantification using both label free methods places high demands on the reproducibility of the LC system, as the measured peptide precursor masses are matched to their corresponding retention times (Neilson *et al*., 2011, Megger *et al.*, 2013). Label-free quantification methods are considered prone to quantification errors compared to the isotope labeling methods esp. metabolic labeling, where the samples are mixed at the very beginning. The samples are processed in parallel in label-free quantification, which can lead to the introduction of experimental variation, such as pipetting errors during the sample preparation (Bantscheff *et al.*, 2012).

In spite of these challenges, label-free quantification is becoming increasingly more popular. It holds the advantage of inexpensive sample preparation compared to the isotope-based labeling techniques, and the lack of extra steps in the procedure. Thanks to constantly improving instrumentation and software solutions, label-free methods have become fully capable of providing trustworthy quantitative data.

2.1.3 Limitations of proteomic methods

The “classical” proteomic approach has long been the standard for quantitative analyses of proteome research. The principal method, 2-DE, possesses several limitations, however. Most importantly, the vast majority of the protein spots (over 80%) contain multiple co-migrating proteins (Gygi *et al.*, 2000, Thiede *et al.*, 2013). Information about protein quantity obtained from

densitometric analysis of spots containing multiple proteins is therefore inaccurate. Conversely, most proteins exist in the form of multiple proteoforms and produce multiple spots. In extreme cases, even over 30 proteoforms can be detected, as in the case of heat shock protein 27 (Hsp27) and enolase-1 (Jungblut *et al.*, 2008, Thiede *et al.*, 2013). This leads to the situation where the differential expression attributed to a protein in a differential 2-DE analysis actually concerns only one of its many proteoforms. This can be considered both an advantage and a disadvantage of the method, depending on the objectives of the analysis.

Another major concern is the inability of 2-DE to resolve all the proteins within a sample, given its limited dynamic range, and the inability to separate extremely acidic or basic, extremely large or small, and hydrophobic proteins, i.e. mainly integral membrane proteins. The latter is mainly caused by the limits of the solubilization power of running buffers used for IEF (Magdeldin *et al.*, 2014). The narrow dynamic range stems from the limited sensitivity of either the staining method used, or in mass spectrometry, when the amount of the peptides extracted from the gel is low. Up to several hundred (over 800, Thiede *et al.*, 2013) unique proteins can be identified on a typical 2-DE gel, i.e. one order of magnitude less than in a shotgun approach.

The “shotgun” proteomic approach is in many ways better suited for large-scale quantitative proteomic analyses. It is able to cover a broader dynamic range of protein concentrations and is somewhat more suitable for proteins with extreme properties. On the other hand, in this approach, the information about some proteoforms, such as differentially spliced or post-translationally truncated proteins, is lost at the start of the procedure, when the proteins are digested into a complex mix of peptides. It also becomes impossible to assign which such proteoform contains or does not contain a post-translational modification.

In the shotgun approach, difficulties with determining the protein identity from the identified peptides may appear. Unique peptides, i.e. peptides with sequences that are unique for one protein, are needed for the identification of proteins. Peptides that are not unique are called degenerate, i.e. their sequence is shared by multiple proteins, often homologous ones. It is not possible to distinguish from which protein such a peptide comes, or to assess whether only one, several, or all proteins that share such a degenerate peptide are present in the sample. (Huang *et al.*, 2012)

The sampling rate of current mass spectrometers also presents a limitation: the precursor ion peptides selected during on-line LC-MS represent only a subset of all peptides in the sample, due to the limited speed of current mass spectrometers, given by the need for cycling between MS and MS/MS modes. Each repeated analysis of the same sample therefore leads to overlapping but

somewhat different data sets. This problem can be overcome by repeating the analysis of the same sample, typically by running triplicates. This solution, however, comes at a cost of prolonged analysis time and increased price (Domon & Aebersold, 2010).

One limitation that is common to both proteomic approaches (although it is more pronounced in the classical approach) is the reduced suitability for the analysis of hydrophobic (and also low-abundant) integral membrane proteins. Due to their specific properties, integral membrane proteins are frequently neglected by the standard proteomic methods. Proteomic strategies aimed at integral membrane proteins are discussed in the Section II (chapter 4).

Regardless of the practical and technical limitations listed above, the striking technological advances achieved in the past decade have made proteomics very useful to cell biology and biomedical research. Current sample preparation techniques in combination with accurate LC-MS instrumentation routinely allow the identification and quantification of several thousand proteins from a few micrograms of sample. The first description of a nearly complete model proteome (de Godoy *et al.*, 2008) and the identification of more than 10,000 different proteins in human cell lines (Beck *et al.*, 2011, Nagaraj *et al.*, 2011) and publication of reference maps of human proteome (Kim *et al.*, 2014, Wilhelm *et al.*, 2014) are some of the major recent breakthroughs. Very recently, similar coverage of complex proteomes can be achieved even much faster and with fewer sample preparation steps (Hebert *et al.*, 2014). If the development of robust and economical proteomic workflows and mass spectrometers continues, proteomics may soon play a similar role in biomedicine as next generation sequencing plays now (Mann *et al.*, 2013).

2.2 The biomedical issues studied in this thesis

In the works presented in this thesis, we studied drug resistance in mantle cell lymphoma with the use of quantitative proteomic methods. The first section of this thesis presents three proteomic analyses of drug resistance in MCL cells. In the second section, a novel proteomic method addresses problematic integral membrane proteins. We optimized and tested this method on MCL cells and used it to inventarize their membrane proteome. In the following chapters, I will briefly introduce the topics of drug resistance in cancer and mantle cell lymphoma.

2.2.1 Drug resistance in cancer cells

Drug resistance currently presents one of the most crucial obstacles to the effective treatment of cancer, including MCL. Although most malignancies initially respond to chemotherapy, the eventual development of drug resistance is the main cause of therapeutic failure and death of cancer patients.

Resistance occurs in response to both conventional chemotherapy as well as targeted or biological therapies. This either stems from the genetic background present before treatment, (primary/intrinsic resistance, refractory disease), or represents a response to drug treatment (secondary/acquired resistance). Either way, resistance is caused by mutations in the genome of cancer cells and/or epigenetic changes and altered expression of miscellaneous proteins.

There are several universal mechanisms of drug resistance. One important mechanism is detoxification. This consists of chemical modification of the drug by cytochrome P450 superfamily of enzymes, conjugation with glutathione S-transferase and other molecules, and active drug efflux of modified drugs, facilitated by multidrug resistance proteins (Fodale *et al.*, 2011). These are efflux pumps with broad specificity, belonging to the ATP-binding cassette (ABC) transporter family. Efficient drug efflux lowers intracellular drug concentrations and therefore decreases their effects (Wu *et al.*, 2011[Mol Pharm]).

Deregulation of DNA damage response (DDR) also plays an important role in drug resistance. While in normal cells DDR is tightly connected with cell cycle arrest and apoptosis, cancer cells can circumvent drug-induced DNA damage by switching off signaling in DDR pathways, e.g. the ATM pathway (Wang *et al.*, 2012). In other cases, enhanced DDR can ensure the survival of cancer cells treated by genotoxic drugs by correcting the errors induced by the drugs, e.g. enhancement of nucleotide excision repair against the action of cisplatin (Furuta *et al.*, 2002) or modification of mismatch repair against the effects of 5-fluorouracil (Meyers *et al.*, 2001).

In a similar fashion, cancer cells may limit or circumvent drug effects by avoiding programmed cell death. This may happen by either the overexpression of anti-apoptotic proteins like Bcl-2, IAPs, FLIP etc., or mutational inactivation of pro-apoptotic genes, i.e. caspases, Bax or alterations in the p53 pathway (Igney & Krammer, 2002).

In addition to these general mechanisms, several proliferative signaling pathways also provide survival stimuli that may participate in preventing cancer cell death caused by drug-induced stress. Such mechanisms may comprise overactivation of PI3K/Akt/mTOR, Ras/Raf/MAPK, or constitutive activation of NF-κB pro-survival pathways, or suppressing proliferation inhibitors, such as PTEN phosphatase or pRb (Rebucci & Michiels, 2013).

In addition to nonspecific drug resistance, mechanisms specific to a certain drug or a class of drugs may play even more important role in cancer cell survival. In general, such drug-specific mechanisms may involve:

- downregulation of specific receptors that are the drug targets themselves
- downregulation of specific transporters required for the drug's transport into the cell
- downregulation of specific enzymes required for activation of the prodrug
- upregulation of enzymes that may specifically metabolize or inactivate the active drug
- mutation or deregulation of genes that are the targets of a inhibitor drug, typically by a mutation of the drug's binding site
- other mechanisms specific to individual drug targets.

Elucidation of the molecular mechanisms of resistance has enormous value for drug design and efficient therapy. Detailed molecular analyses of therapy-resistant tumor cells using quantitative proteomic approaches may allow an understanding of the mechanisms of drug resistance. Moreover, such analyses may lead to the identification of contributing and compensatory processes. This knowledge may ultimately lead to the identification of suitable drug targets. Such a global view then potentially opens a way to the personalized therapy of drug-resistant malignancies.

2.2.2 Mantle cell lymphoma

Mantle cell lymphoma (MCL) is a mature B-cell neoplasm classified as a non-Hodgkin lymphoma. It is a rare lymphoid malignancy, the annual incidence of which is 0.5/100 000 in the USA and Europe. MCL is more common in males than in women with a 3:1 ratio, and the median age at diagnosis is 68 years (Cheah *et al.*, 2016).

The molecular hallmark and presumptively the initiating event is the t(11;14)(q13;q32) translocation (Li *et al.*, 1999), which transposes the *CCND1* gene (11q13), next to the immunoglobulin heavy chain locus control region (14q32). This leads to the constitutive overexpression of cyclin D1, encoded by the *CCND1* gene (Jares *et al.*, 2012). Cyclin D1 binds to cyclin-dependent kinases 4 and 6 (CDK4/6), and the complexes phosphorylate the retinoblastoma protein (pRb). This releases E2F transcription factors inhibited by pRb, and E2F transcription factors activate the expression of genes involved in the G_1/S transition, S-phase and DNA replication (Sherr 1994).

Newly diagnosed MCL patients are typically treated by a combinatorial immunochemotherapy including the anti-CD20 antibody rituximab, combined with classical chemotherapy. Most commonly, rituximab (R) is combined with R-CHOP [cyclophosphamide, hydroxydaunorubicin (doxorubicin), oncovin (vincristine), and prednisone], or R-HDAC (high-dose ara-C). Even if the disease is not refractory, the response is typically short-term and remission is commonly followed by a relapse. Prognosis of relapsed/refractory MCL is dismal (Kluin-Nelemans *et al.*, 2012, Dreyling *et al.*, 2013), which makes MCL an untreatable malignancy, median survival being 5-7 years (Herrmann *et al.*, 2009).

There is no standard therapy for patients with relapsed/refractory MCL. Chemoimmunotherapeutic regimens that have been explored include R-DHAP [rituximab with dexamethasone, high-dose ara-C, platinol (carboplatin)], R-FCM (rituximab with fludarabine, cyclophosphamide and mitoxantrone), the combination of rituximab with gemcitabine and oxaliplatin, and others. In these studies, overall response rates were high, but progression-free survival was less than 2 years (Cheah *et al.*, 2016).

Newer agents that have recently received regulatory approval for relapsed/refractory MCL treatment include bortezomib, lenalidomide, temsirolimus and ibrutinib; other drugs are in ongoing clinical trials, and several novel agents are in development.

3 Section I: Proteomic analyses of drug-resistant MCL cells

The studies described in this first section employed proteomic approaches to analyze the changes in MCL cells with acquired drug resistance to experimental or clinically used drugs. We were interested in 1) the causal changes, i.e. the mechanisms of drug resistance, and 2) secondary (contributing and compensatory) changes. Both types of alterations may provide a better understanding of the affected molecular processes and may indicate novel therapeutic targets in such drug resistant cells.

The individual objectives of this part of my thesis were:

1. To identify the molecular changes associated with TRAIL resistance in MCL cells
2. To elucidate the mechanism of resistance to cytarabine in MCL cells
3. To elucidate the mechanism of resistance to fludarabine in MCL cells

3.1 Identification of potential therapeutic molecular targets in TRAIL-resistant MCL cells

Novel therapeutic molecules specifically targeting cancer cells are being developed in order to improve the efficacy of therapy. Such molecules are designed to induce apoptosis specifically in cancer cells. An example of such a molecule is the recombinant soluble form of the proapoptotic cytokine Tumor necrosis factor-related apoptosis-inducing ligand (TRAIL).

TRAIL is a transmembrane glycoprotein (Wiley *et al.*, 1995) localized on the surface of several types of immune system cells (NK cells, cytotoxic T-lymphocytes, dendritic cells and macrophages). The extrinsic apoptosis pathway is triggered after binding of a TRAIL trimer to the death receptor, resulting in its trimerization and recruitment of Fas-associated death domain (FADD) to the receptor's intracellular death domain. FADD recruits procaspase 8 and 10, forming the death-inducing signaling complex (DISC) (Bodmer *et al*., 2000). This leads to the activation of other initiator and effector caspases, launching the process of programmed cell death itself (Riedl *et al.*, 2004).

TRAIL has been implicated in numerous functions related to the immune system: TRAIL and its receptors have been shown to play important roles in the immune response to viral infections and in the immune surveillance of tumors and metastases. TRAIL has also been implicated in the process of activation-induced cell death mediating peripheral immune tolerance (Falschlehner *et al.*, 2009, Dimberg *et al.*, 2013).

TRAIL binds to death receptors (DR) capable of triggering apoptosis TRAIL-R1/DR4 and TRAIL-R2/DR5 (Pan *et al*., 1997, Schneider *et al.*, 1997). Besides these death receptors, TRAIL can also bind to the decoy receptors TRAIL-R3/DcR1 (Pan *et al.*, 1997) and TRAIL-R4/DcR2 (Marsters *et al.*, 1997) and soluble receptor osteoprotegerin (Emery *et al*., 1998), which do not possess the functional cytoplasmic death domain required for the induction of apoptosis (Degli-Esposti *et al*., 1997[J Exp Med], Degli-Esposti *et al.*, 1997[Immunity]). Decoy receptors and osteoprotegerin were suggested to inhibit apoptosis by ligand scavenging (Mérino *et al.*, 2006, Morizot *et al.*, 2011) and by forming inactive complexes with apoptosis-competent TRAIL receptors (Clancy *et al*., 2005).

Several *in vitro* studies have shown that recombinant soluble TRAIL possesses cytostatic and cytotoxic activity in malignant transformed cells (Wiley *et al.*, 1995, Petrák *et al*., 2009, Molinský *et al.*, 2013). Conversely, normal non-transformed cells were shown to be resistant to

TRAIL (Ashkenazi *et al.*, 1999). Most importantly, in tumor xenograft models, TRAIL has been shown to selectively kill cancer cells while sparing normal cells (Walczak *et al*., 1999, Castro Alves *et al.*, 2012). Because both TRAIL death receptors are highly expressed in various malignancies (Pan *et al.*, 1997, Walczak *et al*., 1999, Kurbanov *et al.*, 2005, Voortman *et al*., 2007), recombinant soluble TRAIL is an attractive therapeutic molecule.

As with many other anti-cancer therapeutics, the development of resistance has been frequently observed in *in vitro* and *in vivo* studies (Thorburn *et al.*, 2008, Lovric & Hawkins, 2010, Dimberg *et al*., 2013). The most common mechanisms of resistance were found to be the loss of expression or mutation of the TRAIL "death" receptors, or inhibition of DISC and initiator and effector caspases signaling (Cheng *et al.*, 2006, Dimberg *et al*., 2013).

In this study, we aimed to identify changes in protein expression associated with acquired resistance to TRAIL in MCL cells. Molecular changes associated with the adaptation of drug-sensitive cells to chemotherapy are either directly associated with resistance, or represent additional potentially adaptive changes in the physiology of drug-resistant cells. Proteomic analysis can provide insights into such changes and offer valuable information about potential new therapeutic targets. Using classical differential proteomic analysis, we attempted to find such changes in TRAIL resistant MCL cells.

3.1.1 Derivation of a TRAIL-resistant cell line

For our study, we used the human HBL-2 cell line, an established model of MCL, which is sensitive to recombinant TRAIL (IC_{50} 1 ng/ml after 48 hours according to our control measurements). Long-term exposure to sublethal doses however leads to development of resistance in these cells. A resistant subclone designated HBL-2/R was derived by exposing HBL-2 to increasing concentrations of TRAIL in medium for five weeks. The resulting HBL-2/R proliferated in up to 1000 ng/ml TRAIL in medium (see Figure 3.1).

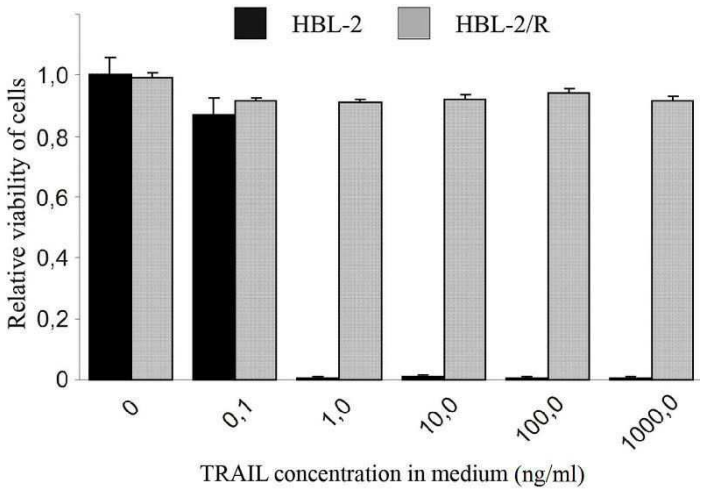

Figure 3.1. *Relative viability of TRAIL-sensitive HBL-2 cells and TRAIL-resistant HBL-2/R cells after 78 h in medium with recombinant TRAIL as determined by WST-8-based colorimetric assay.*

As one of the most common mechanisms of resistance to TRAIL is downregulation of TRAIL receptors, we performed flow cytometry analysis to determine the surface expression of death receptors DR4 and DR5 and decoy receptors DcR1 and DcR2. All four receptors were markedly downregulated in HBL-2/R compared to HBL-2 (see Figure 3.2). Therefore, the downregulation of the death receptors is the likely mechanism of resistance (Cheng *et al.*, 2006) and downregulation of the decoy receptors indicates further, more complex changes.

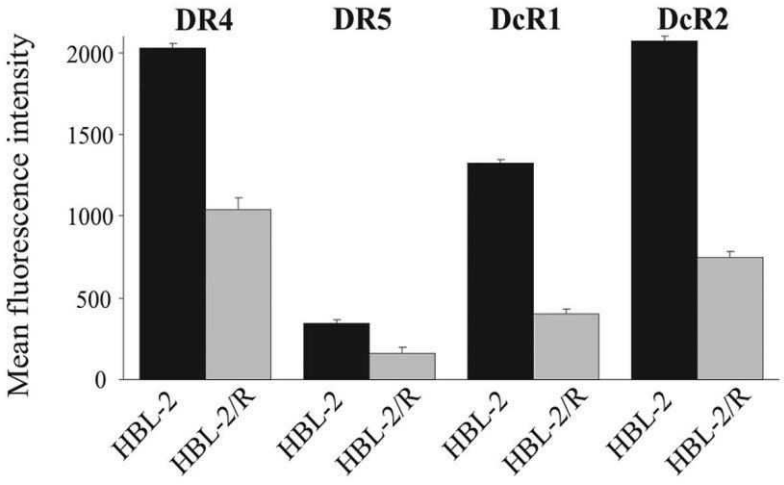

Figure 3.2. *Cell surface expression of TRAIL receptors on HBL-2 and HBL-2/R cell lines. Cells were labeled with phycoerythrin-conjugated antibodies against DR4, DR5, DcR1 and DcR2 receptors and the expression of the receptors was analyzed by flow cytometry.*

3.1.2 Proteomic analysis of the HBL-2 and HBL-2/R cell lines using 2-DE

To explore the molecular changes associated with the development of resistance, the derived TRAIL-resistant HBL-2/R cells along with the original HBL-2 cells were subjected to 2-DE analysis. Cell lysates of HBL-2 and HBL-2/R were loaded onto IPG strips, subjected to isoelectric focusing and separated in the second dimension by SDS-PAGE in 6 replicates each. Coomassie-stained gels were subjected to image analysis and 820 protein spots were reproducibly detected. Significantly quantitatively changed spots (11 upregulated and 10 downregulated in HBL-2/R cells, see Figure 3.3) were subjected to identification using MALDI-MS (see Table 3.1).

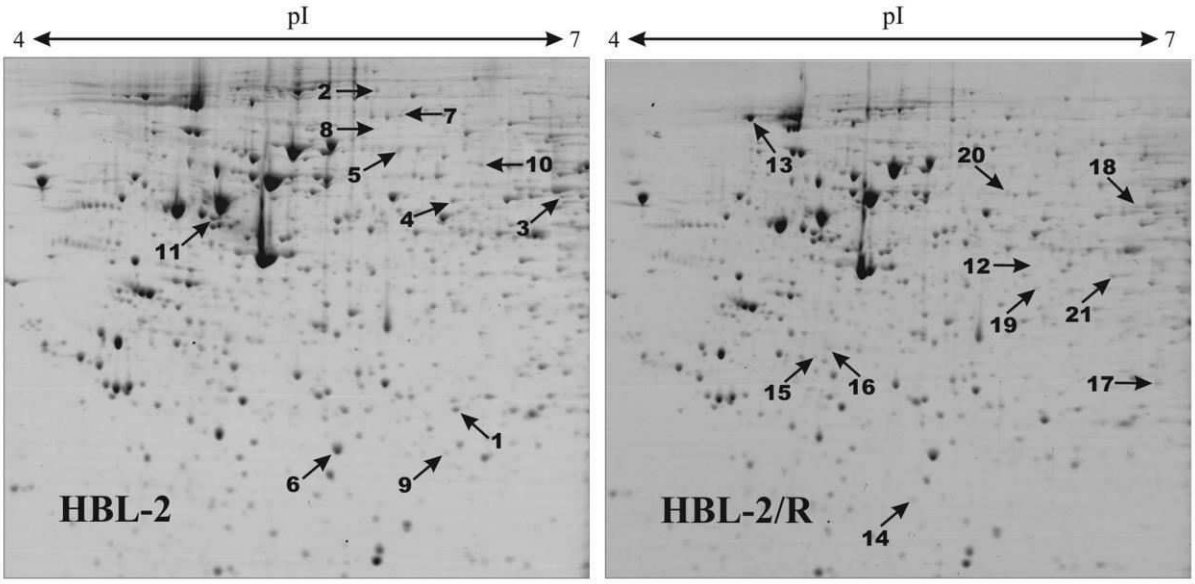

Figure 3.3. *Two-dimensional electrophoresis of HBL-2 and HBL-2/R cells performed on 24-cm gel strips, pH 4.0–7.0 and 10% SDS-PAGE stained with Coomassie Brilliant Blue. Differentially expressed proteins are indicated by numbered arrows (spots 1–11 indicate downregulated proteins and spots 12–21 indicate upregulated proteins in HBL-2/R cells).*

Using the Kyoto Encyclopedia of Genes and Genomes (KEGG) database, differentially expressed proteins were checked for their functional annotation. Three of them belonged to one metabolic pathway, hsa00230 – purine metabolism: adenine phosphoribosyltransferase (APRT, downregulatred 2.2-fold), inosine-5’-monophosphate dehydrogenase 2 (IMPDH2, downregulated 1.6-fold) and purine nucleoside phosphorylase (PNP, downregulated 1.6-fold).

Table 3.1. *List of differentially expressed in proteins HBL-2/R cells (minimal 1.5-fold change and statistical significance $p<0.05$).*

Spot no.	Uniprot Acession	Protein name	Fold change	Mascot score	Sequence coverage (%)	Mole-cular weight
Proteins upregulated in HBL-2/R cells						
1	P04792	Heat shock protein β-1	3.9	84	51	22826
2	P42704	Leucine-rich PPR motif-containing protein	2.6	100	23	159003
3	O75351	Vacuolar protein sorting-associated protein 4B	2.6	171	32	49443
4	P23381	Tryptophanyl-tRNA synthetase	2.4	240	54	53474
5	P20591	Interferon-induced GTP-binding protein Mx1	2.2	176	42	75872
6	P09211	Glutathione S-transferase P	1.9	110	56	23569
7	P06396	Gelsolin	1.9	115	22	86043
8	P13010	X-ray repair cross-complementing protein 5	1.7	262	46	83222
9	Q9HAV7	GrpE protein homolog 1	1.6	99	44	24492
10	O43776	Asparaginyl-tRNA synthetase	1.5	250	41	63758
11	Q15084	Protein disulfide-isomerase A6	1.5	76	29	48490
Proteins downregulated in HBL-2/R cells						
12	P08559	Pyruvate dehydrogenase E1 component subunit α	3.2	111	32	43952
13	P19338	Nucleolin	2.4	146	29	76625
14	P07741	Adenine phosphoribosyltransferase	2.2	227	79	19766
15	O75792	Ribonuclease H2 subunit A	1.7	348	72	33716
16	Q07955	Serine/arginine-rich splicing factor 1	1.7	82	35	27842
17	P00491	Purine nucleoside phosphorylase	1.6	182	68	32325
18	P12268	Inosine-5'-monophosphate dehydrogenase 2	1.6	230	44	56226
19	P40121	Macrophage-capping protein	1.6	102	41	38760
20	P13674	Prolyl 4-hydroxylase subunit α-1	1.5	234	48	61296
21	Q15019	Septin-2	1.5	62	23	41689

The results of the proteomic analysis were verified using western blots with specific antibodies against APRT and PNP (see Figure 3.4).

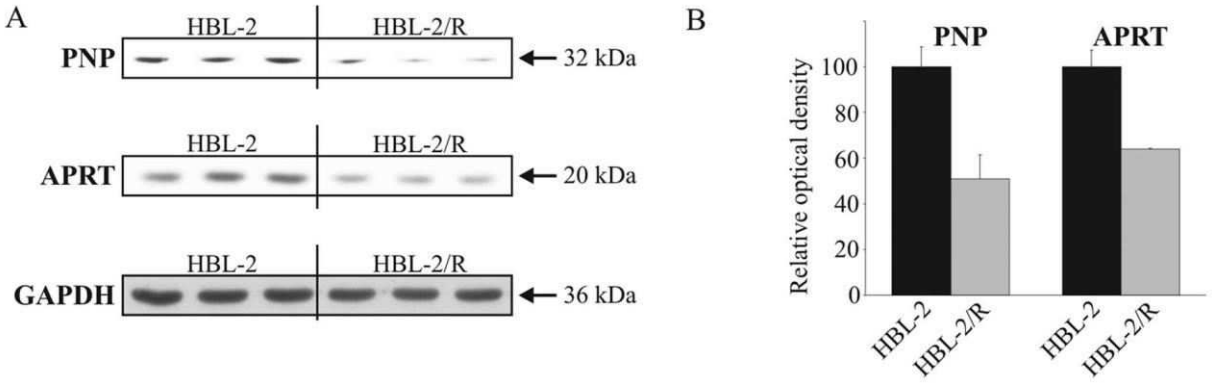

Figure 3.4. *Relative expression of PNP and APRT in HBL-2 and HBL-2/R cell lysates determined by western blot analysis.* ***A.*** *Triplicate cell lysates were probed on 12% SDS-PAGE minigels with anti-APRT, anti-PNP and anti-GAPDH primary antibodies. GAPDH was used as the loading control.* ***B.*** *Relative optical densities of the detected bands.*

3.1.3 Discussion

In our analysis of the TRAIL-resistant MCL cells, our aim was to find the causal changes of TRAIL resistance and secondary contributing and compensatory changes. The downregulation of TRAIL death receptors DR4 and DR5 that we observed has already been established as the common cause of resistance to TRAIL-induced apoptosis (Cheng *et al.*, 2006). **The downregulation of three key enzymes of purine metabolism, detected by 2-D electrophoresis and identified by MALDI-MS, represents a significant secondary change, which may have a profound effect on nucleotide homeostasis in TRAIL-resistant lymphoma cells.** Purine nucleotides are vital for the synthesis of DNA and RNA and as enzyme cofactors. They can be obtained either by *de novo* synthesis, or by being recycled in the so-called salvage pathway, a part of which are the three downregulated enzymes (see Figure 3.5). Both pathways can supply nucleotides independently, but their importance varies throughout different tissues. **In leukemic and lymphoma cells, the salvage pathway is considered the major source of nucleotides** (Scavennec *et al.*, 1982, Natsumeda *et al.*, 1984).

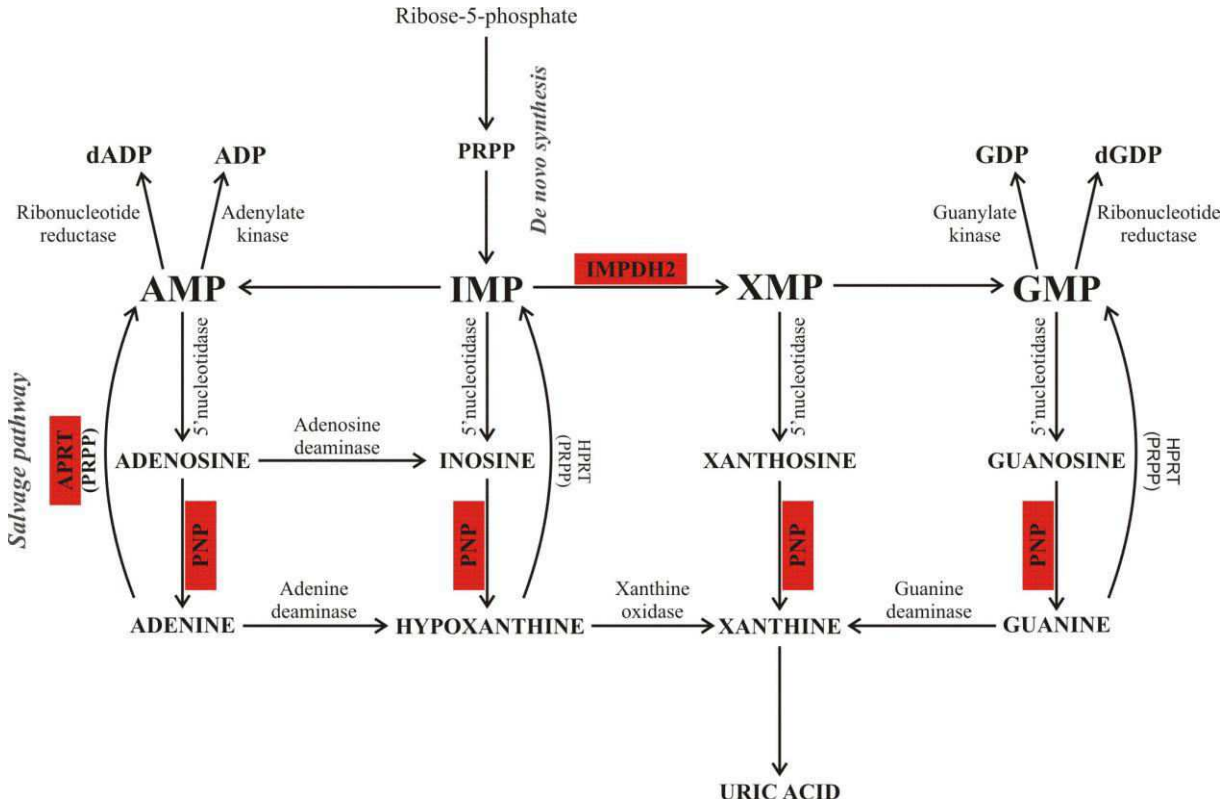

Figure 3.5. *Simplified scheme of purine metabolism, showing the position of APRT, IMPDH2 and PNP in purine nucleotide biosynthesis. The de novo synthesis of purine nucleotides begins with the phosphorylation of ribose-5-phosphate to form PRPP. In a number of reactions, PRPP forms the first fully formed nucleotide, IMP, which is converted by IMPDH2 to GMP. PNP catalyzes the reversible cleavage of purine nucleosides, releasing purine nucleobases (adenine, hypoxanthine, xanthine and guanine). In the salvage pathway the free nucleobases can be reconverted to nucleoside-5'-monophosphates in a reaction with activated sugar (PRPP) catalyzed by APRT.*

The *de novo* pathway for the synthesis of purine nucleotides leads to inosine-5'-monophosphate (IMP), which is a branch point intermediate for purine biosynthesis. IMP can be converted to either adenosine-5'-monophosphate (AMP) or guanine-5'-monophosphate (GMP) by IMPDH2 via another intermediate, xanthosine-5'-monophosphate (XMP). The catabolism of purine nucleosides is carried out by PNP, which liberates free purine bases. The salvage pathway allows the reconversion of the free bases to nucleotide-5'-monophosphates, catalyzed by either APRT in the case of adenine, or HPRT (hypoxanthine phosphoribosyltransferase) in the case of hypoxanthine and guanine (summarized in Figure 3.5).

Balanced enzymatic activities and concentrations of products and intermediates are critical for purine (nucleotide) homeostasis. Inhibition of PNP has been showed to result in accumulation of its substrate, 2′-deoxyguanosine, as well as deoxyguanosine triphosphate (dGTP). High

intracellular concentrations of dGTP inhibit cell proliferation and induce apoptosis (Bantia *et al.*, 1996, Galmarini *et al*., 2008). Likewise, inhibition of APRT has been showed to cause the accumulation of adenine, which is oxidized to insoluble 2,8-dihydroxyadenine; the resulting precipitate causes cell death (Bollée *et al*., 2012). The inhibition of IMPDH2 causes the depletion of guanosine nucleotides, blocking DNA synthesis and cell division (Allison & Engui 2000, Hedstrom, 2009).

The decreased expression of the three enzymes of purine metabolism observed in our analysis may thus affect both *de novo* synthesis and the salvage pathway of purine nucleosides in HBL-2/R cells. This may represent a selective disadvantage, or "weakness" of the resistant cells. Although it was not apparent in the rich cell culture media (where the proliferation rates of HBL-2/R and HBL-2 cells were comparable), such an imbalance in purine nucleotide metabolism may become critical under the less nutritionally rich environment of the human body.

A therapeutic inhibition of the already "weakened" purine metabolism may further augment the imbalance and become fatal. Such inhibition could therefore be effective for the selective elimination of TRAIL-resistant MCL cells in an experimental therapy. Several inhibitors of purine metabolism exist and are available for clinical use, such as methotrexate (inhibits purine *de novo* synthesis via dihydrofolate reductase) (Fairbanks *et al.*, 1999), ribavirin and mycophenolic acid (inhibitors of IMPDH2) (Allison & Engui 1993, Zhou *et al.*, 2003) or forodesine (inhibitor of PNP) (Gandhi *et al*., 2005).

In this study, we identified altered expression of several proteins including 3 enzymes of the purine metabolism pathway in a TRAIL-resistant MCL cell line. These molecular changes in the drug resistant cells (although not directly responsible for the resistance) represent a "weakness" that might be potentially used as a therapeutic target for the selective elimination of such resistant cells.

The results of this work were published in:

Resistance to TRAIL in mantle cell lymphoma cells is associated with the decreased expression of purine metabolism enzymes. Pospisilova J, Vit O, Lorkova L, Klanova M, Zivny J, Klener P, Petrak J.. *International Journal of Molecular Medicine* 2013; 31(5):1273 (IF 2013: 1.880).

(See Appendix 1.)

3.2 Elucidation of the mechanism of resistance to cytarabine in MCL cells

In our next study, we attempted to identify the molecular mechanism of resistance to cytarabine, a drug used clinically in the treatment of MCL. Cytarabine (cytosine arabinoside, or ara-C) is a structural analog of deoxycytidine (see Figure 3.6) and is being used primarily in the treatment of leukemias and lymphomas (Galmarini *et al.*, 2002[Lancet Oncol]) such as acute myeloid leukemia (AML) and non-Hodgkin lymphomas (NHL) (Kantarjian *et al*., 1983, Capizzi, 1996). Implementation of high-dose cytarabine into the therapy of MCL, typically by alternating R-CHOP (rituximab, cyclophosphamide, hydroxydaunorubicin, oncovin/vincristin, prednisone) and R-DHAP (rituximab, dexamethasone, high-dose ara-C, cisplatin) has led to higher response rates and prolonged progression-free patient survival (Delarue *et al*., 2013).

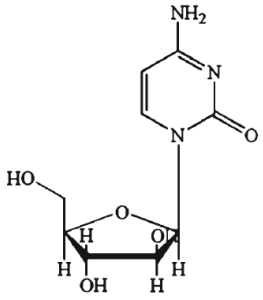

Figure 3.6. *Chemical structure of the cytidine analog cytarabine. Taken from Zhang et al., 2007[Cancer Mut Rev].*

Equilibrative nucleoside transporter ENT1 (SLC29A1) is the primary transporter responsible for the cellular uptake of cytarabine, along with ENT2 (SLC29A2) (Zhang *et al*., 2007[Cancer Mut Rev]). At high concentrations, cytarabine also diffuses across cell membranes independent of the transporters (Capizzi *et al*., 1991). Upon entry, cytarabine is phosphorylated by deoxycytidine kinase (dCK) and forms cytarabine monophosphate (ara-CMP). This phosphorylation retains the drug in the cell and allows its further phosphorylation to the active metabolite cytarabine triphosphate (ara-CTP), which can be incorporated into DNA. This causes chain termination, thereby blocking DNA synthesis and inducing apoptosis. Cytarabine also directly inhibits DNA polymerases. (Grant, 1998)

The development of resistance to cytarabine is common in MCL patients and leads to relapsed/refractory stage of the disease with poor prognosis. Currently there is no second line standard of care for relapsed/refractory MCL (Ferrero & Dreyling, 2013). The molecular mechanisms of resistance to cytarabine in MCL are unknown and had not been studied in detail.

The altered expression of several enzymes has been implicated in resistance to cytarabine. Reduced transporter activity may play a role in resistance to cytarabine by blocking its transport into the cells (Mackey *et al.*, 1998, Clarke *et al.*, 2002). dCK, as a bottleneck factor, influences the amount of the drug being activated and retained in the cells. The inactivation of dCK has also been implicated as a possible mechanism of cytarabine resistance (Dumontet *et al.*, 1999, Galmarini *et al.*, 2002[Br J Haematol]). Further enzymes involved in pyrimidine metabolism can also play role in cytarabine resistance: Deamination by cytidine deaminase (CDA) inactivates cytarabine through its conversion to uracil arabinoside (Laliberté & Momparler, 1994). The monophosphorylated form of the drug (ara-CMP) can be dephosphorylated by nucleotidases, such as cytosolic 5' nucleotidase (NT5C2) (Hunsucker *et al.*, 2005) and cytosolic 5' nucleotidase 3A (NT5C3A) (Amici *et al.*, 1997) or deaminated by deoxycytidylate deaminase (DCTD) (Mancini & Cheng, 1983). Ribonucleotide reductase (RR) reduces ribonucleotides to their corresponding deoxyribonucleotides, including dCTP. This can contribute to cytarabine resistance by multiple mechanisms including the feedback inhibition of dCK by increased production of deoxynucleotides (Lamba *et al.*, 2009). These enzymes, summarized in Figure 3.7, can all decrease the pool of ara-CTP, and therefore may be involved in cytarabine resistance.

Cytarabine resistance in lymphomas including MCL had not yet been studied in detail and no standard of care exists for MCL patients with resistance to this drug. Therefore, we derived a cytarabine resistant MCL cell line, tested the sensitivity of cytarabine-resistant MCL cell lines to a battery of different anti-cancer drugs in order to uncover eventual cross-resistance, and performed a proteomic analysis of the drug resistant cells. The goal of this work was to elucidate the mechanism of resistance to cytarabine and to find suitable therapeutic strategy based on the results.

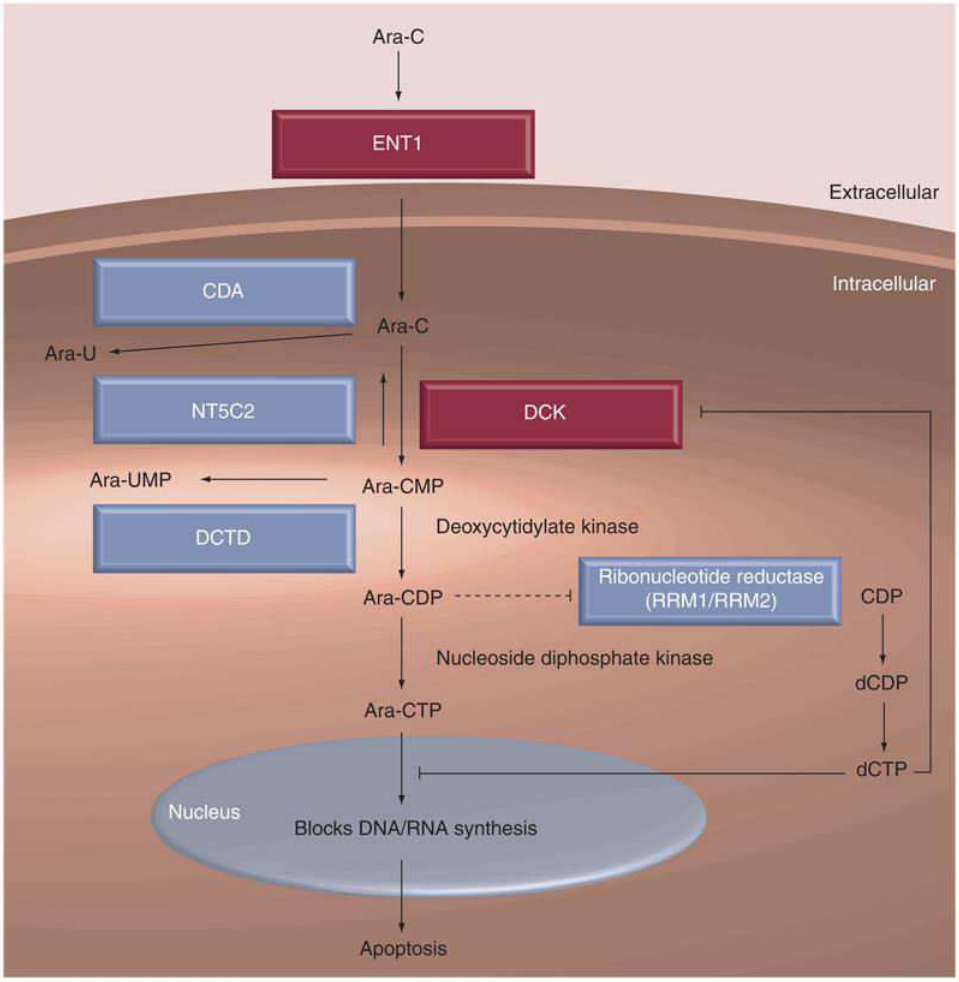

Figure 3.7. *Main enzymes involved in the transport and metabolism of purines and activation/inactivation of cytarabine that can contribute to its resistance. dCK and ENT1 (red) are needed for therapeutic efficacy of cytarabine, and CDA, DCTD and NT5C2 (blue) can diminish the amounts of the active drug (Taken from Lamba et al., 2009).*

3.2.1 Derivation of a cytarabine-resistant cell line

To analyze resistance to cytarabine in MCL, we employed five model cell lines derived from MCL (GRANTA-519, HBL-2, JEKO-1, MINO and REC-1), all sensitive to cytarabine. The cell lines were exposed to increasing doses of cytarabine, up to 50 μM. After five weeks, we established resistant subclones (GRANTA-519/R, HBL-2/R, JEKO-1/R, MINO/R and REC-1/R), which tolerated 125-1000-fold higher concentrations of cytarabine in media compared to the original sensitive cell lines (see Figure 3.8).

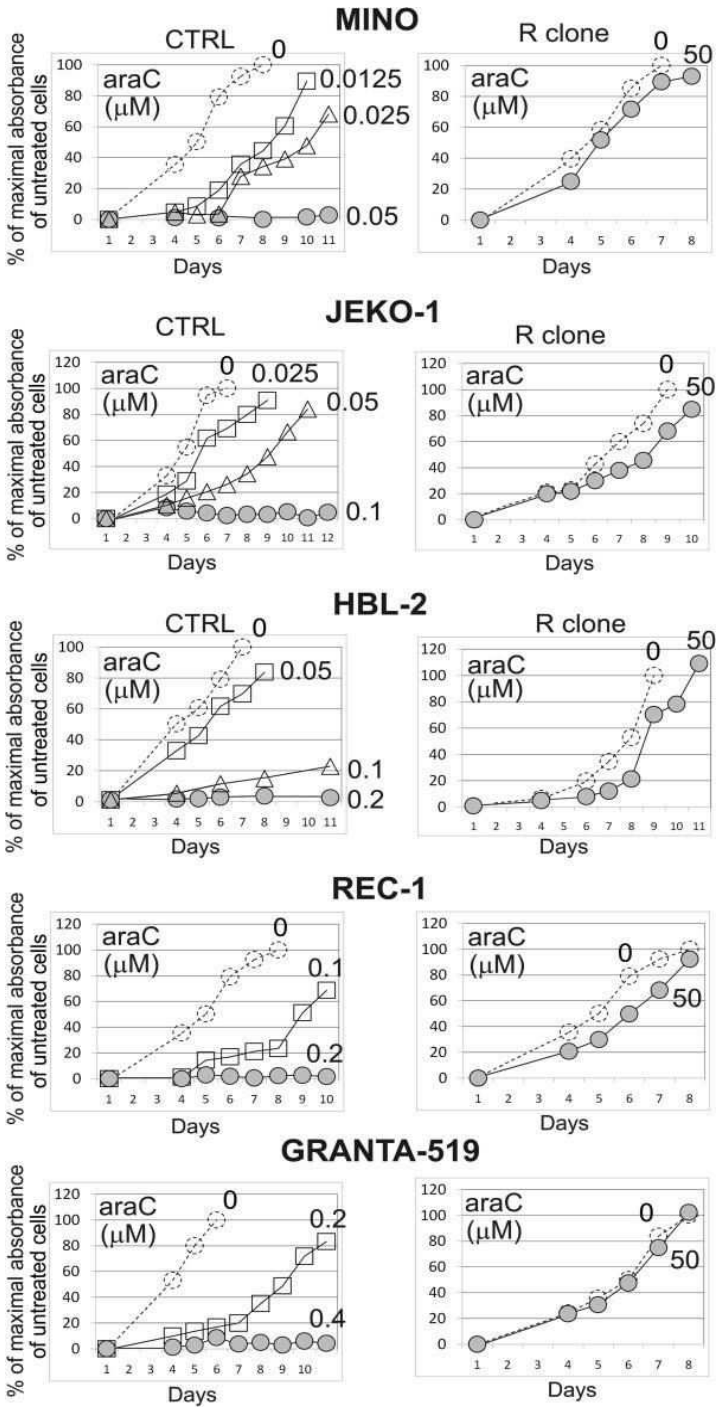

Figure 3.8. *WST-8-based cell proliferation assay of the five original MCL cell lines (left column) and five R-subclones shows that the lethal dose of cytarabine for CTRL cells ranged from 0.05 to 0.4 μM, while the proliferation rate of R-subclones in 50 μM araC was virtually unaffected. Full lines denote cells in the presence of the indicated concentration of cytarabine, dashed lines denote control cells in media without cytarabine.*

3.2.2 Assessment of cross-resistances of cytarabine resistant cells to other therapeutic molecules *in vitro*

To evaluate the sensitivity of the cytarabine resistant cells to other anti-cancer drugs, we performed cytotoxicity tests using a panel of clinically used drugs, including the alkylating agents bendamustine, cisplatin and doxorubicin, the nucleoside analogs cladribine, fludarabine and gemcitabine, and the inhibitory agents bortezomib (proteasome ihibitor), ibrutinib (Bruton tyrosine kinase, BTK) and temsirolimus (mammalian target of rapamycin, mTOR). All of the five R-subclones showed cross-resistance to all of the nucleoside analogs (see Figure 3.9 A,B). Interestingly, the cross-resistance involved both pyrimidine (gemcitabine) and purine (cladribine and fludarabine) nucleoside analogs.

Sensitivity to other classes of anti-lymphoma drugs remained unchanged, with the exception of ibrutinib, which proved to be more toxic to the resistant subclones than the original cell lines (see Figures 3.9 C,D). In addition to the cytotoxicity tests, sensitivity to anti-CD20 monoclonal antibody rituximab was determined by a ^{51}Cr release assay, a tool to evaluate the antibody-dependent and complement-mediated cytotoxicity of antibody-based drugs. In this case, the sensitivity of the original cell lines and the R-subclones was comparable.

Taken together, the observed cross-resistance to purine and pyrimidine nucleoside analogs and retained sensitivity to all other types of drugs indicates that the mechanism of resistance is nucleoside specific.

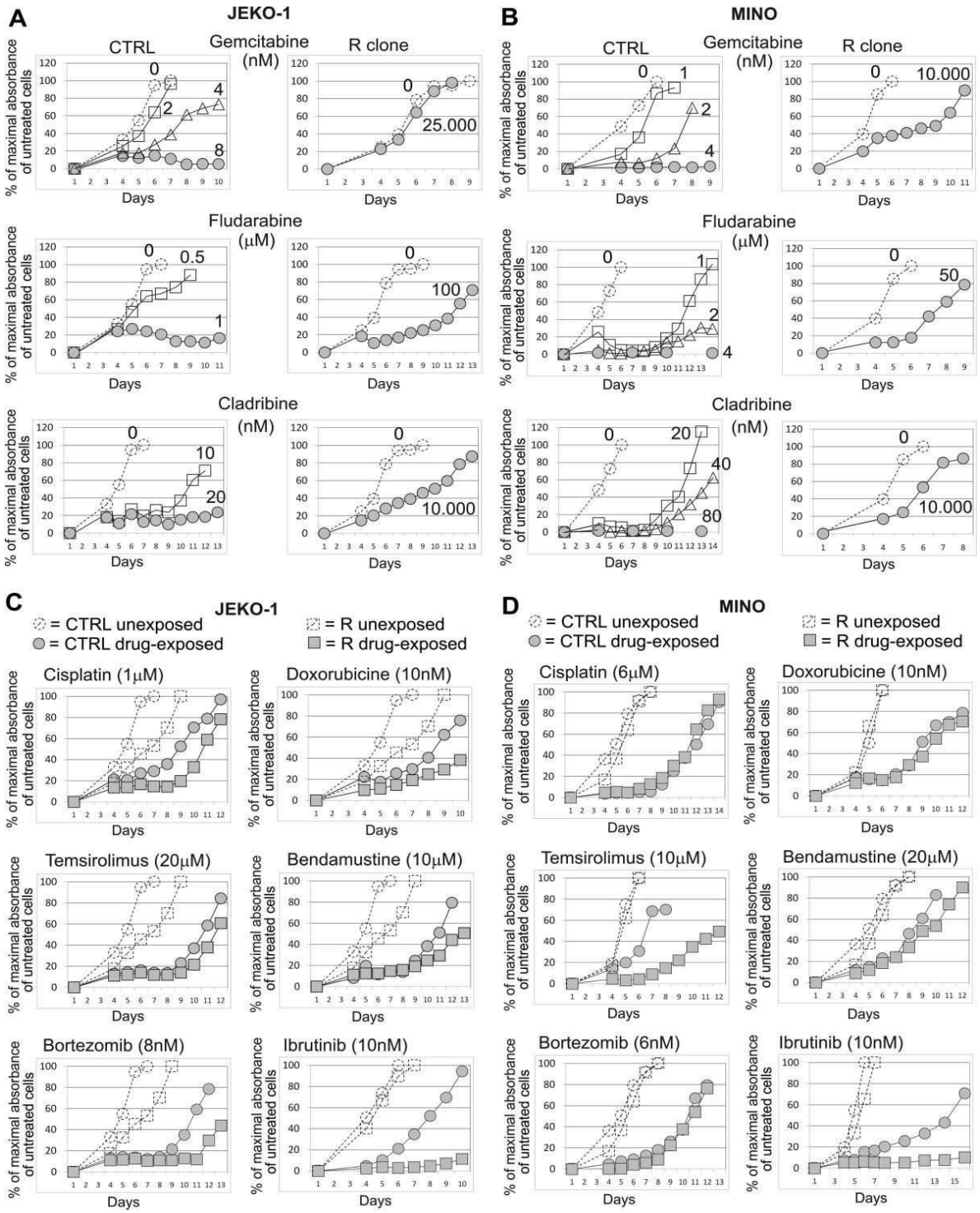

Figure 3.9. *Proliferation curves (determined by the WST-8 cell proliferation assay) of JEKO-1 (**A**, **C**) and MINO (**B**, **D**) cells and their R-subclones in the presence of nucleoside analogs gemcitabine, fludarabine and cladribine (**A**, **B**) and other types of anti-lymphoma drugs (**C**, **D**) in media (full lines). Controls (dashed lines) are cells without any anti-cancer agents in the media.*

3.2.3 Assessment of cross-resistances of cytarabine resistant cells to other therapeutic molecules *in vivo*

The in vitro tests of cellular toxicity provided important information on direct cellular effects of the tested drugs to the resistant cells. However, in vitro assays do not take into account important systemic pharmacokinetic and pharmacodynamic variables, which can have large impact on drug efficacy in vivo.

We therefore validated the information provided by the *in vitro* analyses by an *in vivo* model, which reflects the complexity of drug metabolism more accurately. We used a model of human MCL cells xenografted into immunodeficient mice (lacking B and T lymphocytes, NK cells, the complement and macrophage and dendritic cell deficiency – NOD.Cg-*Prkdc*^{scid} *Il2rg*^{tm1Wjl}/SzJ mice; Shultz *et al.*, 2005) to simulate *in vivo* treatment of cyarabine sensitive and resistant MCL. JEKO-1 or JEKO-1/R cells (10^6) were intravenously injected into the animals. This led to the development of disseminated lymphomas in the xenografted mice with a median survival rate of 38 days. Treatment with the nucleoside analogs fludarabine and gemcitabine demonstrated the loss of their therapeutic effect in animals xenografted with JEKO-1/R cells, while the remaining anti-tumor drugs bendamustine, bortezomib, cisplatin, cyclophosphamide, rituximab and temsirolimus had similar effects in both JEKO-1 and JEKO-1/R xenografted mice (see Figure 3.10).

Using the *in vivo* model, we therefore confirmed the results of the *in vitro* tests, i.e. cross-resistance of cytarabine resistant cells to both pyrimidine and purine derived nucleoside analogs, and retained sensitivity toward other types of drugs. These results provide further evidence that cytarabine resistance in MCL cells is caused by a nucleoside-specific mechanism.

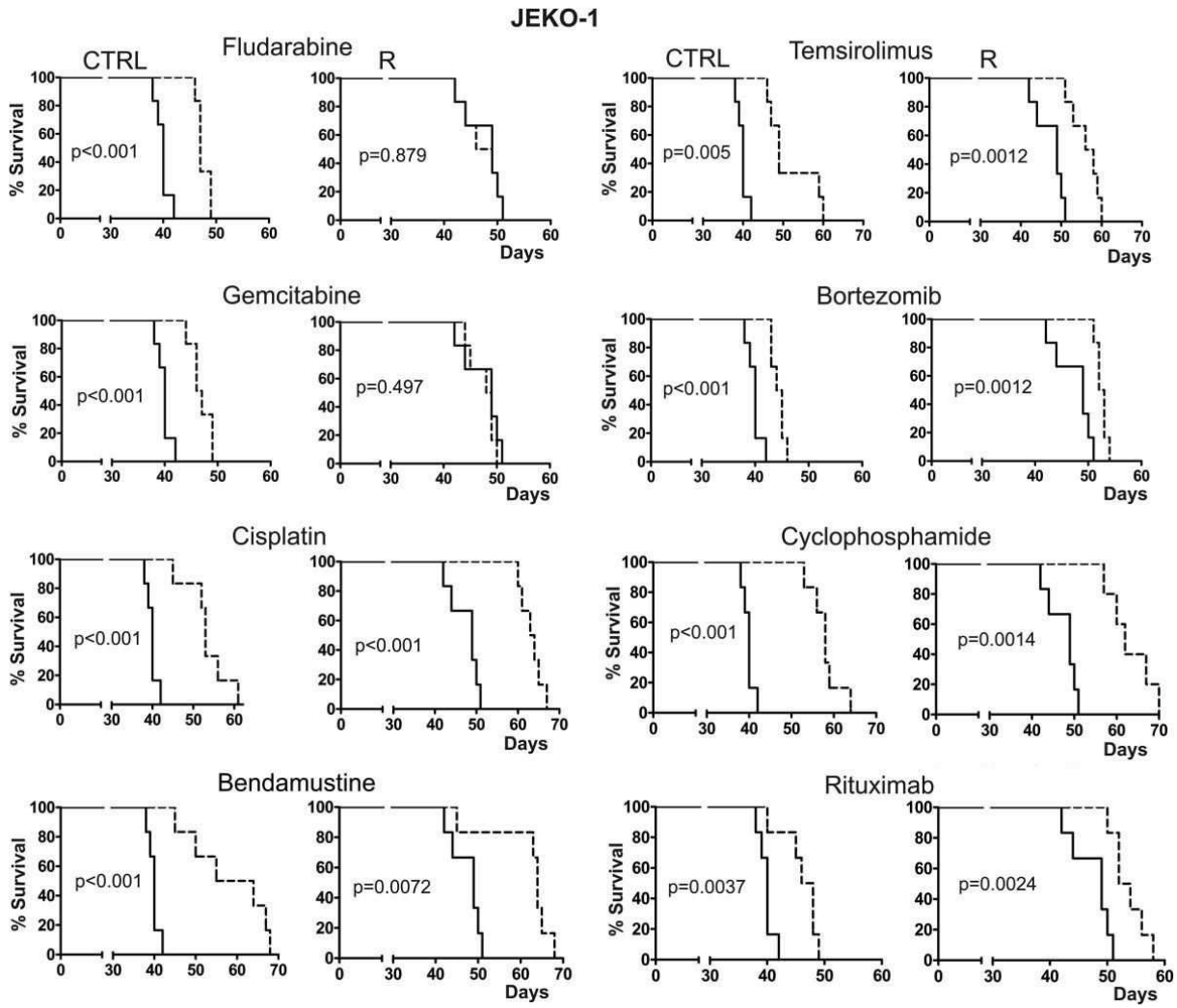

Figure 3.10. *Kaplan-Meier survival curves of immunodeficient mice xenografted with JEKO-1 or JEKO-1/R treated with stated anti-tumor drugs (dashed lines) and corresponding untreated control animals (full lines).*

3.2.4 Proteomic and transcriptomic analysis of the resistant MCL cell lines

In order to analyze the molecular changes responsible for and associated with the development of resistance in MCL cells, we analyzed the newly established MINO/R along with control MINO cell lines by 2-D electrophoresis in the same fashion as described in chapter 3.1.2. Spots with significant changes in density were in-gel digested with trypsin and the differentially expressed proteins were identified with MALDI-MS. Among the seven identified differentially expressed proteins (see Table 3.2 and Figure 3.11), we found massive downregulation of dCK in the MINO/R subclone.

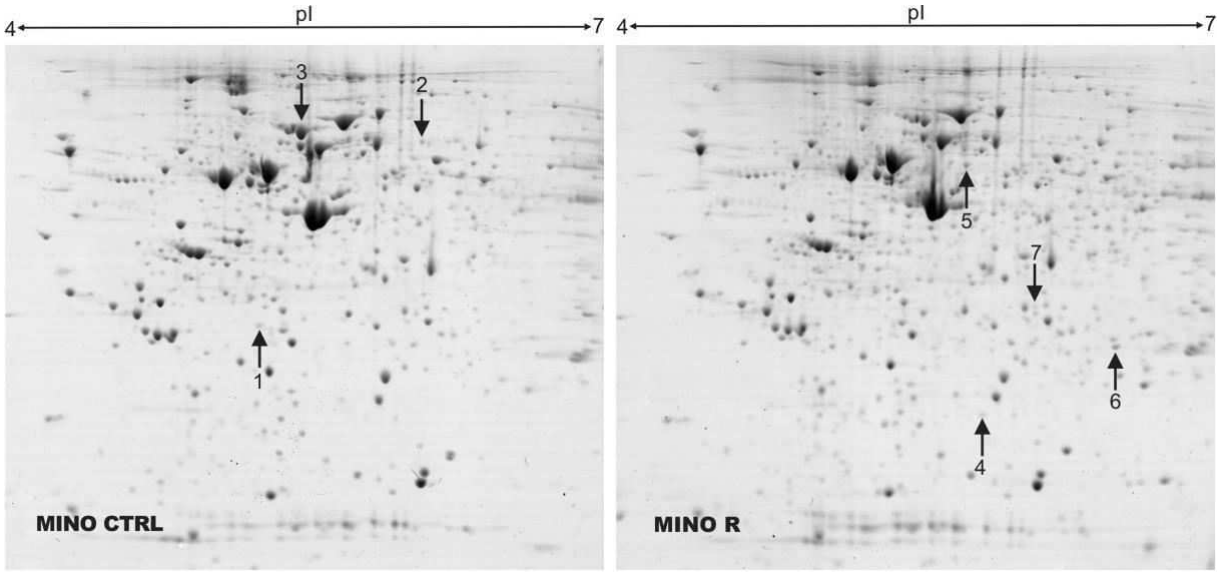

Figure 3.11. *Two-dimensional electrophoresis of MINO and MINO/R cells performed on 24-cm gel strips, pH 4.0–7.0 and 10% SDS-PAGE stained with Coomassie Brilliant Blue. Differentially expressed proteins are indicated by numbered arrows (spots 1–3 indicate downregulated proteins and spots 4–7 indicate upregulated proteins in HBL-2/R cells).*

Table 3.2. *List of differentially expressed in proteins MINO/R cells (minimal 1.5-fold change and statistical significance $p<0.05$).*

Spot no.	Uniprot accession	Protein name	Fold change	Mascot score	Sequence coverage (%)	Molecular weight
Proteins downregulated in MINO/R cells						
1	P27707	Deoxycytidine kinase	4.6	44*	16	30841
2	Q99829	Copine-1	4.3	102	17	59649
3	P13796	Plastin-2	2	453	65	70814
Proteins upregulated in MINO/R cells						
4	P07741	Adenine phosphoribosyltransferase	5	70	40	19766
5	P68363	Tubulin α-1B chain	5	169	32	50804
6	P04792	Heat shock protein β-1	2.3	73	32	22826
7	P31937	3-Hydroxyisobutyrate dehydrogenase	2.1	43*	8	35712

* Identity of proteins with low Mascot score was verified by MS/MS:

Spot no.	Uniprot accession	Protein name	Peptide sequences	Mascot score
1	P27707	Deoxycytidine kinase	LKDAEKPVLFFER QLCEDWEVVPEPVAR	41 46
2	P31937	3-Hydroxyisobutyrate dehydrogenase	DFSSVFQFLREEETF SPILLGSLAHQIYR	49 28

In parallel with the proteomic analysis, transcriptome profiling using Illumina BeadChips was performed for each of the five MCL cell lines and their cytarabine-resistant subclones. Only one gene, *DCK* (coding dCK) was consistently differentially expressed (downregulated) in all of the cell lines. The massive downregulation of dCK, identified in our proteomic analysis was further verified using Western blots in all five cell lines and their resistant subclones, and its expression was found to be under the limit of detection in four of the resistant subclones and several-fold downregulated in the remaining one (see Figure 3.12).

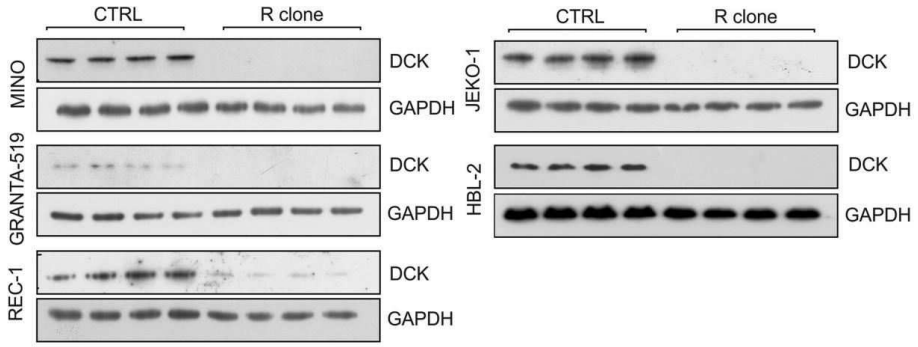

Figure 3.12. *Western blot verification of the marked downregulation of dCK in all R-subclones. GAPDH was used as the loading control.*

The fact that the downregulation of dCK (or the complete loss of its expression) was the only change observed on both the transcript and protein levels and consistently in multiple MCL cell lines led us to conclude that the downregulation of dCK is the causal mechanism of resistance in MCL cells. dCK is the enzyme responsible for the activation of cytarabine and other purine and pyrimidine nucleoside analogs, which also explains the observed cross-resistance of all five cytarabine resistant subclones to both purine and pyrimidine nucleoside analogs *in vitro* and *in vivo*. This cross-resistance concurrently supports our assumption that the downregulation of dCK is the causal mechanism of cytarabine resistance in our MCL model.

3.2.5 DCK expression in primary cells

In order to verify whether the acquired cytarabine resistance is also associated with the downregulation of dCK in human patients, we analyzed the expression of dCK protein and transcript levels in primary patient cells.

Primary MCL cells from ten patients were obtained by isolation of CD19 positive cells from peripheral blood, pleural effusion or lymph node samples at diagnosis (D1-10) and at relapse after failure of high-dose cytarabine based treatment (R1-8) or after 14 days of administration to patients refractory to cytarabine treatment (R9-10). The samples were analyzed by real-time RT PCR and by Western blot. In five cases (R2, R3, R4, R7, R9), downregulation of *DCK* was observed on the transcript level. Downregulation of dCK was confirmed by Western blots in samples R2 and R9. One sample (R6) revealed the downregulation of dCK only on the protein level (see Figure 3.13). The observed downregulation of dCK in several primary cell samples from patients resistant or refractory to cytarabine treatment is evidence that the downregulation of dCK

occurs in the clinical setting in response to cytarabine treatment. This further indicates that the probable mechanism of resistance to cytarabine is the downregulation of dCK.

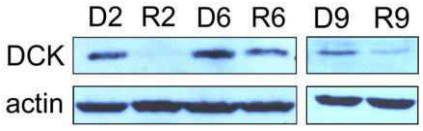

Figure 3.13. *Relative expression of DCK in post-treatment primary MCL samples (R2, R6, R9) compared to pre-treatment samples (D2, D6, D9). Actin was used as the loading control.*

3.2.6 Discussion

We analyzed the molecular changes associated with cytarabine resistance in five MCL cell lines. We observed cross-resistance to the nucleoside analogs gemcitabine, fludarabine and cladribine in cytarabine-resistant MCL cells, while sensitivity towards other classes of anti-lymphoma drugs remained unchanged. The cross-resistance to nucleoside analogs and the retained sensitivity towards other therapeutic molecules was confirmed by the mouse xenograft model *in vivo*. The retained sensitivity to all other types of anticancer drugs suggests that the resistance is not caused by pro-survival processes, such as avoiding apoptosis. Most importantly, together with the retained sensitivity to most types of drugs, the observed cross-resistance to antinucleosides indicates a nucleoside-specific mechanism of drug resistance.

Proteomic analysis using 2-D electrophoresis identified dCK as one of the most significantly downregulated proteins in the cytarabine resistant cell line MINO/R. Transcriptomic analysis revealed markedly lowered expression of *DCK* in five cytarabine resistant MCL cell line subclones. The downregulation of dCK was further confirmed by Western blots of all five cytarabine resistant subclones. dCK catalyzes the first phosphorylation of nucleosides and nucleoside analogs, leading to their activation from a pro-drug to active drug form. This is a rate-limiting step in the activation of dCK. dCK possesses low substrate specificity, which allows it to phosphorylate both pyrimidine and purine nucleosides, as well as nucleoside analogs (Arnér & Eriksson, 1995). This explains the observed cross-resistance to all tested antinucleoside drugs. Moreover, downregulation of dCK has been previously shown to be a causal mechanism of resistance to another cytidine analog, decitabine (5-aza-2′-deoxycytidine, Qin *et al.*, 2009).

Analysis of primary MCL samples was performed in order to verify whether downregulation of dCK occurs in response to a cytarabine-based regimen in clinical settings. We observed significant downregulation of *DCK* in 50% of samples obtained from patients who relapsed after or progressed on cytarabine-based treatment.

Taken together, our results indicate that patients with cytarabine-resistant MCL should not be treated with pyrimidine nor purine analogs, because the lowered expression of dCK is likely the molecular mechanism of resistance to cytarabine and cross-resistance to other antinucleoside drugs. Instead, other types of anti-cancer drugs should be used, such as alkylating agents (e.g. bendamustine) or targeted drugs recently approved for the treatment of relapsed/refractory MCL: bortezomib, ibrutinib and temsirolimus.

The results of this work were published in:

Downregulation of deoxycytidine kinase in cytarabine-resistant mantle cell lymphoma cells confers cross-resistance to nucleoside analogs gemcitabine, fludarabine and cladribine, but not to other classes of anti-lymphoma agents. Klánová M, Lorková L, Vít O, Maswabi B, Molinský J, Pospíšilová J, Vočková P, Mavis C, Latečková L, Kulvait V, Vejmělková D, Jaksa R, Hernandez F, Trněný M, Vokurka M, Petrák J, Klener P Jr. *Molecular Cancer.* 2014;13:159 (IF 2014: 4.257).

(See Appendix 2.)

3.3 Functional and proteomic analysis of fludarabine resistant MCL cells

In the work described in previous chapter, we showed that the downregulation of dCK is the likely mechanism of the resistance to pyrimidine antimetabolite cytarabine in MCL cells. Because the mechanism of resistance to other structurally distinct nucleoside antimetabolites can be entirely different, in our next study we analyzed the molecular changes associated with resistance of MCL cells to the purine nucleoside analog fludarabine. Fludarabine (2-fluoroadenosine arabinoside, see Figure 3.14) is being widely used for the salvage therapy of relapsed/refractory MCL (Forstpointner *et al.*, 2004, Johnson *et al.*, 2004).

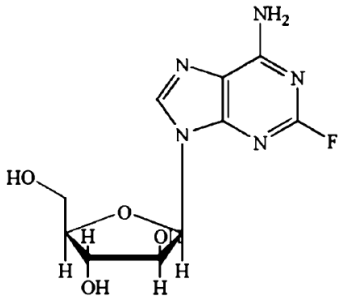

Figure 3.14. *Chemical structure of adenosine analog fludarabine (dephosphorylated form). Taken from Zhang et al., 2007*[CMR].

Fludarabine is administered in the form of a monophosphate prodrug. Upon administration, it undergoes dephosphorylation in vivo (Gandhi & Plunkett, 2002) and is then transported into the cells by equilibrative nucleoside transporters, mainly ENT1 (Molina-Arcas *et al.*, 2003). Similarly to cytarabine, its metabolic activation is carried out by phosphorylation by dCK (Danhauser *et al.*, 1986). This is the rate-limiting step for the formation of fludarabine triphosphate (F-ara-ATP). F-ara-ATP directly inhibits DNA polymerases and is incorporated into the DNA strand. Incorporation of F-ara-ATP into DNA results in chain termination, replication fork stalling, and DNA breaks. The replication stress activates DNA damage response, resulting in either DNA repair or apoptosis (Gandhi & Plunkett, 2002, de Campos-Nebel *et al.*, 2008). Fludarabine also directly inhibits ribonucleotide reductase, which leads to lowered cellular dNTP pools and increasing the fludarabine:dNTPs ratio (Gandhi & Plunkett, 2002).

Fludarabine-based regimens are mainly used for the first-line therapy of chronic lymphocytic leukemia (CLL) and for salvage therapy of indolent lymphomas (Lukenbill & Kalaycio 2013)

and acute myelogeneous leukemias (AML). Acquired resistance to fludarabine is unfortunately common. Its mechanisms in lymphomas are, however, largely unknown. Several studies have reported various molecules mutated or deregulated in association with inherent or acquired resistance to fludarabine in leukemic cells (CLL, AML), including molecules/genes involved in the nucleotide salvage pathway (dCK, nucleotide transporters, ribonucleotide reductase) (Månsson *et al.*, 2003, Mackey *et al.*, 2005), the antiapoptotic molecules BIRC3 and Bcl-2 family proteins (Rossi *et al.*, 2012, Sharma *et al.*, 2013, Messina *et al.*, 2014), the transcription factors Myc and Notch 1 (Moussay *et al.*, 2010, Messina *et al.*, 2014), the mediators of genotoxic stress ATM, p53 and SF3B1 (Austen *et al.*, 2007, Zenz *et al.*, 2009, Messina *et al.*, 2014) and others. Molecular mechanisms of fludarabine resistance may therefore vary to a great extent in different types of cancer. The molecular mechanisms of fludarabine resistance in MCL have not been studied so far.

The goal of this work was to 1) identify the mechanism of fludarabine resistance, 2) to obtain as much information about the molecular changes in fludarabine resistant cells as possible, and based on the obtained information to suggest optimal strategies for the elimination of fludarabine-resistant MCL cells. We derived fludarabine resistant subclones of MCL cells and subjected them to detailed large-scale semi-quantitative SILAC-based proteomic analysis to describe causative, contributing and compensatory molecular changes associated with fludarabine resistance in cellular model of MCL.

3.3.1 Derivation of a fludarabine-resistant cell line and assessment of sensitivity to other drugs

For our study of fludarabine resistance in MCL, we employed an established model of MCL – the cell line MINO. This cell line is sensitive to fludarabine exposure, with a LD_{100} of approximately 1-2 µM. The cells were grown in the presence of increasing doses of fludarabine to derive fludarabine-resistant MINO/FR cells. The derived subclone proliferated in medium with 100 µM fludarabine (see Figure 3.15 A). We performed cytotoxicity tests using a panel of clinically used drugs in order to assess the sensitivity to several drug classes.

The MINO/FR subclone displayed cross-resistance to all three tested nucleoside analogs: purine-derived cladribine and pyrimidine-derived cytarabine and gemcitabine (see Figure 3.15 B-D). In addition, MINO/FR cells showed to be significantly resistant to ibrutinib (a Bruton tyrosine kinase inhibitor, see Figure 3.21 E) and slightly less sensitive to methotrexate (anti-folate, see Figure 3.21 J). The sensitivity to other tested anti-tumor drugs was comparable to the original MINO cells or slightly higher (see Figure 3.15 F-I).

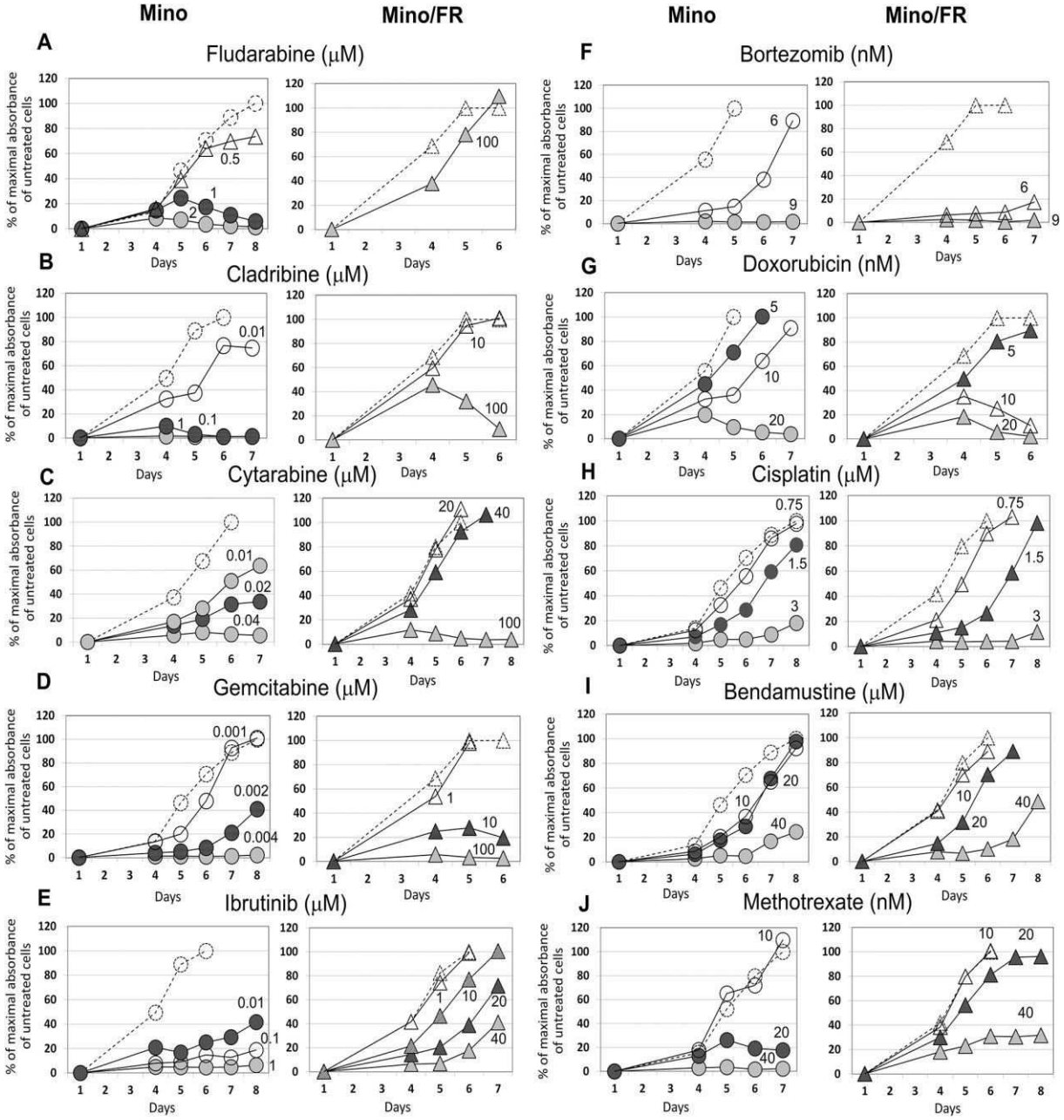

Figure 3.15. *Proliferation curves (determined by the WST-8 cell proliferation assay) of MINO and MINO/FR cells in the presence of fludarabine, cladribine, cytarabine, gemcitabine, ibrutinib, bortezomib, doxorubicin, cisplatin, bendamustine, and methotrexate in media (full lines). Controls (dashed lines) are cells without any anti-cancer agents in the media.*

This data may indicate multiple deregulated metabolic and signaling pathways associated with the acquired fludarabine resistance. The distinct cross-resistance of MINO/FR cells to purine and pyrimidine antinucleosides suggests that the resistance is caused by a nucleoside-specific mechanism similarly to in our previous work (chapter 3.2). The observed resistance to ibrutinib (an inhibitor of Bruton tyrosine kinase) may suggest a deregulation of B-cell receptor (BCR) signaling in MINO/FR cells (further discussed in chapter 3.3.6).

3.3.2 Quantitative proteomic analysis of fludarabine sensitive and resistant cell lines

In order to identify the changes in protein expression associated with the development of fludarabine resistance, we performed a large-scale quantitative proteomic analysis of MINO versus MINO/FR cells. We employed stable isotope labeling in cell culture (SILAC, Ong *et al.*, 2002). The cells were supplemented with ^{13}C and ^{15}N-labeled arginine and lysine (heavy medium), or standard unlabeled amino acids (light medium). To provide sufficient robustness of the analysis, we set up two experiments. The experiment where MINO cells were grown in heavy medium and MINO/FR cells in light medium was designated “forward”, and vice versa, MINO cells grown in light medium and MINO/FR in heavy medium was denoted “reverse”.

The identical amounts of heavy and light cells in each of the forward and reverse experiments were mixed, and whole cell lysates were subjected to filter-aided sample preparation (FASP, Wiśniewski *et al.*, 2009$^{\text{Nat Methods}}$) for detergent removal, reduction, alkylation and digestion. Resulting peptide samples were analyzed by LC-MS/MS using nano UHPLC coupled to a quadrupole Orbitrap Q Exactive plus mass spectrometer. Proteome Discoverer v. 1.4 software was used for protein identification and quantification. Quantitative analysis was based on the area under curve of the peptide precursors and the protein ratio was calculated as the median of peptide ratios, only unique peptides being considered.

We identified 1942 and 1700 proteins in forward and reverse experiments, respectively, 1377 of which were identified in both analyses. For the quantitative analysis, we considered 1201 proteins, which were detected with at least 3 SILAC pairs and with a variability of protein ratios below 40% in both (forward and reverse) experiments. The expression ratios in the forward and reverse experiments were highly correlated (see Figure 3.16), which indicates a high reproducibility of the used quantitative approach. 152 proteins were found to be downregulated and 160 upregulated with a fold change of at least 1.5 (see Table 3.3). We subjected the differentially expressed proteins to functional annotation using the Kyoto Encyclopedia of Genes and Genomes (KEGG) via Database for Annotation, Visualization and Integrated Discovery (DAVID) to identify the cellular

processes most affected by fludarabine resistance. DNA replication and repair (mismatch repair and nucleotide excision repair), purine and pyrimidine metabolism and aminoacyl tRNA biosynthesis among upregulated proteins and fatty acid metabolism, glutathione metabolism and adherens junctions among downregulated proteins were the most enriched annotations.

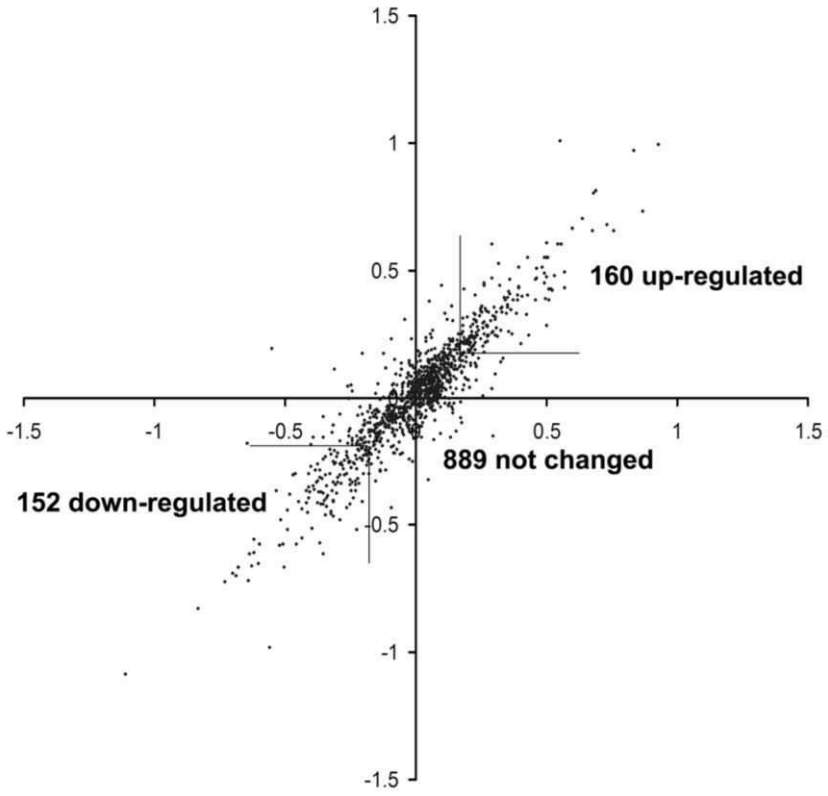

Figure 3.16. *Correlation of protein expression ratios in forward and reverse SILAC experiments. Log values of Heavy/Light protein ratios from the forward experiment were plotted against log values of Light/Heavy protein ratios from the reverse labeling experiment.*

Table 3.3. *Differentially expressed proteins in MINO/FR cells with a fold change of at least 1.5. Gene names are shown, proteins with a fold change >3 are highlighted.*

Proteins upregulated in MINO/FR cells	
DNA replication and repair	FANCI, LIG1, MCM2, MCM3, MCM4, MCM5, MCM6, MCM7, MSH2, MSH6, NCAPD2, NCAPD3, NCAPG, NCAPH, PARP1, PDE12, RFC2, RFC3, **RFC4**, RFC5, RUVBL1, RUVBL2, SMC2, SMC4
Purine and pyrimidine metabolism	**ADA**, CTPS1, GMPS, HPRT1, IMPDH2, PNP, **RRM2**, UMPS, TYMS
Aminoacyl tRNA biosynthesis	CARS, DARS, GARS, EPRS, IARS, LARS, MARS, NARS, YARS
Other processes	ABCF1, ABCF3, **ACAD9**, ACLY, ACO2, ADRBK1, ALDH5A1, **ALOX5**, ANP32B, AP2M1, APEH, ATG3, ATP1A1, ATP1B3, ATP6V1C1, ATXN10, **BCL2**, **BLVRA**, CD2AP, CKAP5, CLPTM1L, COBRA1, CPNE1, **CPNE3**, CUL1, CYB5R3, **DCUN1D1**, DCXR, DDX17, DHCR24, DHCR7, **DHRS7B**, DHX30, DNAJC2, DNMT1, EEF1E1, EHD1, EIF2A, **EIF4A2**, EIF4E, EIF4G1, ERLIN1, ERO1L, ERP44, EXOSC7, **EZR**, FAM105B, FAM162A, FAM213A, FASN, FDFT1, FKBP5, **FXR1**, GAPVD1, GNA13, GNL1, GNL3, GOT1, **GRHPR**, GYG1, HEATR2, HMGB2, HNRNPD, HS2ST1, HSPA14, KHSRP, KIF11, KNTC1, KPNA2, **LBR**, LRMP, LSS, MYH10, NAA25, NAP1L4, NDUFAF4, NUP210, PA2G4, PAICS, PDCD6IP, PFKM, PFKP, **PHGDH**, PLCG2, PPM1G, PPP2R4, PRDX6, **PSAT1**, PSMD5, PSMG2, PTBP1, PTPRC, PTPRCAP, RAB7A, RRAS2, SBDS, SEC11C, SEC24A, SET, SFXN1, **SLC1A4**, SLC1A5, SLC25A1, SLC2A1, SRPR, ST13, **TPD52**, TRIP13, TROVE2, TUBA4A, TUBB4B, TUBGCP2, UBE2E1, VPRBP, XPNPEP1, XPO7, XPOT, ZW10
Proteins downregulated in MINO/FR cells	
Fatty acid metabolism	ACAA2, **ACADVL**, **ACOT1** ACSL4, CPT2, HADHB
Glutathione metabolism	GSTK1, **GSTP1**, **G6PD**, IDH2, PGD
CD molecules	CD20 (MS4A1), CD38, **CD43**, **CD70**, **CD74**
Adherens junctions	CSNK2A2, MAPK1, PTPN1, **PTPN6**, SMAD3
Other processes	ALG5, ANXA2, APMAP, ARHGAP1, ARHGAP17, ARHGAP4, ARHGEF2, **ARL6IP5**, ARL8B, ASCC2, ATAD1, ATP2A3, ATPAF2, AUP1, BAX, **BCAP31**, BCAT2, **BTK**, CFA20, C1QBP, **CNDP2**, COPG2, CSTF3, CTPS2, DAGLB, **DCK**, DDX24, DDX3X, DKC1, DLST, DNAJA2, EIF4A1, EIF5A, ELMO1, EML4, FAM129C, FAM3C, FBXO7, FLAD1, **FLNA**, GBE1, GFPT1, GLOD4, GNPDA1, GOT2, HIST1H2AH, HIST1H2BK, HIST1H4A, HM13, HMGB3, HSP90B1, HSPH1, **ICAM1**, ICAM3, IER3IP1, IGF2BP3, INPP5D, IQSEC1, ITPR2, KPNA3, LTA4H, LRRFIP1, M6PR, MAT2A, ME2, MPDU1, MSN, MTA2, MYBBP1A, **NAGK**, NDUFA13, NDUFA9, NDUFB8, NDUFS1, NEK9, NLN, NRD1, NUDT19, MOB1B, OGDH, PDIA4, PEPD, PFAS, PGRMC1, POLR2B, POR, PPCS, PPIB, PRMT1,PRPF6, PRPSAP2, PSAP, PSME1, PSME2, PSMF1, PTPN2, PUS1, RASAL3, RNH1, **ROCK1**, RUFY1, SCRIB, SEC23IP, SEPT9, SLC25A5, SLC25A6, SLC38A5, SND1, SNRNP200, SRP54, STK4, TDP1, TMED4, TMX3, TOM1, TPM3, TPP2, TRMT6, TSR1, **TST**, **TSTA3**, UBLCP1, VARS, VAT1, VPS13C, VPS26A,VPS35, WDR1, XPO5, ZMPSTE24

Expression changes of selected proteins with marked (>5 fold) differential expression were verified. Downregulation of dCK, protein tyrosine phosphatase non-receptor type 6 (PTPN6, alias Src homology region 2 domain-containing phosphatase-1 – SHP-1) and upregulation of proteins B-cell lymphoma 2 (Bcl-2) and phosphoserine aminotransferase 1 (PSAT-1) was verified using Western blot (see Figure 3.17 A). In addition, downregulation of CD20 and CD38 surface markers was confirmed by flow cytometry (see Figure 3.17 B).

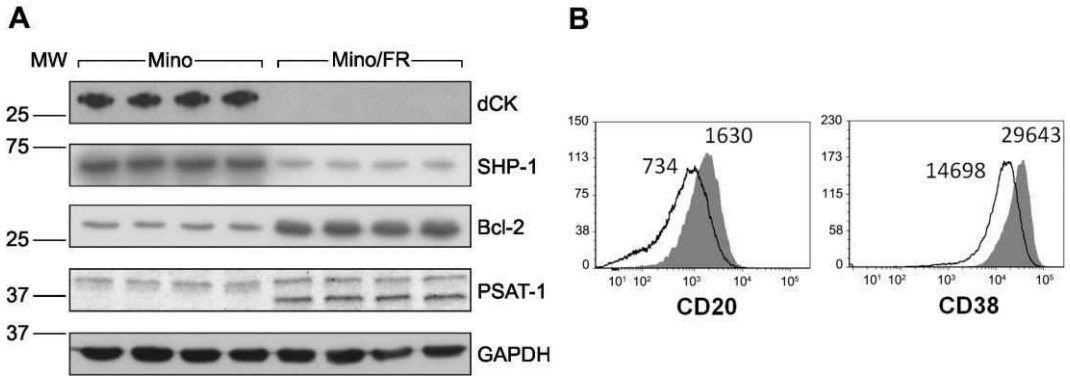

Figure 3.17. *Verification of differential expression of the key proteins identified by our proteomic analysis.* ***A.*** *Relative expression of four differentially expressed proteins - dCK, SHP-1 (alias PTPN6), Bcl-2 and PSAT-1 in MINO and MINO/FR cells determined by Western blots. GAPDH was used as a loading control.* ***B.*** *Relative expression of CD20 and CD38 determined by flow cytometry. Open histograms represent MINO/FR cells, full histograms show MINO cells. Decreased median fluorescence intensity indicate approximately 2-fold decreased expression of CD20 and CD38 in MINO/FR cells.*

3.3.3 Purine and pyrimidine metabolism

The utilization of a shotgun quantitative proteomic approach allowed us to observe 312 differentially expressed proteins. This analysis provided a detailed snapshot of the molecular changes associated with fludarabine resistance in MCL cells. Several-fold downregulation of dCK was one of the most prominent changes detected in our analysis.

In our previous work discussed in chapter 3.2, we showed that downregulation of dCK is responsible for the resistance to cytarabine in MCL cells, and for cross-resistance of the cytarabine-resistant cells to other nucleoside antimetabolites, including purine-derived fludarabine. dCK phosphorylates and thus activates both pyrimidine and purine nucleosides and nucleoside analogs including fludarabine (Månsson *et al*., 2003). The downregulation of dCK

has been previously shown as a mechanism of fludarabine resistance in leukemia cells (Bai *et al*., 1998, Månsson *et al.*, 2003). The massive downregulation detected in our analysis is therefore most likely the critical change responsible for fludarabine resistance in our MCL model.

Rapidly proliferating leukemia and lymphoma cells typically exploit the nucleotide salvage pathway to supply the needed high amounts of nucleosides (Natsumeda *et al.*, 1984). However, we detected the upregulation of numerous enzymes of *de novo* synthesis and nucleoside interconversion: GMP synthase, CTP synthase 1, inosine-5'-monophosphate dehydrogenase, uridine-5'-monophosphate synthase, purine nucleoside phosphorylase, adenosine deaminase, purine nucleoside phosphorylase, thymidilate synthase, and ribonucleoide reductase subunit M2.

In addition to the enzymes directly involved in nucleoside metabolism, the strong upregulation of two enzymes of the serine biosynthesis pathway, D-3-phosphoglycerate dehydrogenase (PHGDH) and PSAT-1, can be linked to nucleotide *de novo* biosynthesis, since serine is essential as a source of carbon moieties in the folate cycle (Tedeschi *et al.*, 2013). This is further supported by the observed upregulation of neutral amino acid transporters A and B (SLC1A4 and SLC1A5), which among others transport serine.

Aside from preventing antinucleotide drug toxicity, the downregulation (or even absence) of dCK makes the utilization of natural nucleosides from the environment impossible and thus leads to dependence on de novo nucleotide synthesis (Natsumeda *et al.*, 1984, Austin *et al.*, 2012). The upregulation of numerous enzymes of nucleoside metabolism and other proteins, mentioned above, may reflect the increased demand for deoxyribonucleotide (dNTP) synthesis after the loss of dCK.

3.3.4 Anti-apoptotic changes

The ultimate consequence of fludarabine toxicity is DNA damage. The upregulation of the enzymes of DNA replication and repair in our study seems to reflect this, leading presumably to averting apoptosis by increasing the efficiency of DNA repair. Furthermore, replication stress caused by the shortage of dNTPs can cause their misincorporation into DNA and the need for a DNA damage response (Austin *et al.*, 2012). Among the proteins known to contribute to DNA repair, we identified the upregulated poly(ADP-ribose) polymerase 1, all five subunits of the condensin I protein complex, Fanconi anemia group I protein (FANCI), the DNA replication licensing factors MCM2, MCM3, MCM4 MCM5, MCM6 and MCM7, Nek9 ligase, replication factor C subunits 2, 3, 4 and 5, pontin, reptin, and DNA ligase 1.

In addition to the stimulation of the DNA repair, the most prominent anti-apoptotic change we observed was the strong upregulation of the negative regulator of apoptosis Bcl-2 in MINO/FR cells. Its upregulation is a common mechanism of avoiding apoptosis in drug resistant cancer cells (Reed 1997). Our results also showed downregulation of the Bcl-2 antagonist Bax (Oltvai *et al.*, 1993), which suggests a coordinated deregulation of protein expression in a pro-survival and anti-apoptotic direction in MINO/FR cells. Because the upregulation of Bcl-2 represents a potential therapeutic target, we decided to test the sensitivity of MINO/FR cells to inhibition of Bcl-2.

3.3.5 The effect of Bcl-2 inhibition on fludarabine and cytarabine-resistant cells

Several inhibitors of Bcl-2 have been developed and are being clinically tested. One of them, ABT-199, has been tested in a wide range of B-cell malignancies and showed promising results in chronic lymphocytic leukemia (Souers *et al.*, 2013) and MCL (Saba & Wiestner, 2014). We therefore tested the relative toxicity of ABT-199 in MINO and MINO/FR cells to evaluate its potential for the therapy of anti-nucleoside-resistant MCL. In MINO/FR cells, we observed markedly increased sensitivity to ABT-199 compared to the original MINO cell line (100-fold: 1 μM in MINO cells, 0.01 μM in MINO/FR, see Figure 3.18). Furthermore, to show that this change in sensitivity is not exclusive to fludarabine resistant cells, we also evaluated ABT-199 cytotoxicity in the REC-1 cell line and its cytarabine resistant sub-clone REC-1/R (cross-resistant to fludarabine) derived and characterized earlier (see chapter 3.2.1). We found that REC-1/R also overexpress Bcl-2 and is more sensitive to ABT199 (see Figure 3.19). These results suggest that ABT-199 has a high potential for the therapy of both fludarabine- and cytarabine-resistant MCL.

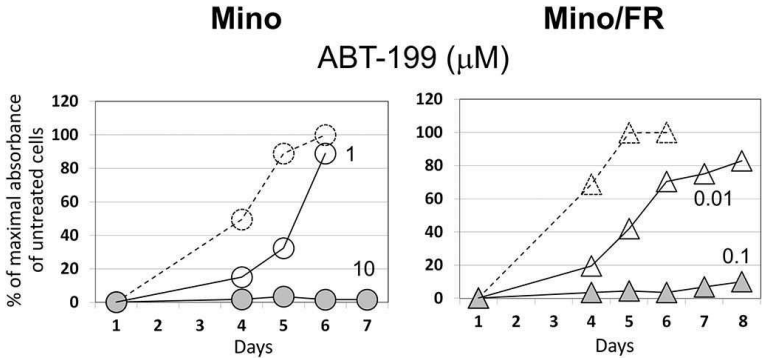

Figure 3.18. *Proliferation curves (determined by the WST-8 cell proliferation assay) of MINO and MINO/FR cells in the presence of the indicated concentrations of the Bcl-2 inhibitor ABT-199 in the media (full lines). Controls (dashed lines) are cells without the inhibitor in the media.*

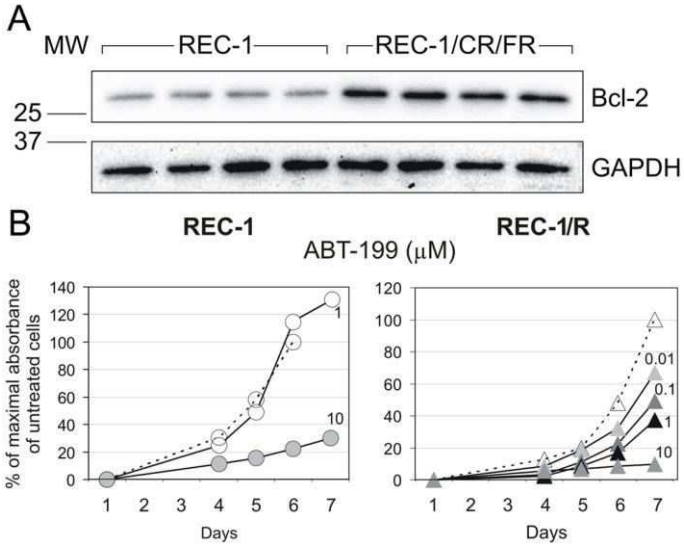

Figure 3.19. A. *Expression of Bcl-2 in REC-1 and REC-1/R cells determined by Western blots. GAPDH was used as the loading control.* ***B.*** *Proliferation curves (determined by the WST-8 cell proliferation assay) of REC-1 and REC-1/R cells in the presence of the indicated concentrations of Bcl-2 inhibitor ABT-199 in the media (full lines). Controls (dashed lines) are cells grown without the inhibitor in the media.*

3.3.6 BTK and ibrutinib resistance in MINO/FR cells

Our initial cytotoxicity tests showed significant cross-resistance of MINO/FR cells to the inhibitor of Bruton tyrosine kinase (BTK) ibrutinib (see chapter 3.3.1 and Figure 3.15 E). BTK is a key component of B-cell receptor (BCR) signaling, which is crucial to proliferation during B-cell development (Satterthwaite & Witte, 2000) and has been implicated in the pathogenesis of B-cell malignancies including MCL (Jares *et al*., 2012). In response to BCR stimulation, BTK is phosphorylated and in turn phosphorylates phospholipase C gamma 2. This leads to the activation of several signaling pathways that promote cell survival and proliferation, including NF-κB, mTOR and MAP kinase pathways (Kurosaki & Hikida, 2009).

Importantly, in our proteomic analysis, BTK was identified among the proteins substantially downregulated in MINO/FR cells. Ibrutinib was recently approved for the therapy of relapsed/refractory mantle cell lymphoma (Wang *et al*., 2013). We therefore verified both total and activated (phoshpo-BTK^{Y233}) BTK levels in MINO and MINO/FR cells using Western blotting (see Figure 3.20). BTK expression and p-BTK levels were markedly decreased in MINO/FR cells, clearly indicating the disruption of BCR signaling in MINO/FR cells. This provides a mechanistic explanation for the observed resistance of MINO/FR cells to ibrutinib.

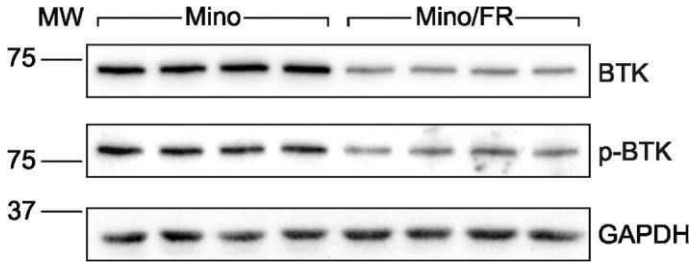

Figure 3.20. *Relative expression of total and phosphorylated (active) p-BTK233 was determined by Western blotting using specific antibodies in MINO and MINO/FR cells. GAPDH was used as the loading control.*

In addition to BTK, we also observed downregulation of other proteins involved in BCR signaling – PTPN6 (SHP-1, Cyster & Goodnow, 1995) and phosphatidylinositol 3,4,5-triphosphate 5-phosphatase 1 (SHIP-1, Chacko *et al*., 1996), and also MAPK kinase, a downstream effector of BCR signaling.

3.3.7 Changes in the expression of CD20 and other surface antigens

We identified five leukocyte surface CD (cluster of differentiation) antigens downregulated in MINO/FR cells, namely B-lymphocyte antigen CD20, CD38 (ADP-ribosyl cyclase), CD43 (leukosialin), CD70 antigen and CD74 (HLA class II histocompatibility antigen γ chain). No CD antigens were among the proteins upregulated in MINO/FR cells. Loss of the CD antigens in the resistant cells may be specific to the development of resistance and/or may reflect a shift of the resistant lymphoma cells toward differently matured B-cell phenotype. A lowered expression of CD molecules may theoretically limit the efficacy of therapeutic antibodies, namely rituximab (anti-CD20), used in lymphoma therapy.

3.3.8 Summary

In this work, we observed a **substantial cross-resistance of MINO/FR cells to purine and pyrimidine nucleoside antimetabolites**. Importantly, we identified a **massive downregulation of dCK in the fludarabine-resistant MCL cells**. As discussed in chapter 3.2, dCK is responsible for the activation of both pyrimidine and purine nucleosides and nucleoside analogs including fludarabine (Månsson *et al*., 2003) and its downregulation was previously shown to be the mechanism of fludarabine resistance in leukemia cells (Bai *et al*., 1998, Månsson *et al*., 2003). **Our work further underlies the downregulation of dCK as a key mechanism of**

antinucleoside drug resistance, and provides evidence for this mechanism of resistance in MCL cells.

Besides limiting the activation of fludarabine and other antinucleosides, the downregulation/loss of dCK also inevitably limits the supply of natural deoxynucleotides. This may lead to replication stress and activation of a DNA-damage response (Austin *et al.*, 2012). In our study, we observed the upregulation of numerous proteins involved in DNA repair. Other prominent anti-apoptotic changes identified were the upregulation of Bcl-2 and a decrease of Bax expression, and therefore a decrease of the Bax/Bcl-2 ratio in MINO/FR cells. Importantly, **the upregulation of Bcl-2 makes this regulatory protein a potential therapeutic target for fludarabine-resistant MCL cells, as demonstrated by the increased sensitivity of the MINO/FR cells towards the Bcl-2 inhibitor ABT-199**.

Among others, we also detected changes that may well result in the loss of sensitivity towards other drugs. **Downregulation of CD20 may limit the efficacy of the chimeric anti-CD20 monoclonal antibody rituximab** used in lymphoma therapy. Furthermore, **the strong downregulation of BTK and resultant loss of sensitivity of the fludarabine resistant cells to the BTK inhibitor ibrutinib** suggests deregulation of B-cell receptor (BCR) signaling in MINO/FR cells. The key changes observed in fludarabine-resistant MINO/FR cells are summarized in Figure 3.20.

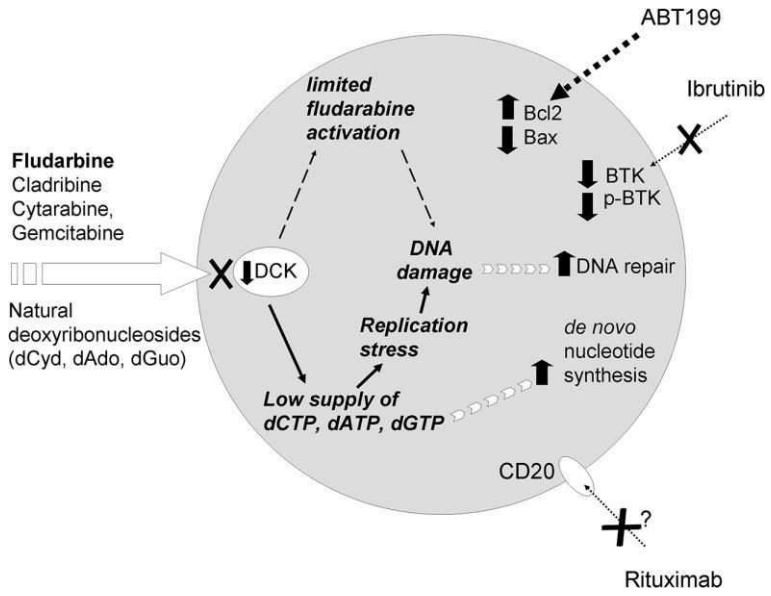

Figure 3.20. *Summary of the processes associated with fludarabine resistance in MINO/FR cells observed in our analyses. Details in the text.*

Taken together, this work provides evidence that the downregulation of dCK is the likely mechanism of the resistance of MCL cells to fludarabine and other antinucleoside drugs. The downregulation of BTK (associated with the decreased sensitivity of fludarabine-resistant cells to ibrutinib), the upregulation of Bcl-2 (responsible for an increased sensitivity to ABT-199) and the downregulation of CD20 (which may cause the loss of sensitivity to rituximab) are further valuable information that could be used for the prediction of optimal treatment strategies in patients who fail a fludarabine-based regimen.

Our analysis of a MCL model of acquired resistance to fludarabine thus provides a proof-of-concept that proteomics might be used in clinical settings for the prediction of optimal treatment strategies. The characterization of small populations of cancer cells from individual patients may allow proteomics to contribute to the formulation of individualized therapies in the near future.

The results of this work were published in:

Detailed functional and proteomic characterization of fludarabine resistance in mantle cell lymphoma cells. Lorkova L, Scigelova M, Arrey TN, Vit O, Pospisilova J, Doktorova E, Klanova M, Alam M, Vockova P, Maswabi B, Klener P Jr., Petrak J. *PLoS One.* 2015;10(8):e0135314 (IF 2015: 3.057).

(See Appendix 3.)

3.4 Conclusions to Section I

The exposure of cancer cells to cytotoxic drugs can lead to their adaptation and to the emergence of drug resistant cell populations. Depending on the drug's mechanism of action, the adaptation generally affects one or more cellular processes or pathways (metabolic, signaling or others). Some of the molecular changes are causal, some may contribute to the survival of the resistant cells, and some may be seemingly unrelated to the mechanism of resistance and represent complex secondary adaptive changes. These changes are specific for the resistant cells and can be therefore specifically targeted in order to eliminate such a resistant population. These specific changes may be considered a potential weakness – an “Achilles’ heel” – of such cells. Identification of such a specific feature or “weakness” may be exploited as a therapeutic target.

The works presented in chapters 3.1, 3.2 and 3.3 demonstrate that proteomics has the potential to describe the molecular “landscape” of drug resistance in cancer cell in detail, and reveal both causative changes and additional processes contributing to or associated with resistance. This gives us the in-depth view of the resistant cell biology, which is essential for therapy rationalization, optimization, and personalization.

Based on the proteomic analyses of both the cytarabine and fludarabine resistant MCL cells, we can reasonably conclude that the marked downregulation (or possibly even a total silencing) of dCK is the causative alteration responsible for the resistance in our MCL model and also in patient samples. The substrate promiscuity of dCK explains the cross-resistance of the resistant cells to the remaining purine- and pyrimidine-derived antinucleosides included in these studies. This provides a critical message for clinical practice: MCL patients who become unresponsive to antinucleoside-based therapy should not be treated with pyrimidine nor purine analogs. Instead, other types of anti-cancer drugs should be used.

Additionally, in the case of our fludarabine resistance study, we demonstrated that based on a detailed analysis we can, to some extent, predict the toxicity of various existing drugs, and thus help to prioritize which drug should be (ABT199) or should not be (ibrutinib) be used. In the clinical setting, such findings could be used for the prediction of optimal treatment strategies, in this instance for patients who fail a fludarabine-based regimen.

Our studies were based on cell culture models and their relevance for clinical practice is therefore limited. They nevertheless demonstrated that the information obtained from a proteomic analysis of a small biological sample can be used for the prediction of an appropriate therapeutic strategy.

In the clinical setting, lymphoma cells could be isolated from patients and analyzed in a similar manner. Although the standard SILAC used in our analysis of fludarabine resistant MCL cells is not applicable for patient samples, other quantitative proteomic methods, such as iTRAQ, super-SILAC or label-free analysis could be used. In this way, the analysis results could be used for patient-tailored therapy, i.e. the choice of an optimal treatment strategy based on the molecular profile of the disease, the patient's clinical profile and the pharmacological properties of the drug.

4 Section II: Proteomics of integral membrane proteins

The objective of the second part of this thesis was to develop and optimize a method for the proteomic analysis of integral membrane proteins and to perform inventarization of the membrane proteome of human MCL cells.

The works described in Section I of this thesis employed standard and well-established proteomic procedures. These techniques, especially the so-called “shotgun” methods, enable the identification of thousands of proteins in single sample. Unfortunately, not all proteins are well suited for the established proteomic methods. In fact, due to their different physical and chemical properties, integral membrane proteins (IMPs) are frequently omitted by these approaches. The following chapter 4.1, which is a concise version of our review (Vít & Petrák, 2017) summarizes the recent developments in the field of proteomics of integral membrane proteins.

4.1 Current proteomic approaches to the analysis of the membrane proteome

4.1.1 Properties of IMPs, obstacles for proteomic analysis

Integral membrane proteins (IMPs), i.e. proteins that cross the phospholipid bilayer, are coded by roughly a quarter of human genes (Fagerberg *et al.*, 2010) and represent about 7-8 % of all cellular protein mass in human cells (Nagaraj *et al.*, 2011). IMPs serve as transporters, channels, receptors, adhesion molecules and enzymes, and are responsible for signal transduction, regulatory processes and cell-cell and cell-environment interactions. This makes IMPs attractive targets for therapeutic molecules. In fact, approximately half of the currently approved drugs in human medicine target IMPs (Yildirim *et al.*, 2007).

IMPs can be divided into α-helical and β-barrel types. The latter are rare in eukaryotes and do not pose analytical difficulty, since they do not have long stretches of hydrophobic amino acids. Therefore, I further discuss only α-helical IMPs.

Standard proteomic approaches are unsuitable for α-helical IMPs and our knowledge of their expression dynamics and function is therefore vastly limited for three major reasons:

1) α-helical IMPs are amphipathic: they consist of hydrophilic extra-membrane segments and one or multiple hydrophobic α-helices that span the phospholipid bilayer. This amphipathy causes the insolubility of IMPs in aqueous buffers, which makes them difficult to analyze using standard proteomic approaches.

2) The charged amino acids lysine (K) and arginine (R) are rare in IMPs, which have numerous hydrophobic stretches in their sequences. K and R are indispensable for digestion with trypsin, the most widely used protease in conventional proteomic procedures. The hydrophilic extra-membrane segments are often of limited length and may not provide enough tryptic peptides for identification.

3) IMPs frequently exhibit low expression levels, which further complicates their analysis (Vuckovic *et al*. 2013).

These three obstacles, each to various extents for individual IMPs, together complicate the proteomic analyses of IMPs. 2-DE is not suitable for the analysis of IMPs at all, primarily due to their insolubility in running buffers used for IEF (Magdeldin *et al.*, 2014). While the “shotgun” approaches, e.g. with the use of FASP, has been declared to be unbiased towards membrane

proteins (Wiśniewski *et al.*, 2009[Nat Methods]), these approaches still predominantly use trypsin for digestion (2nd obstacle) and do not adequately address the low expression levels of many IMPs (3rd obstacle). Specific approaches that reflect the different physico-chemical properties of IMPs are therefore needed to access the membrane proteome.

Such approaches typically combine or include three specifically designed steps, namely the enrichment of membrane material, solubilization of membrane proteins, and alternative digestion or cleavage strategies.

4.1.2 Enrichment of membrane material

Enrichment of membrane material is performed most often by differential centrifugation. However, regardless of the isolation complexity, the isolated "membrane enriched fraction" is inevitably contaminated by abundant soluble proteins. If not removed, these molecules later dominate the MS spectra and hamper the analysis of less-abundant IMPs. To further enrich IMPs, the membrane fractions are often "washed" with aqueous, high ionic strength buffers, typically high pH sodium carbonate washes (Fujiki *et al.*, 1982). Unfortunately, carbonate washing, or even some more vigorous methods such as high salt and trifluoroethanol washes, only partially remove non-membrane proteins from the membrane sample.

Current membrane proteomics uses two principal strategies that follow the enrichment of membrane material:

a) IMPs are solubilized with the help of a detergent or organic solvents and targeted as whole molecules.

b) The hydrophilic (extramembrane) or hydrophobic (transmembrane) segments of IMP are targeted separately or exclusively.

Detergents, organic solvents, chaotropes and alternative cleavage strategies that assist in the proteomic analyses of membrane proteins will be discussed in the following paragraphs.

4.1.3 Detergents in the proteomics of IMPs

Detergents are amphipathic molecules that mimic the properties of membrane phospholipids and therefore are capable of dissolving membranes and solubilizing IMPs. Various detergents differ in their solubilizing power and denaturing effects. On top of that, some inactivate trypsin and other proteases, interfere with chromatographic separation and/or suppress peptide ionization,

and contaminate mass spectrometers. Their removal prior to digestion or LC-MS analysis is therefore essential.

Sodium dodecyl sulfate (SDS) is one of the most widely used detergents in protein biochemistry. It is a strong ionic linear-chain detergent, and besides the effective solubilization of membranes and IMPs it also promotes protein denaturation (Reynolds *et al.*, 1970). Trypsin activity is limited in 0.1% SDS, however, and even lower concentrations can reduce the separation power of LC and hamper peptide ionization during MS analysis (Botelho *et al.*, 2010).

To remove SDS from a membrane sample, numerous methods have been developed, including effective filter assisted sample preparation (FASP). This method makes use of centrifugal ultrafilters with a 10-30 kDa cut-off to deplete small molecules including SDS and other detergents from a protein sample using 8 M urea washes, followed by on-filter sample digestion. FASP has been reported as being unbiased against hydrophobic proteins (Wiśniewski *et al.*, 2009$^{\text{Nat Methods}}$) and its potential for large scale proteomic analysis of membrane samples was demonstrated by the identification of over 1,600 IMPs in mouse hippocampal membranes (Wiśniewski *et al.*, 2009$^{\text{J Proteome Res}}$). More recently, the application of FASP and SDS in combination with extensive fractionation enabled the identification of 2,090 IMPs in human leukemic cell membranes (Yu *et al.*, 2012).

Although SDS has been the detergent of choice for the solubilization of IMPs, alternatives with simpler removal methods have been sought. **Sodium deoxycholate (SDC)** is an ionic detergent with a steroidal hydrophobic part and a charged carboxyl group. Compared to SDS, it is a less potent denaturant and solubilizing agent (Masuda *et al.*, 2008); nevertheless, it is highly compatible with trypsin, which tolerates SDC concentrations up to 5-10% (Masuda *et al.*, 2008, Lin *et al.*, 2008).

SDC can be removed by phase transfer into water-immiscible ethyl acetate (Masuda *et al.*, 2008) or, alternatively, by acid precipitation with trifluoroacetic or formic acid (Lin *et al.*, 2008). The use of SDC allowed the identification of nearly 2,000 IMPs in human breast tumor samples (Muraoka *et al.*, 2013) and over 1,500 IMPs in human colorectal cancer samples (Kume *et al.*, 2014).

To enable an even more straightforward removal prior to LC-MS, a novel class of detergents, **acid-labile surfactants (ALS),** has been developed. These detergents are cleaved by a low-pH environment at elevated temperature and their hydrophobic part precipitates, while the remaining part of the molecule is LC- and MS-compatible. RapiGest™ (Yu *et al.*, 2003) is currently the most widely used ALS. It effectively solubilizes membranes, while not limiting trypsin activity in

concentrations up to 1% (Yu *et al.*, 2003, Mbeunkui *et al.*, 2011). Although ALS are easy to remove and were shown to be comparably efficient when used side-by-side with SDS (Wu *et al.*, 2011[Anal Chim Acta], Sun *et al.*, 2012), ALS possess two limitations: 1) they are expensive compared to conventional detergents, 2) the loss of the most hydrophobic peptides has been reported, due to co-precipitation with the hydrophobic RapiGest fragment (Yu *et al.*, 2003, Masuda *et al.*, 2008).

4.1.4 Organic solvents in proteomics of IMPs

Organic solvents have mainly been used as an alternative to detergents in the "pre FASP" era to perform large-scale proteomic analyses of IMPs. Most commonly, methanol has been used as a co-solvent for IMP solubilization and digestion. In **60% methanol**, trypsin activity is reduced to one-fifth compared to aqueous buffer (Blonder *et al.*, 2004[Proteomics]) and its specificity may also decrease (Rietschel *et al.*, 2009[Mol Cell Proteomics]). Nevertheless, trypsin digestion assisted by sonication in 60% methanol enabled the identification of over 700 IMPs in murine macrophage membranes (Blonder *et al.*, 2004[J Proteome Res]). Similarly, **50% trifluoroethanol** has been used as an agent for the solubilization of membranes (Zhang *et al.*, 2007[Proteomics]) and delipidated IMPs (Ghosh *et al.*, 2010). However, a recent side-by-side comparison showed that the use of organic solvents is markedly inferior compared to detergents in terms of the total number of identified IMPs (Moore *et al.*, 2016).

Concentrated **formic acid** (FA) is an excellent solvent for the solubilization of membranes, hydrophobic proteins and peptides (Zhao *et al.*, 2013, Doucette *et al.*, 2014). It is, however, incompatible with most proteases including trypsin, and tends to generate uncontrolled damage to protein samples, e.g. D-P bond cleavage (Piszkiewicz *et al.*, 1970), and cause protein formylation (Loo *et al.*, 2007). This can, however, be prevented by working at low temperatures (Doucette *et al.*, 2014). Importantly, formic acid is an optimal solvent for the cleavage of proteins and peptides with cyanogen bromide (CNBr, see chapter 4.1.6) (Fischer *et al.*, 2006, Blackler *et al.*, 2008).

4.1.5 Chaotropes in the proteomics of IMPs

Chaotropes are used in proteomics for the disruption of protein-protein interactions and maintaining the unfolded state of proteins. Urea and guanidine hydrochloride are used most often. In contrast to detergents and organic solvents, chaotropes only denature proteins but do not solubilize membranes or IMPs. Their optimal concentrations for protein denaturation (6 M guanidine and 8 M urea) are, however, incompatible with reasonable trypsin activity, and lowering

of their concentrations leads to protein refolding (Dormeyer *et al.*, 2008, Mbeunkui *et al.*, 2011, Waas *et al.*, 2014).

The role of chaotropes in membrane proteomics cannot be dismissed, as endoprotease Lys-C remains active even at high urea concentrations. Digestion of a membrane sample with Lys-C in 6-8 M urea preceding the dilution of the chaotrope and sample re-digestion with trypsin has been shown to improve the identification and coverage of IMPs in complex samples, and has become one of the new standards in sample preparation (Dormeyer *et al.*, 2008, Lund *et al.*, 2009, Wiśniewski *et al.*, 2009[J Proteome Res], Wiśniewski & Mann, 2012). Digestion with Lys-C in 6-8 M urea facilitates the solubilization and digestion of extra-membrane domains of IMPs; however, it does not help to digest the long transmembrane segments that do not contain lysines.

4.1.6 Alternative cleavage strategies of IMPs

With the use of the novel or optimized solubilization strategies mentioned above, the number of identified IMPs and their sequence coverage can be improved. Unfortunately, however, only to a limited extent. Peptides of suitable size, compatible with LC-MS/MS, can be generated only with an appropriate cleavage agent. Trypsin is optimal for standard soluble protein sequences containing advantageous distributions of K and R residues (Ulmschneider *et al.*, 2005). In transmembrane segments of IMPs, however, these residues are scarce. The size of trypsin-cleavable portions of IMPs varies from proteins with large extracellular domains down to very short terminal or loop segments that may not provide enough sequence coverage for protein identification (Eichacker *et al.*, 2004, Sharpe *et al.*, 2010). Peptides containing a transmembrane α-helix are inevitably large (>30 amino acids) and highly hydrophobic, and may therefore adhere to plastic surfaces, get lost during sample preparation, be retained on LC columns or exceed the optimal mass for their efficient detection in MS. The use of different cleavage agents or their combination for a proteomic analysis of IMPs may therefore represent a solution to this problem.

Chymotrypsin cleaves peptide bonds following the large aromatic amino acids phenylalanine, tyrosine and tryptophan. It also cleaves (although with lower efficiency) after leucine and methionine, i.e. amino acids occurring frequently in the hydrophobic transmembrane segments of IMPs. Therefore, it has been suggested that digestion with chymotrypsin should be advantageous in the analysis of IMPs (Fischer & Poetsch, 2006). Chymotrypsin has, however, been used in only a limited number of technical studies and with varying results (Fischer *et al.*, 2006, Dormeyer *et* al., 2008, Fränzel *et al.*, 2009, Moore *et al.*, 2016).

Elastase cleaves at the C-terminal side of small neutral amino acids. It has been tested for use in the analysis of a bacterial membrane proteome and was found to allow the identification of IMPs based on transmembrane peptides (Rietschel *et al.*, 2009[Mol Cell Proteomics]).

Pepsin is a gastric enzyme active in an acidic environment. It cleaves mainly after aromatic (Y, F, W) and hydrophobic (L, A, G) residues (Han *et al.*, 2004, Rietschel *et al.*, 2009[Proteomics], López-Ferrer *et al.*, 2011). Its activity in acidic environments favors combination with FA, which has been shown to be a potent solvent for hydrophobic proteins, and this combination was demonstrated in Ma *et al.*, 2010. The sequential pepsin and trypsin digestion was shown as being beneficial, increasing the sequence coverage of IMPs compared to cleavage with trypsin only (Golizeh *et al.*, 2013).

Proteinase K is a nonspecific protease. It was used by Wu *et al.* to digest or "shave" the extra-membrane domains of IMPs (Wu *et* al., 2003). More importantly, the method was later extended to also include analysis of the hydrophobic transmembrane segments that remain protected from the protease activity by the phospholipid bilayer (Blackler *et al.*, 2008, see section 4.4).

The use of semi- or nonspecific proteases for the analysis of IMPs may seem advantageous, as it overcomes the relative scarcity of tryptic cleavage sites - lysines and arginines. It should be noted, however, that non-specifically cleaved peptides are usually more difficult to identify than tryptic peptides due to their poorer ionization and fragmentation, which is caused by the lack of defined positively charged C-termini. This also markedly increases the database search space, as more possible peptides fall within the precursor mass tolerance and thus increases the false positive rates (Gupta *et al.*, 2011).

In addition to the available proteases, non-enzymatic protein cleavage is a less frequently used alternative. **Cyanogen bromide (CNBr)** allows the sequence specific digestion of proteins in an acidic environment (usually 90% FA or 70% trifluoroacetic acid). It reacts with methionine and yields homoserine or homoserine lactone and an aminoacyl peptide fragment (see Figure 4.1) Compared to endoproteases, CNBr treatment is very robust, reaching 90–100% cleaved methionine sites with the exception of oxidized methionines (Gross & Witkop, 1962).

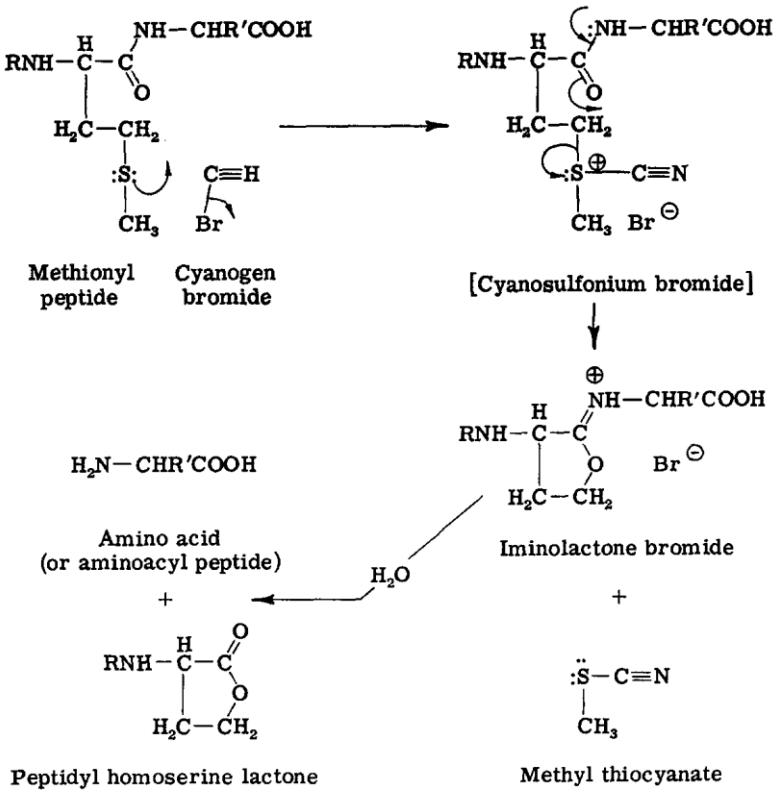

Figure 4.1. *The mode of action of CNBr. Taken from Gross, 1967.*

CNBr is a convenient tool for the digestion of IMPs, since methionines occur at relatively favorable intervals in transmembrane helices (Eichacker *et al.*, 2004). A combination of trypsin and CNBr digestion allows a higher sequence coverage of IMPs (van Montfort *et al.*, 2002, Fischer & Poetsch, 2006) and this approach has been applied to complex membrane samples (Washburn *et al.*, 2001, Fischer *et al.*, 2006). Despite its advantages, CNBr has been rather neglected, perhaps because of safety concerns due to its high toxicity. The minute amounts needed for cleavage of a typical protein sample, however, do not pose a significant health risk.

4.1.7 "Divide and conquer" approaches

4.1.7.1 Proteomic approaches targeting the hydrophilic segments of IMPs

The amphipathic nature of IMPs represents the main obstacle to their solubilization, hampering their analysis in the form of whole intact molecules by the standard proteomic methods. To overcome this, several strategies that aim exclusively at either hydrophilic (extramembrane) or hydrophobic (transmembrane) segments have been developed. The hydrophilic extra-membrane segments of IMPs seem to provide an easier target.

Currently, the most successful approach for the isolation of extracellular (soluble) segments of plasma membrane proteins is **cell surface capture (CSC)**. CSC uses the labeling of intact cells with biotin-containing tags for subsequent streptavidin-based affinity capture. Biotinylation is done with either primary amine-reactive tags (Elia *et al.*, 2008, Hofmann *et al.*, 2010), or, more often, by labeling of periodate-oxidized sugar moieties of glycoproteins with hydrazide chemistry (Gahmberg & Andesson, 1977, Bayer *et al.*, 1988). After solubilization, digestion, and affinity purification using streptavidin-coated beads, the glycopeptides are released enzymatically by peptide-N-glycosidase F (PNGase F) and are subjected to MS/MS analysis. Wollscheid *et al.* optimized this protocol (Wollscheid *et al.*, 2009) and applied it to study a number of various biological processes in combination with quantitative proteomic methods, either SILAC or label-free analysis (Schiess *et al.*, 2009, Hofmann *et al.*, 2010, Gundry *et al.*, 2012, Bock *et al.*, 2012, Moest *et al.*, 2013, DeVeale *et al.*, 2014, Tylečková *et al.*, 2016)

This method enables unprecedented enrichment of IMPs (reaching up to 90%) and has led to the identification of up to 600 surface IMPs. Its success in the extensive number of publications has even given rise to a new term - “surfaceomics.” Despite this, the CSC method has several limitations: it requires live cells, and preferentially targets the N-glycoproteins of the plasma membrane. Moreover, its laboriousness is possibly to blame for the limited number of research groups that have adopted this technique.

The alternative to CSC for fresh or frozen tissues is called **solid phase extraction of formerly N-glycosylated glycoproteins (SPEG)**. This employs the conjugation of oxidized sugars to hydrazide-coated beads (Zhang *et al.*, 2003, Tian *et al.*, 2007); washed glycopeptides are then eluted with PNGase F and subjected to LC-MS. This has recently allowed the identification of nearly 900 glycoproteins, with more than a half predicted as IMPs (Liu *et al.*, 2014).

A similar surface-oriented approach combines **FASP with lectin-affinity capture**. Standard FASP is followed by incubation of the digest with free lectins to enrich for N-glycosylated peptides, and the peptides are then released by PNGase (Zielinska *et al.*, 2010). This method was shown to produce a high enrichment of IMPs (70%) and the identification of over 900 IMPs (Deeb *et al.*, 2014).

Despite the impressive numbers of identified IMPs, the methods that use the capture of glycopeptides have an identical limitation: by exclusively targeting N-glycosylated peptides, other peptides and proteins are omitted by these methods, limiting a complete and accurate description of membrane proteomes.

4.1.7.2 Proteomic approaches targeting the hydrophobic segments of IMPs

The methods targeting the extra-membrane soluble domains of IMPs are attractive, as they seem to be the path of least resistance. A significant portion of each IMP, frequently a major part of the molecule, remains hidden in the phospholipid bilayer. This makes it difficult to solubilize and, more importantly, renders the transmembrane segments of IMPs inaccessible to standard proteolytic digestion. On the other hand, this protective effect of the membrane can be exploited after proteolytic digestion of all non-membrane proteins and extra-membrane parts of IMPs. The protected transmembrane segments can be enriched and isolated.

The pioneering step taking advantage of the protective effect of phospholipid bilayer was taken by Adele Blackler *et al*. (Blackler *et al.*, 2008). In their approach, abbreviated as hppK-CNBr (high pH, proteinase K and CNBr), a crude membrane fraction was washed with carbonate buffer and treated with proteinase K, enabling the removal of soluble and membrane-associated proteins and the extra-membrane parts of IMPs. Because the alkaline carbonate wash performed at low temperature promotes the opening of membrane vesicles (Fujiki *et al.*, 1982), it enabled the digestion at both membrane surfaces (Wu *et al.*, 2003). To achieve the optimal peptide length for LC-MS, the enriched membrane-embedded segments of IMPs were solubilized in 90% formic acid and re-digested with CNBr. Using this method, 670 proteins in human HeLa cells were identified and 479 (72%) of them were IMPs. Importantly, two thirds of the identified IMPs were identified by peptides overlapping with predicted transmembrane segments.

4.1.8 The current status of the proteomics of IMPs

The novel detergent removal methods have significantly improved the outputs of conventional, trypsin-based approaches. The conventional approaches, however, still possess only a limited ability to access the membrane proteome. Namely, the isolation and purification of membrane material by centrifugation and carbonate and/or high-salt washes provides only limited enrichment, which can lead to the omission of less-abundant IMPs in the analyses. Furthermore, the deficit of trypsin (and Lys-C etc.) cleavage sites in a large part of IMPs leads to the omission of highly hydrophobic proteins (containing several transmembrane helices) in the conventional, trypsin-based approaches.

The alternative “divide & conquer” strategies circumvent the problem of the amphipathy of IMPs by targeting either hydrophilic (extra-membrane) or hydrophobic (transmembrane) parts of IMPs. An equally important principle in the “divide & conquer” strategies is the specific enrichment of IMPs by isolating either glycosylated proteins/peptides (in CSC, glyco-FASP or SPEG) or

phospholipid bilayer-protected segments of IMPs (hppK-CNBr). The use of an alternative cleavage strategy, such as cleavage with CNBr, in combination with specific enrichment, may be fundamental for accessing the insufficiently explored parts of the membrane proteome.

This introduction to proteomics of IMPs is based on our review, published in:

Integral membrane proteins in proteomics: How to break open the black box? Vit O, Petrak J. *Journal of Proteomics.* 2017;153:8-20. (IF 2015: 3.867).

(See Appendix 4.)

4.2 Development and application of a new method for proteomic analysis of integral membrane proteins based on their transmembrane segments

A “divide & conquer” approach, targeting transmembrane segments of IMPs and employing an alternative cleavage strategy potentially opens a new way to a description of the membrane proteome. For this reason, we chose to follow the path indicated by the work of Wu & Blackler. Their work (Blackler et al., 2008) specifically deals with two general problems of membrane proteomics, namely IMP enrichment and the lack of trypsin cleavage sites. To enrich for IMPs (or their transmembrane segments) their “hppK-CNBr” method combined a carbonate wash of isolated membranes with proteolytic “shaving” of extra-membrane protein material with proteinase K in carbonate buffer. This allowed digestion at both sides of membranes and a very high enrichment of transmembrane segments of IMPs. The lack of lysine and arginines in the hydrophobic stretches of IMPs has thus been elegantly solved by the inclusion of peptide cleavage with CNBr.

This method allowed the identification of hundreds of IMPs in human cells with very high enrichment. Another advantage of this pioneering method is that it is not limited to plasma membrane proteins, since whole cell membrane material can be processed in this manner. In the glyco-centric “divide and conquer” approaches, the enrichment is limited to glycosylated proteins, i.e. predominantly plasma membrane proteins. Importantly, hppK-CNBr can also be applied to frozen samples or tissue biopsies, contrary to other “divide and conquer” approaches such as CSC.

Despite the obvious potential for tapping the valuable information hidden in the phospholipid bilayer, the strategy has some features that precluded its universal adoption in the proteomic community. These include the laborious multi-step workflow and application of less common cleavage strategies (non-specific proteinase K and CNBr), and potentially also safety concerns regarding CNBr. The non-specific proteinase K produces numerous overlapping peptides, leading to excessive sample complexity. A sequence specific protease such as trypsin would preclude this complication. Moreover, the use of trypsin would enable a quantitative analysis of IMPs – for instance in connection with SILAC. In our presented work we modified several critical steps of the method, namely a) we modified the membrane isolation and IMP enrichment, b) we used trypsin instead of proteinase K, c) we optimized the conditions of peptide cleavage with CNBr, and d) we applied an alternative method of sample delipidation.

In reference to the acronym "hppK" of the original method, we propose the acronym "hpTC" for our method, standing for high pH, Trypsin, CNBr. We applied the hpTC strategy to the analysis of IMPs of human lymphoma cells.

4.2.1 Optimization of the membrane isolation and digestion protocol

The original method used time-consuming and laborious ultracentrifugation steps for membrane enrichment. We replaced these unnecessary steps with a simple method combining cell homogenization with a hypodermic needle, sedimentation of the unbroken cells and nuclei at 500×*g*, DNAse treatment to prevent the co-isolation of chromosomal DNA, and sedimentation of the crude membrane fraction in a bench-top centrifuge at 18,000×*g*.

Alkaline carbonate washing at low temperatures opens membrane vesicles (Fujiki *et al.*, 1982), facilitates the removal of membrane associated proteins, and enables the non-specific proteinase K used in the original hppK method to have access to both sides of the membrane. The non-specific proteinase K produces numerous overlapping peptides, leading to excessive sample complexity. We therefore replaced the proteinase K with specific trypsin. This required a decrease in the pH of the buffer from ~11.5 of the carbonate buffer to pH ~8.5, to ensure high trypsin activity. A simple exchange of the buffer to 50 mM ammonium bicarbonate (pH = ~8.5, already containing trypsin) after pelleting the carbonate washed membranes proved to work well and to be more elegant. To remove the extra-membrane peptides trapped inside of the re-formed vesicles, we further washed the membranes with repeated freeze-thaw cycles in the alkaline carbonate buffer. This process effectively digests most non-membrane proteins and the extra-membrane segments of IMPs. As can be seen on the electron micrographs in Figure 4.2 C, the vesicles that have undergone tryptic "shaving" are more sharply defined.

The carbonate wash of a crude whole-cell membrane fraction also introduced a major obstacle, denaturation of chromosomal DNA in the basic environment. This was solved by short centrifugation of the lysate (500×*g*, 5 minutes) to pellet the nuclei, and brief incubation of the remaining lysate with deoxyribonuclease before the isolation of the final membrane fraction.

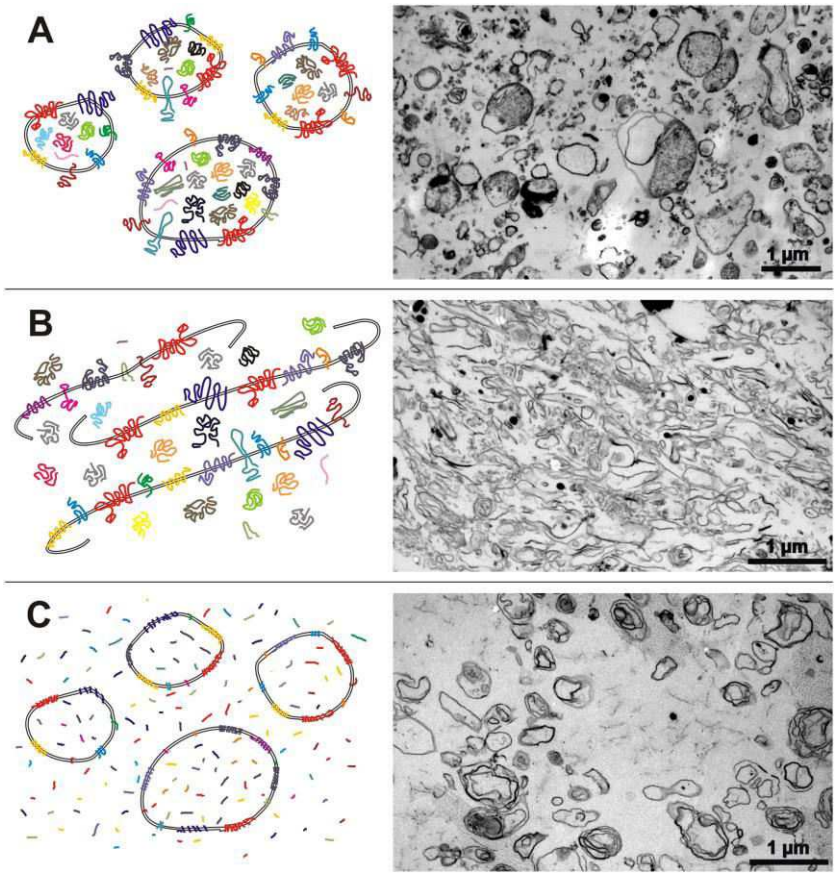

Figure 4.2. *Isolation, carbonate stripping and proteolytic shaving of membranes steps visualized by transmission electron microscopy (TEM).* ***A.*** *The isolated crude membrane fraction consists of variously sized membrane vesicles containing trapped proteins and other material.* ***B.*** *Carbonate stripping opens the vesicles and allows release of trapped content. Since the sample was centrifuged during fixation for TEM, the opened membranes appear to be stacked.* ***C.*** *After tryptic digestion, the membrane outlines are more sharply defined and the vesicles appear empty compared to A. Because of previous opening and stacking, some of the resulting vesicles are multilayered.*

4.2.2 Re-digestion of trypsin-protected transmembrane segments and sample delipidation

Transmembrane segments of IMP protected from trypsin activity remain embedded in the phospholipid bilayer. A typical vertebrate transmembrane α-helix consists of 20-30 amino acids (Sharpe *et al*., 2010) and the nearest trypsin cleavage sites from the edge of the phospholipid bilayer adds some more residues. The resulting transmembrane peptides are therefore often too large (5-8 kDa) for optimal LC-MS analysis and need to be further cleaved. Methionine residues tend to occur frequently in the transmembrane alpha helices, and the specific chemical cleavage with cyanogen bromide (CNBr) at methionine residues is therefore an optimal solution, and was

used in the original hppK protocol. As the solvent for CNBr cleavage, the original protocol employed 90% FA. This solvent, however, can cause damage to the peptide sample (as discussed in chapter 4.1.4) even at the prolonged incubation at room temperature needed for CNBr cleavage. For this reason, we decided to replace 90% FA with 70% trifluoroacetic acid (TFA).

After the chemical cleavage, the sample must be delipidated prior to the LC-MS. In the original hppK-CNBr protocol, delipidation was done by lipid precipitation in aqueous-organic buffer. We replaced the precipitation step with on-column delipidation using dichloromethane, originally designed for the removal of non-ionic detergents (Rey *et al.*, 2010). More importantly, as shown in Figure 4.4, the resulting peptides identified in our study were on average more hydrophobic than peptides identified in the original hppK-CNBr work, which may be a result of the different method of sample delipidation. A summary of the hpTC workflow and key differences compared to the original hppK-CNBr method are highlighted in Figure 4.3.

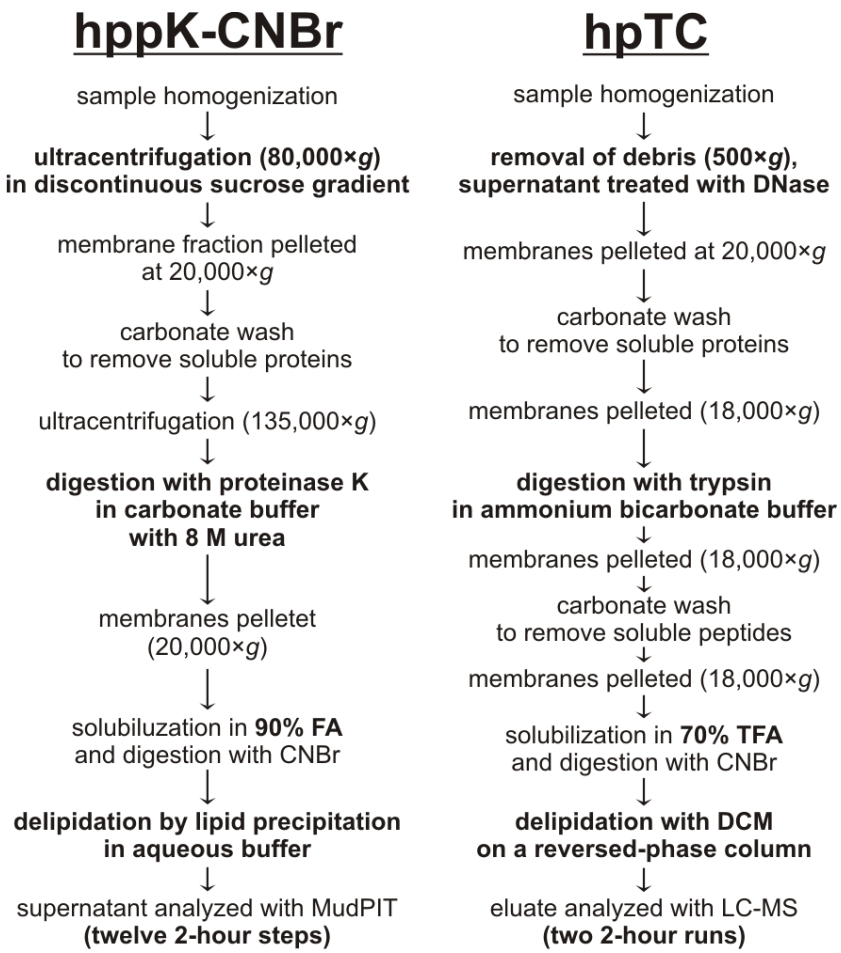

Figure 4.3. *Comparison of the hppT-CNBr and hpTC workflows. Key differences are highlighted in bold.*

4.2.3 Proteomic analysis and bioinformatic assessment of the results

After optimization of the protocol, we employed our modified method for the analysis of the IMPs of the human MCL cell line MINO. We aimed to validate the potential of the approach as a stand-alone or complementary method to a standard proteomic analysis, and to inventarize the membrane proteome of MCL cells. The works presented in Section I of this thesis used conventional proteomic approaches for the analysis of changes associated with drug resistance. Those conventional methods, however, do not enable the coverage of a significant part of IMPs, among which potential drug targets may be included. Proteomic analysis aimed at IMPs might therefore provide valuable data.

LC-MS/MS analysis of the sample generated by our hpTC approach from the human lymphoma cell line MINO was performed using nano UHPLC with a 50 cm Thermo Scientific Acclaim Easy-Spray PepMap C18 RSLC column heated to 40 °C. Peptides were eluted using a 90-minute linear gradient of solvent B (80% acetonitrile) and detected with a Hybrid Quadrupole-Orbitrap Mass Spectrometer Q Exactive plus (Thermo Fisher Scientific).

Proteome Discoverer v. 1.4 software was used for protein identification. The spectra were searched using Sequest HT search engine against the human subset of the Swiss-Prot database with added contaminant protein sequences. The search results were validated with a decoy database search using Percolator with 0.01 FDR.

4.2.3.1 Protein and peptide structure

In two runs, 1,224 proteins with average sequence coverage of 12.2% were identified in the MCL cell line MINO. 802 (65.5%) of the identifications were predicted to contain at least one transmembrane domain by TMHMM (Tied Mixture Hidden Markov Model, Krogh *et al.*, 2001). We compared the hydrophobicity (GRAVY score, Kyte & Doolittle, 1982) of the identified peptides in our dataset with the hydrophobicity of the peptides measured in Blackler *et al.*, 2008. The distribution of GRAVY scores supports the notion that our method of delipidation allows the better recovery of hydrophobic peptides, since out dataset was slightly shifted towards peptides with positive GRAVY scores, i.e. more hydrophobic peptides (see Figure 4.4).

The 802 identified IMPs contained 1-16 transmembrane segments (see Figure 4.5) according to the TMHMM prediction. The distribution of transmembrane segments is in agreement with a genome-wide prediction of the human proteome (Fagerberg *et al.*, 2010), suggesting that hpTC is not biased against more hydrophilic, nor against the most hydrophobic IMPs with many

transmembrane segments. A bioinformatic assessment further showed that approximately half of the unique identified peptides overlapped with the predicted transmembrane segments. A few examples of the coverage of some of the identified proteins are shown in Figure 4.6.

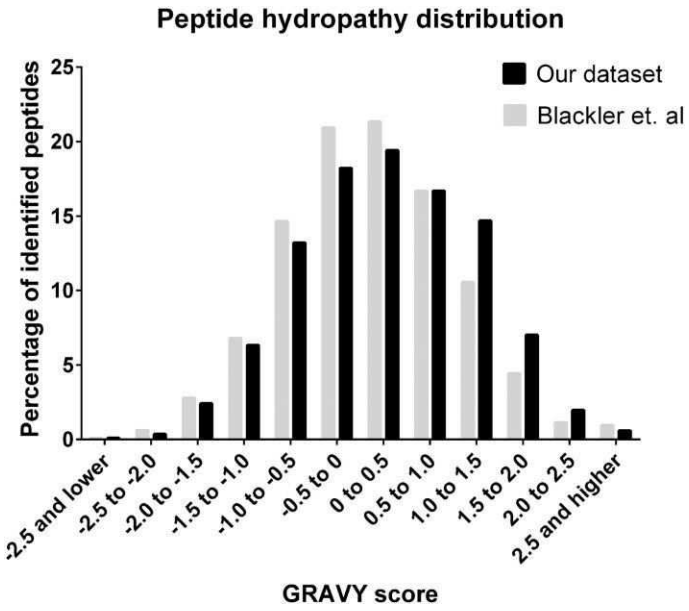

Figure 4.4. *Comparison of the distribution of peptide hydrophobicity GRAVY score in our dataset with the results of the original method by Blackler et al.*

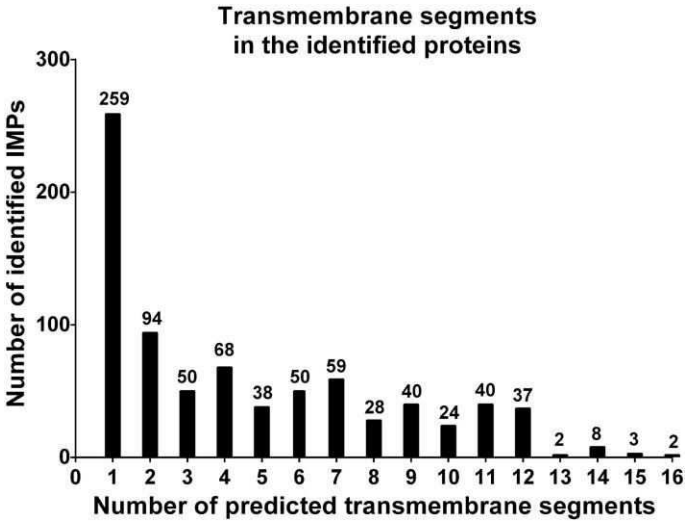

Figure 4.5. *Number of predicted transmembrane regions (based on TMHMM prediction) in the 802 IMPs identified in our dataset.*

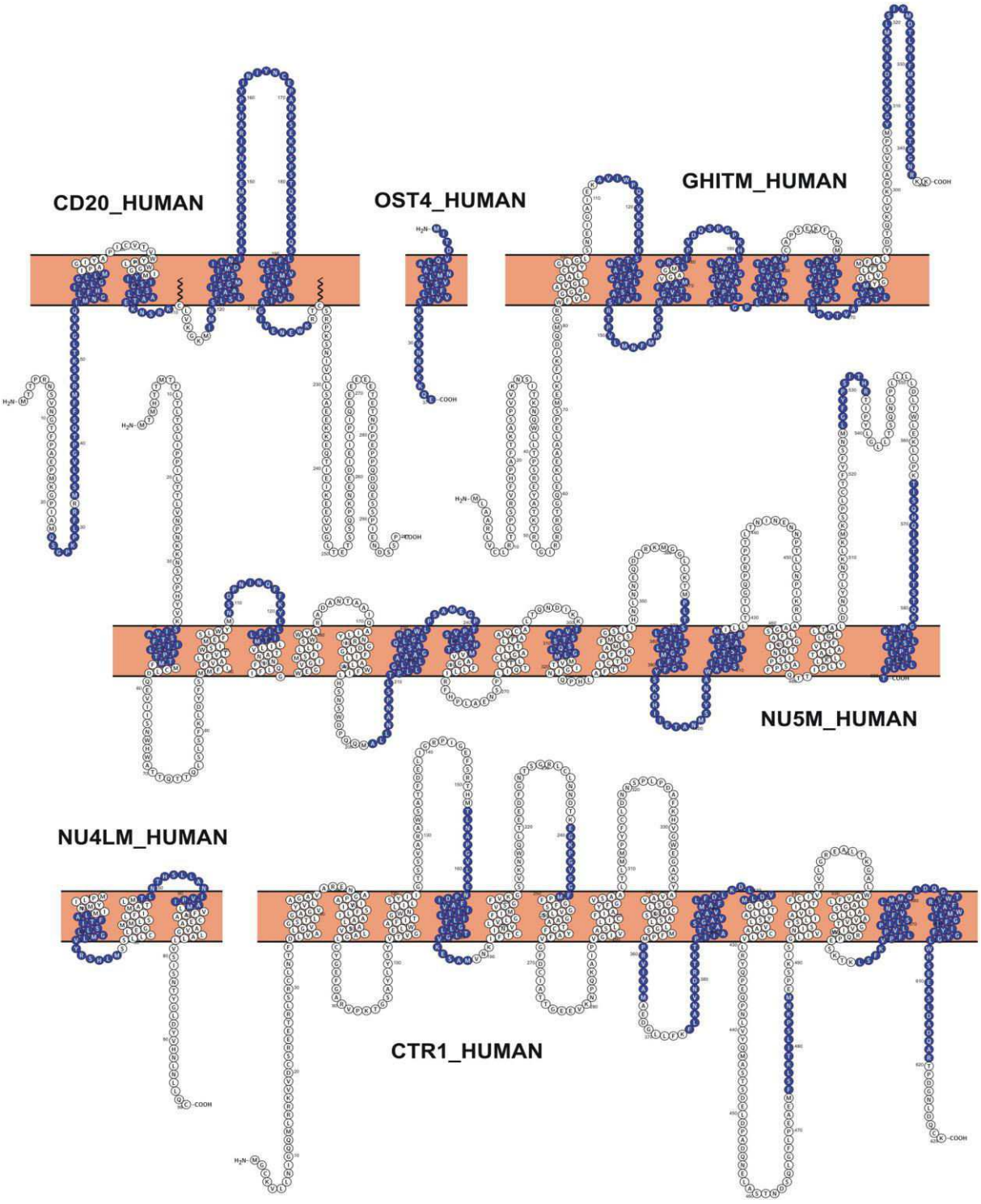

Figure 4.6. *Examples of sequence coverage of identified IMPs on topological prediction maps, generated using Protter (http://wlab.ethz.ch/protter). Identified peptides are labeled blue. These examples illustrate, that peptides overlapping with transmembrane segments significantly contribute to the protein identification.*

The importance of CNBr cleavage for the protocol is apparent from the high contribution of CNBr cleaved peptides in the identification of IMPs. Approximately 75% of all observed peptides were generated either with CNBr alone, or in combination with trypsin digestion. The CNBr contribution, however, rose to 97% in the case of peptides overlapping with transmembrane segments (Figure 4.7).

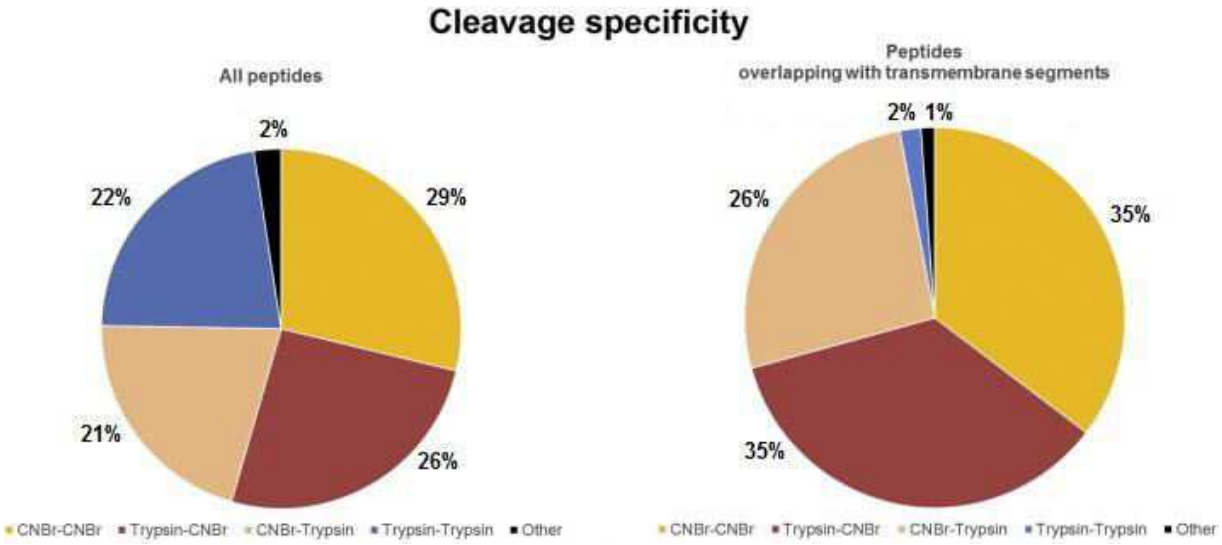

Figure 4.7. *Relative contribution of CNBr and trypsin in our dataset. CNBr-CNBr denotes peptides formed by CNBr cleavages on both termini, similarly Trypsin-Trypsin denotes fully tryptic peptides. Trypsin-CNBr represents peptides formed by trypsin cleavage on N-terminus and CNBr cleavage on C-terminus and vice versa. Others are peptides originating from protein N- or C-terminus.*

4.2.3.2 Identity, localization and biology of the identified proteins

Among the identified IMPs were numerous transporters (both plasma membrane and inner organellar transporters – ion channels, small molecule transporters, subunits of various ATPases), membrane enzymes (e.g. enzymes that take part in the post-translational processing of proteins in the endoplasmic reticulum and Golgi apparatus), receptors and signal transduction proteins (growth factor receptors etc.), proteins with immunity-related activities (human leukocyte antigens, cytokine receptors, various CD proteins) and other proteins. High abundant subunits of the inner mitochondrial electron transport chain complexes were among the IMPs with the highest number of identified peptides. The Gene Ontology annotations of a significant part of the identified proteins, however, did not contain any information in the domains “biological function” (127 proteins) or “molecular function” (274 proteins).

The potential of the hpTC method is further accented by the identification of several so-called “missing proteins.” These are the products of protein coding genes that have not been previously detected on the protein level. This set of proteins has recently attracted the attention of the Human Proteome Project, and the search for strategies to detect the remaining “missing proteins” has become one of the priorities of the project (Lane *et al.*, 2014). In our dataset, we found 13 such “previously unseen” proteins that were in the NeXtProt database of missing proteins (www.nextprot.org) at the time of submission of our paper. Six of them had been previously detected only on transcript level (O15342, O60478, Q14330, Q14656, Q5SWH9, Q6UWH6), the existence of 4 was based on homology (A8MWL7, A2A368, C9J798, P69849), and 3 were classified as “uncertain” (O60361, Q5T1J5, Q92928).

The high share of unknown proteins or proteins with unknown function illustrates how under-explored the membrane environment is, and demonstrates the potential of our method for the analysis of this membrane “black box”. The most problematic are small, highly hydrophobic IMPs that do not contain enough trypsin cleavage sites and otherwise would not be identified using standard trypsin-based proteomic approaches. The topological diagrams of OST4_HUMAN and NU4LM_HUMAN in Figure 4.6 are examples of such IMPs.

We evaluated the localization of the identified IMPs based of their Gene Ontology annotations in order to show whether the hpTC method allows access to all cellular membrane compartments. Several identified proteins were annotated exclusively to the inner mitochondrial membrane (ADP/ATP translocases 1–3, numerous components of respiratory chain), the endoplasmic reticulum membrane (GlcNAc-1-P transferase, UDP-glucuronic acid/UDP-N-acetylgalactosamine transporter), the Golgi apparatus membrane (Alpha-(1,6)-fucosyltransferase, Beta-1,4-galactosyltransferase 3) and the nuclear membrane (lamin-B receptor, nucleoporin NDC). Surface proteins of the plasma membrane were also identified, represented for instance by 48 CD (cluster of differentiation) molecules (see Table 5.1). CD proteins expressed on the cell surface represent promising targets of modern anti-cancer drugs including therapeutic antibodies, as exemplified by rituximab targeting CD20, trastuzumab targeting-HER2 (CD340), and ipilimumab targeting CTLA-4 (CD152) (Zhu *et al.*, 2015). Information on the expression of CD markers in cancer cells is therefore potentially valuable. Taken together, the identification of numerous proteins from each cellular compartmental membrane confirms the ability of the method to access not only the plasma membrane, but all cellular membranes.

Table 5.1. *The list of identified CD molecules.*

CD No.	Accession	Entry name	Protein name
CD10	P08473	NEP_HUMAN	Neprilysin
CD11a	P20701	ITAL_HUMAN	Integrin α-L
CD18	P05107	ITB2_HUMAN	Integrin β-2
CD19	P15391	CD19_HUMAN	B-lymphocyte antigen CD19
CD20	P11836	CD20_HUMAN	B-lymphocyte antigen CD20
CD21	P41597	CCR2_HUMAN	C-C chemokine receptor type 2
CD27	P26842	CD27_HUMAN	CD27 antigen
CD32	P31994	FCG2B_HUMAN	Low affinity immunoglobulin γ Fc region receptor II-b
CD39	P49961	ENTP1_HUMAN	Ectonucleoside triphosphate diphosphohydrolase 1
CD40	P25942	TNR5_HUMAN	Tumor necrosis factor receptor superfamily member 5
CD43	P16150	LEUK_HUMAN	Leukosialin
CD45	P08575	PTPRC_HUMAN	Receptor-type tyrosine-protein phosphatase C
CD47	Q08722	CD47_HUMAN	Leukocyte surface antigen CD47
CD48	P09326	CD48_HUMAN	CD48 antigen
CD50	P32942	ICAM3_HUMAN	Intercellular adhesion molecule 3
CD53	P19397	CD53_HUMAN	Leukocyte surface antigen CD53
CD54	P05362	ICAM1_HUMAN	Intercellular adhesion molecule 1
CD63	P08962	CD63_HUMAN	CD63 antigen
CD70	P32970	CD70_HUMAN	CD70 antigen
CD71	P02786	TFR1_HUMAN	Transferrin receptor protein 1
CD72	P21854	CD72_HUMAN	B-cell differentiation antigen CD72
CD74	P04233	HG2A_HUMAN	HLA class II histocompatibility antigen γ chain
CD79a	P11912	CD79A_HUMAN	B-cell antigen receptor complex-associated protein α chain
CD79b	P40259	CD79B_HUMAN	B-cell antigen receptor complex-associated protein β chain
CD81	P60033	CD81_HUMAN	CD81 antigen
CD82	P27701	CD82_HUMAN	CD82 antigen
CD84	Q9UIB8	SLAF5_HUMAN	SLAM family member 5
CD92	Q8WWI5	CTL1_HUMAN	Choline transporter-like protein 1
CD97	P48960	CD97_HUMAN	CD97 antigen
CD98	P08195	4F2_HUMAN	4F2 cell-surface antigen heavy chain
CD99	P14209	CD99_HUMAN	CD99 antigen
CD102	P13598	ICAM2_HUMAN	Intercellular adhesion molecule 2
CD107a	P11279	LAMP1_HUMAN	Lysosome-associated membrane glycoprotein 1
CD132	P31785	IL2RG_HUMAN	Cytokine receptor common subunit γ
CD147	P35613	BASI_HUMAN	Basigin
CD159a	P26715	NKG2A_HUMAN	NKG2-A/NKG2-B type II integral membrane protein
CD184	P61073	CXCR4_HUMAN	C-X-C chemokine receptor type 4
CD185	P32302	CXCR5_HUMAN	C-X-C chemokine receptor type 5
CD192	P41597	CCR2_HUMAN	C-C chemokine receptor type 2
CD197	P32248	CCR7_HUMAN	C-C chemokine receptor type 7
CD205	O60449	LY75_HUMAN	Lymphocyte antigen 75
CD217	Q96F46	I17RA_HUMAN	Interleukin-17 receptor A
CD222	P11717	MPRI_HUMAN	Cation-independent mannose-6-phosphate receptor
CD225	P13164	IFM1_HUMAN	Interferon-induced transmembrane protein 1
CD230	P04156	PRIO_HUMAN	Major prion protein
CD289	Q9NR96	TLR9_HUMAN	Toll-like receptor 9
CD298	P54709	AT1B3_HUMAN	Sodium/potassium-transporting ATPase subunit β-3
CD361	P34910	EVI2B_HUMAN	Protein EVI2B

4.2.3.3 Contaminants

The carbonate washes and digestion with trypsin were efficient in removing the majority of soluble proteins and peptides, but not all. Besides IMPs, approximately a third of the list of proteins identified in our study were non-membrane proteins (proteins without predicted membrane domains). There may be several explanations or reasons for this.

We observed contamination with high-abundant cytosolic, cytoskeletal as well as nuclear proteins. The cleavage products of these high copy number proteins may nonspecifically interact with phospholipid bilayers, and this may prevent their complete removal. Some soluble proteins, as in the case of histones, have even been shown to directly interact with membranes (Watson *et al.*, 1999, Hariton-Gazal *et al.*, 2003). Membrane-associated proteins and subunits of transmembrane multi-protein complexes with no predicted transmembrane segment may have tight specific interactions with the membrane, or can be shielded from the proteolytic activity of trypsin by other subunit components.

Despite the presence of contaminating soluble proteins in our analysis results, two thirds of the identified proteins were IMPs. This enrichment of IMPs is high compared to conventional proteomic analyses of membrane proteins, usually ranging between 20-40% of IMPs, and demonstrates the high efficacy of the hpTC method.

4.2.4 The potential use of hpTC in quantitative proteomic analyses

Our hpTC strategy enables high enrichment and identification of hundreds of IMPs in complex samples, and can be used as a stand-alone method. The combination of hpTC with a complementary method, such as cell surface capture, or a standard proteomic analysis, should provide even more robust information on the membrane proteome. To obtain relevant biological data, however, quantitative analysis is usually needed. Implementation of trypsin instead of proteinase K not only decreases the sample complexity, but also makes it compatible with SILAC labeling (see chapter 2.1.2.2) potentially enabling such a quantitative analysis (at least in growing cells).

We evaluated the content of the SILAC-suitable amino acids arginine (R) and lysine (K) in the unique peptides identified in our analysis. Nearly 83% of the peptides contained either R or K (see Figure 4.8). This would theoretically allow “double” SILAC labeling to provide semi-quantitative information from our hpTC analysis. With the addition of labeled leucine (L), which

by itself also accounts for 83%, the “triple” labeling with R, K and L would provide semi-quantitative data on 97% of all identified peptides.

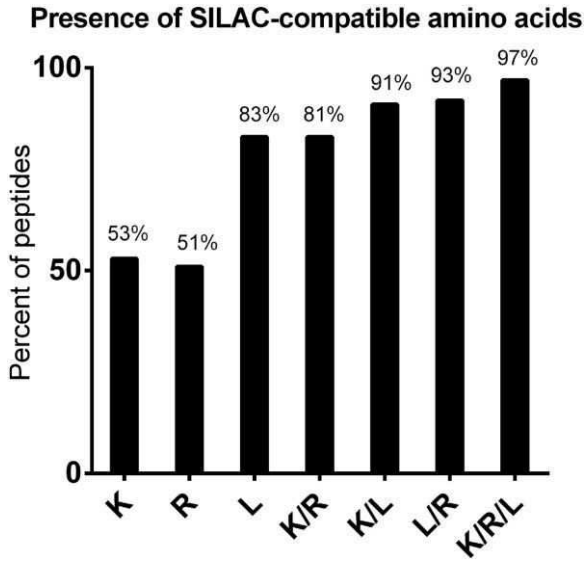

Figure 4.8. *Percentage of unique peptides identified in our analysis containing SILAC-compatible amino acids lysine (K), arginine (R) and leucine (L).*

4.2.5 Discussion

We modified the original hppK-CNBr method, and in reference to it, we use the abbreviation hpTC (high pH, trypsin, CNBr). We demonstrated that our hPTC strategy, combining trypsin digestion of the intact membrane fraction with the CNBr cleavage of trypsin-protected transmembrane segments, enables very high enrichment and the analysis of hundreds of IMPs from all cellular compartments.

We modified several steps of the original method. In particular, we eliminated the use of ultracentrifugation, used deoxyribonuclease for the removal of co-isolated chromosomal DNA, and, most importantly, we replaced the non-specific proteinase K with trypsin. This modification eliminates the production of multiple overlapping peptides and increases the method's sensitivity, and opens a new way toward combining this method with SILAC or label-free quantification. We also employed on-column sample delipidation with dichloromethane, a method originally devised for detergent removal (Rey *et al*., 2010) instead of lipid precipitation in the aqueous-organic solvent used in Blackler *et al.*, 2008.

Our improved strategy enabled us to identify 1,224 proteins in human lymphoma cells, including 802 (65.5%) IMPs with 1 to 16 transmembrane domains. Roughly half of the unique peptides belonging to IMPs overlapped with predicted transmembrane segments. Membrane proteins annotated to all cellular compartments were present among the identified proteins. Moreover, this method enabled us to identify thirteen so-called “missing proteins”, i.e. proteins with no previous evidence at the protein level.

In contrast to several other strategies, our method is not limited to glycosylated IMPs of the plasma membrane, as in glyco-capture methods such as CSC and glyco-FASP (described in detail in chapter 4.1.7.1). By focusing on membrane-embedded segments of IMPs, the method enables the effective enrichment of IMPs. In combination with the dual trypsin-CNBr cleavage, this allows the identification of otherwise problematic small, hydrophobic and low-abundant proteins. Taken together, this method is well suited for sensitive analysis of the membrane proteome. Due to the amphipathic nature of IMPs, a combination of the hpTC approach with a soluble-peptide oriented method such as CSC or glycoFASP and a suitable quantitative approach might provide the best results and enable deep expression analyses of membrane proteomes.

The results of this work were published in:

Large-scale identification of membrane proteins based onanalysis of trypsin-protected transmembrane segments. Vit O, Man P, Kadek A, Hausner J, Sklenar J, Harant K, Novak P, Scigelova M,Woffendin G, Petrak J. *Journal of Proteomics* 2016;149:15-22. (IF 2015: 3.867).

(See Appendix 5.)

4.3 Conclusions to Section II

In the last decade, technological progress in mass spectrometry, novel methods for detergent removal, and methods for the enrichment of glycoproteins has enabled significant improvements in analyzing the previously nearly-inaccessible membrane proteome.

The conventional proteomic approaches for analysis of IMPs, which target IMPs as whole molecules, benefited significantly from the introduction of FASP for SDS removal and the use of SDC and its removal by phase separation. These improvements allowed several impressive large-scale analyses of membrane proteins. Alternative strategies that utilize the “divide and conquer” principle, oriented toward soluble glycosylated peptides of IMPs (CSC, SPEG and glyco-FASP), also significantly improved our knowledge of the membrane proteome. Our modified “hpTC” method based on the “hppK-CNBr” has a potential to shed light on the so-far unexplored depths of the membrane proteome. Its major advantages that enable the detection of the least-explored IMPs are primarily:

- the high enrichment of hydrophobic IMPs, based on membrane protection of the transmembrane segments from protease activity
- the combination of the conventional and alternative sequence-specific proteolytic agents trypsin and CNBr.

The information provided by the three approaches –conventional methods, glyco-capture methods and hpTC – are nonetheless complementary. A combination of all three will probably be needed to obtain more comprehensive insights into the inaccessible parts of the membrane proteome. For instance, a combination of the glyco-capture approach with complementary analysis of the hydrophobic segments in one biological sample can be envisioned. Such a combination might provide unprecedented coverage of the membrane proteome. If combined with a quantitative method, e.g. SILAC labeling, such a combined analysis should provide a thorough and more complete snapshot.

Ultimately, more efficient analyses of the membrane proteome could provide valuable data about changes in the expression of IMPs, which have been difficult to obtain with conventional proteomic methods. That there are plenty of target proteins of already-approved drugs among IMPs. By widening the global view of protein expression on such an important class of proteins, a complementary analysis of IMPs could allow the identification of suitable drug targets and treatment strategies in disease models or even in personalized medicine.

5 Final conclusions

In the works presented in this thesis, we demonstrated that proteomics can provide detailed insights into quantitative changes in the proteomes of drug resistant cancer cells. Namely, we identified causal and secondary contributing or compensatory changes in MCL cells with acquired resistance to three different anti-cancer drugs. Detailed knowledge of the molecular landscape of drug-resistant cancer cells is a prerequisite for successful therapy. Based on the information obtained by proteomics, we were able to propose appropriate therapeutic strategies, or conversely, predict which drugs would be ineffective in the treatment of drug resistant cells. We believe that our works provide a proof of concept that a detailed proteomic analyses of small populations of cancer cells can be used in the clinical setting and direct individualized therapies in the near future.

Despite the enormous progress in proteomic technologies in the last decade, there are still shortcomings that need to be addressed. The inadequacy of standard proteomic workflows for integral membrane proteins is one of the most insistent. New paradigms and innovative approaches are needed. We followed an unexplored path toward the analysis of the membrane proteome, and presented a modified and improved method for the analysis of membrane proteins via their membrane-embedded peptides. This method, abbreviated as hpTC, allows the detection of the least-accessible, less-abundant and highly hydrophobic IMPs. We applied the method in the analysis of the membrane proteome of MCL cells. IMPs are an important part of the proteome and physiology of cells and the majority of current drugs target IMPs. Methods such as hpTC capable of accessing the membrane proteome are therefore essential to biomedical research. We believe that future applications of hpTC may provide new insights into biomedical problems including cancer drug resistance, identification of sensitive diagnostic markers and suitable drug targets.

6 List of references

Aggarwal S, Yadav AK. Dissecting the iTRAQ Data Analysis. Methods Mol Biol 2016;1362:277-91.

Allison AC, Eugui EM. The design and development of an immunosuppressive drug, mycophenolate mofetil. Springer Semin Immunopathol 1993;14:353-80. Review.

Allison AC, Eugui EM. Mycophenolate mofetil and its mechanisms of action. Immunopharmacology 2000;47(2-3):85-118. Review.

Amici A, Emanuelli M, Magni G, Raffaelli N, Ruggieri S. Pyrimidine nucleotidases from human erythrocyte possess phosphotransferase activities specific for pyrimidine nucleotides. FEBS Lett 1997;419(2-3):263-7.

Anderson NL, Polanski M, Pieper R, Gatlin T, Tirumalai RS, Conrads TP, Veenstra TD, Adkins JN, Pounds JG, Fagan R, Lobley A. The human plasma proteome: a nonredundant list developed by combination of four separate sources. Mol Cell Proteomics 2004;3(4):311-26.

Arnér ES, Eriksson S. Mammalian deoxyribonucleoside kinases. Pharmacol Ther 1995;67(2):155-86. Review.

Ashkenazi A, Pai RC, Fong S, Leung S, Lawrence DA, Marsters SA, Blackie C, Chang L, McMurtrey AE, Hebert A, DeForge L, Koumenis IL, Lewis D, Harris L *et al.* Safety and antitumor activity of recombinant soluble Apo2 ligand. J Clin Invest 1999;104(2):155-62.

Austen B, Skowronska A, Baker C, Powell JE, Gardiner A, Oscier D, Majid A, Dyer M, Siebert R, Taylor AM, Moss PA, Stankovic T. Mutation status of the residual ATM allele is an important determinant of the cellular response to chemotherapy and survival in patients with chronic lymphocytic leukemia containing an 11q deletion. J Clin Oncol 2007;25(34):5448-57.

Austin WR, Armijo AL, Campbell DO, Singh AS, Hsieh T, Nathanson D, Herschman HR, Phelps ME, Witte ON, Czernin J, Radu CG. Nucleoside salvage pathway kinases regulate hematopoiesis by linking nucleotide metabolism with replication stress. J Exp Med 2012;209(12):2215-28.

Bai L, Yamaguchi M, Tatsumi M, Kon K, Bräutigam M. Mechanisms responsible for resistance of sublines derived from leukemia cell lines to an antitumor agent 9-beta-D-arabinofuranosyl-2-fluoroadenine. J Cancer Res Clin Oncol 1998;124(7):367-73.

Bantia S, Montgomery JA, Johnson HG, Walsh GM. In vivo and in vitro pharmacologic activity of the purine nucleoside phosphorylase inhibitor BCX-34: the role of GTP and dGTP. Immunopharmacology 1996;35(1):53-63.

Bayer EA, Ben-Hur H, Wilchek M. Biocytin hydrazide-a selective label for sialic acids, galactose, and other sugars in glycoconjugates using avidin-biotin technology. Anal Biochem 1988;170:271-81.

Bantscheff M, Lemeer S, Savitski MM, Kuster B. Quantitative mass spectrometry in proteomics: critical review update from 2007 to the present. Anal Bioanal Chem 2012;404(4):939-65.

Beck M, Schmidt A, Malmstroem J, Claassen M, Ori A, Szymborska A, Herzog F, Rinner O, Ellenberg J, Aebersold R. The quantitative proteome of a human cell line. Mol Syst Biol. 2011;7:549.

Blackler AR, Speers AE, Ladinsky MS, Wu CC. A shotgun proteomic method for the identification of membrane-embedded proteins and peptides. J Proteome Res. 2008 Jul;7(7):3028-34.

Blonder J, Rodriguez-Galan MC, Chan KC, Lucas DA, Yu LR, Conrads TP, Issaq HJ, Young HA, Veenstra TD. Analysis of murine natural killer cell microsomal proteins using two-dimensional liquid chromatography coupled to tandem electrospray ionization mass spectrometry. J Proteome Res 2004;3:862-70.

Blonder J, Conrads TP, Yu LR, Terunuma A, Janini GM, Issaq HJ, Vogel JC, Veenstra TD. A detergent- and cyanogen bromide-free method for integral membrane proteomics: application to Halobacterium purple membranes and the human epidermal membrane proteome. Proteomics 2004;4:31-45.

Bock T, Moest H, Omasits U, Dolski S, Lundberg E, Frei A, Hofmann A, Bausch-Fluck D, Jacobs A, Krayenbuehl N, Uhlen M, Aebersold R, Frei K, Wollscheid B. Proteomic analysis reveals drug accessible cell surface N-glycoproteins of primary and established glioblastoma cell lines. J Proteome Res 2012;11:4885-93.

Bodmer JL, Holler N, Reynard S, Vinciguerra P, Schneider P, Juo P, Blenis J, Tschopp J. TRAIL receptor-2 signals apoptosis through FADD and caspase-8. Nat Cell Biol 2000;2(4):241-3.

Bollée G, Harambat J, Bensman A, Knebelmann B, Daudon M, Ceballos-Picot I. Adenine phosphoribosyltransferase deficiency. Clin J Am Soc Nephrol 2012;7(9):1521-7. Review.

Botelho D, Wall MJ, Vieira DB, Fitzsimmons S, Liu F, Doucette A. Top-down and bottom-up proteomics of SDS-containing solutions following mass-based separation. J Proteome Res 2010;9:2863-70.

Brodbelt JS. Ion activation methods for peptides and roteins. Anal Chem. 2016 Jan 5;88(1):30-51.

Capizzi RL, White JC, Powell BL, Perrino F. Effect of dose on the pharmacokinetic and pharmacodynamic effects of cytarabine. Semin Hematol 1991;28(3 Suppl 4):54-69. Review.

Capizzi RL. Curative chemotherapy for acute myeloid leukemia: the development of high-dose ara-C from the laboratory to bedside. Invest New Drugs. 1996;14(3):249-56. Review.

Castro Alves C, Terziyska N, Grunert M, Gündisch S, Graubner U, Quintanilla-Martinez L, Jeremias I. Leukemia-initiating cells of patient-derived acute lymphoblastic leukemia xenografts are sensitive toward TRAIL. Blood 2012;119(18):4224-7.

Chacko GW, Tridandapani S, Damen JE, Liu L, Krystal G, Coggeshall KM. Negative signaling in B lymphocytes induces tyrosine phosphorylation of the 145-kDa inositol polyphosphate 5-phosphatase, SHIP. J Immunol 1996;157(6):2234-8.

Cheah CY, Seymour JF, Wang ML. Mantle Cell Lymphoma. J Clin Oncol 2016;34(11):1256-69. Review.

Cheng J, Hylander BL, Baer MR, Chen X, Repasky EA. Multiple mechanisms underlie resistance of leukemia cells to Apo2 Ligand/TRAIL. Mol Cancer Ther 2006;5(7):1844-53.

Clamp M, Fry B, Kamal M, Xie X, Cuff J, Lin MF, Kellis M, Lindblad-Toh K, Lander ES. Distinguishing protein-coding and noncoding genes in the human genome. Proc Natl Acad Sci USA. 2007;104(49):19428-33.

Clancy L, Mruk K, Archer K, Woelfel M, Mongkolsapaya J, Screaton G, Lenardo MJ, Chan FK. Preligand assembly domain-mediated ligand-independent association between TRAIL receptor 4 (TR4) and TR2 regulates TRAIL-induced apoptosis. Proc Natl Acad Sci USA 2005;102(50):18099-104.

Clarke ML, Mackey JR, Baldwin SA, Young JD, Cass CE. The role of membrane transporters in cellular resistance to anticancer nucleoside drugs. Cancer Treat Res 2002;112:27-47. Review.

Cyster JG, Goodnow CC. Protein tyrosine phosphatase 1C negatively regulates antigen receptor signaling in B lymphocytes and determines thresholds for negative selection. Immunity 1995;2(1):13-24.

Danhauser L, Plunkett W, Keating M, Cabanillas F. 9-beta-D-arabinofuranosyl-2-fluoroadenine 5'-monophosphate pharmacokinetics in plasma and tumor cells of patients with relapsed leukemia and lymphoma. Cancer Chemother Pharmacol 1986;18(2):145-52.

de Campos-Nebel M, Larripa I, González-Cid M. Non-homologous end joining is the responsible pathway for the repair of fludarabine-induced DNA double strand breaks in mammalian cells. Mutat Res 2008;646(1-2):8-16.

Deeb SJ, Cox J, Schmidt-Supprian M, Mann M. N-linked glycosylation enrichment for in-depth cell surface proteomics of diffuse large B-cell lymphoma subtypes. Mol Cell Proteomics 2014 Jan;13:240-51.

Degli-Esposti MA, Dougall WC, Smolak PJ, Waugh JY, Smith CA, Goodwin RG. The novel receptor TRAIL-R4 induces NF-kappaB and protects against TRAIL-mediated apoptosis, yet retains an incomplete death domain. Immunity 1997;7(6):813-20.

Degli-Esposti MA, Smolak PJ, Walczak H, Waugh J, Huang CP, DuBose RF, Goodwin RG, Smith CA. Cloning and characterization of TRAIL-R3, a novel member of the emerging TRAIL receptor family. J Exp Med 1997;186(7):1165-70.

de Godoy LM, Olsen JV, Cox J, Nielsen ML, Hubner NC, Fröhlich F, Walther TC, Mann M. Comprehensive mass-spectrometry-based proteome quantification of haploid versus diploid yeast. Nature. 2008;455(7217):1251-4.

Delarue R, Haioun C, Ribrag V, Brice P, Delmer A, Tilly H, Salles G, Van Hoof A, Casasnovas O, Brousse N, Lefrere F, Hermine O. CHOP and DHAP plus rituximab followed by autologous stem cell transplantation in mantle cell lymphoma: a phase 2 study from the Groupe d'Etude des Lymphomes de l'Adulte. Blood 2013;121(1):48-53.

DeVeale B, Bausch-Fluck D, Seaberg R, Runciman S, Akbarian V, Karpowicz P, Yoon C, Song H, Leeder R, Zandstra PW, Wollscheid B, van der Kooy D. Surfaceome profiling reveals regulators of neural stem cell function. Stem Cells 2014;32:258-68.

Dimberg LY, Anderson CK, Camidge R, Behbakht K, Thorburn A, Ford HL. On the TRAIL to successful cancer therapy? Predicting and counteracting resistance against TRAIL-based therapeutics. Oncogene 2013 14;32(11):1341-50. Review.

Domon B, Aebersold R. Options and considerations when selecting a quantitative proteomics strategy. Nat Biotechnol 2010;28(7):710-21.

Dormeyer W, van Hoof D, Mummery CL, Krijgsveld J, Heck AJ. A practical guide for the identification of membrane and plasma membrane proteins in human embryonic stem cells and human embryonal carcinoma cells. Proteomics 2008;8:4036-53.

Doucette AA, Vieira DB, Orton DJ, Wall MJ. Resolubilization of precipitated intact membrane proteins with cold formic acid for analysis by mass spectrometry. J Proteome Res 2014;13:6001-12.

Dreyling M, Kluin-Nelemans HC, Beà S, Klapper W, Vogt N, Delfau-Larue MH, Hutter G, Cheah C, Chiappella A, Cortelazzo S, Pott C, Hess G, Visco C, Vitolo U *et al.* Update on the molecular pathogenesis and clinical treatment of mantle cell lymphoma: report of the 11th annual conference of the European Mantle Cell Lymphoma Network. Leuk Lymphoma 2013;54(4):699-707. Review.

Dumontet C, Fabianowska-Majewska K, Mantincic D, Callet Bauchu E, Tigaud I, Gandhi V, Lepoivre M, Peters GJ, Rolland MO, Wyczechowska D, Fang X, Gazzo S, Voorn DA, Vanier-Viornery A, MacKey J. Common resistance mechanisms to deoxynucleoside analogues in variants of the human erythroleukaemic line K562. Br J Haematol 1999;106(1):78-85.

Eichacker LA, Granvogl B, Mirus O, Müller BC, Miess C, Schleiff E. Hiding behind hydrophobicity. Transmembrane segments in mass spectrometry. J Biol Chem 2004;279:50915-22.

Elia G. Biotinylation reagents for the study of cell surface proteins. Proteomics 2008;8:4012-24.

Emery JG, McDonnell P, Burke MB, Deen KC, Lyn S, Silverman C, Dul E, Appelbaum ER, Eichman C, DiPrinzio R, Dodds RA, James IE, Rosenberg M, Lee JC, Young PR. Osteoprotegerin is a receptor for the cytotoxic ligand TRAIL. J Biol Chem 1998;273(23):14363-7.

Eng JK, McCormack AL, Yates JR. An approach to correlate tandem mass spectral data of peptides with amino acid sequences in a protein database. J Am Soc Mass Spectrom 1994;5(11):976-89.

Fagerberg L, Jonasson K, von Heijne G, Uhlén M, Berglund L. Prediction of the human membrane proteome. Proteomics. 2010 Mar;10(6):1141-9.

Fairbanks LD, Rückemann K, Qiu Y, Hawrylowicz CM, Richards DF, Swaminathan R, Kirschbaum B, Simmonds HA. Methotrexate inhibits the first committed step of purine biosynthesis in mitogen-stimulated human T-lymphocytes: a metabolic basis for efficacy in rheumatoid arthritis? Biochem J 1999;342(Pt 1):143-52.

Falschlehner C, Schaefer U, Walczak H. Following TRAIL's path in the immune system. Immunology 2009;127(2):145-54. Review.

Fenn JB, Mann M, Meng CK, Wong SF, Whitehouse CM. Electrospray ionization for mass spectrometry of large biomolecules. Science 1989;246(4926):64-71. Review.

Ferrero S, Dreyling M. The current therapeutic scenario for relapsed mantle cell lymphoma. Curr Opin Oncol 2013;25(5):452-62. Review.

Fischer F, Poetsch A. Protein cleavage strategies for an improved analysis of the membrane proteome. Proteome Sci 2006;4:2.

Fischer F, Wolters D, Rögner M, Poetsch A. Toward the complete membrane proteome: high coverage of integral membrane proteins through transmembrane peptide detection. Mol Cell Proteomics 2006;5:444-53.

Fodale V, Pierobon M, Liotta L, Petricoin E. Mechanism of cell adaptation: when and how do cancer cells develop chemoresistance? Cancer J 2011;17(2):89-95. Review.

Forstpointner R, Dreyling M, Repp R, Hermann S, Hänel A, Metzner B, Pott C, Hartmann F, Rothmann F, Rohrberg R, Böck HP, Wandt H, Unterhalt M, Hiddemann W. The addition of rituximab to a combination of fludarabine, cyclophosphamide, mitoxantrone (FCM) significantly increases the response rate and prolongs survival as compared with FCM alone in patients with relapsed and refractory follicular and mantle cell lymphomas: results of a prospective randomized study of the German Low-Grade Lymphoma Study Group. Blood 2004;104(10):3064-71.

Fränzel B, Fischer F, Trötschel C, Poetsch A, Wolters D. The two-phase partitioning system – a powerful technique to purify integral membrane proteins of Corynebacterium glutamicum for quantitative shotgun analysis. Proteomics 2009;9:2263-72.

Fujiki Y, Hubbard AL, Fowler S, Lazarow PB. Isolation of intracellular membranes by means of sodium carbonate treatment: application to endoplasmic reticulum. J Cell Biol 1982;93:97-102.

Furuta T, Ueda T, Aune G, Sarasin A, Kraemer KH, Pommier Y. Transcription-coupled nucleotide excision repair as a determinant of cisplatin sensitivity of human cells. Cancer Res 2002;62(17):4899-902.

Gahmberg CG, Andersson LC. Selective radioactive labeling of cell surface sialoglycoproteins by periodate-tritiated borohydride. J Biol Chem 1977;252:5888-94.

Galmarini CM, Thomas X, Calvo F, Rousselot P, Rabilloud M, El Jaffari A, Cros E, Dumontet C. In vivo mechanisms of resistance to cytarabine in acute myeloid leukaemia. Br J Haematol 2002;117(4):860-8.

Galmarini CM, Mackey JR, Dumontet C. Nucleoside analogues and nucleobases in cancer treatment. Lancet Oncol 2002;3(7):415-24. Review.

Galmarini CM, Popowycz F, Joseph B. Cytotoxic nucleoside analogues: different strategies to improve their clinical efficacy. Curr Med Chem 2008;15(11):1072-82. Review.

Gandhi V, Plunkett W. Cellular and clinical pharmacology of fludarabine. Clin Pharmacokinet 2002;41(2):93-103. Review.

Gandhi V, Kilpatrick JM, Plunkett W, Ayres M, Harman L, Du M, Bantia S, Davisson J, Wierda WG, Faderl S, Kantarjian H, Thomas D. A proof-of-principle pharmacokinetic, pharmacodynamic, and clinical study with purine nucleoside phosphorylase inhibitor immucillin-H (BCX-1777, forodesine). Blood 2005;106(13):4253-60.

Geiger T, Cox J, Ostasiewicz P, Wisniewski JR, Mann M. Super-SILAC mix for quantitative proteomics of human tumor tissue. Nat Methods 2010;7(5):383-5.

Ghosh D, Lippert D, Krokhin O, Cortens JP, Wilkins JA. Defining the membrane proteome of NK cells. J Mass Spectrom 2010;45:1-25.

Golizeh M, Sleno L. Optimized proteomic analysis of rat liver microsomes using dual enzyme digestion with 2D-LC-MS/MS. J Proteomics 2013;82:166-78.

Görg A, Weiss W, Dunn MJ. Current two-dimensional electrophoresis technology for proteomics. Proteomics 2004;4(12):3665-85. Review.

Grant S. Ara-C: cellular and molecular pharmacology. Adv Cancer Res 1998;72:197-233. Review.

Gross E. The cyanogen bromide reaction. In: Hirs CHW, editor. Methods in Enzymology, vol. 11: Enzyme Structure; Academic Press; 1967, p.238-255.

Gross E, Witkop B. Nonenzymatic cleavage of peptide bonds: the methionine residues in bovine pancreatic ribonuclease. J Biol Chem 1962;237:1856-60.

Gstaiger M, Aebersold R. Applying mass spectrometry-based proteomics to genetics, genomics and network biology. Nat Rev Genet 2009;10(9):617-27. Review.

Gundry RL, Riordon DR, Tarasova Y, Chuppa S, Bhattacharya S, Juhasz O, Wiedemeier O, Milanovich S, Noto FK, Tchernyshyov I, Raginski K, Bausch-Fluck D, Tae HJ, Marshall S *et al.* A cell surfaceome map for immunophenotyping and sorting pluripotent stem cells. Mol Cell Proteomics 2012;11:303-16.

Gupta N, Bandeira N, Keich U, Pevzner PA. Target-decoy approach and false discovery rate: when things may go wrong. J Am Soc Mass Spectrom 2011;22:1111-20.

Gygi SP, Corthals GL, Zhang Y, Rochon Y, Aebersold R. Evaluation of two-dimensional gel electrophoresis-based proteome analysis technology. Proc Natl Acad Sci U S A 2000;97(17):9390-5.

Han J, Schey KL. Proteolysis and mass spectrometric analysis of an integral membrane: aquaporin 0. J Proteome Res 2004;3(4):807-12.

Hariton-Gazal E, Rosenbluh J, Graessmann A, Gilon C, Loyter A. Direct translocation of histone molecules across cell membranes. J Cell Sci. 2003;116(Pt 22):4577-86.

Hebert AS, Richards AL, Bailey DJ, Ulbrich A, Coughlin EE, Westphall MS, Coon JJ. The one hour yeast proteome. Mol Cell Proteomics 2014;13(1):339-47.

Hedstrom L. IMP dehydrogenase: structure, mechanism, and inhibition. Chem Rev 2009;109(7):2903-28. Review.

Herrmann A, Hoster E, Zwingers T, Brittinger G, Engelhard M, Meusers P, Reiser M, Forstpointner R, Metzner B, Peter N, Wörmann B, Trümper L, Pfreundschuh M, Einsele H, *et al.* Improvement of overall survival in advanced stage mantle cell lymphoma. J Clin Oncol 2009;27(4):511-8.

Hoedt E, Chaoui K, Huvent I, Mariller C, Monsarrat B, Burlet-Schiltz O, Pierce A. SILAC-based proteomic profiling of the human MDA-MB-231 metastatic breast cancer cell line in response to the two antitumoral lactoferrin isoforms: the secreted lactoferrin and the intracellular delta-lactoferrin. PLoS One 2014;9(8):e104563.

Hofmann A, Gerrits B, Schmidt A, Bock T, Bausch-Fluck D, Aebersold R, Wollscheid B. Proteomic cell surface phenotyping of differentiating acute myeloid leukemia cells. Blood 2010;116:e26-34.

Hu Q, Noll RJ, Li H, Makarov A, Hardman M, Graham Cooks R. The Orbitrap: a new mass spectrometer. J Mass Spectrom 2005;40(4):430-43.

Huang T, Wang J, Yu W, He Z. Protein inference: a review. Brief Bioinform 2012;13(5):586-614

Hunsucker SA, Mitchell BS, Spychala J. The 5'-nucleotidases as regulators of nucleotide and drug metabolism. Pharmacol Ther 2005;107(1):1-30. Review.

Igney FH, Krammer PH. Death and anti-death: tumour resistance to apoptosis. Nat Rev Cancer 2002;2(4):277-88. Review.

Jares P, Colomer D, Campo E. Molecular pathogenesis of mantle cell lymphoma. J Clin Invest 2012;122(10):3416-23. Review.

Jensen ON. Modification-specific proteomics: characterization of post-translational modifications by mass spectrometry. Curr Opin Chem Biol 2004;8(1):33-41. Review.

Johnson SA. Use of fludarabine in the treatment of mantle cell lymphoma, Waldenström's macroglobulinemia and other uncommon B- and T-cell lymphoid malignancies. Hematol J 2004;5 Suppl 1:S50-61. Review.

Jungblut PR, Holzhütter HG, Apweiler R, Schlüter H. The speciation of the proteome. Chem Cent J 2008 Jul 18;2:16.

Kaiser J. Proteomics. Public-private group maps out initiatives. Science 2002;296(5569):827.

Kantarjian H, Barlogie B, Plunkett W, Velasquez W, McLaughlin P, Riggs S, Cabanillas F. High-dose cytosine arabinoside in non-Hodgkin's lymphoma. J Clin Oncol 1983;1(11):689-94.

Karas M, Bachmann D, Hillenkamp F. Influence of the wavelength in high-irradiance ultraviolet laser desorption mass spectrometry of organic molecules. Anal Chem 1985;57(14):2935-9.

Kelleher NL. A cell-based approach to the human proteome project. J Am Soc Mass Spectrom 2012;23(10):1617-24.

Kim MS, Pinto SM, Getnet D, Nirujogi RS, Manda SS, Chaerkady R, Madugundu AK, Kelkar DS, Isserlin R, Jain S, Thomas JK, Muthusamy B, Leal-Rojas P, Kumar P *et al.* A draft map of the human proteome. Nature 2014;509(7502):575-81.

Kluin-Nelemans HC, Hoster E, Hermine O, Walewski J, Trneny M, Geisler CH, Stilgenbauer S, Thieblemont C, Vehling-Kaiser U, Doorduijn JK, Coiffier B, Forstpointner R, Tilly H, Kanz L *et al.* Treatment of older patients with mantle-cell lymphoma. N Engl J Med 2012;367(6):520-31.

Krogh A, Larsson B, von Heijne G, Sonnhammer EL. Predicting transmembrane protein topology with a hidden Markov model: application to complete genomes. J Mol Biol 2001;305(3):567-80.

Kurbanov BM, Geilen CC, Fecker LF, Orfanos CE, Eberle J. Efficient TRAIL-R1/DR4-mediated apoptosis in melanoma cells by tumor necrosis factor-related apoptosis-inducing ligand (TRAIL). J Invest Dermatol 2005;125(5):1010-9.

Kume H, Muraoka S, Kuga T, Adachi J, Narumi R, Watanabe S, Kuwano M, Kodera Y, Matsushita K, Fukuoka J, Masuda T, Ishihama Y, Matsubara H, Nomura F, Tomonaga T. Discovery of colorectal cancer biomarker candidates by membrane proteomic analysis and subsequent verification using selected reaction monitoring (SRM) and tissue microarray (TMA) analysis. Mol Cell Proteomics 2014;13:1471-84.

Kurosaki T, Hikida M. Tyrosine kinases and their substrates in B lymphocytes. Immunol Rev 2009;228(1):132-48. Review.

Kyte J, Doolittle RF. A simple method for displaying the hydropathic character of a protein. J Mol Biol 1982;157(1):105-32.

Laliberté J, Momparler RL. Human cytidine deaminase: purification of enzyme, cloning, and expression of its complementary DNA. Cancer Res 1994;54(20):5401-7.

Lamba JK. Genetic factors influencing cytarabine therapy. Pharmacogenomics 2009;10(10):1657-74. Review.

Lane L, Bairoch A, Beavis RC, Deutsch EW, Gaudet P, Lundberg E, Omenn GS. Metrics for the Human Proteome Project 2013-2014 and strategies for finding missing proteins. J Proteome Res 2014;13(1):15-20.

Li JY, Gaillard F, Moreau A, Harousseau JL, Laboisse C, Milpied N, Bataille R, Avet-Loiseau H. Detection of translocation t(11;14)(q13;q32) in mantle cell lymphoma by fluorescence in situ hybridization. Am J Pathol 1999;154(5):1449-52.

Lin Y, Zhou J, Bi D, Chen P, Wang X, Liang S. Sodium-deoxycholate-assisted tryptic digestion and identification of proteolytically resistant proteins. Anal Biochem 2008;377:259-66.

Liu Y, Chen J, Sethi A, Li QK, Chen L, Collins B, Gillet LC, Wollscheid B, Zhang H, Aebersold R. Glycoproteomic analysis of prostate cancer tissues by SWATH mass spectrometry discovers N-acylethanolamine acid amidase and protein tyrosine kinase 7 as signatures for tumor aggressiveness. Mol Cell Proteomics 2014;13:1753-68.

Loo RR, Loo JA. Matrix-assisted laser desorption/ionization-mass spectrometry of hydrophobic proteins in mixtures using formic acid, perfluorooctanoic acid, and sorbitol. Anal Chem 2007;79:1115-25.

López-Ferrer D, Petritis K, Robinson EW, Hixson KK, Tian Z, Lee JH, Lee SW, Tolić N, Weitz KK, Belov ME, Smith RD, Pasa-Tolić L. Pressurized pepsin digestion in proteomics: an automatable alternative to trypsin for integrated top-down bottom-up proteomics. Mol Cell Proteomics 2011;10(2):M110.001479.

Lovric MM, Hawkins CJ. TRAIL treatment provokes mutations in surviving cells. Oncogene 2010;29(36):5048-60.

Lukenbill J, Kalaycio M. Fludarabine: a review of the clear benefits and potential harms. Leuk Res 2013;37(9):986-94. Review.

Lund R, Leth-Larsen R, Jensen ON, Ditzel HJ. Efficient isolation and quantitative proteomic analysis of cancer cell plasma membrane proteins for identification of metastasis-associated cell surface markers. J Proteome Res. 2009;8:3078-90.

Ma J, Hou C, Sun L, Tao D, Zhang Y, Shan Y, Liang Z, Zhang L, Yang L, Zhang Y. Coupling formic acid assisted solubilization and online immobilized pepsin digestion with strong cation exchange and microflow reversed-phase liquid chromatography with electrospray ionization tandem mass spectrometry for integral membrane proteome analysis. Anal Chem 2010;82:9622-5.

MacCoss MJ, Wu CC, Liu H, Sadygov R, Yates JR 3rd. A correlation algorithm for the automated quantitative analysis of shotgun proteomics data. Anal Chem 2003;75(24):6912-21.

Mackey JR, Baldwin SA, Young JD, Cass CE. Nucleoside transport and its significance for anticancer drug resistance. Drug Resist Updat 1998;1(5):310-24.

Mackey JR, Galmarini CM, Graham KA, Joy AA, Delmer A, Dabbagh L, Glubrecht D, Jewell LD, Lai R, Lang T, Hanson J, Young JD, Merle-Béral H, Binet JL *et al*. Quantitative analysis of nucleoside transporter and metabolism gene expression in chronic lymphocytic leukemia (CLL): identification of fludarabine-sensitive and -insensitive populations. Blood 2005;105(2):767-74.

Magdeldin S, Enany S, Yoshida Y, Xu B, Zhang Y, Zureena Z, Lokamani I, Yaoita E, Yamamoto T. Basics and recent advances of two dimensional-polyacrylamide gel electrophoresis. Clin Proteomics 2014;11(1):16. Review.

Mancini WR, Cheng YC. Human deoxycytidylate deaminase. Substrate and regulator specificities and their chemotherapeutic implications. Mol Pharmacol 1983;23(1):159-64.

Mann M, Kulak NA, Nagaraj N, Cox J. The coming age of complete, accurate, and ubiquitous proteomes. Mol Cell 2013;49(4):583-90.

Månsson E, Flordal E, Liliemark J, Spasokoukotskaja T, Elford H, Lagercrantz S, Eriksson S, Albertioni F. Down-regulation of deoxycytidine kinase in human leukemic cell lines resistant to cladribine and clofarabine and increased ribonucleotide reductase activity contributes to fludarabine resistance. Biochem Pharmacol 2003;65(2):237-47.

March RE. Quadrupole ion trap mass spectrometry: a view at the turn of the century. Int J Mass Spec 2000;200(1-3): 285-312. Review.

Marshall AG, Hendrickson CL, Jackson GS. Fourier transform ion cyclotron resonance mass spectrometry: a primer. Mass Spectrom Rev 1998;17(1):1-35. Review.

Marsters SA, Sheridan JP, Pitti RM, Huang A, Skubatch M, Baldwin D, Yuan J, Gurney A, Goddard AD, Godowski P, Ashkenazi A. A novel receptor for Apo2L/TRAIL contains a truncated death domain. Curr Biol 1997;7(12):1003-6.

Masuda T, Tomita M, Ishihama Y. Phase transfer surfactant-aided trypsin digestion for membrane proteome analysis. J Proteome Res 2008;7:731-40.

Mbeunkui F, Goshe MB. Investigation of solubilization and digestion methods for microsomal membrane proteome analysis using data-independent LC-MSE. Proteomics 2011;11:898-911.

Megger DA, Bracht T, Meyer HE, Sitek B. Label-free quantification in clinical proteomics. Biochim Biophys Acta 2013;1834(8):1581-90.

Mérino D, Lalaoui N, Morizot A, Schneider P, Solary E, Micheau O. Differential inhibition of TRAIL-mediated DR5-DISC formation by decoy receptors 1 and 2. Mol Cell Biol 2006;26(19):7046-55.

Merrill AE, Hebert AS, MacGilvray ME, Rose CM, Bailey DJ, Bradley JC, Wood WW, El Masri M, Westphall MS, Gasch AP, Coon JJ. NeuCode labels for relative protein quantification. Mol Cell Proteomics 2014;13(9):2503-12.

Messina M, Del Giudice I, Khiabanian H, Rossi D, Chiaretti S, Rasi S, Spina V, Holmes AB, Marinelli M, Fabbri G, Piciocchi A, Mauro FR, Guarini A, Gaidano G *et al.* Genetic lesions associated with chronic lymphocytic leukemia chemo-refractoriness. Blood 2014;123(15):2378-88.

Meyers M, Wagner MW, Hwang HS, Kinsella TJ, Boothman DA. Role of the hMLH1 DNA mismatch repair protein in fluoropyrimidine-mediated cell death and cell cycle responses. Cancer Res 2001;61(13):5193-201.

Moest H, Frei AP, Bhattacharya I, Geiger M, Wollscheid B, Wolfrum C. Malfunctioning of adipocytes in obesity is linked to quantitative surfaceome changes. Biochim Biophys Acta 2013;1831:1208-16.

Molina-Arcas M, Bellosillo B, Casado FJ, Montserrat E, Gil J, Colomer D, Pastor-Anglada M. Fludarabine uptake mechanisms in B-cell chronic lymphocytic leukemia. Blood 2003;101(6):2328-34.

Molinský J, Klánová M, Koc M, Beranová L, Anděra L, Ludvíková Z, Böhmová M, Gašová Z, Strnad M, Ivánek R, Trněný M, Nečas E, Živný J, Klener P. Roscovitine sensitizes leukemia and lymphoma cells to tumor necrosis factor-related apoptosis-inducing ligand-induced apoptosis. Leuk Lymphoma. 2013;54(2):372-80.

Moore SM, Hess SM, Jorgenson JW. Extraction, enrichment, solubilization, and digestion techniques for membrane proteomics. J Proteome Res 2016;15(4):1243-52.

Morizot A, Mérino D, Lalaoui N, Jacquemin G, Granci V, Iessi E, Lanneau D, Bouyer F, Solary E, Chauffert B, Saas P, Garrido C, Micheau O. Chemotherapy overcomes TRAIL-R4-mediated TRAIL resistance at the DISC level. Cell Death Differ 2011;18(4):700-11.

Moussay E, Palissot V, Vallar L, Poirel HA, Wenner T, El Khoury V, Aouali N, Van Moer K, Leners B, Bernardin F, Muller A, Cornillet-Lefebvre P, Delmer A, Duhem C *et al.* Determination of genes and microRNAs involved in the resistance to fludarabine in vivo in chronic lymphocytic leukemia. Mol Cancer 2010;9:115.

Muraoka S, Kume H, Adachi J, Shiromizu T, Watanabe S, Masuda T, Ishihama Y, Tomonaga T. In-depth membrane proteomic study of breast cancer tissues for the generation of a chromosome-based protein list. J Proteome Res 2013;12:208-13.

Nagaraj N, Wisniewski JR, Geiger T, Cox J, Kircher M, Kelso J, Pääbo S, Mann M. Deep proteome and transcriptome mapping of a human cancer cell line. Mol Syst Biol 2011 Nov 8;7:548.

Natsumeda Y, Prajda N, Donohue JP, Glover JL, Weber G. Enzymic capacities of purine de novo and salvage pathways for nucleotide synthesis in normal and neoplastic tissues. Cancer Res 1984;44(6):2475-9.

Neilson KA, Ali NA, Muralidharan S, Mirzaei M, Mariani M, Assadourian G, Lee A, van Sluyter SC, Haynes PA. Less label, more free: approaches in label-free quantitative mass spectrometry. Proteomics 2011;11(4):535-53. Review.

Nesvizhskii AI. A survey of computational methods and error rate estimation procedures for peptide and protein identification in shotgun proteomics. J Proteomics 2010;73(11):2092-123. Review.

Oltvai ZN, Milliman CL, Korsmeyer SJ. Bcl-2 heterodimerizes in vivo with a conserved homolog, Bax, that accelerates programmed cell death. Cell 1993;74(4):609-19.

Omenn GS, States DJ, Adamski M, Blackwell TW, Menon R, Hermjakob H, Apweiler R, Haab BB, Simpson RJ, Eddes JS, Kapp EA, Moritz RL, Chan DW, Rai AJ *et al.* Overview of the HUPO Plasma Proteome Project: results from the pilot phase with 35 collaborating laboratories and multiple analytical groups, generating a core dataset of 3020 proteins and a publicly-available database. Proteomics 2005;5(13):3226-45.

Ong SE, Blagoev B, Kratchmarova I, Kristensen DB, Steen H, Pandey A, Mann M. Stable isotope labeling by amino acids in cell culture, SILAC, as a simple and accurate approach to expression proteomics. Mol Cell Proteomics 2002;1(5):376-86.

Ong SE, Mann M. A practical recipe for stable isotope labeling by amino acids in cell culture (SILAC). Nat Protoc 2006;1(6):2650-60.

Pan G, O'Rourke K, Chinnaiyan AM, Gentz R, Ebner R, Ni J, Dixit VM. The receptor for the cytotoxic ligand TRAIL. Science. 1997;276(5309):111-3.

Pappin DJ, Hojrup P, Bleasby AJ. Rapid identification of proteins by peptide-mass fingerprinting. Curr Biol 1993;3(6):327-32.

Perkins DN, Pappin DJ, Creasy DM, Cottrell JS. Probability-based protein identification by searching sequence databases using mass spectrometry data. Electrophoresis 1999;20(18):3551-67.

Pernemalm M, Lehtiö J. Mass spectrometry-based plasma proteomics: state of the art and future outlook. Expert Rev Proteomics 2014;11(4):431-48. Review.

Petrák J, Toman O, Simonova T, Halada P, Cmejla R, Klener P, Zivny J. Identification of molecular targets for selective elimination of TRAIL-resistant leukemia cells. From spots to in vitro assays using TOP15 charts. Proteomics 2009;9(22):5006-15.

Piszkiewicz D, Landon M, Smith EL. Anomalous cleavage of aspartyl-proline peptide bonds during amino acid sequence determinations. Biochem Biophys Res Commun 1970;40:1173-8.

Qin T, Jelinek J, Si J, Shu J, Issa JP. Mechanisms of resistance to 5-aza-2'-deoxycytidine in human cancer cell lines. Blood 2009;113(3):659-67.

Rauniyar N, Yates JR 3rd. Isobaric labeling-based relative quantification in shotgun proteomics. J Proteome Res 2014;13(12):5293-309. Review.

Rebucci M, Michiels C. Molecular aspects of cancer cell resistance to chemotherapy. Biochem Pharmacol 2013;85(9):1219-26. Review.

Reed JC. Bcl-2 family proteins: regulators of apoptosis and chemoresistance in hematologic malignancies. Semin Hematol 1997;34(4 Suppl 5):9-19. Review.

Rey M, Mrázek H, Pompach P, Novák P, Pelosi L, Brandolin G, Forest E, Havlícek V, Man P. Effective removal of nonionic detergents in protein mass spectrometry, hydrogen/deuterium exchange, and proteomics. Anal Chem 2010;82(12):5107-16.

Reynolds JA, Tanford C. Binding of dodecyl sulfate to proteins at high binding ratios. Possible implications for the state of proteins in biological membranes. Proc Natl Acad Sci USA 1970;66:1002-7.

Riedl SJ, Shi Y. Molecular mechanisms of caspase regulation during apoptosis. Nat Rev Mol Cell Biol 2004;5(11):897-907. Review.

Rietschel B, Arrey TN, Meyer B, Bornemann S, Schuerken M, Karas M, Poetsch A. Elastase digests: new ammunition for shotgun membrane proteomics. Mol Cell Proteomics 2009;8:1029-43.

Rietschel B, Bornemann S, Arrey TN, Baeumlisberger D, Karas M, Meyer B. Membrane protein analysis using an improved peptic in-solution digestion protocol. Proteomics. 2009;9(24):5553-7.

Ross PL, Huang YN, Marchese JN, Williamson B, Parker K, Hattan S, Khainovski N, Pillai S, Dey S, Daniels S, Purkayastha S, Juhasz P, Martin S, Bartlet-Jones M *et al.* Multiplexed protein quantitation in Saccharomyces cerevisiae using amine-reactive isobaric tagging reagents. Mol Cell Proteomics 2004;3(12):1154-69.

Rossi D, Fangazio M, Rasi S, Vaisitti T, Monti S, Cresta S, Chiaretti S, Del Giudice I, Fabbri G, Bruscaggin A, Spina V, Deambrogi C, Marinelli M, Famà R *et al.* Disruption of BIRC3 associates with fludarabine chemorefractoriness in TP53 wild-type chronic lymphocytic leukemia. Blood 2012;119(12):2854-62.

Saba N, Wiestner A. Do mantle cell lymphomas have an 'Achilles heel'? Curr Opin Hematol 2014;21(4):350-7. Review.

Satterthwaite AB, Witte ON. The role of Bruton's tyrosine kinase in B-cell development and function: a genetic perspective. Immunol Rev 2000;175:120-7. Review.

Scavennec J, Maraninchi D, Gastaut JA, Carcassonne Y, Cailla HL. Purine and pyrimidine ribonucleoside monophosphate patterns of peripheral blood and bone marrow cells in human acute leukemias. Cancer Res 1982;42(4):1326-30.

Schiess R, Mueller LN, Schmidt A, Mueller M, Wollscheid B, Aebersold R. Analysis of cell surface proteome changes via label-free, quantitative mass spectrometry. Mol Cell Proteomics 2009;8:624-38.

Schneider P, Bodmer JL, Thome M, Hofmann K, Holler N, Tschopp J. Characterization of two receptors for TRAIL. FEBS Lett. 1997;416(3):329-34.

Schwanhäusser B, Busse D, Li N, Dittmar G, Schuchhardt J, Wolf J, Chen W, Selbach M. Global quantification of mammalian gene expression control. Nature 2011;473(7347):337-42.

Schwartz JC, Senko MW, Syka JE. A two-dimensional quadrupole ion trap mass spectrometer. J Am Soc Mass Spectrom 2002;13(6):659-69.

Sharma A, Singh K, Mazumder S, Hill BT, Kalaycio M, Almasan A. BECN1 and BIM interactions with MCL-1 determine fludarabine resistance in leukemic B cells. Cell Death Dis 2013;4:e628.

Sharpe HJ, Stevens TJ, Munro S. A comprehensive comparison of transmembrane domains reveals organelle-specific properties. Cell 2010;142:158-69.

Sherr CJ. G1 phase progression: cycling on cue. Cell 1994;79(4):551-5. Review.

Shultz LD, Lyons BL, Burzenski LM, Gott B, Chen X, Chaleff S, Kotb M, Gillies SD, King M, Mangada J, Greiner DL, Handgretinger R. Human lymphoid and myeloid cell development in NOD/LtSz-scid IL2R gamma null mice engrafted with mobilized human hemopoietic stem cells. J Immunol 2005;174(10):6477-89.

Smith LM, Kelleher NL. Consortium for Top Down Proteomics. Proteoform: a single term describing protein complexity. Nat Methods 2013;10(3):186-7.

Souers AJ, Leverson JD, Boghaert ER, Ackler SL, Catron ND, Chen J, Dayton BD, Ding H, Enschede SH, Fairbrother WJ, Huang DC, Hymowitz SG, Jin S, Khaw SL *et al.* ABT-199, a potent and selective BCL-2 inhibitor, achieves antitumor activity while sparing platelets. Nat Med 2013;19(2):202-8.

Sun D, Wang N, Li L. Integrated SDS removal and peptide separation by strong-cation exchange liquid chromatography for SDS-assisted shotgun proteome analysis. J Proteome Res 2012;11(2):818-28.

Tedeschi PM, Markert EK, Gounder M, Lin H, Dvorzhinski D, Dolfi SC, Chan LL, Qiu J, DiPaola RS, Hirshfield KM, Boros LG, Bertino JR, Oltvai ZN, Vazquez A. Contribution of serine, folate and glycine metabolism to the ATP, NADPH and purine requirements of cancer cells. Cell Death Dis 2013;4:e877.

Thiede B, Koehler CJ, Strozynski M, Treumann A, Stein R, Zimny-Arndt U, Schmid M, Jungblut PR. High resolution quantitative proteomics of HeLa cells protein species using stable isotope labeling with amino acids in cell culture(SILAC), two-dimensional gel electrophoresis(2DE) and nano-liquid chromatograpohy coupled to an LTQ-OrbitrapMass spectrometer. Mol Cell Proteomics 2013;12(2):529-38.

Thompson A, Schäfer J, Kuhn K, Kienle S, Schwarz J, Schmidt G, Neumann T, Johnstone R, Mohammed AK, Hamon C. Tandem mass tags: a novel quantification strategy for comparative analysis of complex protein mixtures by MS/MS. Anal Chem 2003;75(8):1895-904.

Thorburn A, Behbakht K, Ford H. TRAIL receptor-targeted therapeutics: resistance mechanisms and strategies to avoid them. Drug Resist Updat. 2008;11(1-2):17-24. Review.

Tian Y, Zhou Y, Elliott S, Aebersold R, Zhang H. Solid-phase extraction of N-linked glycopeptides. Nat Protoc 2007;2:334-9.

Tylečková J, Valeková I, Žižková M, Rakocyová M, Marsala S, Marsala M, Gadher SJ, Kovářová H. Surface N-glycoproteome patterns reveal key proteins of neuronal differentiation. J Proteomics 2016;132:13-20.

Ulmschneider MB, Sansom MS, Di Nola A. Properties of integral membrane protein structures: derivation of an implicit membrane potential. Proteins 2005;59:252-65.

Van Damme P, Maurer-Stroh S, Plasman K, Van Durme J, Colaert N, Timmerman E, De Bock PJ, Goethals M, Rousseau F, Schymkowitz J, Vandekerckhove J, Gevaert K. Analysis of protein processing by N-terminal proteomics reveals novel species-specific substrate determinants of granzyme B orthologs. Mol Cell Proteomics 2009;8(2):258-72.

van Montfort BA, Doeven MK, Canas B, Veenhoff LM, Poolman B, Robillard GT. Combined in-gel tryptic digestion and CNBr cleavage for the generation of peptide maps of an integral membrane protein with MALDI-TOF mass spectrometry. Biochim Biophys Acta 2002;1555:111-5.

Vit O, Petrak J. Integral membrane proteins in proteomics. How to break open the black box? J Proteomics 2017;153:8-20.

Voortman J, Resende TP, Abou El Hassan MA, Giaccone G, Kruyt FA. TRAIL therapy in non-small cell lung cancer cells: sensitization to death receptor-mediated apoptosis by proteasome inhibitor bortezomib. Mol Cancer Ther 2007;6(7):2103-12.

Vuckovic D, Dagley LF, Purcell AW, Emili A. Membrane proteomics by high performance liquid chromatography-tandem mass spectrometry: Analytical approaches and challenges. Proteomics 2013;13:404-23.

Waas M, Bhattacharya S, Chuppa S, Wu X, Jensen DR, Omasits U, Wollscheid B, Volkman BF, Noon KR, Gundry RL. Combine and conquer: surfactants, solvents, and chaotropes for robust mass spectrometry based analyses of membrane proteins. Anal Chem 2014;86:1551-9.

Washburn MP, Wolters D, Yates JR 3rd. Large-scale analysis of the yeast proteome by multidimensional protein identification technology. Nat Biotechnol 2001;19(3):242-7.

Walczak H, Miller RE, Ariail K, Gliniak B, Griffith TS, Kubin M, Chin W, Jones J, Woodward A, Le T, Smith C, Smolak P, Goodwin RG, Rauch CT *et al*. Tumoricidal activity of tumor necrosis factor-related apoptosis-inducing ligand in vivo. Nat Med 1999;5(2):157-63.

Wang L, Mosel AJ, Oakley GG, Peng A. Deficient DNA damage signaling leads to chemoresistance to cisplatin in oral cancer. Mol Cancer Ther 2012;11(11):2401-9.

Wang ML, Rule S, Martin P, Goy A, Auer R, Kahl BS, Jurczak W, Advani RH, Romaguera JE, Williams ME, Barrientos JC, Chmielowska E, Radford J, Stilgenbauer S *et al*. Targeting BTK with ibrutinib in relapsed or refractory mantle-cell lymphoma. N Engl J Med 2013;369(6):507-16.

Wasinger VC, Cordwell SJ, Cerpa-Poljak A, Yan JX, Gooley AA, Wilkins MR, Duncan MW, Harris R, Williams KL, Humphery-Smith I. Progress with gene-product mapping of the Mollicutes: Mycoplasma genitalium. Electrophoresis 1995;16(7):1090-4.

Watson K, Gooderham NJ, Davies DS, Edwards RJ. Nucleosomes bind to cell surface proteoglycans. J Biol Chem 1999;274(31):21707-13.

Weickhardt C, Moritz F, Grotemeyer J. Time-of-flight mass spectrometry: State-of the-art in chemical analysis and molecular science. Mass Spectrom Rev 1996;15(3):139-62. Review.

Wiley SR, Schooley K, Smolak PJ, Din WS, Huang CP, Nicholl JK, Sutherland GR, Smith TD, Rauch C, Smith CA, et al. Identification and characterization of a new member of the TNF family that induces apoptosis. Immunity 1995;3(6):673-82.

Wilhelm M, Schlegl J, Hahne H, Gholami AM, Lieberenz M, Savitski MM, Ziegler E, Butzmann L, Gessulat S, Marx H, Mathieson T, Lemeer S, Schnatbaum K, Reimer U *et al*. Mass-spectrometry-based draft of the human proteome. Nature 2014;509(7502):582-7.

Wilkins M. Proteomics data mining. Expert Rev Proteomics 2009;6(6):599-603.

Wilson SR, Vehus T, Berg HS, Lundanes E. Nano-LC in proteomics: recent advances and approaches. Bioanalysis 2015;7(14):1799-815. Review.

Wiśniewski JR, Zougman A, Mann M. Combination of FASP and StageTip-based fractionation allows in-depth analysis of the hippocampal membrane proteome. J Proteome Res 2009;8:5674-8.

Wiśniewski JR, Zougman A, Nagaraj N, Mann M. Universal sample preparation method for proteome analysis. Nat Methods 2009;6:359-62.

Wiśniewski JR, Mann M. Consecutive proteolytic digestion in an enzyme reactor increases depth of proteomic and phosphoproteomic analysis. Anal Chem 2012;84:2631-7.

Wollscheid B, Bausch-Fluck D, Henderson C, O'Brien R, Bibel M, Schiess R, Aebersold R, Watts JD. Mass-spectrometric identification and relative quantification of N-linked cell surface glycoproteins. Nat Biotechnol 2009;27:378-86.

Wu CC, MacCoss MJ, Howell KE, Yates JR 3rd. A method for the comprehensive proteomic analysis of membrane proteins. Nat Biotechnol 2003;21:532-8.

Wu F, Sun D, Wang N, Gong Y, Li L. Comparison of surfactant-assisted shotgun methods using acid-labile surfactants and sodium dodecyl sulfate for membrane proteome analysis. Anal Chim Acta 2011;698:36-43.

Wu CP, Hsieh CH, Wu YS. The emergence of drug transporter-mediated multidrug resistance to cancer chemotherapy. Mol Pharm 2011;8(6):1996-2011. Review.

Wu L, Candille SI, Choi Y, Xie D, Jiang L, Li-Pook-Than J, Tang H, Snyder M. Variation and genetic control of protein abundance in humans. Nature 2013;499(7456):79-82.

Yang F, Shen Y, Camp DG, Smith RD. High pH reversed-phase chromatography with fraction concatenation as an alternative to strong-cation exchange chromatography for two-dimensional proteomic analysis. Expert Rev Proteomics 2012;9(2):129-134.

Yao X, Freas A, Ramirez J, Demirev PA, Fenselau C. Proteolytic 18O labeling for comparative proteomics: model studies with two serotypes of adenovirus. Anal Chem 2001;73(13):2836-42.

Yildirim MA, Goh KI, Cusick ME, Barabási AL, Vidal M. Drug-target network. Nat Biotechnol 2007;25):1119-26.

Yu YQ, Gilar M, Lee PJ, Bouvier ES, Gebler JC. Enzyme-friendly, mass spectrometry-compatible surfactant for in-solution enzymatic digestion of proteins. Anal Chem 2003;75:6023-8.

Yu Y, Xie L, Gunawardena HP, Khatun J, Maier C, Spitzer W, Leerkes M, Giddings MC, Chen X. GOFAST: an integrated approach for efficient and comprehensive membrane proteome analysis. Anal Chem 2012;84:9008-14.

Zenz T, Häbe S, Denzel T, Mohr J, Winkler D, Bühler A, Sarno A, Groner S, Mertens D, Busch R, Hallek M, Döhner H, Stilgenbauer S. Detailed analysis of p53 pathway defects in fludarabine-refractory chronic lymphocytic leukemia (CLL): dissecting the contribution of 17p deletion, TP53 mutation, p53-p21 dysfunction, and miR34a in a prospective clinical trial. Blood 2009;114(13):2589-97.

Zhang R, Sioma CS, Wang S, Regnier FE. Fractionation of isotopically labeled peptides in quantitative proteomics. Anal Chem. 2001;73(21):5142-9.

Zhang H, Li XJ, Martin DB, Aebersold R. Identification and quantification of N-linked glycoproteins using hydrazide chemistry, stable isotope labeling and mass spectrometry. Nat Biotechnol 2003;21:660-6.

Zhang J, Visser F, King KM, Baldwin SA, Young JD, Cass CE. The role of nucleoside transporters in cancer chemotherapy with nucleoside drugs. Cancer Metastasis Rev 2007;26(1):85-110. Review.

Zhang H, Lin Q, Ponnusamy S, Kothandaraman N, Lim TK, Zhao C, Kit HS, Arijit B, Rauff M, Hew CL, Chung MC, Joshi SB, Choolani M. Differential recovery of membrane proteins after extraction by aqueous methanol and trifluoroethanol. Proteomics 2007;7:1654-63.

Zhao Q, Liang Y, Yuan H, Sui Z, Wu Q, Liang Z, Zhang L, Zhang Y. Biphasic microreactor for efficient membrane protein pretreatment with a combination of formic acid assisted solubilization, on-column pH adjustment, reduction, alkylation, and tryptic digestion. Anal Chem 2013;85:8507-12.

Zhou S, Liu R, Baroudy BM, Malcolm BA, Reyes GR. The effect of ribavirin and IMPDH inhibitors on hepatitis C virus subgenomic replicon RNA. Virology 2003;310(2):333-42.

Zhu Y, Choi SH, Shah K. Multifunctional receptor-targeting antibodies for cancer therapy. Lancet Oncol 2015;16(15):e543-54. Review.

Zielinska DF, Gnad F, Wiśniewski JR, Mann M. Precision mapping of an in vivo N-glycoproteome reveals rigid topological and sequence constraints. Cell 2010;141:897-907.

7 Appendices

7.1 Appendix 1

Resistance to TRAIL in mantle cell lymphoma cells is associated with the decreased expression of purine metabolism enzymes. Pospisilova J, Vit O, Lorkova L, Klanova M, Zivny J, Klener P, Petrak J. *International Journal of Molecular Medicine* 2013; 31(5):1273 (IF 2013: 1.880).

Resistance to TRAIL in mantle cell lymphoma cells is associated with the decreased expression of purine metabolism enzymes

JANA POSPISILOVA[1], ONDREJ VIT[1], LUCIE LORKOVA[1], MAGDALENA KLANOVA[1], JAN ZIVNY[1], PAVEL KLENER[1] and JIRI PETRAK[1,2]

[1]Institute of Pathological Physiology, First Faculty of Medicine, Charles University in Prague, 128 53 Prague; [2]Institute of Hematology and Blood Transfusion, 128 20 Prague, Czech Republic

Received January 25, 2013; Accepted March 1, 2013

DOI: 10.3892/ijmm.2013.1302

Abstract. Mantle cell lymphoma (MCL) is a rare aggressive type of B-cell non-Hodgkin's lymphoma. Response to chemotherapy tends to be short and virtually all patients sooner or later relapse. The prognosis of relapsed patients is extremely poor. The tumor necrosis factor-related apoptosis-inducing ligand (TRAIL) is considered one of the novel experimental molecules with strong antitumor effects. TRAIL triggers extrinsic apoptotis in tumor cells by binding to TRAIL 'death receptors' on the cell surface. Recombinant TRAIL has shown promising pro-apoptotic effects in a variety of malignancies including lymphoma. However, as with other drugs, lymphoma cells can develop resistance to TRAIL. Therefore, the aim of this study was to identify the molecular mechanisms responsible for, and associated with TRAIL resistance in MCL cells. If identified, these features may be used as molecular targets for the effective elimination of TRAIL-resistant lymphoma cells. From an established TRAIL-sensitive mantle cell lymphoma cell line (HBL-2) we derived a TRAIL-resistant HBL-2/R subclone. By TRAIL receptor analysis and differential proteomic analysis of HBL-2 and HBL-2/R cells we revealed a marked downregulation of all TRAIL receptors and, among others, the decreased expression of 3 key enzymes of purine nucleotide metabolism, namely purine nucleoside phosphorylase, adenine phosphoribosyltransferase and inosine-5'-monophosphate dehydrogenase 2, in the resistant HBL-2/R cells. The downregulation of the 3 key enzymes of purine metabolism can have profound effects on nucleotide homeostasis in TRAIL-resistant lymphoma cells and can render such cells vulnerable to any further disruption of purine nucleotide metabolism. This pathway represents a 'weakness' of the TRAIL-resistant MCL cells and has potential as a therapeutic target for the selective elimination of such cells.

Correspondence to: Ms. Jana Pospisilova, Institute of Pathological Physiology, First Faculty of Medicine, Charles University in Prague, U Nemocnice 5, 128 53 Prague, Czech Republic
E-mail: jana.pospisilova@lf1.cuni.cz

Key words: mantle cell lymphoma, TRAIL, drug resistance, purine nucleotide metabolism, proteomics

Introduction

Mantle cell lymphoma (MCL) is a rare agressive type of B-cell non-Hodgkin's lymphoma with an estimated annual incidence in Europe of 0.45/100,000 individuals (1). MCL is a biologically and clinically heterogeneous disease; the immunophenotype of neoplastic cells reflects the phenotype of cells similar to lymphocytes in the mantle zone of normal germinal follicles (2). The genetic hallmark of MCL cells is a translocation between chromosomes 11 and 14, t(11;14)(q13;q32), juxtaposing the gene for immunoglobulin heavy chain and the gene encoding cyclin D1. This results in cyclin D1 overexpression (3,4).

The standard of care for newly diagnosed MCL patients is combined immunochemotherapy alternating rituximab-CHOP (R-CHOP; cyclophosphamide, vincristine, doxorubicin and prednisone) and R-HDAC (high-dose cytarabine). The addition of rituximab and HDAC to CHOP has improved the survival of MCL patients in the last 2 decades from 3 to 5 years. However, the response to therapy tends to be short and virtually all patients sooner or later relapse. There is no standard of care for relapsed or refractory MCL patients. Salvage therapy usually comprises diverse regimens based on fludarabine, gemcitabine, cisplatin, bendamustine, bortezomib (inhibitor of 26S proteasome) or temsirolimus (inhibitor of mTOR). Recently, several new experimental molecules have shown promise in the therapy of relapsed or resistant MCL, including lenalidomide (immunomodulatory agent), ibrutinib (PCI-32765, inhibitor of Bruton's tyrosine-kinase), new monoclonal antibodies (e.g., anti-CD20 ofatumumab), as well as other agents (5). Combination therapies are currently being evaluated in clinical trials; however, novel drugs are required.

The tumor necrosis factor-related apoptosis-inducing ligand (TRAIL) is considered one of the novel experimental molecules with strong antitumor effects. TRAIL is a type II transmembrane protein from the tumor necrosis factor superfamily (6,7) expressed mostly by cells of the immune system (natural killer cells, cytotoxic T-cells, macrophages and dendritic cells). The main function of this molecule is thought to be in tumor immunosurveillance, but its actual molecular role remains to be elucidated.

TRAIL can trigger extrinsic apoptotis in target cells by binding to TRAIL death receptors located on the cell surface (8). This interaction is performed by a long extracellular C-terminal

region of the TRAIL molecule. There are 4 distinct cell surface TRAIL receptors in humans (DcR1, DcR2, DR4 and DR5) encoded by separate genes (9,10). However, only DR4 and DR5 contain a functional death domain (structurally conserved protein interaction domain) and are capable of signaling apoptosis. Two decoy receptors (DcR1 and DcR2) lack a functional death domain and inhibit TRAIL signaling by competing with death receptors for TRAIL (9,10). The binding of TRAIL to DR4 or DR5 leads to receptor homotrimerization and formation of the death-inducing signaling complex (DISC) (11). Through the DISC a caspase machinery is activated, which results in apoptosis (12). TRAIL death receptors DR4 and DR5 are ubiquitously expressed, indicating that most tissues and cell types are potential targets of TRAIL signaling (13). Nevertheless, TRAIL seems to induce apoptosis only in tumor cells but not in healthy tissues. Due to its selective pro-apoptotic effect, TRAIL has attracted much attention for its possible use in cancer therapy. *In vitro*, a recombinant soluble TRAIL molecule has shown cytostatic or cytotoxic effects in a wide variety of tumor cell lines, including leukemia and lymphoma cells, but not in normal cells (6,7,10,11,14-19). The administration of a recombinant soluble TRAIL molecule has been shown to induce the regression or complete remission of tumors in tumor xenograft models (11,20-26). The efficacy of recombinant TRAIL and agonistic antibodies recognizing either receptor DR4 or DR5 has been investigated in numerous clinical trials, as recently reviewed (27).

TRAIL has also shown promising pro-apoptotic effects in a variety of lymphoma cell lines including MCL (15). However, as with other drugs, cancer cells can develop resistance to TRAIL following prolonged exposure to sublethal doses of TRAIL (14,28). Resistance to TRAIL-mediated apoptosis can arise due to changes at the cell membrane level (typically by loss of expression or mutation of functional DR4 and/or DR5 at the cell surface) or on the intracellular level (such as incorrect formation of DISC and abberant expression of caspases) (29). The successful therapy of malignancies in general, and particularly those with very poor prognosis, such as MCL, depends on the effective management of drug resistance. An in-depth understanding of the processes involved in the development of drug resistance and a detailed description of secondary molecular changes associated with resistance are essential for successful cancer therapy. Specific molecular changes which occur in drug-resistant cells can confer a potential selective disadvatage to such cells and may be used as targets for the effective elimination of drug-resistant lymphoma cells.

The aim of this study was to elucidate the molecular mechanisms responsible for TRAIL resistance in MCL cells, as well as the secondary molecular alterations associated with this process. We also aimed to identify the phenotypic features specific for TRAIL-resistant MCL cells. If identified, these molecular features can be, at least theoretically, used as molecular targets for the effective elimination of TRAIL-resistant lymphoma cells in experimental therapies.

Materials and methods

Cell growth and cellular toxicity assay. HBL-2 cells were grown in Iscove's modified Dulbecco's medium in the presence of 10% foetal bovine serum, 1% penicillin-streptomycin solution in a 37˚C humidified atmosphere with 5% CO_2. TRAIL-resistant HBL-2/R cells were derived by selective pressure of increasing concentrations of human recombinant TRAIL (Apronex Biotechnologies, Czech Republic) up to 1,000 ng/ml in medium from the wild-type HBL-2 cells in 5 weeks. The toxicity of TRAIL to HBL-2 and HBL-2/R was measured using the colorimetric WST-8-based Quick Cell proliferation Assay kit II (BioVision, San Francisco, CA, USA) according to the manufacturer's instructions. Briefly, 40,000 cells were seeded in a 96-well plate in 300 μl of medium supplemented with increased concentrations of TRAIL up to 1,000 ng/ml in medium for 1-4 days. After the addition of WST reagent, absorbance was measured on a Sunrise microplate absorbance reader (Tecan Group Ltd., Männedorf, Switzerland) with a 450 nm reading filter and 630 nm reference filter. The absorbance of free medium was used as the background level, triplicate samples were grown and measured for each cell type and TRAIL concentration. Mean values were calculated. All chemicals were purchased from Sigma-Aldrich (St. Louis, MO, USA) unless specified otherwise.

Flow cytometric analysis. HBL-2 and HBL-2/R cells ($2x10^5$ cells for each assay) were washed in PBS buffer (0.5% foetal bovine serum in PBS), stained with phycoerythrin-conjugated antibodies against TRAIL receptors DR4, DR5, DcR1 and DcR2 (anti-hTRAIL R1, anti-hTRAIL R2, anti-hTRAIL R3 and anti-hTRAIL R4; R&D Systems, Minneapolis, MN, USA) and analyzed by flow cytometry in triplicate (FASCCanto II, BD Biosciences, San Jose, CA, USA). Unstained cells and cells incubated with isotype controls served as the background fluorescence controls.

Sample preparation for two-dimensional electrophoresis. HBL-2 and HBL-2/R cells ($6x10^7$) were harvested, washed twice with PBS and cell pellets were frozen and stored at -80˚C. Samples were thawed and homogenized in lysis buffer [7 M urea, 2 M thiourea, 4% CHAPS, 60 mM dithiothreitol (DTT) and 1% ampholytes (Bio-Lyte 3-10 Buffer, Bio-Rad, Hercules, CA, USA)] and protease inhibitor cocktail (Roche Diagnostics GmbH, Mannheim, Germany) for 20 min at room temperature with occasional vortexing. Samples were sedimented at 18,000 x g for 20 min at room temperature, supernatants were collected and protein concentration was determined by the Bradford assay (Bio-Rad). Protein concentrations in all samples were equalized to 3.3 mg/ml by dilution with lysis buffer.

Two-dimensional electrophoresis. IPG strips (pH 4.0-7.0, 24 cm; ReadyStrip, Bio-Rad) were rehydrated overnight in 450 μl of sample, representing 1.5 mg of protein. Isoelectric focusing was performed for 70 kVh, with maximum voltage not exceeding 5 kV, current limited to 50 μA per strip and temperature set to 20˚C (Protean IEF Cell, Bio-Rad). Six replicates were run for each cell type. Focused strips were briefly rinsed in deionized water, equilibrated and reduced in equilibration buffer supplemented with DTT (6 M urea, 50 mM Tris pH 8.8, 30% glycerol, 2% SDS and 450 mg DTT per 50 ml) for 15 min and then alkylated in equilibration buffer with iodacetamide (1.125 mg iodacetamide per 50 ml of the buffer). Equilibrated strips were then secured on 10% SDS-PAGE and secured in place by molten agarose. SDS-PAGE electrophoresis was performed in

a Tris-glycine-SDS system using a 12-gel Protean Dodeca Cell apparatus (Bio-Rad) with buffer circulation and external cooling (20˚C). Gels were run at a constant voltage of 45 V per gel for 30 min and then at a constant voltage of 200 V for 6 h. Gels were washed 3 times for 15 min in deionized water to remove redundant SDS. Gels were then stained with colloidal Coomassie Brilliant Blue (SimplyBlue™ Safestain, Invitrogen, Carlsbad, CA, USA) overnight and briefly de-stained in deionized water.

Gel image analysis and extraction of peptides. Stained gels were scanned with GS 800 calibrated densitometer (Bio-Rad) and image analysis was performed with Progenesis™ software (Nonlinear Dynamics, Ltd., Newcastle upon Tyne, UK) in semi-manual mode with 6 gel replicates for each cell type. Normalization of gel images was based on total spot density, and integrated spot density values (spot volumes) were then calculated after background subtraction. Average spot volume values (averages from the all 6 gels in the group) for each spot were compared between the groups. Protein spots were considered differentially expressed if their average normalized spot volume difference was >1.5-fold. As determined by the Student's t-test, a p-value <0.05 was considered to indicate a statistically significant difference.

Protein digestion and peptide extraction. Spots containing differentially expressed proteins were excised from the gels, cut into small pieces and washed 3 times with 25 mM ammonium bicarbonate in 50% acetonitrile (ACN). The gels were then dried in a SpeedVac Concentrator (Eppendorf, Hamburg, Germany). Sequencing grade modified trypsin (Promega, Madison, WI, USA) (6 ng/μl of trypsin in 25 mM ammonium bicarbonate in 5% ACN) was added. Following overnight incubation at 37˚C, the resulting peptides were extracted with 50% ACN.

Matrix-assisted laser desorption/ionization-time of flight mass spectrometry (MALDI-TOF MS) and identification of selected proteins. Peptide samples were spotted on a polished steel target plate (Bruker Daltonics, Bremen, Germany) and allowed to dry at room temperature. Matrix solution (3 mg α-cyano-4-hydroxycinnamic acid in 1 ml of 50% ACN containing 0.1% trifluoroacetic acid) was then added. MS was performed on an Autoflex II MALDI-TOF/TOF mass spectrometer (Bruker Daltonics) using a solid nitrogen laser (337 nm) and FlexControl software (Bruker Daltonics) in reflectron mode with positive ion mass spectra detection. The mass spectrometer was externally calibrated with Peptide Calibration Standard II (Bruker Daltonics). Spectra were acquired in the mass range 800-4,000 Da. The peak lists were generated using FlexAnalysis and searched against Swiss-Prot (2011 version, 524420 sequences) using Mascot software. The peptide mass tolerance was set to 50 ppm, taxonomy *Homo sapiens*, missed cleavage was set to 2, fixed modification for cysteine carbamidomethylation, and variable modifications for methionine oxidation and protein N-terminal acetylation.

Western blot analysis. Cells were lysed in NHT buffer (140 mM NaCl, 10 mM HEPES, 1.5% Triton X-100, pH 7.4). Protein concentration in the collected supernatants was determined by the Bradford assay (Bio-Rad). Lysate samples (25-70 μg) were combined with SDS loading buffer containing 2-mercaptoethanol and boiled for 5 min. Triplicate samples were separated on 12% SDS-PAGE minigels in Tris-glycine buffer (Bio-Rad). Electrophoresis was performed at a constant voltage for 30 min at 45 V per gel, and then at 90 V per gel until the dye front reached the gel bottom. Proteins were transferred onto 0.45 μm PVDF membranes (Milipore, Billerica, MA, USA) in a semi-dry blotter (Hoefer, San Francisco, CA, USA) at 0.8 mA/cm^2 of membrane. Membranes were incubated with blocking buffer containing PBS (Invitrogen), 0.1% Tween-20 and 5% non-fat dried milk for 1 h. As primary antibodies anti-adenine phosphoribosyltransferase (APRT; 1:1,000, rabbit polyclonal antibody), anti-purine nucleoside phosphorylase (PNP; 1:1,000, mouse monoclonal antibody) and anti-GAPDH (1:10,000, rabbit polyclonal antibody) were used. After thoroughly washing in blocking buffer, a secondary horseradish peroxidase-conjugated anti-mouse or anti-rabbit antibody was added (1:10,000). GAPDH was used as the loading control. The signal was detected using Western Blotting Luminol Reagent (Santa Cruz Biotechnology, Inc., Santa Cruz, CA, USA) and membranes were exposed to X-ray films (Kodak, Rochester, NY, USA). All used antibodies were from Santa Cruz Biotechnology.

Results

Molecular changes associated with the generation of drug-resistant cells can confer potential selective disadvantage. Such a 'weakness' may be used as druggable target for effective elimination of drug-resistant lymphoma cells. Our aim was to elucidate the molecular changes associated with the development of TRAIL resistance in (originally TRAIL-sensitive) MCL cells in order to identify such a cellular 'weakness' of TRAIL-resistant MCL cells. To identify the specific protein expression changes in the TRAIL-resistant cells, we derived a TRAIL-resistant HBL-2 subclone (HBL-2/R) from the originally TRAIL-sensitive HBL-2 cell line, and performed differential analysis of the surface expression of TRAIL receptors and comparative proteomic analysis of the HBL-2/R and HBL-2 cells.

TRAIL-resistant cell line. The TRAIL-resistant HBL-2 subclone (HBL-2/R) was derived from the originally TRAIL-sensitive HBL-2 cell line by selective pressure of increasing TRAIL concentration in medium over 5 weeks. While the IC_{50} for TRAIL in the originally sensitive HBL-2 cells was 1 ng/ml at 48 h (data not shown), the resulting HBL-2/R subclone proliferated in up to 1,000 ng/ml TRAIL concentration in medium and was therefore >1,000-fold more resistant to TRAIL than the HBL-2 cells (Fig. 1).

TRAIL receptors - flow cytometric analysis of cell surface expression. The attenuated expression of TRAIL death receptors DR4 and DR5 has been previously described as a cause of TRAIL resistance. We therefore determined the relative expression of TRAIL receptors in HBL-2 and HBL-2/R cells by flow cytometry (Fig. 2). The expression of DR4, DR5, DcR1 and DcR2 in the HBL-2/R cells was markedly decreased compared to the HBL-2 cells. The marked downregulation of death receptors DR4 and DR5 explains the resistance of the HBL-2/R cells to TRAIL, while the downregulation of decoy receptors DcR1 and DcR2 may indicate further, more complex phenotypic changes in the HBL-2/R cells.

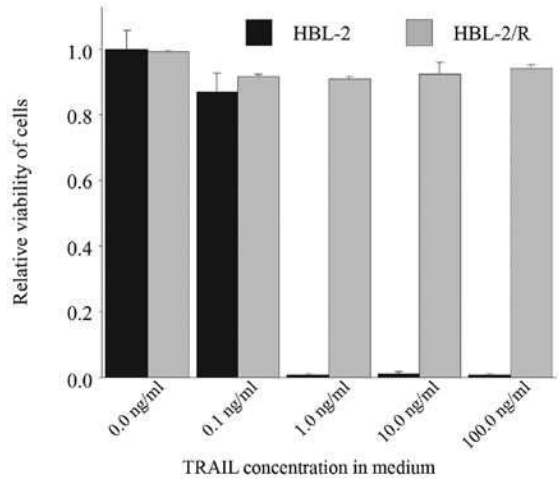

Figure 1. Relative cytotoxicity of TRAIL. Viability of TRAIL-sensitive HBL-2 cells and TRAIL-resistant HBL-2/R cells after 78 h in medium with recombinant TRAIL was determined by WTS-based colorimetric assay. Absorbance value of HBL-2 cells grown in medium without TRAIL was set to 1.

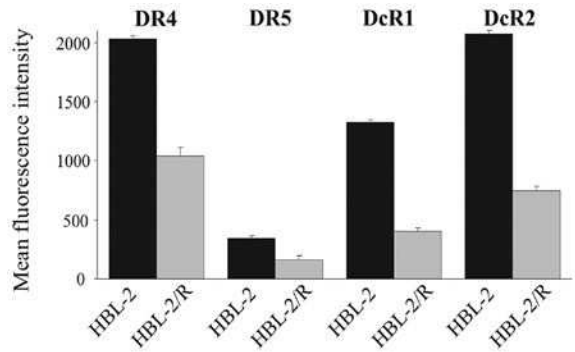

Figure 2. Cell surface expression of TRAIL receptors. HBL-2 and HBL-2/R cells were labeled with phycoerythrin-conjugated antibodies against the TRAIL cell surface receptors, DR4, DR5, DcR1 and DcR2, and the expression of the receptors was analyzed by flow cytometry. Cells without staining and isotype controls served as the blank controls.

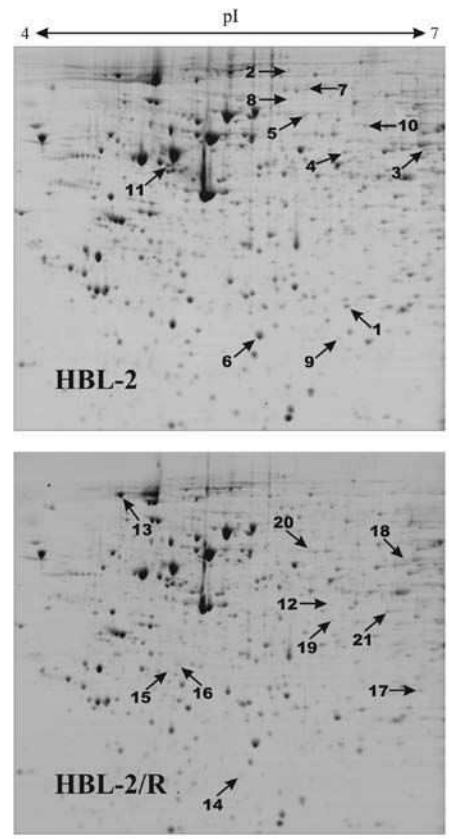

Figure 3. Two-dimensional electrophoresis of HBL-2 and HBL-2/R cells was performed on 24-cm gel strips, pH 4.0-7.0, 10% SDS-PAGE. Proteins were stained with Coomassie Brilliant Blue. Differentially expressed proteins are indicated by numbered arrows (spots 1-11 indicate downregulated proteins in HBL-2/R cells, and spots 12-21 indicate upregulated proteins in HBL-2/R cells).

Proteomic analysis. In order to identify specific changes in protein expression associated with TRAIL resistance in HBL-2/R cells, we performed comparative proteomic analysis of cellular homogenates of HBL-2/R and TRAIL-sensitive HBL-2 cells. Using two-dimensional electrophoresis of total cell lysates, we reproducibly detected 820 protein spots on Coomassie Brilliant Blue-stained gels. We found 21 protein spots to be significantly quantitatively changed (upregulated or downregulated, change >1.5-fold; $p<0.05$) in HBL-2/R cells (Fig. 3). Using MALDI-TOF/TOF mass spectrometry we identified all 21 proteins differentially expressed in HBL-2/R cells (Table I).

Functional annotations of the identified differentially expressed proteins were analyzed using the Kyoto Encyclopedia of Genes and Genomes (KEGG) database. Among the 21 identified proteins we found molecules involved in diverse functions, including cytoskeleton regulation, ribosome synthesis and maturation, RNA metabolism, chromosome translocation, DNA repair and replication, as well as protein folding. However, one pathway was markedly enriched in our set (hsa00230 - purine metabolism) represented by 3 differentially expressed proteins. These 3 molecules are key enzymes of the purine nucleotide metabolism (Fig. 5) and all 3 are downregulated in TRAIL-resistant HBL-2/R cells [PNP (downregulated 1.6-fold in HBL-2/R cells), APRT (downregulated 2.2-fold in HBL-2/R cells) and inosine-5'-monophosphate dehydrogenase 2 (IMPDH2, downregulated 1.6-fold in HBL-2/R cells)].

Verification of proteomic analysis. To confirm the results of proteomic analysis by an independent method we verified the decreased expression of the 2 proteins involved in purine metabolism, namely PNP and APRT, by western blot analysis in HBL-2 and HBL-2/R cell lysates (Fig. 4).

Discussion

The downregulation of the 3 key enzymes of purine metabolism can have a profound effect on nucleotide homeostasis in TRAIL-resistant lymphoma cells. Purine nucleotides, the building blocks for synthesis of DNA, RNA and enzyme co-factors, are recruited either from *de novo* purine synthesis from low molecular weight precursors or by recycling of free nucleobases in the so-called salvage pathway. Both pathways lead to the production of nucleoside-5'-phosphates (Fig. 5). Both pathways can supply cellular demand independently; however, their importance in different tissues is variable. In leukemic and lymphoma cells the salvage pathway is considered the major source of purine nucleotides (30,31).

Table I. List of proteins differentially expressed in HBL-2/R cells (difference at least 1.5-fold and statistical significance p<0.05).

Spot no.	Swiss-Prot no.[a]	Protein name	Fold change	Mascot score[b]	Sequence cov. (%)[c]	Mr
Proteins upregulated in HBL-2/R cells						
1	P04792	Heat shock protein β-1	3.9	84	51	22826
2	P42704	Leucine-rich PPR motif-containing protein, mitochondrial	2.6	100	23	159003
3	O75351	Vacuolar protein sorting-associated protein 4B	2.6	171	32	49443
4	P23381	Tryptophanyl-tRNA synthetase, cytoplasmic	2.4	240	54	53474
5	P20591	Interferon-induced GTP-binding protein Mx1	2.2	176	42	75872
6	P09211	Glutathione S-transferase P	1.9	110	56	23569
7	P06396	Gelsolin	1.9	115	22	86043
8	P13010	X-ray repair cross-complementing protein 5	1.7	262	46	83222
9	Q9HAV7	GrpE protein homolog 1, mitochondrial	1.6	99	44	24492
10	O43776	Asparaginyl-tRNA synthetase, cytoplasmic	1.5	250	41	63758
11	Q15084	Protein disulfide-isomerase A6	1.5	76	29	48490
Proteins downregulated in HBL-2/R cells						
12	P08559	Pyruvate dehydrogenase E1 component subunit α	3.2	111	32	43952
13	P19338	Nucleolin	2.4	146	29	76625
14	P07741	Adenine phosphoribosyltransferase	2.2	227	79	19766
15	O75792	Ribonuclease H2 subunit A	1.7	348	72	33716
16	Q07955	Serine/arginine-rich splicing factor 1	1.7	82	35	27842
17	P00491	Purine nucleoside phosphorylase	1.6	182	68	32325
18	P12268	Inosine-5'-monophosphate dehydrogenase 2	1.6	230	44	56226
19	P40121	Macrophage-capping protein	1.6	102	41	38760
20	P13674	Prolyl 4-hydroxylase subunit α-1	1.5	234	48	61296
21	Q15019	Septin-2	1.5	62	26	41689

[a]Swiss-Prot no. is the code under which the identified protein is deposited in the Swiss-Prot database. [b]Mascot score helps to estimate the correctness of the individual hit. It is expressed as -10 x log(P) where P is the probability that the observed match is a random event. [c]Sequence coverage is the number of amino acids spanned by the assigned peptides divided by the sequence length.

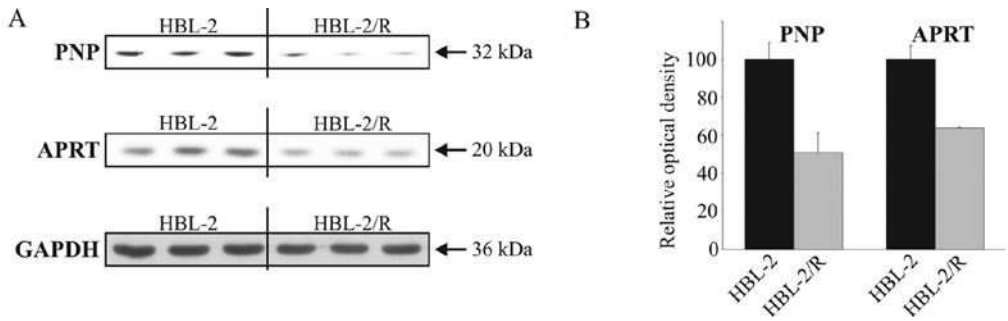

Figure 4. Relative expression of purine nucleoside phosphorylase (PNP) and adenine phosphoribosyltransferase (APRT) in HBL-2 and HBL-2/R cell lysates determined by western blot analysis. (A) Triplicate cell lysates were separated on 12% SDS-PAGE minigels. Proteins were then transferred onto PVDF membranes, blocked and probed with either anti-APRT, or anti-PNP antibody. Anti-GAPDH antibody was used as the loading control. The bands were visualized by HRP-conjugated secondary antibodies. (B) The values of integrated optical densities of PNP and APRT in HBL-2 cells were set to 100.

The *de novo* synthesis of purine nucleotides requires 5-phosphoribosyl-1-pyrophosphate (PRPP), ATP, glutamine, glycine, CO_2, aspartate and formate to create the first fully formed nucleotide, inosine-5'-monophosphate (IMP). IMP represents a branch point for purine biosynthesis, since it can be converted either to guanosine-5'-monophosphate (GMP) by IMPDH2 (downregulated in HBL-2/R cells) or to adenosine-5'-monophosphate (Fig. 5).

The catabolism of purine nucleotides leads to the liberation of free purine bases by PNP (downregulated in HBL-2/R cells). In the salvage pathway the free bases are reconverted back to nucleoside-5'-monophosphates in a reaction with activated sugar (PRPP) catalyzed by APRT (downregulated in HBL-2/R cells) or hypoxanthine-guanine phosphoribosyltransferase (32) (Fig. 5). Ribonucleotides are converted by ribonucleotide reductase into the corresponding deoxyribonucleotides.

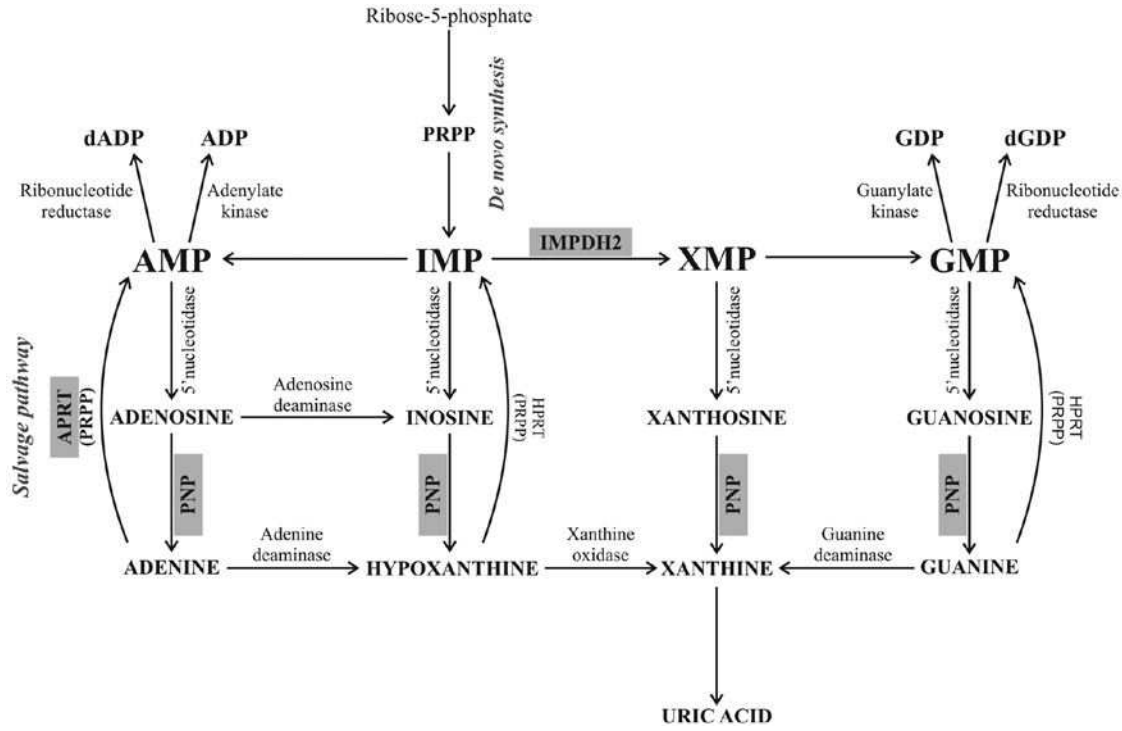

Figure 5. Scheme of the purine metabolism pathways, showing the position of IMPDH2, APRT and PNP in purine nucleotide biosynthesis, adopted from a previous study (35). The *de novo* synthesis of purine nucleotides begins with the phosphorylation of ribose-5-phosphate to form PRPP. In a number of reactions, PRPP creates the first fully formed nucleotide, IMP. IMP is converted by IMPDH2 to GMP. PNP catalyzes the reversible cleavage of purine nucleosides, releasing purine nucleobases (adenine, hypoxanthine, xanthine and guanine). In the salvage pathway the free nucleobases can be reconverted back to nucleoside-5'-monophosphates in a reaction with activated sugar (PRPP) catalyzed by APRT. IMPDH2, inosine-5'-monophosphate dehydrogenase 2; APRT, adenine phosphoribosyltransferase; PNP, purine nucleoside phosphorylase; PRPP, 5-phosphoribosyl-1-pyrophosphate; IMP, inosine-5'-monophosphate; GMP, guanosine-5'-monophosphate; dADP, deoxyadenosine diphosphate; ADP, adenosine diphosphate; GDP, guanosine diphosphate; dGDP, deoxyguanosine diphosphate; AMP, adenosine monophosphate; XMP, xanthosine monophosphate.

The delicate balance of enzyme activities and concentrations of products and intermediates are critical for purine (nucleotide) homeostasis. The inhibition of PNP results in the accumulation of its substrate, 2'-deoxyguanosine which is further phosphorylated to deoxyguanosine triphosphate (dGTP). A high intracellular concentration of dGTP inhibits cell proliferation and induces apoptosis (33-35). If APRT is inhibited, accumulated adenine is oxidized to insoluble 2,8-dihydroxyadenine. Accumulation of this precipitate results in cell death (32). Similarly, the inhibition of IMPDH2 leads to depletion of guanosine nucleotides, which blocks DNA synthesis and cell division (36,37).

Disruption of the purine nucleotide metabolism generally results in an accumulation and/or a lack of ribonucleotides or deoxyribonucleotides or metabolic intermediates with potentially cytotoxic consequences. The observed decreased expression of the 3 purine metabolism enzymes affects both *de novo* synthesis and the salvage pathway of purine metabolism and may also affect purine nucleotide homeostasis in TRAIL-resistant HBL-2/R cells. Such an imbalance may represent a selective disadvantage for the affected cells. Such a 'weakness' may not be apparent under normal circumstances but may become critical under stress or unfavorable conditions. As the proliferation rates of HBL-2/R and HBL-2 cells are comparable, the proposed imbalance in purine nucleotide metabolism in TRAIL-resistant cells is possibly mild and/or well compensated *in vitro*. However, this 'weakness' may become apparent due to lack of building blocks for DNA and RNA synthesis in the environment or upon further disruption of purine metabolism. Since both pathways of purine metabolism are compromised in TRAIL-resistant MCL cells, these cells should be vulnerable to further inactivation of purine nucleotide metabolism enzymes. Therefore, drugs that target (already disbalanced) purine metabolism should be highly cytotoxic to TRAIL-resistant cells (compared to non-malignant cells) and may therefore be selectively effective in the elimination of TRAIL-resistant MCL cells in experimental therapy. There are several approved inhibitors of purine metabolism, such as methotrexate (inhibits purine *de novo* synthesis via dihydrofolate reductase) (38), ribavirin and mycophenolic acid (inhibitors of IMPDH2) (39,40) or forodesine (a novel inhibitor of PNP) (41,42), available for clinical use.

The adaptation of cancer cells to cytostatic and cytotoxic drugs is associated to a certain degree with extensive changes in the cell phenotype. Some of the molecular changes, although seemingly unrelated to the mechanism of resistance, can provide a selective disadvantage to the cells and such a 'weakness' may be used as a potential therapeutic target. By the presented proteomic analysis of the changes associated with resistance to TRAIL in MCL HBL-2 cells, we demonstrated the downregulation of all types of TRAIL receptors and identified the altered expression of several proteins including 3 enzymes of the purine metabolism pathway. This downregulated pathway potentially represents a 'weakness' of the TRAIL-resistant MCL cells and has potential as a therapeutic target for the selective elimination of such cells in the future.

Acknowledgements

This study was supported by the Grant Agency of Charles University (GAUK 251180 111210 and 253284 700712), by the Grant Agency of the Czech Republic (305/09/1390), by the Ministry of Education, Youth and Sports (PRVOUK P24/LF1/3 and SVV 2012-264507), UNCE 204021 and the Ministry of Health of the Czech Republic (IGA MZ NT12248-5, IGA-MZ NT13201-4).

References

1. Sant M, Allemani C, Tereanu C, *et al*: Incidence of hematologic malignancies in Europe by morphologic subtype: results of the HAEMACARE project. Blood 116: 3724-3734, 2010.
2. Perez-Galan P, Dreyling M and Wiestner A: Mantle cell lymphoma: biology, pathogenesis, and the molecular basis of treatment in the genomic era. Blood 117: 26-38, 2011.
3. Tsujimoto Y, Yunis J, Onorato-Showe L, Erikson J, Nowell PC and Croce CM: Molecular cloning of the chromosomal breakpoint of B-cell lymphomas and leukemias with the t(11;14) chromosome translocation. Science 224: 1403-1406, 1984.
4. Williams ME, Swerdlow SH, Rosenberg CL and Arnold A: Characterization of chromosome 11 translocation breakpoints at the bcl-1 and PRAD1 loci in centrocytic lymphoma. Cancer Res 52: 5541S-5544S, 1992.
5. Humala K and Younes A: Current and emerging new treatment strategies for mantle cell lymphoma. Leuk Lymphoma: Feb 19, 2013 (Epub ahead of print).
6. Wiley SR, Schooley K, Smolak PJ, *et al*: Identification and characterization of a new member of the TNF family that induces apoptosis. Immunity 3: 673-682, 1995.
7. Pitti RM, Marsters SA, Ruppert S, Donahue CJ, Moore A and Ashkenazi A: Induction of apoptosis by Apo-2 ligand, a new member of the tumor necrosis factor cytokine family. J Biol Chem 271: 12687-12690, 1996.
8. Ashkenazi A and Dixit VM: Death receptors: signaling and modulation. Science 281: 1305-1308, 1998.
9. Sheridan JP, Marsters SA, Pitti RM, *et al*: Control of TRAIL-induced apoptosis by a family of signaling and decoy receptors. Science 277: 818-821, 1997.
10. Ashkenazi A: Targeting death and decoy receptors of the tumour-necrosis factor superfamily. Nat Rev Cancer 2: 420-430, 2002.
11. Castro Alves C, Terziyska N, Grunert M, *et al*: Leukemia-initiating cells of patient-derived acute lymphoblastic leukemia xenografts are sensitive toward TRAIL. Blood 119: 4224-4227, 2012.
12. Peter ME and Krammer PH: The CD95(APO-1/Fas) DISC and beyond. Cell Death Differ 10: 26-35, 2003.
13. Spierings DC: Tissue distribution of the death ligand TRAIL and its receptors. J Histochem Cytochem 52: 821-831, 2004.
14. Petrak J, Toman O, Simonova T, *et al*: Identification of molecular targets for selective elimination of TRAIL-resistant leukemia cells. From spots to in vitro assays using TOP15 charts. Proteomics 9: 5006-5015, 2009.
15. Molinsky J, Klanova M, Koc M, *et al*: Roscovitine sensitizes leukemia and lymphoma cells to tumor necrosis factor-related apoptosis-inducing ligand-induced apoptosis. Leuk Lymphoma 54: 372-380, 2013.
16. Klener P, Leahomschi S, Molinsky J, *et al*: TRAIL-induced apoptosis of HL60 leukemia cells: two distinct phenotypes of acquired TRAIL resistance that are accompanied with resistance to TNFalpha but not to idarubicin and cytarabine. Blood Cells Mol Dis 42: 77-84, 2009.
17. Leahomschi S, Molinsky J, Klanova M, *et al*: Multi-level disruption of the extrinsic apoptotic pathway mediates resistance of leukemia cells to TNF-related apoptosis-inducing ligand (TRAIL). Neoplasma 60: 223-231, 2013.
18. Wen J, Ramadevi N, Nguyen D, Perkins C, Worthington E and Bhalla K: Antileukemic drugs increase death receptor 5 levels and enhance Apo-2L-induced apoptosis of human acute leukemia cells. Blood 96: 3900-3906, 2000.
19. Plasilova M, Zivny J, Jelinek J, *et al*: TRAIL (Apo2L) suppresses growth of primary human leukemia and myelodysplasia progenitors. Leukemia 16: 67-73, 2002.
20. Ashkenazi A, Pai RC, Fong S, *et al*: Safety and antitumor activity of recombinant soluble Apo2 ligand. J Clin Invest 104: 155-162, 1999.
21. Di Pietro R and Zauli G: Emerging non-apoptotic functions of tumor necrosis factor-related apoptosis-inducing ligand (TRAIL)/Apo2L. J Cell Physiol 201: 331-340, 2004.
22. Kelley SK, Harris LA, Xie D, *et al*: Preclinical studies to predict the disposition of Apo2L/tumor necrosis factor-related apoptosis-inducing ligand in humans: characterization of in vivo efficacy, pharmacokinetics, and safety. J Pharmacol Exp Ther 299: 31-38, 2001.
23. Lawrence D, Shahrokh Z, Marsters S, *et al*: Differential hepatocyte toxicity of recombinant Apo2L/TRAIL versions. Nat Med 7: 383-385, 2001.
24. Roth W, Isenmann S, Naumann U, *et al*: Locoregional Apo2L/TRAIL eradicates intracranial human malignant glioma xenografts in athymic mice in the absence of neurotoxicity. Biochem Biophys Res Commun 265: 479-483, 1999.
25. Walczak H, Miller RE, Ariail K, *et al*: Tumoricidal activity of tumor necrosis factor-related apoptosis-inducing ligand in vivo. Nat Med 5: 157-163, 1999.
26. Hylander BL, Pitoniak R, Penetrante RB, *et al*: The anti-tumor effect of Apo2L/TRAIL on patient pancreatic adenocarcinomas grown as xenografts in SCID mice. J Transl Med 3: 22, 2005.
27. Dimberg LY, Anderson CK, Camidge R, Behbakht K, Thorburn A and Ford HL: On the TRAIL to successful cancer therapy? Predicting and counteracting resistance against TRAIL-based therapeutics. Oncogene: 14 May, 2012 (Epub ahead of print). doi: 10.1038/onc.2012.164, 2012.
28. Zhang L and Fang B: Mechanisms of resistance to TRAIL-induced apoptosis in cancer. Cancer Gene Ther 12: 228-237, 2005.
29. Maksimovic-Ivanic D, Stosic-Grujicic S, Nicoletti F and Mijatovic S: Resistance to TRAIL and how to surmount it. Immunol Res 52: 157-168, 2012.
30. Scavennec J, Maraninchi D, Gastaut JA, Carcassonne Y and Cailla HL: Purine and pyrimidine ribonucleoside monophosphate patterns of peripheral blood and bone marrow cells in human acute leukemias. Cancer Res 42: 1326-1330, 1982.
31. Natsumeda Y, Prajda N, Donohue JP, Glover JL and Weber G: Enzymic capacities of purine de novo and salvage pathways for nucleotide synthesis in normal and neoplastic tissues. Cancer Res 44: 2475-2479, 1984.
32. Bollee G, Harambat J, Bensman A, Knebelmann B, Daudon M and Ceballos-Picot I: Adenine phosphoribosyltransferase deficiency. Clin J Am Soc Nephrol 7: 1521-1527, 2012.
33. Bantia S, Miller PJ, Parker CD, *et al*: Purine nucleoside phosphorylase inhibitor BCX-1777 (Immucillin-H) - a novel potent and orally active immunosuppressive agent. Int Immunopharmacol 1: 1199-1210, 2001.
34. Bantia S, Montgomery JA, Johnson HG and Walsh GM: In vivo and in vitro pharmacologic activity of the purine nucleoside phosphorylase inhibitor BCX-34: the role of GTP and dGTP. Immunopharmacology 35: 53-63, 1996.
35. Galmarini CM, Popowycz F and Joseph B: Cytotoxic nucleoside analogues: different strategies to improve their clinical efficacy. Curr Med Chem 15: 1072-1082, 2008.
36. Allison AC and Eugui EM: Mycophenolate mofetil and its mechanisms of action. Immunopharmacology 47: 85-118, 2000.
37. Hedstrom L: IMP dehydrogenase: structure, mechanism, and inhibition. Chem Rev 109: 2903-2928, 2009.
38. Fairbanks LD, Ruckemann K, Qiu Y, *et al*: Methotrexate inhibits the first committed step of purine biosynthesis in mitogen-stimulated human T-lymphocytes: a metabolic basis for efficacy in rheumatoid arthritis? Biochem J 342: 143-152, 1999.
39. Allison AC and Eugui EM: The design and development of an immunosuppressive drug, mycophenolate mofetil. Springer Semin Immunopathol 14: 353-380, 1993.
40. Zhou S, Liu R, Baroudy BM, Malcolm BA and Reyes GR: The effect of ribavirin and IMPDH inhibitors on hepatitis C virus subgenomic replicon RNA. Virology 310: 333-342, 2003.
41. Gandhi V, Kilpatrick JM, Plunkett W, *et al*: A proof-of-principle pharmacokinetic, pharmacodynamic, and clinical study with purine nucleoside phosphorylase inhibitor immucillin-H (BCX-1777, forodesine). Blood 106: 4253-4260, 2005.
42. Miles RW, Tyler PC, Furneaux RH, Bagdassarian CK and Schramm VL: One-third-the-sites transition-state inhibitors for purine nucleoside phosphorylase. Biochemistry 37: 8615-8621, 1998.

7.2 Appendix 2

Downregulation of deoxycytidine kinase in cytarabine-resistant mantle cell lymphoma cells confers cross-resistance to nucleoside analogs gemcitabine, fludarabine and cladribine, but not to other classes of anti-lymphoma agents. Klanova M, Lorkova L, Vit O, Maswabi B, Molinsky J, Pospisilova J, Vocková P, Mavis C, Lateckova L, Kulvait V, Vejmelkova D, Jaksa R, Hernandez F, Trneny M, Vokurka M, Petrak J, Klener P Jr. *Molecular Cancer.* 2014;13:159 (IF 2014: 4.257).

MOLECULAR CANCER

RESEARCH Open Access

Downregulation of deoxycytidine kinase in cytarabine-resistant mantle cell lymphoma cells confers cross-resistance to nucleoside analogs gemcitabine, fludarabine and cladribine, but not to other classes of anti-lymphoma agents

Magdalena Klanova[1,2], Lucie Lorkova[1], Ondrej Vit[1], Bokang Maswabi[1], Jan Molinsky[1,2], Jana Pospisilova[1], Petra Vockova[1,2], Cory Mavis[3], Lucie Lateckova[1,2], Vojtech Kulvait[1], Dana Vejmelkova[2], Radek Jaksa[3], Francisco Hernandez[4], Marek Trneny[2], Martin Vokurka[1], Jiri Petrak[1,5†] and Pavel Klener Jr[1,2*†]

Abstract

Background: Mantle cell lymphoma (MCL) is an aggressive type of B-cell non-Hodgkin lymphoma associated with poor prognosis. Implementation of high-dose cytarabine (araC) into induction therapy became standard-of-care for all newly diagnosed younger MCL patients. However, many patients relapse even after araC-based regimen. Molecular mechanisms responsible for araC resistance in MCL are unknown and optimal treatment strategy for relapsed/refractory MCL patients remains elusive.

Methods: Five araC-resistant (R) clones were derived by long-term culture of five MCL cell lines (CTRL) with increasing doses of araC up to 50 microM. Illumina BeadChip and 2-DE proteomic analysis were used to identify gene and protein expression changes associated with araC resistance in MCL. *In vitro* cytotoxicity assays and experimental therapy of MCL xenografts in immunodeficient mice were used to analyze their relative responsiveness to a set of clinically used anti-MCL drugs. Primary MCL samples were obtained from patients at diagnosis and after failure of araC-based therapies.

Results: Marked downregulation of deoxycytidine-kinase (DCK) mRNA and protein expression was identified as the single most important molecular event associated with araC-resistance in all tested MCL cell lines and in 50% primary MCL samples. All R clones were highly (20-1000x) cross-resistant to all tested nucleoside analogs including gemcitabine, fludarabine and cladribine. *In vitro* sensitivity of R clones to other classes of clinically used anti-MCL agents including genotoxic drugs (cisplatin, doxorubicin, bendamustine) and targeted agents (bortezomib, temsirolimus, rituximab) remained unaffected, or was even increased (ibrutinib). Experimental therapy of immunodeficient mice confirmed the anticipated loss of anti-tumor activity (as determined by overall survival) of the nucleoside analogs gemcitabine and fludarabine in mice transplanted with R clone compared to mice transplanted with CTRL cells, while the anti-tumor activity of cisplatin, temsirolimus, bortezomib, bendamustine, cyclophosphamide and rituximab remained comparable between the two cohorts.

(Continued on next page)

* Correspondence: pavel.klener@gmail.com
†Equal contributors
[1]Institute of Pathological Physiology, Charles University in Prague, First Faculty of Medicine, Prague, Czech Republic
[2]First Department of Medicine - Department of Hematology, General University Hospital and Charles University in Prague, Prague, Czech Republic
Full list of author information is available at the end of the article

(Continued from previous page)

Conclusions: Acquired resistance of MCL cells to araC is associated with downregulation of DCK, enzyme of the nucleotide salvage pathway responsible for the first phosphorylation (=activation) of most nucleoside analogs used in anti-cancer therapy. The data suggest that nucleoside analogs should not be used in the therapy of MCL patients, who relapse after failure of araC-based therapies.

Keywords: Mantle cell lymphoma (MCL), Cytarabine, Drug resistance, Nucleotide salvage pathway, Proteomics, Mass spectrometry

Background

Mantle cell lymphoma (MCL) is an aggressive type of B-cell non-Hodgkin lymphoma (NHL) associated with poor prognosis [1,2]. In recent years several studies brought evidence that implementation of high-dose cytarabine (araC) into induction therapy, e.g. by sequential chemotherapy by R(ituximab)-CHOP and R-DHAP regimens, induced higher response rate and prolonged progression-free survival compared to R-CHOP-only [3-5]. Based on these results, implementation of araC into induction therapy became standard of care for all newly diagnosed younger MCL patients. Despite considerable improvement, however, most high-risk MCL patients relapse even after araC-based first-line regimen. Prognosis of relapsed/refractory (RR) MCL is dismal. Currently, there is no second-line standard-of-care for RR-MCL [6]. Available treatment approaches for RR-MCL include cisplatin, fludarabine, cladribine, gemcitabine, temsirolimus, bortezomib, bendamustine, lenalidomide and ibrutinib-based regimen [7-16].

AraC belongs among the backbone anti-leukemia agents [17]. Both, "standard dose" araC (100-200 mg/m2 continuous i.v. infusion for 7 days), and "high dose" araC (HDAC, 2-3 g/m2, 2–4 i.v. three hour administrations every 12–24 hours) have been widely used in the therapy of acute myelogenous leukemia (AML), as well as in salvage regimen for relapsed B-NHL [18,19]. As mentioned above araC appears particularly effective component of multi-agent aggressive immunochemoterapy regimen used in younger MCL patients.

AraC is a prodrug, which must be 1. transported into the cell, and 2. within the cell converted into an active drug by phosphorylation by specific phosphokinases of the nucleotide salvage pathway [20]. During "standard dose" cytarabine administration araC is transported into the cell by means of specific transporters, primarily via hENT1/SLC29A1 [21]. During high-dose cytarabine administration araC also diffuses across plasma membrane independent of the specific transporters [22]. The rate-limiting enzyme of the nucleotide salvage pathway is deoxycytidine-kinase (DCK), which catalyzes the first phosphorylation of araC into araCMP. AraCMP is retained in the cell and undergoes two additional consecutive phosporylations before it can be incorporated into DNA.

The molecular mechanisms of araC resistance in MCL are unknown. Resistance to araC in myeloid leukemia cells was repeatedly associated with altered expression of genes involved in nucleotide salvage pathway, including downregulation of DCK, or upregulation of key araC-inactivating enzymes, namely cytidine-deaminase (CDA) or cytoplasmic 5′nucleotidase (NT5C2) [20-25].

In this study we derived araC-resistant MCL cells, studied their sensitivity to a battery of anti-cancer drugs and elucidated the molecular mechanism responsible for araC resistance in MCL.

Results

Establishment and characterization of araC-resistant MCL clones (R clones)

Five araC-resistant MCL clones (=R clones) were established by long-term culture of five cytarabine-sensitive MCL cell lines (JEKO-1, MINO, REC-1, HBL-2 and GRANTA-519, =CTRL cell lines) in the presence of increasing doses of araC (up to 50 μM, comparable with plasma concentration reached in patients treated with high-dose araC) [26]. Resistance of R clones to araC was confirmed *in vitro* by proliferation assays (Figure 1). The R clones tolerated at least 125-1000-fold higher concentrations of araC compared to CTRL cells (Figure 1).

Gene expression profiling of R clones revealed downregulation of deoxycytidine-kinase (DCK)

To identify gene and protein expression changes associated with araC resistance in MCL we performed parallel transcriptome profiling and proteomic analysis of R clones compared to CTRL cell lines. Transcriptomic analysis was performed for each of the 5 MCL cell lines and their respective R clones in biological duplicates using Illumina BeadChips. The filtered groups of genes with fold change at least ± 1.5-fold and adjusted p value < 0.05 were annotated and arranged into biologically relevant categories using The Database for Annotation, Visualization and Integrated Discovery (DAVID, Additional file 1: Figure S1). Based on Gene Ontology (GO) terms, the downregulated genes were involved in *ribosome structure and function*, *cell cycle*, *RNA degradation*, *antigen processing and presentation*, *purine metabolism* and *pyrimidine metabolism*

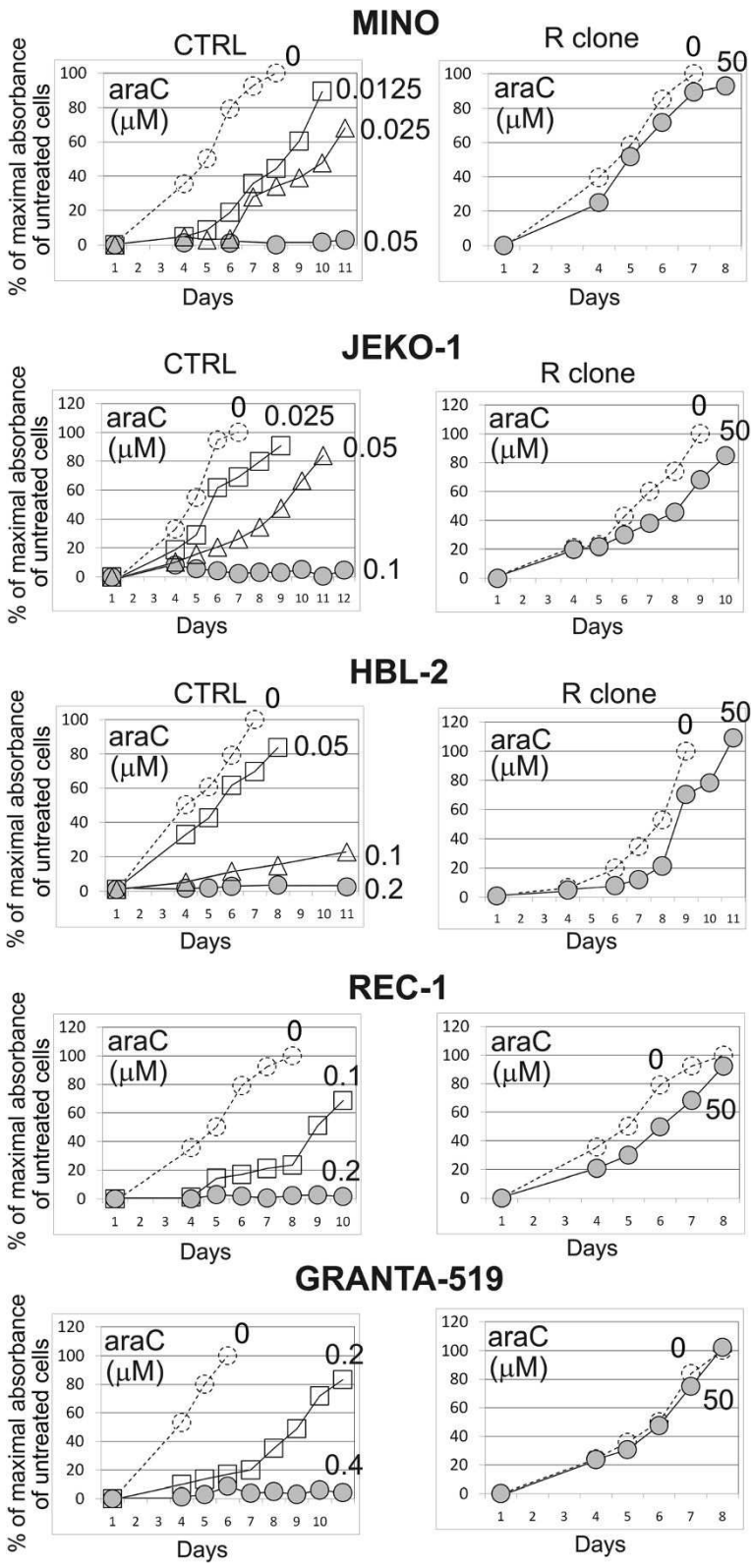

Figure 1 R clones are resistant to 50 μM cytarabine. WST-8 cell proliferation assay of 5 MCL cell lines (CTRL) and 5 R clones was carried out as described in Methods. While the lethal dose of cytarabine for CTRL cells ranged from 0.05 to 0.4 μM, proliferation rate of R clones in 50 μM araC was virtually unaffected. Representative example of two independent experiments is shown. Standard deviations were < 5% for all measurements.

(Additional file 1: Figure S1A). Among the most upregulated gene groups belonged those involved in *graft-vs-host disease*, *alograft rejection*, *B-cell receptor signaling*, *cell adhesion molecules*, *chemokine signaling pathway* and *Toll-like receptor signaling* (Additional file 1: Figure S1B). The only gene consistently differentially expressed across all 5 MCL cell lines was DCK, which was markedly downregulated in all R clones. Other genes differentially expressed in more than one MCL cell line are shown in Additional file 2: Table S1. Proteomic analysis using 2-DE was applied to Mino R subclone compared to Mino CTRL cell line, and revealed differential expression of several proteins, among them almost 5-fold downregulation of DCK in the Mino R subclone was the most apparent (Figure 2, Tables 1 and 2). Downregulation of DCK protein (the rate-limiting enzyme of the nucleotide salvage pathway, which catalyzes the first phosphorylation of araC and other nuclosides into their respective monophosphates) was confirmed by western blotting in all five R clones (Figure 3). DCK expression seemed to be fully abrogated in four R clones (as there was no detectable DCK) and several-fold downregulated in one R clone compared to the CTRL cells.

AraC-resistant clones are cross-resistant to nucleoside analogs, but remain sensitive to other classes of anti-lymphoma agents

To identify optimal treatment strategy for araC-resistant MCL we determined sensitivity (or eventual cross-resistance) of all 5 R clones in a battery of cellular toxicity tests. We exposed R clones and CTRL cells to a panel of clinically used anti-MCL agents in various concentrations and measured their effect on cell proliferation rate. The tested agents included both, classical genotoxic cytostatics and novel targeted drugs. The panel included alkylating agents cisplatin, doxorubicin and bendamustine, nucleoside analogs gemcitabine, cladribine and fludarbine, and targeted drugs bortezomib (proteasome inhibitor), temsirolimus (mTOR inhibitor) and ibrutinib (Bruton tyrosine-kinase (BTK) inhibitor). All five R clones (resistant to a pyrimidine analog cytarabine) showed cross-resistance not only to another pyrimidine analog gemcitabine (up to 3125-fold), but also to purine nucleoside analogs fludarabine and cladribine (approx. 12.5-500-fold, see Figure 4A,B). Sensitivity of the resistant R clones to other classes of anti-lymphoma agents (i.e. other than nucleoside analogs) remained comparable to the respective CTRL cells (Figure 4C,D), with the exception of ibrutinib. The BTK inhibitor ibrutinib proved to be significantly more cytotoxic to R clones compared to CTRL cells *in vitro* (see Figure 4C,D, Additional file 3: Figure S2). R clones also retained *in vitro* sensitivity to anti-CD20 monoclonal antibody rituximab comparable to CTRL cells as determined by ^{51}Cr release assay, which is standardly used to evaluate antibody-dependent cytotoxicity (ADCC) and complement-mediated cytotoxicity (CMC) of therapeutic monoclonal antibodies (Figure 5).

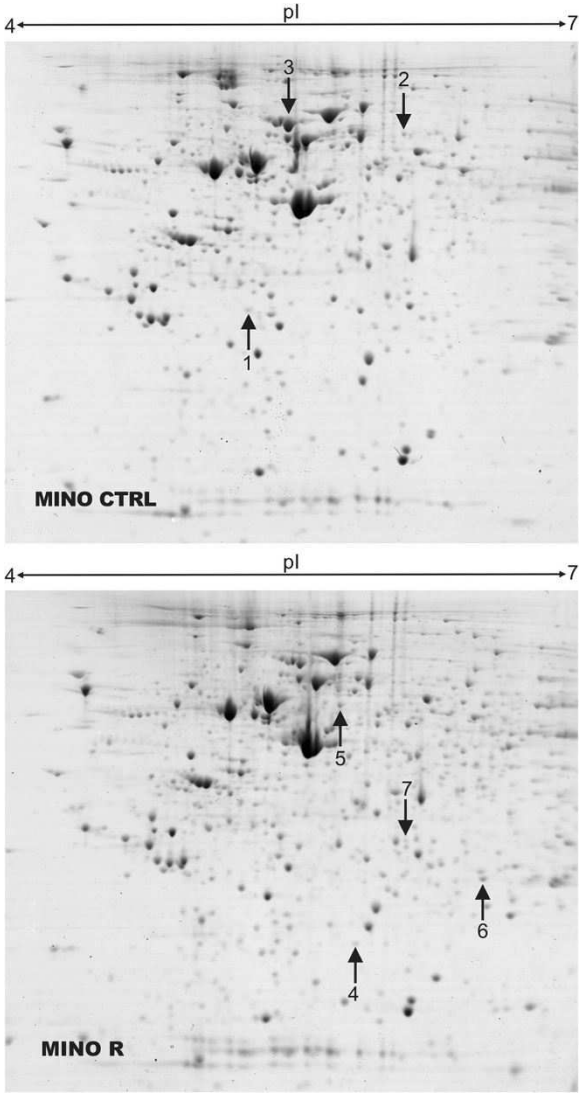

Figure 2 Proteomic analysis of MINO R vs MINO CTRL cells. Two-dimensional electrophoresis of cells MINO R cell versus MINO CTRL cells was performed on 24 cm gel strips, pH 4.0-7.0, 10% SDS-PAGE. Proteins were stained with Coomassie Brilliant Blue. Differentially expressed proteins are indicated by numbered arrows, spots 1–3 indicate proteins significantly downregulated in MINO R cells, and spots 4–7 indicate proteins upregulated in MINO R cells.

Experimental therapy with fludarabine and gemcitabine is ineffective in mice xenografted with araC-resistant clones

The *in vitro* tests of cellular toxicity provided important information on direct cellular effects of the tested drugs to the resistant cells. However, *in vitro* assays do not take into account important systemic pharmacokinetic

Table 1 List of proteins differentially expressed in MINO R cells identified by 2-DE

Spot no.	Accession	Protein name	Fold change	Mascot score	Sequence cov. (%)	Mr
Proteins downregulated in MINO R cells						
1	P27707	Deoxycytidine kinase	−4.6	44*	16	30841
2	Q99829	Copine-1	−4.3	102	17	59649
3	P13796	Plastin-2	−2	453	65	70814
Proteins upregulated in MINO R cells						
4	P07741	Adenine phosphoribosyltransferase	5	70	40	19766
5	P68363	Tubulin alpha-1B chain	5	169	32	50804
6	P04792	Heat shock protein beta-1	2/3	73	32	22826
7	P31937	3-Hydroxyisobutyrate Dehydrogenase, Mitochondrial	2/1	43*	8	35712

*Identity of proteins with low Mascot Score was verified by MS/MS (see Table 2).
Included are the proteins with difference in expression at least 2-fold and statistical significance of the change $p < 0.05$. Swiss-Prot no. is the code under which the identified protein is deposited in the Swiss-Prot database. Mascot score helps to estimate the correctness of the individual hit. It is expressed as $-10 \times \log(P)$ where P is the probability that the observed match is a random event. Sequence coverage is the number of amino acids spanned by the assigned peptides divided by the sequence length.

and pharmacodynamic variables, which can have large impact on the drug efficacy *in vivo*. In addition, some anti-MCL agents cannot be properly tested *in vitro*, because their mechanism of antitumor activity directly or indirectly depends on the *in vivo* context, e.g. activation of a prodrug cyclophosphamide in the liver microsome, cooperation of a monoclonal antibody rituximab with complement and cells of the immune system, or antiangiogenic component of temsirolimus activity. Therefore, we used a mouse xenograft model (NOD.Cg-*Prkdc*^{scid} *Il2rg*^{tm1Wjl}/SzJ mice) of MCL to simulate *in vivo* treatment of araC-sensitive and araC-resistant disease. Intravenous injection of 1 million JEKO-1 MCL cells leads to demise of the xenografted animals due to disseminated lymphoma with median overall survival of approx. 38 days. Experimental therapy of JEKO-1-xenografted immunodeficient mice with single-agent fludarabine and gemcitabine confirmed total loss of anti-tumor activity of purine analog fludarabine and pyrimidine analog gemcitabine (measured as overall survival of experimental animals) in mice transplanted with cytarabine-resistant JEKO-1 R clone compared to mice transplanted with cytarabine-sensitive JEKO-1 CTRL cells (Figure 6). Antitumor activity of cisplatin, temsirolimus, bendamustine, bortezomib, cyclophosphamide and rituximab remained comparable between JEKO-1 R clone and JEKO-1 CTRL-xenografted mice in agreement with the *in vitro* tests (Figure 6).

Analysis of primary MCL samples confirmed that downregulation of DCK is frequently associated with failure of high-dose araC-based treatments

Eight and two primary MCL samples obtained from patients at diagnosis (D1-D8) and at lymphoma relapse after failure of high-dose araC-based treatments (R1-R8) were analyzed by real-time RT-PCR and western blotting, respectively (Table 3, Figure 7A). In four cases downregulation of DCK gene expression was observed in R compared to D samples (difference in ΔCT (DCK-GAPDH) between R and D samples was > 1 cycle), while in four cases no change was observed (difference in ΔCT < 1 cycle) (Table 3). Western blotting analysis of the sample R2 compared to D2 revealed marked downregulation of protein DCK thereby confirming the gene expression results (i.e. 4-fold decrease in total DCK mRNA after araC-based therapy). Interestingly, protein DCK in the sample R6 compared to D6 was also moderately downregulated despite its gene expression remained virtually unchanged (Figure 7A, Table 3). In addition to the analysis of MCL samples obtained from the relapsed patients, paired primary cells isolated from two MCL patients (samples D9/R9, and D10/R10) refractory to araC were subject to analysis of gene and protein expression, and determination of their *ex vivo* sensitivity to nucleoside analogs (Figure 7B,C). The samples were obtained before araC administration (D9, D10), and 14 days after araC administration (R9, R10). Downregulation of both gene

Table 2 Identity of differentially expressed proteins with low mascot score confirmed by MS/MS

Spot no.	Accession	Protein name	Peptide sequence	Score
1	P27707	Deoxycytidine kinase	LKDAEKPVLFFER, QLCEDWEVVPEPVAR	41, 46
7	P31937	3-Hydroxyisobutyrate Dehydrogenase, Mitochondrial	DFSSVFQFLREEETF (C-term), SPILLGSLAHQIYR	49, 28

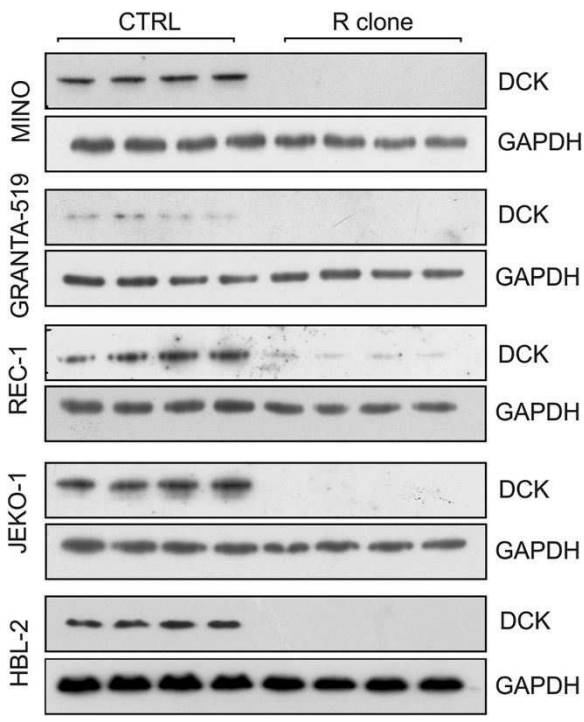

Figure 3 Western blot analysis confirms marked downregulation of protein DCK in all R clones. Relative expression of deoxycytine kinase (DCK) in all five R and CTRL clones. Quadruplicate cell lysates were separated on 12% SDS-PAGE minigels. Proteins were then transferred onto PVDF membranes, blocked and probed with anti-DCK antibody. Anti-GAPDH antibody was used as the loading control.

and protein DCK expression was confirmed in R9 compared to D9 cells (Figure 7B). Sensitivity of R9 cells to araC, fludarabine and gemcitabine was significantly suppressed compared to D9 cells (Figure 7C). Both gene expression and protein expression of R10 compared to D10 sample remained unchanged (Figure 7B). Interestingly, susceptibility of R10 cells compared to D10 cells to undergo apoptosis after their *ex vivo* exposure to araC was increased despite the fact that R10 cells were isolated after administration of four cycles of high-dose araC (Figure 7C).

Discussion

In this study we analyzed molecular mechanisms of araC resistance in five MCL cell lines and ten paired primary MCL samples obtained before and after araC-based therapies. In addition, we tested optimal treatment strategies for cytarabine-resistant MCL. On molecular level we identified marked and principal downregulation of DCK, the rate-limiting enzyme of nucleotide salvage pathway, in all 5 cytarabine-resistant MCL clones, and in 50% primary MCL samples obtained from patients, who progressed on or relapsed after araC-based treatments. In 50% primary MCL samples, no change of DCK expression was observed at time of lymphoma relapse or progression. Importantly, no upregulation of DCK was observed in any of the analyzed post-treatment samples. Although the analysis of the primary MCL samples indicate that the mechanisms responsible for araC resistance *in vivo* are more complex than those observed *in vitro*, it must be emphasized that downregulation of gene and protein DCK was indeed confirmed in a substantial part of the patients' post-treatment samples (Table 3, Figure 7A,B). Interestingly, in one of the two MCL patients primary resistant to araC, no change of DCK expression was observed with slightly increased *ex vivo* sensitivity of post-treatment MCL cells to araC (Figure 7B,C). This observation could be explained by existence of araC-resistant stem cell-like MCL cells that would reside in the niches in lymph nodes (and/or bone marrow) and produce partially araC-sensitive MCL cells mobilized in the peripheral blood. In such a case, elimination of the mobilized MCL cells, but persistence of the stem cell-like MCL compartment, would lead to stable disease, and eventual lymphoma progression (which was the actual course of the disease observed in this patient).

DCK catalyzes the first phosphorylation (=activation necessary for their cytotoxic activity) not only of araC into araCMP, but also of most nucleoside analogs (both pyrimidine and purine-derived) commonly used in anticancer therapy. Using DAVID bioinformatic analyzer *purine/pyrimidine metabolism*, and *B-cell receptor signaling* were among the functional cathegories associated with the most downregulated and upregulated genes, respectively. In accordance with these results we subsequently showed that all R clones were cross-resistant to both pyrimidine analog gemcitabine, and to purine analogs fludarabine and cladribine (all of which are activated by DCK). Sensitivity of R clones to other types of anti-cancer molecules including genotoxic cytostatics (cisplatin, doxorubicin, bendamustine), targeted drugs (temsirolimus, bortezomib) or biological agents (monoclonal anti-CD20 antibody rituximab) remained unaffected, or was even augmented in the case of BTK inhibitor ibrutinib. The reason, why ibrutinib more effectively eliminated araC-resistant MCL cells remained elusive, but might be at least partially explained by the observed upregulation of B-cell receptor signaling in R clones compared to CTRL cells (Additional file 1: Figure S1).

The results of our *in vitro* and *in vivo* tests combined with the observed decreased expression of DCK in all araC-resistant MCL clones and in 50% post-treatment primary MCL samples suggest that the resistance of MCL cells to high-dose araC is caused by suppressed araC activation by DCK due to markedly decreased DCK expression. DCK has low substrate preference and phosphorylates both, purines and pyrimidines, including synthetic analogs cytarabine, fludarabine, gemcitabine and cladribine [27-29]. The fact that above-mentioned nucleoside analogs are

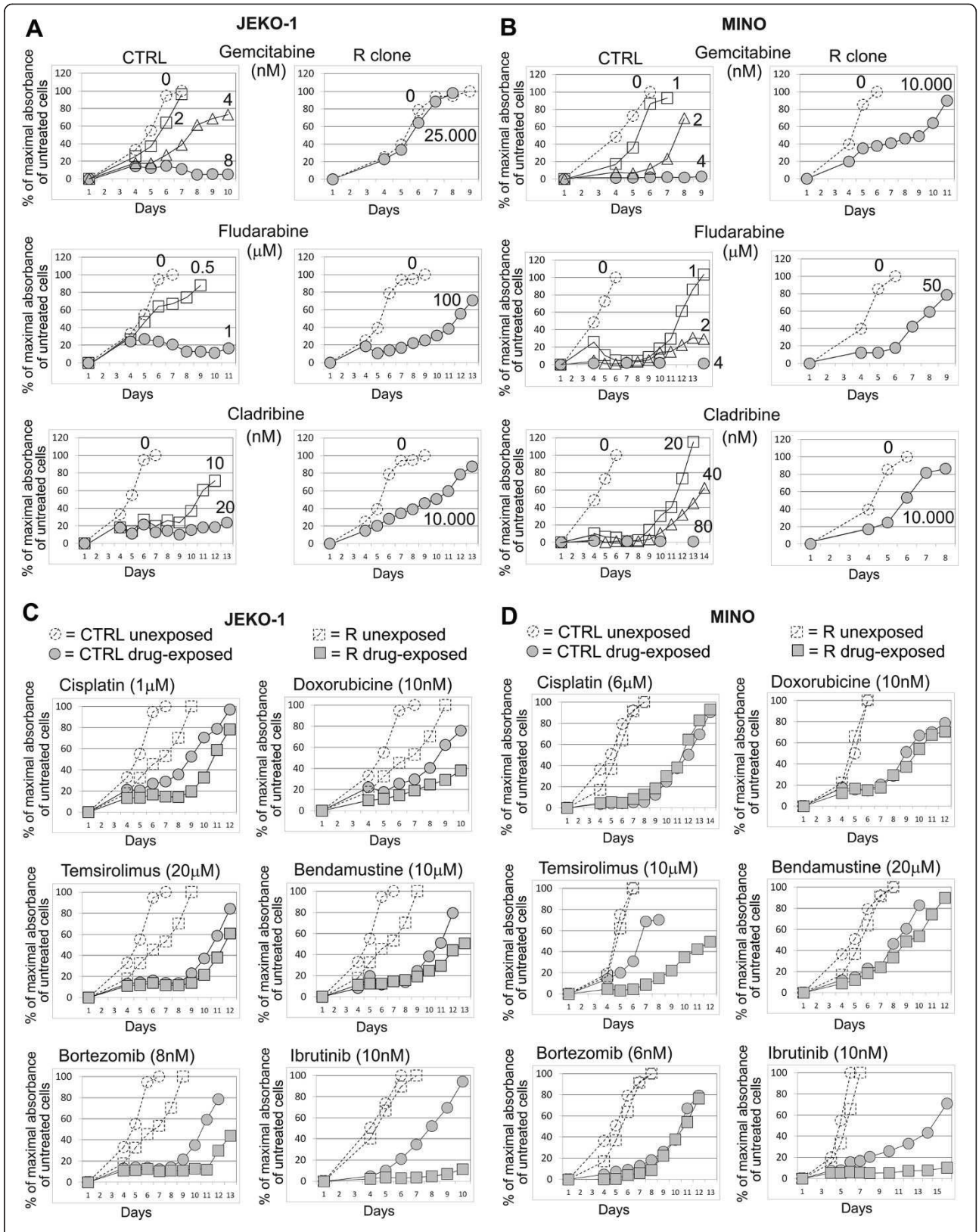

Figure 4 (See legend on next page.)

(See figure on previous page.)
Figure 4 R clones are cross-resistant to nucleoside analogs, but remain sensitive to other classes of anti-lymphoma agents. (A-D) WST-8 cell proliferation assays of CTRL cells and R clones were carried out as described in Methods. Maximal absorbance obtained from the untreated cells during the particular experiment (MAX_u) was arbitrary set as 100%. Absorbance of medium without cells was used as background **(B)**. For each cell population (both, unexposed and drug-exposed) and for each measurement (M_1, M_2, M_3…M_X) the proliferation curve was calculated as follows: (M_X - B)/(MAX_u - B). As a consequence, proliferation curves of untreated cells always peak at 100%, while proliferation curves of drug-exposed cells can terminate below or above 100%. One representative example of two independent experiments carried out both on JEKO-1 **(A, C)** and MINO **(B, D)** is shown. Data from the remaining three MCL cell lines (HBL-2, GRANTA-519 and REC-1) are not shown, because they did not significantly differ from those presented for the JEKO-1 and MINO cells. In summary, all 5 R clones were cross-resistant to the tested nucleoside analogs, but remained sensitive to other classes of anti-lymphoma agents with negligible differences between particular MCL cell lines. The only exception to the rule was markedly (>100-fold) increased sensitivity of REC-1 R clone to ibrutinib compared to REC-1 CTRL cells (see Additional file 3: Figure S2). The remaining 4 MCL cell lines (JEKO-1, MINO, GRANTA-519 and HBL-2) showed only approx. 2-fold increased sensitivity to ibrutinib compared to the corresponding CTRL cells. Standard deviations were < 5% for all measurements presented in Figure 4.

substrates of DCK explains the observed cross-resistance of R clones to all tested nucleoside analogs, both purine- and pyrimidine-derived. Retained sensitivity to other classes of anti-MCL agents (i.e. other than nucleoside analogs) with diverse molecular mechanisms of their respective antitumor activities suggests that no major additional molecular alteration was involved in the development of araC resistance.

Prognosis of patients with relapsed/refractory MCL (RR-MCL) is dismal. Currently there is no standard-of-care for RR-MCL patients. Second-line treatment approaches include fludarabine, gemcitabine, cladribine, cisplatin, bortezomib, temsirolimus, bendamustine, lenalidomide and ibrutinib-based regimen. We have proved *in vitro* and *in vivo* on a mouse xenograft model of MCL that treatment of patients, who progress on or relapse

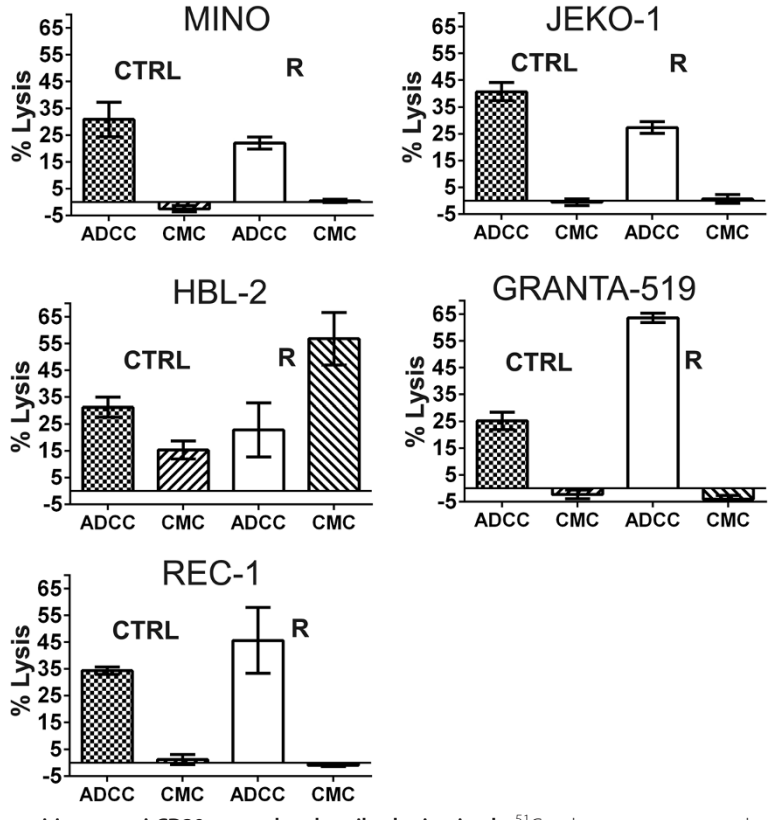

Figure 5 R clones remain sensitive to anti-CD20 monoclonal antibody rituximab. ^{51}Cr release assay was used to assess the impact of the anti-CD20 monoclonal antibody rituximab on complement mediated cytotoxicity (CMC) and antibody dependent cellular cytotoxicity (ADCC). CMC was measurable only in HBL-2 cells (both CTRL and R), but was negligible in the remaining four MCL cell populations (both CTRL and R). In HBL-2 R clone the CMC was significantly increased compared to CTRL. ADCC was measurable in all five MCL cell lines. In JEKO-1 R clone the ADCC was slightly decreased compared to CTRL. In GRANTA-519 R clone the ADCC was significantly increased compared to CTRL. In MINO, REC-1 and HBL-2 the ADCC remained comparable between R clone and CTRL cells.

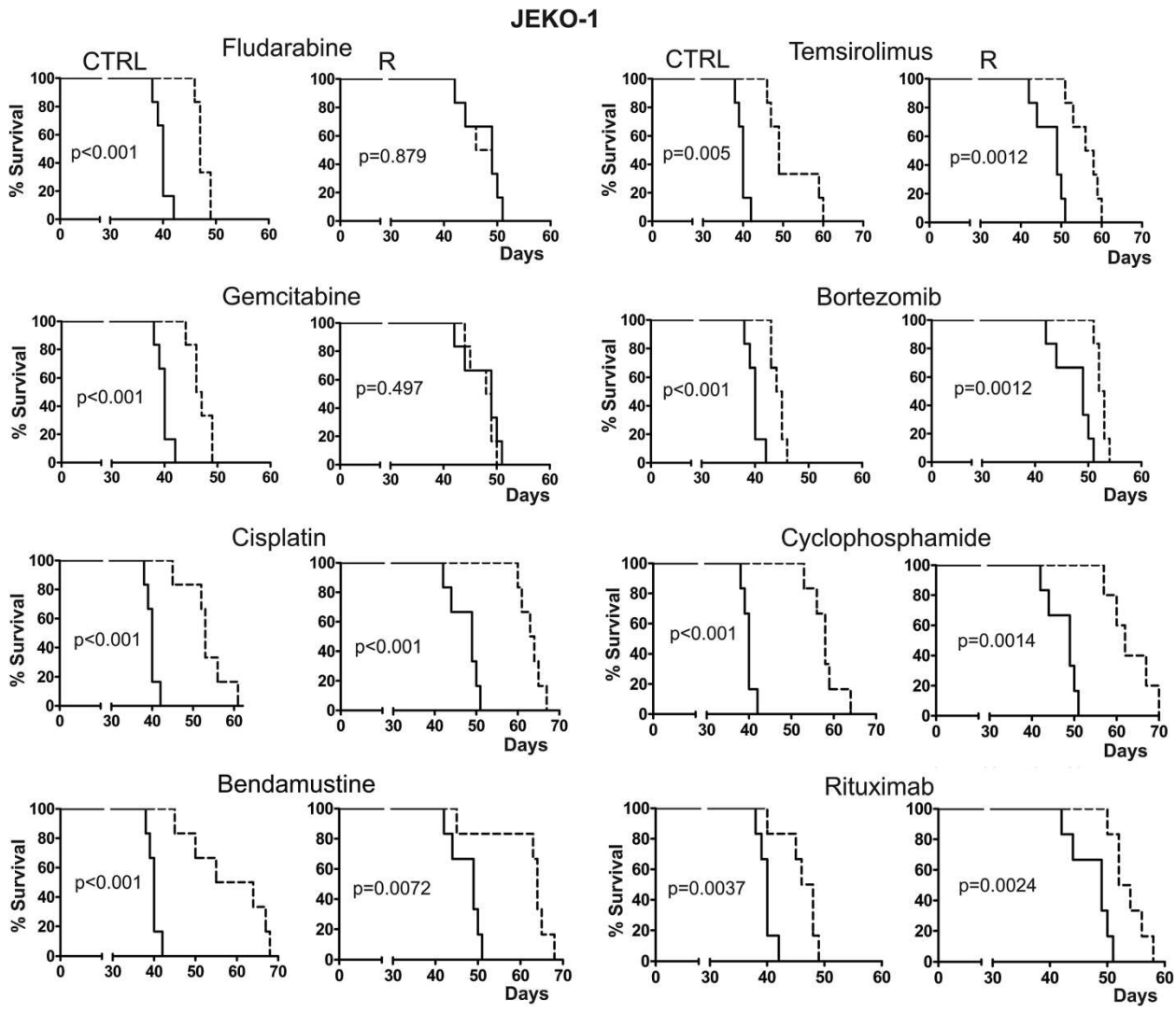

Figure 6 Experimental therapy of mice xenografted with JEKO-1 CTRL and JEKO-1 R cells. Overall survival of experimental animals is shown as Kaplan-Meier survival estimates. Loss of anti-tumor activity was observed for the nucleoside analogs fludarabine and gemcitabine in the therapy of R clone-xenografted mice (dashed lines) when compared to CTRL-xenografted mice (solid lines). Other classes of anti-lymphoma agents retained the antitumor activity in both CTRL- and R clone-xenografted mice. Individual cohorts contained 6 animals. For more details see Methods.

after high-dose araC-based regimen should not rely on nucleoside analogs, namely on the currently used agents fludarabine, gemcitabine and cladribine, since all of them must be phosphorylated by DCK to exert their anti-lymphoma activity. Instead, other classes of anti-lymphoma drugs should be applied in case of araC failure, i.e. in the setting of anticipated araC-resistance. Some of these agents have only recently been approved for the therapy of relapsed/refractory (RR-) MCL, temsirolimus in Europe, bortezomib and ibrutinib in USA. It might be speculated that high-dose therapy (given before autologous stem cell transplant) based on other agents than nucleoside analogs might prove more beneficial especially for those patients with suboptimal responses after induction araC-based immunochemotherapy (e.g. patients, who achieve partial remission, or patients with detectable minimal residual disease). In addition to the currently approved agents, bendamustine represents another extremely promising drug in MCL. Recently it was demonstrated that bendamustine potentiates the effect of araC by augmenting the level of intracellular ara-CTP, and the R-BAC (rituximab, bendamustine, araC) regimen was shown to be effective even in patients resistant to araC thus providing a treatment option even for the elderly and/or frail patients [16,30,31]. It might be speculated that the increased level of ara-CTP might partially offset the anticipated downregulation of DCK thereby explaining, why the combination of bendamustine and araC was shown to be effective even in patients, who relapsed after araC-based therapies [30].

Table 3 Gene expression analysis of DCK in a set of primary MCL samples obtained from patients before and after araC-based therapies

Sample at diagnosis	Source	ΔCT (DCK-GAPDH)	Therapy	Sample at relapse	Disease-free survival (months)	Source	ΔCT (DCK-GAPDH)	Difference in ΔCT between R and D samples
D1	PBMC	3.4	A*	R1	12	PBMC	3.7	+0.3
D2	PE***	3.3	A	R2	10	PE***	5.3	+2.0
D3	FFPE	0.1	A	R3	5	FFPE	1.3	+1.2
D4	FFPE	1.7	B	R4	4	FFPE	3.5	+1.8
D5	PBMC	1.4	A	R5	7	PBMC	2.2	+0.8
D6	PBMC	4.1	B**	R6	3	PBMC	3.9	−0.2
D7	FFPE	1.3	B	R7	13	FFPE	3.5	+2.2
D8	FFPE	2.0	A	R8	25	FFPE	1.8	−0.2
D9	PBMC	1.9	B	R9	N/A	PBMC	3.3	+1.4
D10	PBMC	2.3	A	R10	N/A	PBMC	1.5	−0.8

*A = alternation of R-CHOP and R-araC (2 g/m2, 2 doses a 24 h).
**B = Nordic protocol (alternation of R-MaxiCHOP and R-araC (2-3 g/m2, 4 doses a 12 h).
***PE pleural effusion (CD19-sorted).
Samples from relapsed patients were obtained at diagnosis (D1-D8) and at lymphoma relapse after failure of araC-based therapies (R1-R8). Samples from refractory patients were obtained from primary araC-resistant MCL patients before (D9-D10) and 14 days after (R9-R10) administration of high-dose araC. Real-time RT-PCR was used to determine changes in DCK expression.

Conclusions

Our data from the cell lines and primary MCL samples clearly demonstrate that acquired resistance of MCL cells to araC is associated with downregulation of mRNA and protein expression of DCK, enzyme of the nucleotide salvage pathway responsible for phosphorylation of most nucleoside analogs used in anti-cancer therapy. In translation, the results suggest that 1. nucleoside analogs should not be used for the second-line therapy of MCL patients, who fail after araC-based regimen; 2. non-nucleoside analogs should be employed in this setting, including cisplatin, ibrutinib, temsirolimus, bortezomib or bendamustine; 3. ibrutinib appears particularly effective in eliminating araC-resistant MCL cells.

Methods

Cell culture

JEKO-1, GRANTA-519 and REC-1 were purchased from German Collection of Microorganisms and Cell Cultures (DSMZ), MINO was from American Tissue Culture Collection (ATCC), HBL-2 was a kind gift of prof. Dreyling (University of Munich, Germany). Cell lines were cultured

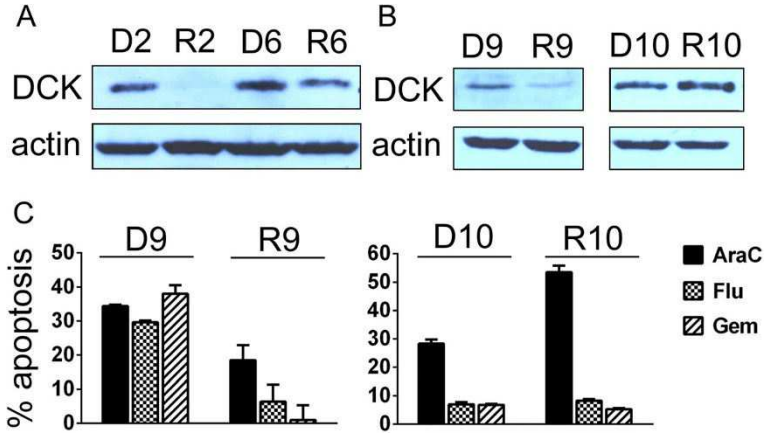

Figure 7 Protein expression of DCK in primary MCL samples, and their *ex vivo* sensitivity to nucleoside analogs. (A-B) Relative expression of deoxycytine kinase (DCK) in post-treatment primary MCL samples (R2, R6, R9, R10) compared to pre-treatment samples (D2, D6, D9, D10). **(C)** CD19-sorted PBMC cells were isolated from two leukemized araC-refractory MCL patients before (D9, D10) and 14 days after (R9, R10) administration of high-dose araC. The cells were *ex vivo/in vitro* exposed to araC (25 μM), fludarabine (Flu, 100 μM) and gemcitabine (Gem, 25 μM). Apoptosis was measured after 24 hours using standard Annexin-V-PE and flow cytometry. Apoptotic cells are shown as Annexin-V-PE-positive cells (Y axis). Basal apoptosis of drug-unexposed cells was subtracted from the apoptosis of the drug-exposed cells.

in Iscove's modified Dulbecco's medium (IMDM) supplemented with 15% fetal bovine serum (FBS) and 1% penicillin/streptomycin.

Reagents

Cytarabine, fludarabine, gemcitabine, cladribine, cyclophosphamide, doxorubicin and cisplatin were from Clinical Dept. of Hematology, University Hospital in Prague, Czech Republic. Temsirolimus, bortezomib, bendamustine and ibrutinib were purchased from Selleck Chemicals. Rituximab was kindly provided by Roche, Czech Republic.

Establishment of araC-resistant clones

MCL cell lines were incubated in Iscove's modified Dulbecco's medium (IMDM) supplemented with 15% fetal bovine serum with increasing concentrations of cytarabine up to 50 μM.

Proliferation assays

Proliferation was estimated using WST-8 Quick Cell Proliferation Assay Kit (BioVision) according to the manufacturer instructions. Briefly, 5.000 cells were seeded into 96-well plate on day 1. Drugs were added on day 1. Proliferation was measured on day 1 and then since day 4 daily. Antiproliferative activity of each drug was analyzed at several concentrations.

Absorbance of the triplicate samples was measured on ELISA reader after 3 hour incubation with WST-8 reagent at 37 grades Celsius in the thermostat. Maximal absorbance (MAX_u) obtained from the untreated cells during the particular experiment was arbitrary set as 100%. Absorbance of medium without cells was used as background (B). For each cell population (both, unexposed and drug-exposed) and for each measurement (M_1, M_2, M_3...M_X) the proliferation curve was calculated as follows: $(M_X - B)/(MAX_u - B)$. As a consequence, the proliferation curve of untreated cells always peaks 100%, while proliferation curves of drug-exposed cells can terminate below or above 100%.

^{51}Cr release assay for the assessment of the impact that CD20 mAbs have on rituximab-mediated complement mediated cytotoxicity (CMC) and antibody dependent cellular cytotoxicity (ADCC)

CTRL MCL cells and R clones were labeled with ^{51}Cr at 37°C, 5% CO2 for 2 hrs. ^{51}Cr-labeled cells were then placed in 96-well plates at a cell concentration of 1×10^5 cells/well (complement-mediated cytotoxicity (CMC) assay) or 1×10^4 cells/well (antibody-dependent cell cytotoxicity (ADCC) assay). Cells were then exposed to rituximab (10 mg/ml) or isotype antibody (10 mg/ml) and human serum (for CMC assay, 1:4 dilution) or peripheral blood mononuclear cells (PBMCs) (for ADCC assay, 40:1 effector: target ratio) for six hrs at 37°C and 5% CO2. ^{51}Cr release was measured from the supernatant by standard gamma counting and the percentage of lysis was calculated. PBMCs were obtained from healthy donors (Roswell Park Cancer Institute IRB-approved protocol CIC-016) and isolated by Histopaque-1077 ultracentrifugation of peripheral whole blood and used at an effector: target ratio of 40:1 for ADCC assays. Pooled human serum was used as the source of complement for CMC assays.

Gene expression profiling and data analysis

A biological duplicate of each araC-resistant MCL clone (R) was compared to a biological duplicate of the original araC-sensitive (CTRL) cell line. In total, five R clones were compared to five corresponding CTRL cell lines using two microarray chips. Total RNA was extracted by RNeasy Mini Kit (Qiagen), and its quality verified using the Agilent 2100 Bioanalyzer (Agilent Technology). Extracted RNA was amplified using the Illumina RNA Amplification Kit (Ambion). Amplified RNA was hybridized to the Illumina HumanRef-8 and HumanRef-12 BeadChips (Illumina). Subsequent data analysis was performed in R-software, mainly in limma package from Bioconductor (http://www.bioconductor.org). Multiple testing correction was performed using Benjamini & Hochberg method. The filtered group of genes with fold change at least ±1.5-fold and adjusted p value < 0.05 were annotated and arranged into biologically relevant categories using The Database for Annotation, Visualization and Integrated Discovery (DAVID, http://david.abcc.ncifcrf.gov).

Primary MCL sample acquisition, real-time RT-PCR analysis, and apoptosis measurement

All primary MCL samples were obtained from patients with MCL at diagnosis (D1-D10), and at the relapse or during progression after failure of high-dose araC-based front-line therapies (R1-R10). Samples were obtained from patients, who signed informed consent according to the Declaration of Helsinki. Mononuclear cells were isolated from all PBMC and PE samples by the standard Ficoll-Hypaque gradient centrifugation. Mononuclear cells were then CD19 sorted on magnetic columns using CD19 microbeads (Miltenyi Biotec). The purity of MCL population after sorting was > 95% in all cases as verified by flow-cytometry. Total RNA was isolated from CD19-sorted PBMC or PE cells stored in RNA*later* solution using RNeasy Mini Kit (Qiagen, Hilden, Germany) and from fresh-frozen paraffin-embedded (FFPE) lymph node samples using High Pure RNA Paraffin Kit (Roche Diagnostics GmbH, Germany) according to the manufacturer's instructions. cDNA synthesis was carried out from 1 μg of total RNA with the High-Capacity cDNA Reverse Transcription Kit (random primers) (Applied Biosystems). Real-time RT-PCR was performed using TaqMan Gene Expression Assays on the ABI 7900HT detection system (Applied

Biosystems). The reference gene was GAPDH. *Ex vivo* apoptosis of primary MCL cells was determined using Annexin-V-PE (Apronex, Czech Republic) and flow cytometry (BD FACS Canto II) according to the manufacturer's instructions after 24 hours exposure to 25 μM araC, 100 μM fludarabine and 25 μM gemcitabine.

Experimental therapy of MCL xenografts

In vivo studies were approved by the institutional Animal Care and Use Committee. Immunodeficient NOD.Cg-*Prkdc*^{scid} *Il2rg*^{tm1Wjl}/SzJ mice (Jackson Laboratory) were maintained in individually ventilated cages. JEKO-1 cell line-based mouse model of MCL was used for experiments [32]. JEKO-1 cells were harvested, suspended in PBS, and injected (1×10^6/mouse) i.v. into tail vein of 8- to 12-week-old female mice on DAY 1. Therapy was initiated on DAY 8. Each cohort of mice contained 6–8 animals. The mice received treatment as follows: temsirolimus 1 mg s.c. 1 x weekly (3 cycles), cyclophosphamide 3 mg i.p. 1 × weekly (3 cycles), bendamustine 0.5 mg i.p. two subsequent days (day 1 + day 2) every two weeks (2 cycles), bortezomib 25 μg i.p. 2 × weekly (3 cycles), cisplatin 180 μg i.p. every two weeks (2 cycles), gemcitabine 10 mg i.p. 1 × weekly (3 cycles), fludarabine 1 mg three subsequent days (day 1–3) weekly (3 cycles), rituximab 250 μg s.c. 1 × weekly (3 cycles). The data were analysed in GraphPad Software.

Two-dimensional electrophoresis

IPG strips (pH 4.0-7.0, 24 cm; ReadyStrip, Bio-Rad) were rehydrated overnight in 450 μL of sample, representing 1.5 mg of protein. Isoelectric focusing was performed for 70 kVh using Protean IEF cell (Bio-Rad). Six replicates were run for each cell type. Focused strips were equilibrated and reduced in equilibration (6 M urea, 50 mM Tris pH 8.8, 30% glycerol, 2% SDS) supplemented with DTT (450 mg per 50 mL) for 15 min and then alkyled in equilibration buffer with added iodacetamide (1.125 mg iodacetamide per 50 mL). SDS-PAGE electrophoresis was performed in a Tris-glycine-SDS system using a 12-gel Protean Dodeca Cell apparatus (Bio-Rad) with buffer circulation and external cooling (20°C). Gels were run at a constant voltage of 80 V per gel for 30 min and then at a constant voltage of 200 V for 6 h. Gels were washed in deionized water to remove redundant SDS and with colloidal Coomassie Brilliant Blue (SimplyBlue™ Safestain, Invitrogen, Carlsbad, CA, USA) overnight.

Gel image analysis and extraction of peptides

Stained gels were scanned with GS 800 calibrated densitometer (Bio-Rad) and image analysis was performed with Progenesis™ software (Nonlinear Dynamics, Ltd., Newcastle upon Tyne, UK) in semi-manual mode with 6 gel replicates for each cell type. Normalization of gel images was based on total spot density, and integrated spot density values (spot volumes) were then calculated after background subtraction. Average spot volume values (averages from the all 6 gels in the group) for each spot were compared between the groups. Protein spots were considered differentially expressed if their average normalized spot volume difference was > 2-fold. As determined by the Student's t-test, a p-value < 0.05 was considered to indicate a statistically significant difference.

Protein digestion and peptide extraction

Spots containing differentially expressed proteins were excised from the gels, cut into small pieces and washed 3 times with 25 mM ammonium bicarbonate in 50% acetonitrile (ACN). The gels were then dried in a Speed-Vac Concentrator (Eppendorf, Hamburg, Germany). Sequencing grade modified trypsin (Promega, Madison, WI, USA) (6 ng/μl in 25 mM ammonium bicarbonate in 5% ACN) was added. Following overnight incubation at 37°C, the resulting peptides were extracted with 50% ACN.

MS analysis and protein identification

Peptide samples were spotted on a steel target plate (Bruker Daltonics, Bremen, Germany) and allowed to dry at room temperature. Matrix solution (3 mg α-cyano-4-hydroxycinnamic acid in 1 ml of 50% ACN containing 0.1% trifluoroacetic acid) was then added. MS was performed on an Autoflex II MALDI-TOF/TOF mass spectrometer (Bruker Daltonics, Bremen, Germany) using a solid nitrogen laser (337 nm) and FlexControl software in reflectron mode with positive ion mass spectra detection. The mass spectrometer was externally calibrated with Peptide Calibration Standard II (Bruker Daltonics). Spectra were acquired in the mass range 800–3,000 Da. The peak lists were generated using FlexAnalysis and searched against Swiss-Prot (2012_07 version, 536 789 sequences) using Mascot software. The peptide mass tolerance was set to 100 ppm, taxonomy Homo sapiens, missed cleavage was set to 1, fixed modification for cysteine carbamidomethylation, and variable modifications for methionine oxidation and protein N-terminal acetylation. Proteins with Mascot score over the threshold 56 for $p < 0.05$ calculated for the used settings were considered as identified. If the score was lower, the identity of protein candidate was confirmed by MS/MS.

Western blot analysis

Cells were lysed in NHT buffer (140 mM NaCl, 10 mM HEPES, 1.5% Triton X-100, pH 7.4). Protein concentration in the collected supernatants was determined by the Bradford assay (Bio-Rad). Lysate samples (50 μg) were combined with SDS loading buffer containing 2-mercaptoethanol and boiled for 5 min. Quadruplicate samples were separated on 12% SDS-PAGE minigels in Tris-glycine buffer (Bio-Rad).

Electrophoresis was performed at a constant voltage for 30 min at 45 V per gel, and then at 90 V per gel until the dye front reached the gel bottom. Proteins were transferred onto 0.45 μm PVDF membranes (Milipore, Billerica, MA, USA) in a semi-dry blotter (Hoefer, San Francisco, CA, USA) at 0.8 mA/cm^2. Membranes were incubated in PBS (Invitrogen) containing 0.1% Tween-20 and 5% non-fat dried milk for 1 h. GAPDH or Actin were used as the loading controls. As primary antibodies anti-deoxycytidine kinase mouse monoclonal antibody (sc 81245 Santa Cruz Biotechnology, Sanat Cruz, CA, USA) diluted 1:200 or polyclonal anti-GAPDH produced in rabbit (Sigma-Aldrich, G9545) diluted 1:10,000 were used. After thorough washing in blocking buffer, a secondary horseradish peroxidase-conjugated anti-mouse (sc2005) or anti-rabbit antibody (sc2313) (both from Santa Cruz Biotechnology) was added (1:10,000). The signal was detected using LumiGLO Reserve, (KPL, Gaithersburg, MD, USA) or Western Blotting Luminol Reagent (Santa Cruz Biotechnology, Inc., Santa Cruz, CA, USA) and membranes were exposed to X-ray films (Kodak, Rochester, NY, USA).

Additional files

Additional file 1: Figure S1. Functional cathegories of genes differentially expressed in R compared to CTRL as determined by DAVID. The filtered group of genes acquired from all five MCL cell lines with fold change at least ±1.5-fold and adjusted p value < 0.05 were annotated and arranged into biologically relevant categories using The Database for Annotation, Visualization and Integrated Discovery (DAVID, http://david.abcc.ncifcrf.gov).

Additional file 2: Table S1. List of genes differentially expressed in more than one R clone compared to the corresponding CTRL cells. Microarray data are shown in Additional file 2: Table S1. 31 genes were differentially expressed in two araC-resistant clones (R) compared to the corresponding araC-sensitive controls (CTRL). 1 gene (TPM1) was differentially expressed in three R clones, and 1 gene (DCK) was differentially expressed in all five R clones compared to the corresponding CTRL.

Additional file 3: Figure S2. Ibrutinib appears more cytotoxic to cytarabine-resistant (R) compared to cytarabine-sensitive (CTRL) MCL cells. WST-8 cell proliferation assays of CTRL cells and R clones were carried out as described in Methods. Maximal absorbance obtained from the untreated cells during the particular experiment (MAX_u) was arbitrary set as 100%. Absorbance of medium without cells was used as background (B). For each cell population (both, unexposed and drug-exposed) and for each measurement (M_1, M_2, M_3…M_X) the proliferation curve was calculated as follows: (M_X - B)/(MAX_u - B). As a consequence, proliferation curves of untreated cells always peak at 100%, while proliferation curves of drug-exposed cells can terminate below or above 100%. One representative example of two independent experiments carried out on REC-1, HBL-2 and GRANTA-519 is shown. In summary, REC-1 R clone was > 100-fold sensitive to Bruton tyrosine-kinase (BTK) inhibitor ibrutinib compared to REC-1 CTRL cells. Both HBL-2 and GRANTA-519 R clones were approx. 2-fold more sensitive to ibrutinib compared to HBL-2 and GRANTA-519 CTRL cells.

Abbreviations

ACN: Acetonitrile; ADCC: Antibody-dependent cytotoxicity; AML: Acute myelogeneous leukemia; BTK: Bruton tyrosine-kinase; araC: Cytarabine, a pyrimidine analog used for anticancer therapy; CDA: Cytidine-deaminase, a key inactivating enzyme of nucleotide salvage pathway; CMC: Complement-mediated cototoxicity; CTRL: araC-sensitive MCL cell line; DCK: Deoxycytidine-kinase, a rate-limiting enzyme of nucleotide salvage pathway; DTT: Dithiothreitol; FFPE: Fresh-frozen paraffin-embedded (lymph node sections); HDAC: High-dose araC; i.v.: Intravenous injection; MCL: Mantle cell lymphoma; NHL: Non-Hodgkin lymphoma; NT5C2: Cytoplasmic 5'nucleotidase II, a key inactivating enzyme of nucleotide salvage pathway; PBMC: Peripheral-blood mononuclear cells; PE: Pleural effusion; R: araC-resistant clone derived from araC-sensitive cell line; R-CHOP: A combination of rituximab, cyclophosphamide, doxorubicin, vincristin and prednisone; R-DHAP: A combination of rituximab, high-dose cytarabine, cisplatin and dexamethasone; RR-MCL: Relapsed/refractory mantle cell lymphoma; s.c.: subcutanous injection.

Competing interests

The authors declare that they have no competing interests.

Authors' contributions

PK and JP conceived of the study and participated in drafting of the manuscript. MK carried out gene expression analysis and *in vivo* experiments, OV, LL and JP carried out proteomic analysis and western blotting. BM, DV, JM, PV and LL participated in *in vitro* experiments. CM carried out chrome-releasing assays. VK performed the statistical analysis. FH and MV participated in the design of the study and helped to review the manuscript. RJ and MT carried out analysis of primary MCL samples. All authors read and approved the final manuscript.

Authors' informations

Jiri Petrak and Pavel Klener Jr are considered senior co-authors.

Acknowledgements

Financial Support: IGA-MZ NT13201-4/2012, GACR14-19590S, GA-UK 446211, GA-UK 253284 700712, GA-UK 595912, GA-UK 1270214, UNCE 204021, PRVOUK-27/LF1/1, PRVOUK P24/LF1/3, SVV-2013-266509 and BIOCEV – Biotechnology and Biomedicine Centre of the Academy of Sciences and Charles University in Vestec" (CZ.1.05/1.1.00/02.0109), from the European Regional Development Fund.

Author details

[1]Institute of Pathological Physiology, Charles University in Prague, First Faculty of Medicine, Prague, Czech Republic. [2]First Department of Medicine - Department of Hematology, General University Hospital and Charles University in Prague, Prague, Czech Republic. [3]Institute of Pathology, General University Hospital and Charles University in Prague, Prague, Czech Republic. [4]Departments of Immunology and Medicine, Roswell Park Cancer Institute, Buffalo, NY, USA. [5]Institute of Hematology and Blood Transfusion, Prague, Czech Republic.

Received: 29 January 2014 Accepted: 23 June 2014
Published: 27 June 2014

References

1. Dreyling M, Kluin-Nelemans HC, Beà S, Klapper W, Vogt N, Delfau-Larue M-H, Hutter G, Cheah C, Chiappella A, Cortelazzo S, Pott C, Hess G, Visco C, Vitolo U, Klener P, Aurer I, Unterhalt M, Ribrag V, Hoster E, Hermine O: **Update on the molecular pathogenesis and clinical treatment of mantle cell lymphoma: report of the 11th annual conference of the European Mantle Cell Lymphoma Network.** *Leuk Lymphoma* 2013, **54:**699–707.
2. Jares P, Colomer D, Campo E: **Molecular pathogenesis of mantle cell lymphoma.** *J Clin Invest* 2012, **122:**3416–3423.
3. Delarue R, Haioun C, Ribrag V, Brice P, Delmer A, Tilly H, Salles G, Van Hoof A, Casasnovas O, Brousse N, Lefrere F, Hermine O: **CHOP and DHAP plus rituximab followed by autologous stem cell transplantation in mantle cell lymphoma: a phase 2 study from the Groupe d'Etude des Lymphomes de l'Adulte.** *Blood* 2013, **121:**48–53.
4. Lefrère F, Delmer A, Suzan F, Levy V, Belanger C, Djabarri M, Arnulf B, Damaj G, Maillard N, Ribrag V, Janvier M, Sebban C, Casasnovas R-O, Bouabdallah R, Dreyfus F, Verkarre V, Delabesse E, Valensi F, McIntyre E, Brousse N, Varet B, Hermine O: **Sequential chemotherapy by CHOP and DHAP regimens followed by high-dose therapy with stem cell transplantation induces a high rate of complete response and improves event-free survival in mantle cell lymphoma: a prospective study.** *Leukemia* 2002, **16:**587–593.
5. Merli F, Luminari S, Ilariucci F, Petrini M, Visco C, Ambrosetti A, Stelitano C, Caracciolo F, Di Renzo N, Angrilli F, Carella AM, Capodanno I, Barbolini E,

Galimberti S, Federico M: **Rituximab plus HyperCVAD alternating with high dose cytarabine and methotrexate for the initial treatment of patients with mantle cell lymphoma, a multicentre trial from Gruppo Italiano Studio Linfomi.** *Br J Haematol* 2012, **156:**346–353.
6. Ferrero S, Dreyling M: **The current therapeutic scenario for relapsed mantle cell lymphoma.** *Curr Opin Oncol* 2013, **25:**452–462.
7. Wang ML, Rule S, Martin P, Goy A, Auer R, Kahl BS, Jurczak W, Advani RH, Romaguera JE, Williams ME, Barrientos JC, Chmielowska E, Radford J, Stilgenbauer S, Dreyling M, Jedrzejczak WW, Johnson P, Spurgeon SE, Li L, Zhang L, Newberry K, Ou Z, Cheng N, Fang B, McGreivy J, Clow F, Buggy JJ, Chang BY, Beaupre DM, Kunkel LA, Blum KA: **Targeting BTK with ibrutinib in relapsed or refractory mantle-cell lymphoma.** *N Engl J Med* 2013, **369:**507–516.
8. Goy A, Sinha R, Williams ME, Kalayoglu Besisik S, Drach J, Ramchandren R, Zhang L, Cicero S, Fu T, Witzig TE: **Single-agent lenalidomide in patients with mantle-cell lymphoma who relapsed or progressed after or were refractory to Bortezomib: phase II MCL-001 (EMERGE) study.** *J Clin Oncol* 2013, **31:**3688–3695.
9. Goy A, Younes A, McLaughlin P, Pro B, Romaguera JE, Hagemeister F, Fayad L, Dang NH, Samaniego F, Wang M, Broglio K, Samuels B, Gilles F, Sarris AH, Hart S, Trehu E, Schenkein D, Cabanillas F, Rodriguez AM: **Phase II study of proteasome inhibitor bortezomib in relapsed or refractory B-cell non-Hodgkin's lymphoma.** *J Clin Oncol* 2005, **23:**667–675.
10. Ansell SM, Tang H, Kurtin PJ, Koenig PA, Inwards DJ, Shah K, Ziesmer SC, Feldman AL, Rao R, Gupta M, Erlichman C, Witzig TE: **Temsirolimus and rituximab in patients with relapsed or refractory mantle cell lymphoma: a phase 2 study.** *Lancet Oncol* 2011, **12:**361–368.
11. Witzig TE, Geyer SM, Ghobrial I, Inwards DJ, Fonseca R, Kurtin P, Ansell SM, Luyun R, Flynn PJ, Morton RF, Dakhil SR, Gross H, Kaufmann SH: **Phase II trial of single-agent temsirolimus (CCI-779) for relapsed mantle cell lymphoma.** *J Clin Oncol* 2005, **23:**5347–5356.
12. Vose JM: **Mantle cell lymphoma: 2012 update on diagnosis, risk-stratification, and clinical management.** *Am J Hematol* 2012, **87:**604–609.
13. Robak T, Lech-Maranda E, Janus A, Blonski J, Wierzbowska A, Gora-Tybor J: **Cladribine combined with cyclophosphamide and mitoxantrone is an active salvage therapy in advanced non-Hodgkin's lymphoma.** *Leuk Lymphoma* 2007, **48:**1092–1101.
14. Morschhauser F, Depil S, Jourdan E, Wetterwald M, Bouabdallah R, Marit G, Solal-Céligny P, Sebban C, Coiffier B, Chouaki N, Bauters F, Dumontet C: **Phase II study of gemcitabine-dexamethasone with or without cisplatin in relapsed or refractory mantle cell lymphoma.** *Ann Oncol* 2007, **18:**370–375.
15. Johnson SA: **Use of fludarabine in the treatment of mantle cell lymphoma, Waldenström's macroglobulinemia and other uncommon B- and T-cell lymphoid malignancies.** *Hematol J* 2004, **5**(Suppl 1):S50–S61.
16. Visco C, Finotto S, Zambello R, Paolini R, Menin A, Zanotti R, Zaja F, Semenzato G, Pizzolo G, D'Amore ESG, Rodeghiero F: **Combination of rituximab, bendamustine, and cytarabine for patients with mantle-cell non-Hodgkin lymphoma ineligible for intensive regimens or autologous transplantation.** *J Clin Oncol* 2013, **31:**1442–1449.
17. Ellison RR, Holland JF, Weil M, Jacquillat C, Boiron M, Bernard J, Sawitsky A, Rosner F, Gussoff B, Silver RT, Karanas A, Cuttner J, Spurr CL, Hayes DM, Blom J, Leone LA, Haurani F, Kyle R, Hutchison JL, Forcier RJ, Moon JH: **Arabinosyl cytosine: a useful agent in the treatment of acute leukemia in adults.** *Blood* 1968, **32:**507–523.
18. Kantarjian H, Barlogie B, Plunkett W, Velasquez W, McLaughlin P, Riggs S, Cabanillas F: **High-dose cytosine arabinoside in non-Hodgkin's lymphoma.** *J Clin Oncol* 1983, **1:**689–694.
19. Capizzi RL: **Curative chemotherapy for acute myeloid leukemia: the development of high-dose ara-C from the laboratory to bedside.** *Invest New Drugs* 1996, **14:**249–256.
20. Lamba JK: **Genetic factors influencing cytarabine therapy.** *Pharmacogenomics* 2009, **10:**1657–1674.
21. Clarke ML, Damaraju VL, Zhang J, Mowles D, Tackaberry T, Lang T, Smith KM, Young JD, Tomkinson B, Cass CE: **The role of human nucleoside transporters in cellular uptake of 4′-thio-beta-D-arabinofuranosylcytosine and beta-D-arabinosylcytosine.** *Mol Pharmacol* 2006, **70:**303–310.
22. Capizzi RL, White JC, Powell BL, Perrino F: **Effect of dose on the pharmacokinetic and pharmacodynamic effects of cytarabine.** *Semin Hematol* 1991, **28**(3 Suppl 4):54–69.
23. Cai J, Damaraju VL, Groulx N, Mowles D, Peng Y, Robins MJ, Cass CE, Gros P: **Two distinct molecular mechanisms underlying cytarabine resistance in human leukemic cells.** *Cancer Res* 2008, **68:**2349–2357.
24. Hubeek I, Stam RW, Peters GJ, Broekhuizen R, Meijerink JPP, van Wering ER, Gibson BES, Creutzig U, Zwaan CM, Cloos J, Kuik DJ, Pieters R, Kaspers GJL: **The human equilibrative nucleoside transporter 1 mediates in vitro cytarabine sensitivity in childhood acute myeloid leukaemia.** *Br J Cancer* 2005, **93:**1388–1394.
25. Tang J, Xie X, Zhang X, Qiao X, Jiang S, Shi W, Shao Y, Zhou X: **Long term cultured HL-60 cells are intrinsically resistant to Ara-C through high CDA activity.** *Front Biosci (Landmark Ed)* 2012, **17:**569–574.
26. DeAngelis LM, Kreis W, Chan K, Dantis E, Akerman S: **Pharmacokinetics of ara-C and ara-U in plasma and CSF after high-dose administration of cytosine arabinoside.** *Cancer Chemother Pharmacol* 1992, **29:**173–177.
27. Qin T, Jelinek J, Si J, Shu J, Issa JP: **Mechanisms of resistance to 5-aza-2'-deoxycytidine in human cancer cell lines.** *Blood* 2009, **113**(3):659–667.
28. Ewald B, Sampath D, Plunkett W: **Nucleoside analogs: molecular mechanisms signaling cell death.** *Oncogene* 2008, **27:**6522–6537.
29. Galmarini CM, Mackey JR, Dumontet C: **Nucleoside analogues: mechanisms of drug resistance and reversal strategies.** *Leukemia* 2001, **15:**875–890.
30. Visco C, Castegnaro S, Chieregato K, Bernardi M, Albiero E, Zanon C, Madeo D, Rodeghiero F: **The cytotoxic effects of bendamustine in combination with cytarabine in mantle cell lymphoma cell lines.** *Blood Cells Mol Dis* 2012, **48:**68–75.
31. Hiraoka N, Kikuchi J, Yamauchi T, Koyama D, Wada T, Uesawa M, Akutsu M, Mori S, Nakamura Y, Ueda T, Kano Y, Furukawa Y: **Purine analog-like properties of bendamustine underlie rapid activation of DNA damage response and synergistic effects with pyrimidine analogues in lymphoid malignancies.** *PLoS One* 2014, **9:**1–14.
32. Klanova M, Soukup T, Jaksa R, Molinsky J, Lateckova L, Maswabi BC, Prukova D, Brezinova J, Michalova K, Vockova P, Hernandez-Ilizaliturri F, Kulvait V, Zivny J, Vokurka M, Necas E, Trneny M, Klener P: **Mouse models of mantle cell lymphoma, complex changes in gene expression and phenotype of engrafted MCL cells: implications for preclinical research.** *Lab Invest* in press.

doi:10.1186/1476-4598-13-159
Cite this article as: Klanova *et al.*: Downregulation of deoxycytidine kinase in cytarabine-resistant mantle cell lymphoma cells confers cross-resistance to nucleoside analogs gemcitabine, fludarabine and cladribine, but not to other classes of anti-lymphoma agents. *Molecular Cancer* 2014 **13**:159.

7.3 Appendix 3

Detailed functional and proteomic characterization of fludarabine resistance in mantle cell lymphoma cells. Lorkova L, Scigelova M, Arrey TN, Vit O, Pospisilova J, Doktorova E, Klanova M, Alam M, Vockova P, Maswabi B, Klener P Jr., Petrak J. *PLoS One.* 2015;10(8):e0135314 (IF 2015: 3.057).

PLOS ONE

RESEARCH ARTICLE

Detailed Functional and Proteomic Characterization of Fludarabine Resistance in Mantle Cell Lymphoma Cells

Lucie Lorkova[1], Michaela Scigelova[2], Tabiwang Ndipanquang Arrey[2], Ondrej Vit[1], Jana Pospisilova[1], Eliska Doktorova[1], Magdalena Klanova[1,3], Mahmudul Alam[1], Petra Vockova[1,3], Bokang Maswabi[1], Pavel Klener, Jr.[1,3☯], Jiri Petrak[1,4☯*]

1 Institute of Pathological Physiology, First Faculty of Medicine, Charles University in Prague, Prague, Czech Republic, **2** Thermo Fisher Scientific, Bremen, Germany, **3** First Department of Medicine—Department of Hematology, General University Hospital and Charles University in Prague, Prague, Czech Republic, **4** Institute of Hematology and Blood Transfusion, Prague, Czech Republic

☯ These joint senior authors contributed equally to this work.
* jpetr@lf1.cuni.cz

Citation: Lorkova L, Scigelova M, Arrey TN, Vit O, Pospisilova J, Doktorova E, et al. (2015) Detailed Functional and Proteomic Characterization of Fludarabine Resistance in Mantle Cell Lymphoma Cells. PLoS ONE 10(8): e0135314. doi:10.1371/journal.pone.0135314

Editor: Yiqun G. Shellman, University of Colorado, School of Medicine, UNITED STATES

Received: April 10, 2015

Accepted: July 20, 2015

Published: August 18, 2015

Data Availability Statement: The mass spectrometry proteomics data have been deposited to the ProteomeXchange Consortium via the PRIDE partner repository with the dataset identifier PXD002034.

Funding: The work was supported by The ministry of health of CR (www.mzcr.cz) via grants: IGA-MZ NT13201-4 (PK), NT12248-5 (JP), 15-32961A (JP) and 15-27757A (PK). The work was also supported by the Minsitry of Education, Youth and Sports of the Czech Republic (www.msmt.cz) via institutional grants PRVOUK P24/LF1/3 (JP) and PRVOUK P27/

Abstract

Mantle cell lymphoma (MCL) is a chronically relapsing aggressive type of B-cell non-Hodgkin lymphoma considered incurable by currently used treatment approaches. Fludarabine is a purine analog clinically still widely used in the therapy of relapsed MCL. Molecular mechanisms of fludarabine resistance have not, however, been studied in the setting of MCL so far. We therefore derived fludarabine-resistant MCL cells (Mino/FR) and performed their detailed functional and proteomic characterization compared to the original fludarabine sensitive cells (Mino). We demonstrated that Mino/FR were highly cross-resistant to other antinucleosides (cytarabine, cladribine, gemcitabine) and to an inhibitor of Bruton tyrosine kinase (BTK) ibrutinib. Sensitivity to other types of anti-lymphoma agents was altered only mildly (methotrexate, doxorubicin, bortezomib) or remained unaffacted (cisplatin, bendamustine). The detailed proteomic analysis of Mino/FR compared to Mino cells unveiled over 300 differentially expressed proteins. Mino/FR were characterized by the marked downregulation of deoxycytidine kinase (dCK) and BTK (thus explaining the observed crossresistance to antinucleosides and ibrutinib), but also by the upregulation of several enzymes of de novo nucleotide synthesis, as well as the up-regulation of the numerous proteins of DNA repair and replication. The significant upregulation of the key antiapoptotic protein Bcl-2 in Mino/FR cells was associated with the markedly increased sensitivity of the fludarabine-resistant MCL cells to Bcl-2-specific inhibitor ABT199 compared to fludarabine-sensitive cells. Our data thus demonstrate that a detailed molecular analysis of drug-resistant tumor cells can indeed open a way to personalized therapy of resistant malignancies.

LF1/1(PK), UNCE 204021 (PK) and SVV-2013-260033 (JP) and grants from Charles University (www.cuni.cz) GAUK 700712 253284 (OV) and 595912 (BM) and from the Czech Science Foundation (www.gacr.cz) grants 15-02986S (PK), 14-19590S (PK) and 15-14200S (JP). The project was also supported by BIOCEV – Biotechnology and Biomedicine Centre of the Academy of Sciences and Charles University in Vestec (CZ.1.05/1.1.00/02.0109), from the ERDF (www.biocev.eu). The funders had no role in study design, data collection and analysis, decision to publish, or preparation of the manuscript.

Competing Interests: Co-authors MS and TA are affiliated with a company Thermo Fisher Scientific. The authors confirm that this involvement does not alter their adherence to all PLOS ONE policies on sharing data and material sharing. Thermo Scientific provided support in the form of salaries for authors MS and TA, but did not have any additional role in the study design, data collection and analysis, decision to publish or preparation of the manuscript. The specific roles of these authors articulated in the "author contributions" section.

Introduction

Mantle cell lymphoma (MCL) is a chronically relapsing aggressive type of B-cell non-Hodgkin lymphoma. Its estimated annual incidence in Europe is 0.45/100,000 persons. MCL remains incurable; despite the fact that most patients achieve an objective response (complete or partial remisison) after induction therapy, virtually all patients relapse sooner or later [1,2]. MCL is characterized by the translocation t(11;14)(q13;q32) leading to the overexpression of cyclin D1 with the ensuing deregulation of cell cycle machinery. Additional molecular aberrations include mutation in ATM, TP53, CDKN2A, RB1, CDK4/6, and MDM2, among other genes [1,3].

Newly diagnosed MCL patients are typically subjected to a combinatorial immunochemotherapy comprising anti-CD20 antibody rituximab (R), intensified anthracycline-based chemotherapy (e.g. R-Maxi-CHOP: cyclophosphamide, vincristine, doxorubicin, and prednisone), high-dose cytarabine (R-HDAC), and consolidation with high-dose therapy and autologous stem cell rescue. Prognosis of relapsed/refractory MCL is poor [1,2], no standard of care has been defined for such a condition. Second-line treatment approaches are based on nucleoside analogs (fludarabine, cladribine), DNA modifying agents (bendamustine, cisplatin), or targeted therapeuticals (bortezomib, temsirolimus, lenalidomide or ibrutinib). In everyday clinical practice, fludarabine-based regimens still remain important and widely used options for the salvage therapy of relapsed/refractory MCL [4]. In addition, several novel multi-agent combinations incorporating fludarabine have been tested and showed promise in the therapy of RR-MCL [5]. Outside MCL, fludarabine-based regimens are used for the first-line therapy of chronic lymphocytic leukemia (CLL), and the salvage therapy of indolent lymphomas and acute myelogeneous leukemias (AML).

Fludarabine (9-beta-D-arabinofuranosyl-2-fluoroadenine) is a prodrug administered in the form of a monophosphate (F-ara-AMP) which is dephosphorylated in vivo by plasma phosphatases and transported into cells. There it is retained after its re-phosphorylation to monophospate by deoxycytidine kinase (dCK) in the rate limiting step of fludarabine utilization. Next, F-ara-AMP is phosphorylated by adenylate kinase to a diphosphate F-ara-ADP, and by nucleoside diphosphate kinase to a triphosphate F-ara-ATP representing the active form of the drug. Incorporation of F-ara-ATP into DNA results in chain termination, replication fork stalling, and DNA breaks [6,7]. The replication stress activates DNA damage response resulting in either DNA repair or apoptosis. In addition, F-ara-ATP also decreases available dNTP pool by inhibiting ribonucleotide reductase, an enzyme critical for sufficient supply of deoxyribonucleotides. Fludarabine is also incorporated into RNA, and has been shown to directly induce apoptosis via caspase activation [6].

Unfortunately, acquired resistance to fludarabine is frequent. Mechanisms of fludarabine resistance in lymphomas are largely unknown. So far, several studies reported various molecules mutated or deregulated in association with fludarabine refractoriness (i.e. inherent resistance or acquired resistance in leukemic cells (CLL, AML)), including molecules/genes involved in the nucleotide salvage pathway (dCK, nucleotide transporters, ribonucleotide reductase) [8–11], antiapoptotic molecules (BCL2 family, BIRC3), transcription factors (MYC, NOTCH), mediators of genotoxic stress (ATM, TP53, SF3B1) and others (SULF2, MTORC2) [12–20]. Molecular mechanisms of fludarabine resistance thus appear highly heterogeneous, and potentially might even be disease-specific, a consequence of different genetic (mutational) background between acute myeloid and chronic lymphoid leukemias. To the best of our knowledge, the molecular mechanisms of fludarabine resistance in MCL have not been studied so far.

In this manuscript we derived fludarabine-resistant MCL cells, and studied their sensitivity to clinically-approved and experimental anti-lymphoma agents in order to empirically identify optimal strategies for elimination of fludarabine-resistant MCL cells. In addition, using detailed SILAC-based proteomic analysis we described molecular events responsible for and associated with fludarabine resistance in MCL, including causative, contributing and adaptive cellular processes.

Materials and Methods

Establishment of fludarabine-resistant clones

MCL cell line Mino [21] was purchased from ATCC, and cultured in Iscove's modified Dulbecco's medium (IMDM) supplemented with 15% fetal bovine serum (FBS) and 1% penicillin/streptomycin under standard tissue culture conditions. Fludarabine-resistant Mino cells (Mino/FR) were derived by co-culture with gradually increasing doses of fludarabine up to 100 μM.

Proliferation assays

Cytarabine, fludarabine, gemcitabine, cladribine, doxorubicin and cisplatin were from Clinical Dept. of Hematology, University Hospital in Prague, Czech Republic. Bortezomib, bendamustine, ABT-199 and ibrutinib were purchased from Selleck Chemicals. Proliferation was estimated using WST-8 Quick Cell Proliferation Assay Kit (BioVision) according to the manufacturer instructions. Briefly, 10,000 cells were seeded into a 96-well plate on day 1. Drugs were added on day 1. Proliferation was measured on day 1, and then starting on day 4 on a daily basis. The antiproliferative activity of each drug was analyzed at several concentrations. Absorbance of the samples (triplicate) was measured on ELISA reader after a three-hour incubation with WST-8 reagent at 37°C in a thermostat. Maximum absorbance (MAXu) obtained from the untreated cells during the particular experiment was arbitrarily set to represent 100%. Absorbance of medium without cells was used as background (B). For each cell population (i.e. unexposed and drug-exposed) and for each measurement (M1, M2, M3. . .MX) the proliferation curve was calculated as follows: (MX—B)/(MAXu—B). As a consequence, the proliferation curve of untreated cells always peaks at 100%, while proliferation curves of drug-exposed cells can terminate below or above 100%.

SILAC labeling

Mino cells were maintained in DMEM medium. To prepare SILAC heavy and light media, SILAC DMEM (Arg, Lys and Leu free) was supplemented with 10% dialyzed fetal bovine serum (FBS), 1% penicillin-streptomycin, sodium pyruvate (1 mM), glucose (4.5 g/L). The light (L) and heavy (H) media were supplemented with either 146 mg/L of L-lysine (L) or L-[$^{13}C_6$, $^{15}N_2$] lysine (H) and either 84 mg/L of L-arginine (L) or L-[$^{13}C_6$, $^{15}N_4$] arginine (H). L-proline (200 mg/L, Thermo Scientific) was added to both media to avoid the conversion of arginine to proline. All other chemicals were obtained from Sigma-Aldrich (St. Louis, MO, USA).

Mino cells were first grown in the "heavy media" (forward labeling) and Mino/FR in the "light media". In a parallel experiment, the media were swapped (reverse labeling). The cells were grown for at least six generations, and the complete incorporation of heavy amino acids was verified by a mass spectrometric analysis.

The same amounts (10 x 10^6 cells) of "light" and "heavy" labeled cells were mixed and processed further. The cells were washed three times with PBS. The mixed cell pellets (20 x 10^6

cells) were homogenized in 160 μL lysis buffer (10 mM HEPES, pH 7.4, 140 mM NaCl, 1.5% Triton X-100) at 4°C for 10 min. The whole cell lysates were centrifuged for 10 min (18,000 g) at 4°C. Protein concentration was determined using Bradford assay (Bio-Rad, CA, USA).

Filter-aided sample preparation (FASP)

Whole cell lysates (H+L) were digested using the filter-aided sample preparation (FASP) method [22] enabling detergent removal, reduction, alkylation and digestion on a filter. Cell lysates (100 μg total protein) were mixed with 300 μL of 8 M urea in 0.1 M Tris/HCl, pH 8.5 (UA buffer) supplemented with 100 mM DTT and incubated for 15 min at room temperature. After centrifugation at 18,000 g for 10 min, the supernatant was loaded on Ultrafree-MC centrifugal filter with a nominal molecular weight cutoff of 10,000 Da (Sigma-Aldrich, St. Louis, MO, USA) and centrifuged at 5,000 g. Retenate was diluted again in 300 μL of UA buffer and centrifuged until the complete removal of UA. The proteins were then alkylated with 100 μL 50 mM iodoacetamide dissolved in UA, incubated for 20 min at room temperature in the dark. Samples were then washed twice with 100 μL UA and three times with 100 μL of 50 mM ammonium bicarbonate. Proteins were digested with trypsin in the filter cone in 40 μL of 50 mM ammoniom bicarbonate at 37°C overnight, at an enzyme to protein ratio of 1:100. Peptides were collected by centrifugation, and the sample was acidified by addition of TFA to a final concentration 0.1% TFA. Samples were desalted using macrotrap (Peptide Macrotrap, Michrom Bioresources, Inc., CA, USA). Peptides were eluted by 200 μL 80% acetonitrile in 1% aqueous TFA. Eluted peptide samples were dried in SpeedVac Concentrator (Eppendorf, CR) and kept at -80°C until analyzed.

LC-MS/MS analysis and data processing

Samples were solubilized in 10 μl of 60% (v/v) aqueous acetonitrile and sonicated for approx. 2 min. Next, 40 μl of 0.1% (v/v) aqueous TFA solution were added, and the samples were sonicated for another 3 min. Peptides were analyzed using nano UHPLC (Easy-nLC 1000; Thermo Fisher Scientific, Odense, Denmark) coupled to the quadrupole-Orbitrap mass analyzer (Q Exactive; Thermo Fisher Scientific, Bremen, Germany). The sample (1 μl) was loaded onto Thermo Scientific Acclaim EasySpray PepMap C18 RSLC column (internal diameter 75 um, length 50 cm, 2 μm particle size, 100 Å pore size) maintained at a constant temperature (40°C) and equilibrated with 5% (v/v) acetonitrile in 0.1% (v/v) aqueous formic acid (FA). Peptides were separated with a 180-minute linear gradient (5–35%) of acetonitrile in 0.1% (v/v) aqueous solution of formic acid, flow rate 250 nl/min. Total run time was 210 min. Each sample was run in quadruplicate.

Data dependent acquisition on the Q Exactive operated in positive mode. Peptide parent ions were detected in a high resolution full scan (mass range 350–1500 *m/z*, 70,000 resolving power setting (resolving power defined as a full peak width at half maximum height at *m/z* 200)). The instrument was set so that 10 most intense ions of every full spectrum, meeting specific threshold criteria (minimum intensity threshold 1.7×10^4, charge state >1), should be selected for MS/MS. Peptides were isolated with an isolation window of 3 Da, fragmented (HCD fragmentation with NCE 27 collision energy setting), and the resulting fragment ions were detected (17,500 resolving power setting). Other settings: target value 3×10^6 and 1×10^5 for full scan and MS/MS scan, respectively; maximum ion time 50 ms and 120 ms for full scan and MS/MS scan, respectively. Following their fragmentation the precursors were put on an exclusion mass list for 30 seconds.

Data processing: Thermo Scientific Proteome Discoverer v. 1.4 (Thermo Fisher Scientific, Bremen, Germany) software package was used for protein identification and quantitation. The

spectra were searched using Mascot (Matrix Science, London, UK) search engine against the human subset of SwissProt database with added contaminant protein sequences (20,249 sequences in total) with the following search settings: cleavage specificity–trypsin; max. 2 missed cleavage sites; precursor mass tolerance 10 ppm; fragment mass tolerance 20 mDa; carbamidomethylation of Cys residues (+57,021) set as a static modification; heavy Arg and Lys residues (+10,008 and +8,014) set as dynamic modifications; maximum 3 dynamic modifications per peptide allowed. The search results were validated with decoy database search strategy using Percolator [23].

Quantitative analysis was based on the area under curve (AUC) for extracted ion chromatograms (6 ppm mass tolerance) of the respective peptide precursors. Protein ratio was calculated as the median of peptide ratios. Only unique peptides were considered.

Proteins confidently identified in both forward and reverse analyses with at least 2 peptides (1377 proteins) were futher evaluated. To normalize for minor differences in protein loading during mixing of "light" and "heavy" cells, SILAC ratios were log normalized. For the semi-quantitative expression analysis only the proteins with with at least 3 SILAC pairs in each (Forward and Reverse) experiment were included. As differentially expressed we considered proteins showing a protein ratio change of at least 1.5-fold and having protein ratio variability lower or equal 40%.

The mass spectrometry proteomics data have been deposited to the ProteomeXchange Consortium via the PRIDE partner repository with the dataset identifier PXD002034 (http://www.ebi.ac.uk/pride/archive/projects/PXD002034).

Western blotting

Cells were lysed in NHT buffer (140 mM NaCl, 10 mM HEPES pH 7.4, 1.5% Triton X-100) and centrifuged at 18,000 g to clear away debris. Protein concentration in resulting supernatants was determined by the Bradford assay. Lysates were combined with SDS loading buffer containing 2-mercaptoethanol, and boiled for 5 min. Quadruplicate samples (50 μg) were separated on Mini-PROTEAN TGX Stain-Free Precast Gels (Bio-Rad) in Tris-glycine-SDS buffer (Bio-Rad). Electrophoresis was performed at a constant voltage for 20 minutes at 300 V per gel until the dye front reached the gel bottom. Proteins were transferred onto 0.45 μm Immobilon-P PVDF membranes (Millipore) in Trans-Blot Turbo™ Transfer System semi-dry blotter (Bio-Rad) using pre-set transfer settings. Membranes were incubated in PBS (Sigma) containing 0.1 Tween-20 (Promega) and 5% non-fat milk for 30 minutes. GAPDH was used as a loading control. As primary antibodies anti-deoxycytidine kinase mouse monoclonal antibody (sc-81245, Santa Cruz Biotechnology) diluted 1:200, anti-Bcl-2 mouse monoclonal antibody (610539, BD Biosciences) diluted 1:1000, anti-Btk rabbit polyclonal antibody and anti-phospho-Btk (Y233) rabbit antibody (3533 and 5082, Cell Signaling Technologies) both diluted 1:1000, anti-phosphoserine aminotransferase rabbit polyclonal antibody (ab96136, Abcam) diluted 1:500, anti-SH-PTP1 rabbit polyclonal antibody (sc-287, Santa Cruz Biotechnology) diluted 1:100,000 and anti-GAPDH rabbit polyclonal antibody (G9545, Sigma) diluted 1:10,000 were used. After thorough washing in PBS with 0.1% Tween-20, secondary horseradish peroxidase-conjugated anti-mouse (sc-2005) or anti-rabbit (sc-2313, both from Santa Cruz Biotechnology) was added (diluted 1:10,000). The signal was detected using LumiGLO Reserve (KPL, Gaithersburg, MD, USA) or Western Blotting Luminol Reagent (Santa Cruz Biotechnology) and membranes were exposed to X-ray films (Kodak, Rochester, NY, USA) or visualised using ChemiDoc MP Imaging System.

Flow cytometry analysis of CD marker expression

Cells were resuspended in 1% immunoglobulin/phosphate-buffered saline solution (IVIG/PBS) to prevent non specific staining. Cells were then labeled with anti-human CD20-APC monoclonal antibody, clone HI40a (EXBIO, Praha, Czech Republic) or anti-human CD38-PE-Cy7 monoclonal antibody, clone HIT2 (BIOLEGEND, San Diego, CA) on ice for 30 minutes. Flow cytometry was then perfomerd on FACS Aria IIu (488 nm; 50 mW orbis, 633 nm, cube coherent 24 mW laser and a 355 nm 5SDU 20 mW laser, BD Biosciences, San Jose, CA, USA). Data were evaluated using BD FACS Diva 6 software.

Results and Discussion

Establishment of fludarabine-resistant Mino/FR cells

Mino cells represent an established model of MCL, derived from a Caucasian male patient [21]. Mino cells are sensitive to fludarabine treatment, with fludarabine LD_{100} approximatelly 1–2 μM. By growing Mino cells in the presence of increasing doses of fludrabine for a prolonged period of time we derived a fludarabine-resistant Mino subclone (Mino/FR). The resistant Mino/FR cells proliferated in 100 μM fludarabine. Toxicity of fludarabine in Mino and Mino/FR cells was determined *in vitro* by cell proliferation assay (Fig 1A).

Mino/FR cells are cross-resistant to all tested purine and pyrimidine antinucleosides and to ibrutinib, but remain sensitive to other anti-cancer drugs

To characterize the Mino/FR cells in terms of their sensitivity to currently used anti-MCL agents we exposed the cells to a range of clinically used anti-lymphoma drugs with different mechanism of action. We included an anti-folate methotrexate, anti-nucleosides cytarabine, gemcitabine and cladribine, a DNA-intercalating agent doxorubicin, a DNA-modifier cisplatin, a proteasome-inhibitor bortezomib, a novel cytostatic with unique mechanism of anti-lymphoma activity bendamustine, and the recently approved taregted inhibitor of Bruton tyrosine kinase–ibrutinib. Mino and Mino/FR cells were exposed to the abovementioned drugs for 6–8 day. The appropriate range of drug concentrations was determined in preliminary experiments. Relative toxicity of the drugs was determined daily using WST-8 cell proliferation assay starting on the day 4 of the experiment. Triplicate samples (10,000 cells/well) were used for each drug concentration and measurement.

Mino/FR cells were significantly more resistant not only to fludarabine (proliferated in 100-fold higher concentrations compared to Mino cells and LD_{100} was not achieved) but also to another purine antinucleoside cladribine (LD_{100} approximately 1,000-fold higher), as well as to pyrimidine-derived cytarabine (LD_{100} approx. 2,000-fold higher) and gemcitabine (LD_{100} approx. 25,000-fold higher) (Fig 1B–1D). Moreover, Mino/FR cells were significantly more resistant to the BTK inhibitor ibrutinib (LD_{100} approx. 4,000-fold higher) (Fig 1E) and slightly more resistant to anti-folate MTX (LD_{100} at least 2-fold higher) (Fig 1J). On the other hand, Mino/FR cells were more sensitive to bortezomib and doxorubicin, tolerating only approximatelly 2-fold lower concentrations compared to Mino cells (Fig 1F and 1G). Sensitivity to alkylating agent bendamustine and cisplatin remained comparable to the original Mino cells (Fig 1H and 1I).

The marked cross-resistance of Mino/FR cells to purine and pyrimidine anti-nucleosides suggests a nucleoside-specific mechanism of resistance, while the observed resistence to BTK-inhibitor ibrutinib may suggest the deregulation of B-cell receptor (BCR) signaling in Mino/FR cells. The slightly increased sensitivity to an intercalating cytostatic doxorubicin suggested a

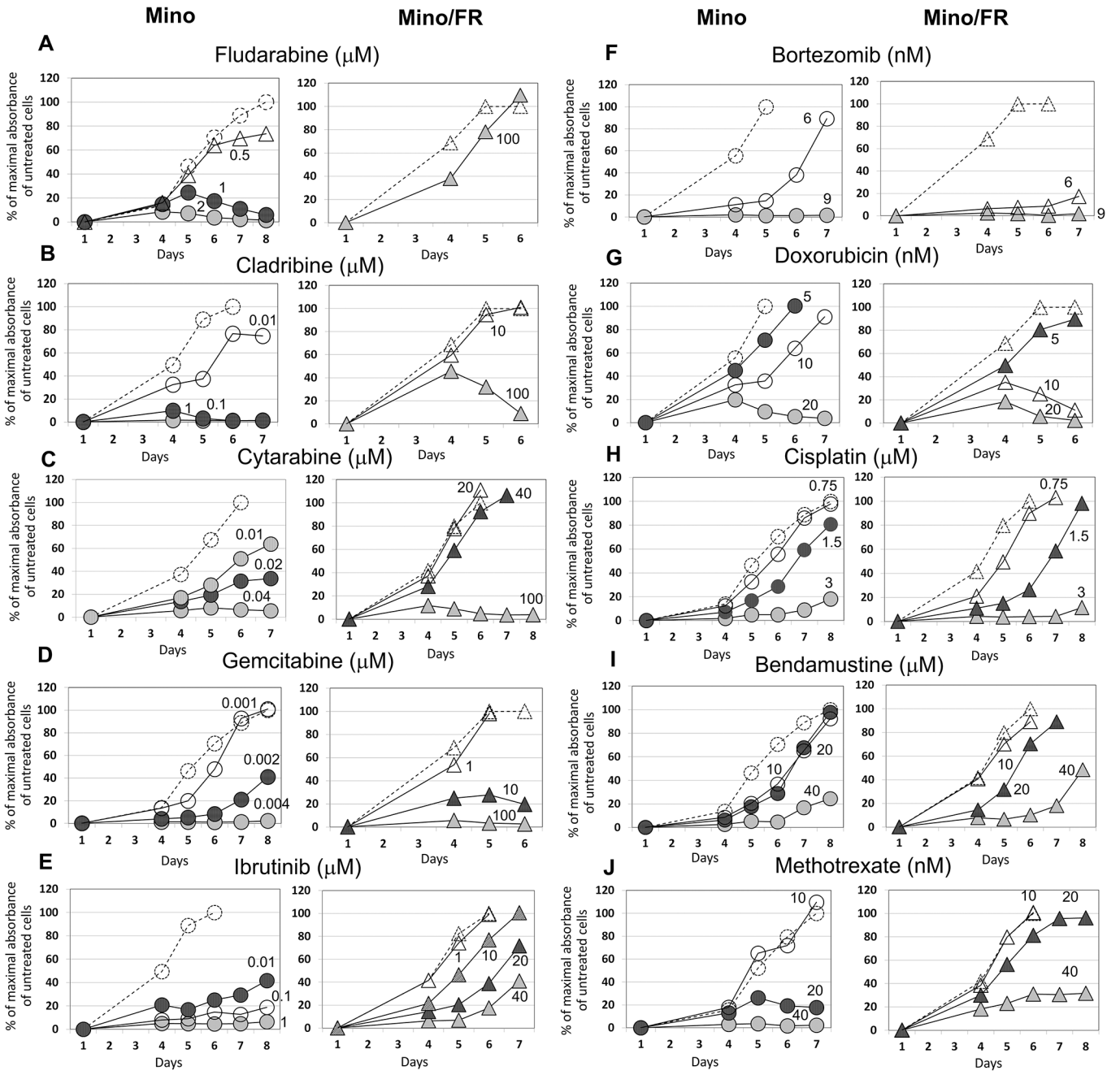

Fig 1. Proliferation of Mino and Mino/FR cells in presence of fludarabine and other anti-lymphoma agents. Cells were grown for 6–8 days in presence of increasing concentrations of **(A)** fludarabine, **(B)** cladribine, **(C)** cytarabine, **(D)** gemcitabine, **(E)** ibrutinib, **(F)** bortezomib, **(G)** doxorubicin, **(H)** cisplatin, **(I)** bendamustine and **(J)** methotrexate. Relative toxicity of the drugs was determined by the WST-8 cell proliferation assay, Dashed lines with open circles or triangles indicate cell proliferation in absence of an anti-lymphoma drug. Other curves represent the cells grown in increasing concentrations (indicated by the associated number) of the tested drug. Maximal absorbance (highest number of viable cells) of cells grown without an anti-lymphoma agent in each experiment was set as 100%. Standard deviations were < 5% for all measurements.

doi:10.1371/journal.pone.0135314.g001

potential deregulation of particular DNA repair mechanisms, while the slightly increased sensitivity to proteasome inhibitor bortezomib might suggest deregulation of NFB pathway. The data thus suggested multiple alterations in MCL cell homeostasis associated with the acquired resistance to fludarabine.

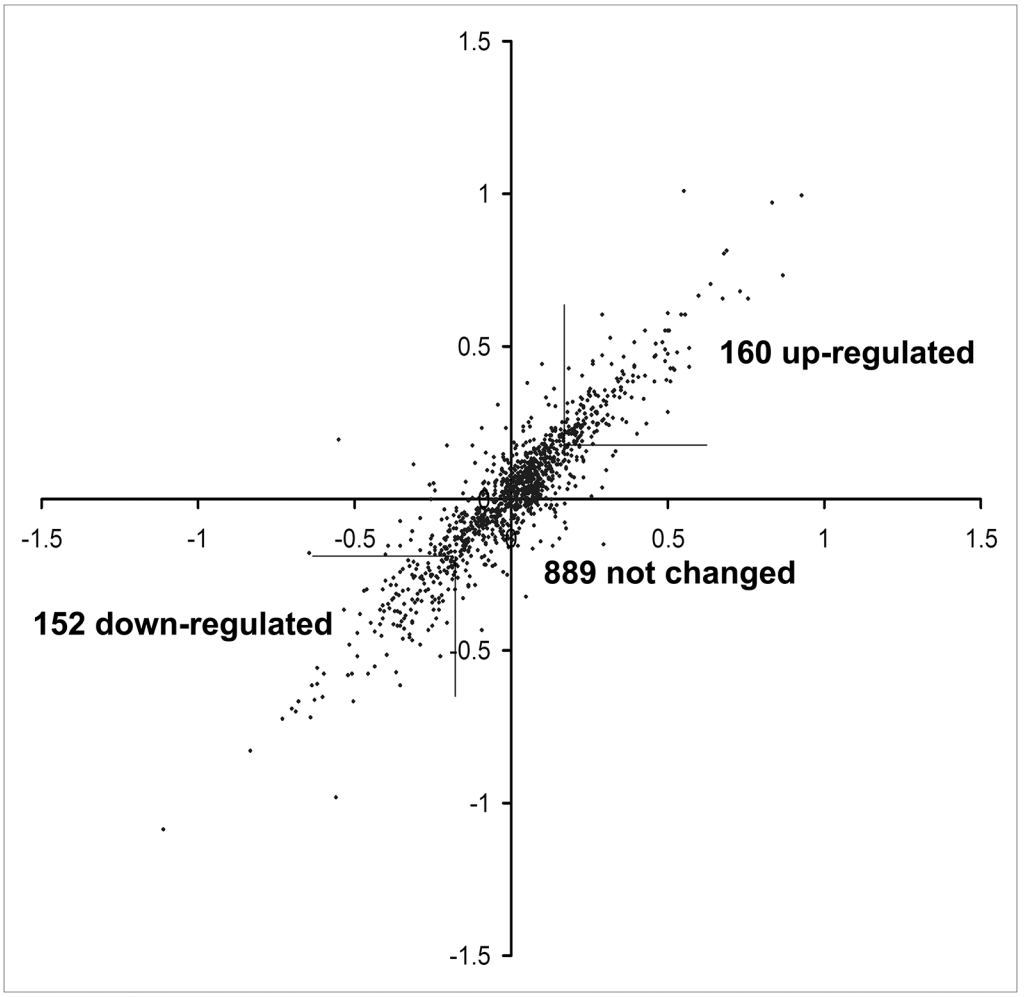

Fig 2. Correlation of protein expression ratios in forward and reverse SILAC experiments. Heavy/Light protein ratios (log values) from the forward experiment were plotted against log values of Light/Heavy protein ratios obtained from the reverse labeling experiment.

doi:10.1371/journal.pone.0135314.g002

Proteomic analysis of Mino versus Mino/FR cells

To uncover the processes responsible for and associated with the fludarabine resistance and to identifie the key molecules we performed in-depth proteomic analysis of Mino and Mino/FR cells.

The differential proteomic analysis of Mino versus Mino/FR cells used metabolic incorporation of stable isotopes in cell culture (SILAC) [24]. Mino cells were first grown in the presence of ^{13}C and ^{15}N-labeled arginine and lysine while Mino/FR cells were grown in normal media with unlabeled amino acids (forward labeling). To make the results sufficiently robust, the experiment was repeated with swapped media (reverse labeling). Fig 2 shows the high correlation of expression ratios between forward and reverse experiments. We identified 1942 and 1700 proteins in forward and reverse experiment, respectively. Only the proteins identified in both analyses (1377 proteins) were further considered. For further quantitative analysis, we used 1201 proteins, each detected with at least 3 SILAC pairs and at the same time showing protein ration variability below 40 percent in both forward and reverse experiments. We identified 312 proteins in the resistant Mino/FR cells showing the fold change of at least 1.5, of which 152 were downregulated and 160 upregulated. (Table 1, for the full report see S1 Table).

Bioinformatic analysis of the proteomic data

Functional annotation and pathway analysis of differentially expressed proteins using KEGG (Kyoto Encykopedia of Genes and Genomes) via DAVID (Database for Annotation, Visualization and Integrated Discovery) highlighted several processes affected by the fludarabine resistance in the Mino-FR cells. Most notably, it pointed toward the upregulation of proteins involved in the processes and pathways responsible for the DNA integrity maintenance. In particular, proteins ionvolved in DNA replication (p-val $1.1x10^{-10}$), mismatch repair (p-val 0.000001), nucleotide excision repair (p-val 0.005) and purine (p-val 0.03) and pyrimidine (p-val 0.06) metabolism were upregulated. In addition, proteins involved in aminoacyl t-RNA biosynthesis (p-val $1.6\ x10^{-7}$) were also enriched among upregulated proteins.

Table 1. Differentially expressed proteins in Mino/FR cells identified by the proteomic analysis. Differentially expressed proteins with fold-change >1.5 are listed. Gene names are shown, proteins with fold-change >3 fold are present in bold letters).

Proteins upregulated in Mino/FR cells	
DNA replication and repair	FANCI, LIG1, MCM2, MCM3, MCM4, MCM5, MCM6, MCM7, MSH2, MSH6, NCAPD2, NCAPD3, NCAPG, NCAPH, PARP1, PDE12, RFC2, RFC3, **RFC4**, RFC5, RUVBL1, RUVBL2, SMC2, SMC4
Purine and pyrimidine metabolism	**ADA**, CTPS1, GMPS, HPRT1, IMPDH2, PNP, **RRM2**, UMPS, TYMS
Aminoacyl tRNA biosynthesis	CARS, DARS, GARS, EPRS, IARS, LARS, MARS, NARS, YARS
Other processes	ABCF1, ABCF3, **ACAD9**, ACLY, ACO2, ADRBK1, ALDH5A1, **ALOX5**, ANP32B, AP2M1, APEH, ATG3, ATP1A1, ATP1B3, ATP6V1C1, ATXN10, **BCL2**, **BLVRA,** CD2AP, CKAP5, CLPTM1L, COBRA1, CPNE1, **CPNE3**, CUL1, CYB5R3, **DCUN1D1**, DCXR, DDX17, DHCR24, DHCR7, **DHRS7B**, DHX30, DNAJC2, DNMT1, EEF1E1, EHD1, EIF2A, **EIF4A2**, EIF4E, EIF4G1, ERLIN1, ERO1L, ERP44, EXOSC7, **EZR**, FAM105B, FAM162A, FAM213A, FASN, FDFT1, FKBP5, **FXR1**, GAPVD1, GNA13, GNL1, GNL3, GOT1, **GRHPR**, GYG1, HEATR2, HMGB2, HNRNPD, HS2ST1, HSPA14, KHSRP, KIF11, KNTC1, KPNA2, **LBR**, LRMP, LSS, MYH10, NAA25, NAP1L4, NDUFAF4, NUP210, PA2G4, PAICS, PDCD6IP, PFKM, PFKP, **PHGDH**, PLCG2, PPM1G, PPP2R4, PRDX6, **PSAT1**, PSMD5, PSMG2, PTBP1, PTPRC, PTPRCAP, RAB7A, RRAS2, SBDS, SEC11C, SEC24A, SET, SFXN1, **SLC1A4**, SLC1A5, SLC25A1, SLC2A1, SRPR, ST13, **TPD52**, TRIP13, TROVE2, TUBA4A, TUBB4B, TUBGCP2, UBE2E1, VPRBP, XPNPEP1, XPO7, XPOT, ZW10
Proteins Downregulated in Mino/FR cells	
Fatty acid metabolism	ACAA2, **ACADVL, ACOT1** ACSL4, CPT2, HADHB
Glutathione metabolism	GSTK1, **GSTP1, G6PD**, IDH2, PGD
CD molecules	CD20 (MS4A1), CD38**, CD43, CD70, CD74**
Adherens junctions	CSNK2A2, MAPK1, PTPN1, **PTPN6**, SMAD3
Other processes	ALG5, ANXA2, APMAP, ARHGAP1, ARHGAP17, ARHGAP4, ARHGEF2, **ARL6IP5**, ARL8B, ASCC2, ATAD1, ATP2A3, ATPAF2, AUP1, BAX, **BCAP31**, BCAT2, **BTK**, CFA20, C1QBP, **CNDP2**, COPG2, CSTF3, CTPS2, DAGLB, **DCK**, DDX24, DDX3X, DKC1, DLST, DNAJA2, EIF4A1, EIF5A, ELMO1, EML4, FAM129C, FAM3C, FBXO7, FLAD1, **FLNA**, GBE1, GFPT1, GLOD4, GNPDA1, GOT2, HIST1H2AH, HIST1H2BK, HIST1H4A, HM13, HMGB3, HSP90B1, HSPH1, **ICAM1**, ICAM3, IER3IP1, IGF2BP3, INPP5D, IQSEC1, ITPR2, KPNA3, LTA4H, LRRFIP1, M6PR, MAT2A, ME2, MPDU1, MSN, MTA2, MYBBP1A, **NAGK**, NDUFA13, NDUFA9, NDUFB8, NDUFS1, NEK9, NLN, NRD1, NUDT19, MOB1B, OGDH, PDIA4, PEPD, PFAS, PGRMC1, POLR2B, POR, PPCS, PPIB, PRMT1,PRPF6, PRPSAP2, PSAP, PSME1, PSME2, PSMF1, PTPN2, PUS1, RASAL3, RNH1, **ROCK1,** RUFY1, SCRIB, SEC23IP, SEPT9, SLC25A5, SLC25A6, SLC38A5, SND1, SNRNP200, SRP54, STK4, TDP1, TMED4, TMX3, TOM1, TPM3, TPP2, TRMT6, TSR1, **TST, TSTA3**, UBLCP1, VARS, VAT1, VPS13C, VPS26A,VPS35, WDR1, XPO5, ZMPSTE24

doi:10.1371/journal.pone.0135314.t001

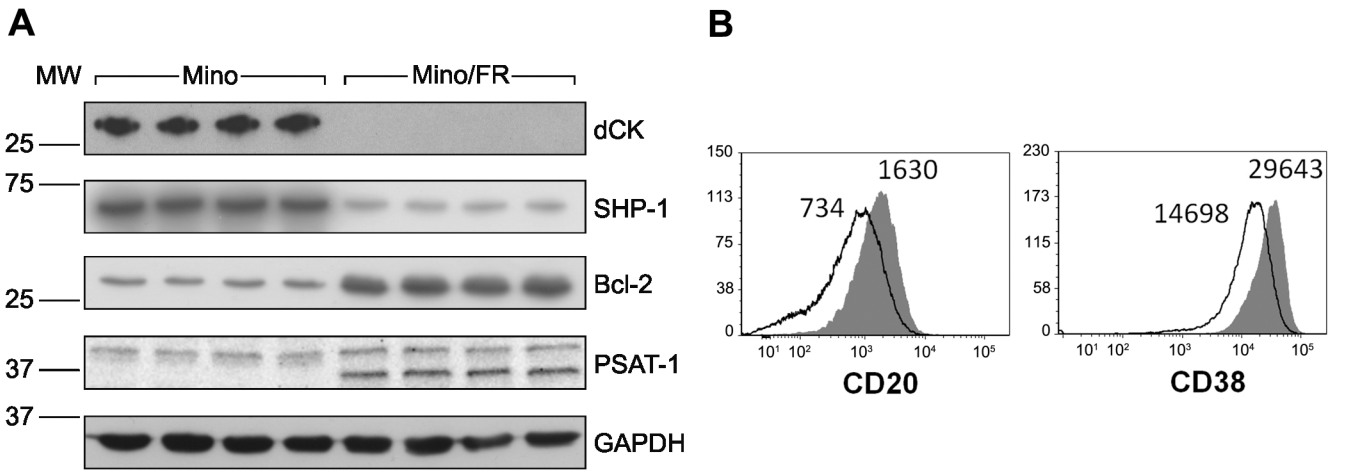

Fig 3. Verification of differential expression of the key proteins identified by proteomics. (A) Relative expression of four differentially expressed proteins—deoxycytidine kinase (dCK), phoshatase SHP-1 (alias PTPN6), Bcl-2 and phoshoserine aminotransferase (PSAT-1)–was determined by Western Blotting using specific antibodies in Mino and Mino/FR cells. GAPDH was used as a loading control. **(B)** Relative expression of two surface CD markers (CD20 and CD38) determined by flow cytometry using specific antibodies. Open histograms represent Mino/FR cells, full histograms show Mino cells. Histograms demonstrate approximately 2-fold decreased expression of CD20 and CD38 in Mino/FR cells as indicated by decreased median fluorescence intensity.

doi:10.1371/journal.pone.0135314.g003

Among the downregulated proteins the enrichment was less significant; proteins implicated in fatty acid metabolism (p-val 0.003), glutathione metabolism (p-val 0.006), and adherens junctions (p-val 0.03) were implicated.

Verification of the landmark expression changes

Among the proteins with the most pronounced (at least 5-fold) differential expression were these downregulated proteins: **deoxycytidine kinase (dCK)** and phosphatase **PTPN6** (alias SHP-1, Tyrosine-protein phosphatase non-receptor type 6), and these upregulated ones: **Bcl-2** and **phosphoserine aminotransferase** (PSAT). Using specific antibodies we confirmed the significantly altered expression of all four landmark proteins (Fig 3A). Observed downregulation of cell surface markers **CD20** (MS4A1) and **CD38** revealed by proteomics in Mino/FR cells was confirmed by flow cytometry using specific antibodies (Fig 3B).

Deoxycitidine kinase, purine and pyrimidine utilization and metabolism

Several-fold downregulation of **deoxycytidine kinase (dCK)** was among the most prominent alterations in the fludarabine-resistant cells detected by the proteomic analysis. In fact, dCK was under detection limit in our Western blotting analysis in Mino/FR cells (Fig 2A), suggesting at least 10-fold downregulation, if not a total absence, of the protein. Deoxycytidine kinase is the key enzyme of deoxyribonucleoside salvage, a metabolic pathway that recycles products of DNA degradation and enables utilization of nucleosides from the environment. Deoxycytidine kinase is responsible for the first intracellular phosphorylation of deoxynucleosides (dCyd, dGuo and dAdo) including clinically relevant analogs cytarabine, cladribine, gemcitabine and fludarabine [9,25]. Despite its name, dCK is promiscuous and phosphorylates both pyrimidine and purine (anti)nucleosides [25]. Downregulation of dCK expression and activity has been demonstrated to cause antinucleoside resistance in human leukemic cell lines by others [8, 9, 26–28]. We have shown recently that the downregulation of dCK is responsible for the resistance to pyrimidine antimetabolite cytarabine in MCL cells, and for cross-resistance of the cytarabine-resistant cells to other antinucleosides [29]. Deoxycytidine kinase is the dominant, if not exclusive, kinase for

fludarabine phosphorylation to its monophosphate [9,25–27]. We can thus reasonably conclude that the marked downregulation (or possibly even a total absence) of dCK is the critical alteration responsible for the fludarabine resistance in our MCL model. Substrate promiscuity of dCK explains the cross-resistance of Mino/FR cells to all other purine and pyrimidine antinucleosides included in our study.

Purine and pyrimidine metabolism

Deoxyribonucleotide triphosphates (dNTPs) essential for DNA replication and repair can be produced either by the *de novo* pathway or by the nucleoside salvage pathway. Rapidly proliferating leukemia and lymphoma cells utilize nucleosides from the environment using the nucleotide salvage pathway [30]. Downregulation of dCK in the resistant Mino/FR cells limits fludarabine activation, preventing or limiting its toxic effect. Simultaneously, it also limits utilization of natural purine and pyrimidine nucleosides (*dCyd*, *dAdo*, *dGuo*) from the environment. Mammalian cells with negligible dCK activity thus become highly dependent on *de novo* nucleotide synthesis [30, 31].

This seems valid also in our model. In the Mino/FR cells we observed a modest, nevertheless, consistent upregulation of many components of purine and pyrimidine metabolism, namely those of *de novo* synthesis and consecutive interconversion reactions. Upregulated were **GMP synthase, CTP synthase 1, inosine-5′-monophosphate dehydrogenase, uridine-5′-monophosphate synthase, purine nucleoside phosphorylase, adenosine deaminase, purine nucleoside phosphorylase, thymidilate synthase, and ribonucleoide reductase subunit M2.**

Ribonucleotide reductase is the key enzyme of the *de novo* pathway for the production of deoxyribonucleosides for DNA synthesis from ribonucleosides. Ribonucleotide reductase activity is known to be directly inhibited by fludarabine [6–9] resulting in depleted dNTP pool. Upregulation of ribonucleotide reductase and its increased activity have been associated with fludarabine resistance in leukemia cells [9].

The concurrent upregulation of the purine and pyrimidine synthetic machinery suggests an increased demand for dNTPs. Resistant cells need to compensate for the loss of deoxynucloside utilization from the environment (normaly facilitated by dCK) by the *de novo* synthesis of both purines and pyrimidines, and their conversion to deoxynucleosides by ribonucleoside reductase.

DNA replication and repair

Fludarabine incorporation into DNA ultimately activates DNA damage response resulting in apoptosis, unless the DNA damage is effectively and rapidly repaired. Increased efficiency of DNA repair is a general mechanism of resistance to DNA-targeting drugs. Mino/FR cells lacking dCK activity face, however, another challenge. Disruption of dNTP pools may cause the misincorporation of nucleotides into DNA resulting in a replication stress which further increases the demand for an effective DNA repair. It has been clearly demonstrated that inactivation of dCK in leukemia cells leads to replication stress and activates DNA-damage response [31].

In general, cells with damaged DNA might escape the damage-triggered apoptosis in so far as they can, at least partially, cope with the inhibited replication, and repair the DNA damage. In agreement with the results of KEGG pathway analysis, we observed upregulation of the large number of proteins participating in both of those processes. DNA repair of a damage in the form of nicks or double-strand breaks is initiated by **poly[ADP-ribose] polymerase 1 (PARP-1).** We found PARP-1 upregulated in Mino/FR cells. PARP-1 acts as a sensor that is thought to

organize the damage site chromatin and/or serve as a scaffold for the subsequent recruitment of repair proteins. PARP-1 directly associates with condensin I protein complex, a conserved multiprotein multifunction assembly partaking in DNA replication and DNA repair [32,33]. We observed upregulation of all five subunits of **condensin I protein complex (condensin complex subunits 1, 2, 3 and structural maintenance of chromosomes proteins 2 and 4).** Similarly, upregulated **Fanconi anemia group I protein (FANCI)** is recruited to stalled replication forks at the sites of DNA damage and aids to the repair of double strand lesions [34]. Among other proteins known to contribute to DNA repair we identified the upregulated **DNA replication licensing factors MCM2, MCM3, MCM4 MCM5, MCM6 and MCM7, replication factor C subunits 2, 3, 4 and 5**, **pontin, reptin, and DNA ligase 1.**

The tight orchestration of replication stress response is mediated by ATM, ATR and checkpoint kinases. Recently, Nek9 kinase has been identified as a key component of the regulatory cascade [35]. **Nek9 kinase** was also found upregulated in Mino/FR cells.

The upregulation of numerous proteins participating in the maintenance of DNA integrity clearly indicates increased demand for DNA repair in Mino/FR cells. Such an upregulation may either contribute to the fludarabine resistance (despite the limited dCK activity, small amounts of fludarabine may still be incoroporated into DNA) and/or compensate for the higher incorporation error rate due to the deficiency of dNTPs caused by insufficient dCK activity [31].

Avoiding apoptosis. Altered Bax /Bcl-2 ratio in Mino/FR

In addition to the processes directly responsible for the resistance (silenced expression of dCK) and the secondary/adaptive changes represented by the changes in nucleotide metabolism, replication and DNA repair, cells can avoid drug-induced apoptosis by the alteration of downstream processes, namely, signaling pathways leading to apoptosis. Apoptosis is regulated, among others, by the Bax/Bcl2 ratio [36, 37], where Bax promotes apoptosis by binding to and antagonizing the anti-apoptotic Bcl-2 protein. Upregulation of Bcl-2 as the mechanism of avoiding cell death has been documented in drug resistant cancer cells previously [38]. In our study, **Bcl-2** was also among the most strongly upregulated proteins in Mino/FR (Fig 3A), while expression of **Bax** was downregulated.

Markedly decreased Bax/Bcl-2 ratio in Mino/FR cells most likely reflects an anti-apoptotic process. This alteration *per se* does not, however, confer universal resistance to apoptosis as demonstrated by the preserved sensitivity of Mino/FR cells to cisplatin and bendamustine (Fig 1H and 1I). We hypothesize that the decreased Bax/Bcl-2 ratio might counterbalance the adverse alterations of the cell metabolism that result from the downregulation of dCK. Importantly, the Bcl-2 upregulation represents a potential therapeutic target for fludarabine-resistant MCL cells.

High sensitivity of Mino/FR to Bcl-2 inhibitor ABT-199

Bcl-2 is an attractive therapeutic target. Sevreal Bcl-2 inhibitors have been developed and are currently in clinical tests. Highly selective Bcl-2 inhibitor ABT-199 showed great promise in a wide range of B-cell malignancies, with greatest efficacy reported in chronic lymphocytic leukemia and mantle cell lymphoma [39, 40]. In order to evaluate the potential of ABT-199 for the therapy of antinucleoside-resistant MCL, we tested relative toxicity of ABT-199 in Mino and Mino/FR cells. We observed markedly increased sensitivity of Mino/FR cells to ABT-199 compared to Mino cells (Fig 4). While Mino cells rapidly proliferated in 1μM ABT-199, proliferation of the Bcl-2 –overexpressing Mino/FR cells was reduced already at 0.01 μM ABT-199 while 0.1 μM ABT-199 effectively killed all Mino/FR cells in culture (LD_{100} 10-100-fold lower).

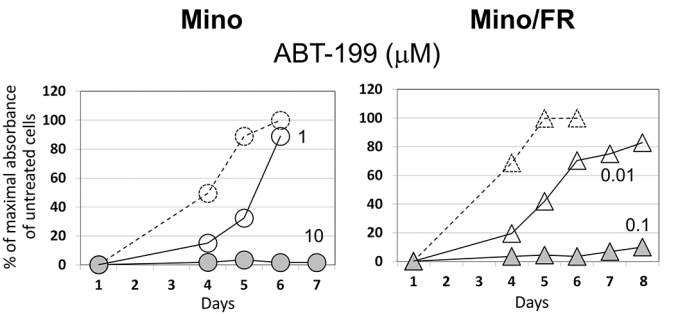

Fig 4. Mino/FR cell are highly sensitive to ABT-199. Proliferation of Mino and Mino/FR cells in presence of of 0.01–10 μM Bcl-2 inhibitor ABT199. Cells were grown for 6–8 days in presence ABT199. Relative toxicity of the drugs was determined by the WST-8 cell proliferation assay. Dashed curves and open circles or triangles indicate cell proliferation in absence of ABT199. Maximum absorbance (highest number of viable cells) of cells grown without ABT199 experiment was set as 100%. Other curves represent the cells grown in increasing concentrations (indicated by the associated number) of ABT199. Standard deviations were < 5% for all measurements.

doi:10.1371/journal.pone.0135314.g004

To ensure, that the phenomenon is not exclusive to Mino/FR cells, we determined the relative expression of Bcl-2 and sensitivity to ABT-199 in another MCL cell line REC-1 and its cytrabine (CR) and fludarabine (FR) resistant subclone REC-1/CR/FR which we derived and characterized previously [29]. We demonstrated that the antinucleoside-resistant REC-1 cells also overexpress Bcl-2 and are more sensitive to ABT199 treatment *in vitro*. (S1 Fig). Our observation thus suggests high potential of the novel anti-Bcl-2 drug ABT-199 for the therapy of fludarabine-resitant MCL.

B-cell receptor signalling. Bruton tyrosine kinase (BTK) and the resistance to ibrutinib

As we demonstrated in the initial battery of toxicity tests, fludarabine-resistant Mino/FR cells were significantly cross-resistant to ibrutinib, an inhibitor of Bruton tyrosine kinase (BTK)—recently approved for the therapy of relapsed/refractory mantle cell lymphoma [41]. BTK is a key component of B-cell receptor (BCR) signaling crucial to cell survival and proliferation during B-cell developement [42], and implicated in pathogenesis of B-cell malignancies, including MCL [3, 43]. Upon complex BCR stimulation, BTK is phosphorylated and the activated BTK phosphorylates phospholipase C gamma 2 (PLCG2). In turn, several downstream target pathways are activated including transcription factor NF-κB and mitogen-activated protein kinase (MAPK), leading to cell survival and proliferation [44]. Our proteomic analysis identified strong downregulation of **BTK** in Mino/FR. Because of its therapeutic importance, we verified both total and activated (phoshpo-BTK^{Y233}) BTK levels in Mino and Mino/FR cells using Western blotting (Fig 5). BTK expression and p-BTK levels were markedly decreased in Mino/FR cells, clearly indicating the disruption of BCR signaling in Mino/FR cells. This provides the explanation for the observed resistance of Mino/FR cells to ibrutinib.

Still, many other players may contribute to the complex sum of signals that decide the cellular fate and response to ibrutinib. Among the downregulated proteins identified in Mino/FR cells there were two phosphatases known to contribute to BCR signalling as well—**phosphatase PTPN6 (alias SHP-1) and phosphatidylinositol 3,4,5-trisphosphate 5-phosphatase 1 (alias SHIP-1)** [45, 46]. We also observed downregulation and **MAPK kinase**, one of the downstream effectors of BCR signalling. Other molecules involved in different signalling cascades (such as **STAT3, kinases CSNK2A2 and ROCK, and phosphatases PTPN1 and PTPN2,** all

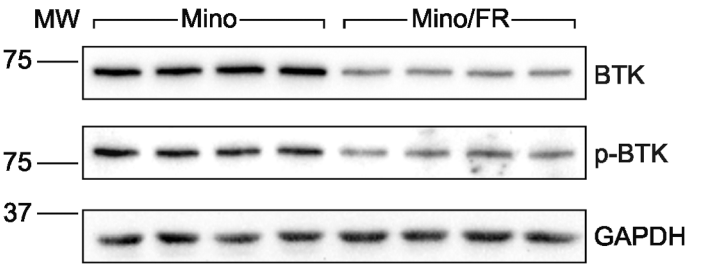

Fig 5. Decreased levels of total BTK and its activated p-BTKY^{233} form in Mino/FR cells. Relative expression of total and phosphorylated (active) p-BTK233 was determined by Western blotting using specific antibodies in Mino and Mino/FR cells. GAPDH was used as the loading control.

doi:10.1371/journal.pone.0135314.g005

downregulated in Mino/FR cells) could also contribute to Mino/FR survival via signalling crosstalk.

Nevertheless, the association of marked ibrutinib resistance with fludarabine resistance in Mino/FR cells, accompanied by the downregulation of BTK and p-BTK, are important observations indicating that disrupted BCR signalling may limit the effective usage of ibrutinib in MCL patients with fludarabine-resistant disease.

Decreased expression of CD20 and other CD antigens, and the potential implications

Among the proteins downregulated in MinoFR cells we found six proteins belonging to the leukocyte CD (cluster of differentiation) antigens, namely, **CD20 (MS4A1), CD38, CD70, CD74 and CD43 (leukosialin).** Importantly, no CD antigen was identified as upregulated. Loss of the CD antigens in the resistant cells may be specific to resistance developement and/or reflect the shift of the resistant lymphoma cells toward differently matured B-cell phenotype.

Since most of the CD proteins are expressed on the cell surface, they represent attractive therapeutic targets. Downregulated expression of CD molecules may theoretically limit the efficacy of therapeutic antibodes such as rituximab (anti-CD20) used in lymphoma therapy. Recently, Kluin-Nelemans et al. published their landmark paper on the survival benefit of maintenance rituximab (R) in the elderly patients with newly diagnosed mantle cell lymphoma [2]. Interestingly, the influence of maintenance rituximab was detected only in patients who received R-CHOP (cyclophosphamide, vincristin, doxorubicin and prednisone), but not in those who received R-FC (fludarabine, cyclophosphamide). In the light of our own data, the downregulation of CD20 in those MCL cells that had survived fludarabine-based induction therapy might at least partially contribute to the failure of rituximab maintenance observed in that cohort of patients.

Metabolic alterations in Mino/FR cells

Among the highly upregulated proteins in the resistant MCL cells were two enzymes responsible for two consecutive steps of serine synthesis, namely **D-3-phosphoglycerate dehydrogenase (PHGDH) and phosphoserine aminotransferase** (PSAT1, verified by Western blotting, Fig 3A). Since serine is an essential compound for the *de novo* nucleotide biosynthesis (as a source of carbon moieties in the folate cycle) the upregulation of serine production may therefore satisfy the increased demand for stimulated *de novo* nucleotide synthesis in Mino/FR cells, which are unable to recycle or obtain nucleosides from the environment due to the missing or defficient dCK activity. This hypothesis seems to be supported by the concomitant

upregulation of **neutral amino acid transporter A (SLC1A4)** and **neutral amino acid transporter B (SLC1A5),** transporters specific for serine, alanine, cysteine, and threonine. Interestingly, upregulation of PSAT1 has been shown to increase proliferation and tumorigenic potential, as well as to protect tumor cells from oxaliplatin toxicity [46]. Whether the PSAT1 effect is directly connected with nucleotide metabolism or rather a more general compensatory metabolic alteration remains to be determined.

The downregulation of six enzymes partaking in the metabolism of fatty acids, (**carnitine O-palmitoyltransferase 2, trifunctional enzyme subunit beta, acyl-CoA thioesterase, 3-ketoacyl-CoA thiolase, long-chain-fatty-acid-CoA ligase 4, and very long chain specific acyl-CoA dehydrogenase**) accompanied by the downregulation of mitochondrial **ADP/ATP translocases 2 and 3** as well as other important mitochondrial proteins, may suggest a complex metabolic re-arrangement in Mino/FR cells.

Marked up-regulation (5-6-fold) of **biliverdin reductase** may contribute to the resistant phenotype. Biliverdin reductase converting biliverdin to bilirubin is a potent intracellular antioxidant, which is induced under hypoxia and contributes to hypoxia-induced resistance to doxycycline, paclitaxel and temozolomide in cancer cells [47, 48]. Whether biliverdin reductase contributes to antinucleoside resistance in our model or merely reflects increased oxidative stress remains to be determined. Similarly, upregulation of two key glutathione transferases, **GSTP1** and **GSTK1,** in Mino/FR may have several explanations. Upregulation of GSTP1 has been linked to an aquired drug resistance, including drugs which are not substrates for glutathionylation-based detoxification (e.g.antimetabolites) [49].

Interestingly, nine **aminoacyl tRNA synthases** were upregulated in the Mino/FR cells. In addition to their canonical roles, these molecules exert various other functions as recently reviewed [50]. Their in contribution to the survival of resistant cells remains to be elucidated.

Conclusions

Detailed molecular analysis of therapy-resistant tumor cells is essential for in-depth understanding of causative mechanisms, as well as contributing and compensatory processes. Such knowledge then potentialy opens a way to the personalized therapy of the drug-resistant malignancy. Here we provided a detailed functional and proteomic snapshot of molecular mechanisms associated with the aquired fludarabine resistance of mantle cell lymphoma cells. Our data suggest the silencing of dCK as the probable causative mechanism of the resistance to fludarabine and of the cross-resistance to other antinucleotides, both pyrimidine- and purine-derived. In addition to the downregulation of dCK, we identified several secondary contributing or compensatory processes associated with the development of fludarabine resistance. Ineffective use of antinucleosides from the environment induces replicative stress and makes the resistant cells highly dependent on *de novo* nucleotide synthesis and effective DNA repair (Fig 6). Some of the identified alterations might have direct therapeutic consequences, including the downregulation of BTK (associated with the decreased sensitivity of fludarabine-resistant cells to ibrutinib) or the upregulation of Bcl-2 (responsible for an increased sensitivity to ABT-199). Our detailed functional and proteomic analysis of mantle cell lymphoma model of acquired resistance to fludarabine thus provides a proof-of-concept that might be exploited in the clinical setting (namely in mantle cell lymphoma and chronic lymphocytic leukemia) for prediction of optimal treatment strategies for those patients who fail fludarabine-based regimen. Due to the remarkable sensitivity and speed of high-resolution mass spectrometry, enabling rapid and detailed molecular characterization of small populations of cancer cells, proteomics may contribute to the formulation of individualized therapies in near future.

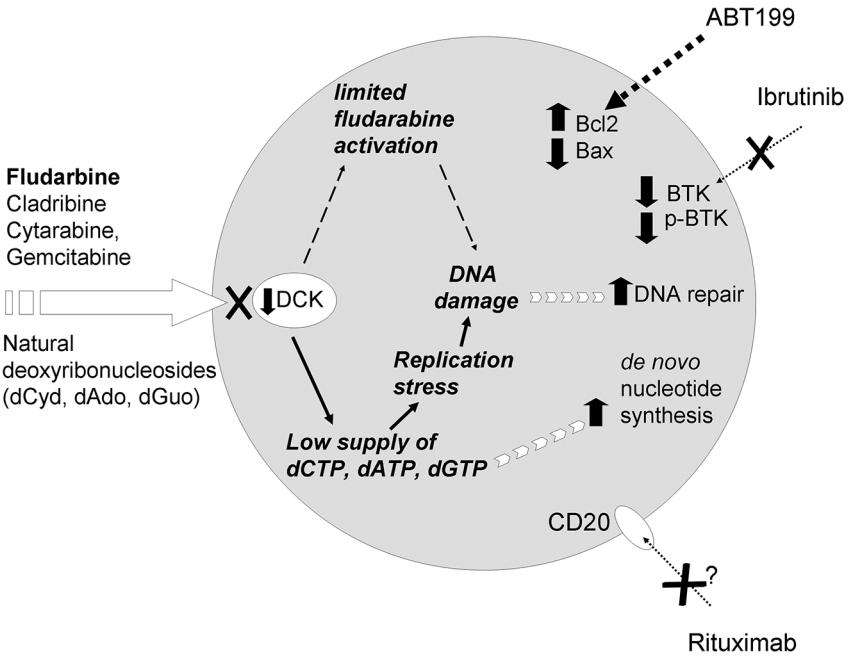

Fig 6. Schematic illustration of the processes associated with fludarabine resistance in Mino/FR cells summarizes the landmark observations in our analyses.

doi:10.1371/journal.pone.0135314.g006

Supporting Information

S1 Fig. Bcl-2 expression and ABT199 toxicity in REC-1 and REC-1/CR/FR cells. Cytrabine- and fludarabine resistant subclone REC-1/CR/FR has been derived and characterized previously from an established MCL cell line REC-1 [29]. A) Expression of Bcl-2 in REC-1 and antinucleoside resiatnt REC-1/CR/FR cells. Relative expression of Bcl-2 was determined by Western blotting using specific antibodies in total cell lystates. GAPDH was used as the loading control. B) Proliferation of REC-1 and REC-1/CR/FR cells in presence of Bcl-2 inhibitro ABT199. Proliferation of REC-1 and REC-1/CR/FR cells in presence of of 0.01–10 μM Bcl-2 inhibitor ABT199 was determined. Cells were grown for 6–7 days in presence ABT199. Relative toxicity of the drugs was determined by the WST-8 cell proliferation assay. Dashed curves and open circles or triangles indicate cell proliferation in absence of ABT199. Maximum absorbance (highest number of viable cells) of cells grown without ABT199 experiment was set as 100%. Other curves represent the cells grown in increasing concentrations (indicated by the associated number) of ABT199. Standard deviations were $< 5\%$ for all measurements.
(TIF)

S1 Table. The complete list of differentially expressed proteins. The list of differentially expressed proteins identified in Mino/FR cells by SILAC analysis. The proteins are ordered according the observed fold-change. Downregulated and upregulated proteins are shown in two separate tables. Number of unique and total peptides identified, number of SILAC pairs and normalized SILAC ratio are diplayed for each protein.
(PDF)

Author Contributions

Conceived and designed the experiments: PK JP. Performed the experiments: LL JP TNA MK BM PV MA ED OV. Analyzed the data: JP PK MS. Wrote the paper: MS PK JP.

References

1. Dreyling M, Kluin-Nelemans HC, Beà S, Klapper W, Vogt N, Delfau-Larue M-H, et al. Update on the molecular pathogenesis and clinical treatment of mantle cell lymphoma: report of the 11th annual conference of the European Mantle Cell Lymphoma Network. Leuk Lymphoma. 2013; 54:699–707. doi: 10.3109/10428194.2012.733882 PMID: 23020649
2. Kluin-Nelemans HC, Hoster E, Hermine O, Walewski J, Trneny M, Geisler CH, et al. Treatment of older patients with mantle-cell lymphoma. N Engl J Med. 2012; 367:520–31. doi: 10.1056/NEJMoa1200920 PMID: 22873532
3. Jares P, Colomer D, Campo E: Molecular pathogenesis of mantle cell lymphoma. J Clin Invest. 2012; 122:3416–23. doi: 10.1172/JCI61272 PMID: 23023712
4. Forstpointner R, Dreyling M, Repp R, Hermann S, Hänel A, Metzner B, et al. The addition of rituximab to a combination of fludarabine, cyclophosphamide, mitoxantrone (FCM) significantly increases the response rate and prolongs survival as compared with FCM alone in patients with relapsed and refractory follicular and mantle cell lymphomas: results of a prospective randomized study of the German Low-Grade Lymphoma Study Group. Blood 2004; 104:3064–71. PMID: 15284112
5. Lin TS, Blum KA, Fischer DB, Mitchell SM, Ruppert AS, Porcu P, et al. Flavopiridol, fludarabine, and rituximab in mantle cell lymphoma and indolent B-cell lymphoproliferative disorders. J Clin Oncol. 2010; 28:418–23. doi: 10.1200/JCO.2009.24.1570 PMID: 20008633
6. Gandhi V, Plunkett W. Cellular and clinical pharmacology of fludarabine. Clin Pharmacokinet. 2002; 41:93–103. PMID: 11888330
7. de Campos-Nebel M, Larripa I, González-Cid M. Non-homologous end joining is the responsible pathway for the repair of fludarabine-induced DNA double strand breaks in mammalian cells. Mutat Res. 2008; 646:8–16. doi: 10.1016/j.mrfmmm.2008.08.013 PMID: 18812179
8. Månsson E, Spasokoukotskaja T, Sällström J, Eriksson S, Albertioni F. Molecular and biochemical mechanisms of fludarabine and cladribine resistance in a human promyelocytic cell line. Cancer Res. 1999; 59:5956–63. PMID: 10606241
9. Månsson E, Flordal E, Liliemark J, Spasokoukotskaja T, Elford H, Lagercrantz S, et al. Down-regulation of deoxycytidine kinase in human leukemic cell lines resistant to cladribine and clofarabine and increased ribonucleotide reductase activity contributes to fludarabine resistance. Biochem Pharmacol. 2003; 65:237–47. PMID: 12504799
10. Mackey JR, Galmarini CM, Graham KA, Joy AA, Delmer A, Dabbagh L, et al. Quantitative analysis of nucleoside transporter and metabolism gene expression in chronic lymphocytic leukemia (CLL): identification of fludarabine-sensitive and-insensitive populations. Blood 2005; 105:767–74. PMID: 15454483
11. Reiman T, Graham KA, Wong J, Belch AR, Coupland R, Young J, et al. Mechanisms of resistance to nucleoside analogue chemotherapy in mantle cell lymphoma: a molecular case study. Leukemia. 2002; 16:1886–87. PMID: 12200718
12. Moussay E, Palissot V, Vallar L, Poirel HA, Wenner T, El Khoury V, et al. Determination of genes and microRNAs involved in the resistance to fludarabine in vivo in chronic lymphocytic leukemia. Mol Cancer 2010; 9:115. doi: 10.1186/1476-4598-9-115 PMID: 20487546
13. Al-Harbi S, Hill BT, Mazumder S, Singh K, Devecchio J, Choudhary G, et al. An antiapoptotic BCL-2 family expression index predicts the response of chronic lymphocytic leukemia to ABT-737. Blood 2011; 118:3579–90. doi: 10.1182/blood-2011-03-340364 PMID: 21772052
14. Sharma A, Singh K, Mazumder S, Hill BT, Kalaycio M, Almasan A. BECN1 and BIM interactions with MCL-1 determine fludarabine resistance in leukemic B cells. Cell Death Dis. 2013; 4:e628. doi: 10.1038/cddis.2013.155 PMID: 23681223
15. de la Fuente MT, Casanova B, Cantero E, Hernández del Cerro M, Garcia-Marco J, Silva A, et al. Involvement of p53 in alpha4beta1 integrin-mediated resistance of B-CLL cells to fludarabine. Biochem Biophys Res Commun. 2003; 311:708–12. PMID: 14623330
16. Zenz T, Häbe S, Denzel T, Mohr J, Winkler D, Bühler A, et al. Detailed analysis of p53 pathway defects in fludarabine-refractory chronic lymphocytic leukemia (CLL): dissecting the contribution of 17p deletion, TP53 mutation, p53-p21 dysfunction, and miR34a in a prospective clinical trial. Blood 2009; 114:2589–97. doi: 10.1182/blood-2009-05-224071 PMID: 19643983
17. Messina M, Del Giudice I, Khiabanian H, Rossi D, Chiaretti S, Rasi S, et al. Genetic lesions associated with chronic lymphocytic leukemia chemo-refractoriness. Blood 2014; 123:2378–88. doi: 10.1182/blood-2013-10-534271 PMID: 24550227
18. Rossi D, Fangazio M, Rasi S, Vaisitti T, Monti S, Cresta S, et al. Disruption of BIRC3 associates with fludarabine chemorefractoriness in TP53 wild-type chronic lymphocytic leukemia. Blood 2012; 119:2854–62. doi: 10.1182/blood-2011-12-395673 PMID: 22308293

19. Sharma A, Janocha AJ, Hill BT, Smith MR, Erzurum SC, Almasan A. Targeting mTORC1-mediated metabolic addiction overcomes fludarabine resistance in malignant B cells. Mol Cancer Res. 2014; 12:1205–15. doi: 10.1158/1541-7786.MCR-14-0124 PMID: 25061101

20. Austen B, Skowronska A, Baker C, Powell JE, Gardiner A, Oscier D, et al. Mutation status of the residual ATM allele is an important determinant of the cellular response to chemotherapy and survival in patients with chronic lymphocytic leukemia containing an 11q deletion. J Clin Oncol. 2007; 25:5448–57. PMID: 17968022

21. Lai R, McDonnell TJ, O'Connor SL, Medeiros LJ, Oudat R, Keating M, et. al. Establishment and characterization of a new mantle cell lymphoma cell line, Mino. Leuk Res. 2002; 26:849–55. PMID: 12127561

22. Wiśniewski JR, Zougman A, Nagaraj N, Mann M. Universal sample preparation method for proteome analysis. Nat Methods 2009; 6:359–62. doi: 10.1038/nmeth.1322 PMID: 19377485

23. Brosch M, Yu L, Hubbard T, Choudhary J. Accurate and sensitive peptide identification with Mascot Percolator. J Proteome Res. 2009; 8:3176–81. doi: 10.1021/pr800982s PMID: 19338334

24. Ong SE, Blagoev B, Kratchmarova I, Kristensen DB, Steen H, Pandey A, et al. Stable isotope labeling by amino acids in cell culture, SILAC, as a simple and accurate approach to expression proteomics. Mol Cell Proteomics 2002; 1:376–86. PMID: 12118079

25. Arnér ES, Eriksson S. Mammalian deoxyribonucleoside kinases. Pharmacol Ther. 1995; 67:155–86. PMID: 7494863

26. Bai L, Yamaguchi M, Tatsumi M, Kon K, Bräutigam M. Mechanisms responsible for resistance of sublines derived from leukemia cell lines to an antitumor agent 9-beta-D-arabinofuranosyl-2-fluoroadenine. J Cancer Res Clin Oncol. 1998; 124:367–73. PMID: 9719499

27. Lotfi K, Månsson E, Spasokoukotskaja T, Pettersson B, Liliemark J, Peterson C. et al. Biochemical pharmacology and resistance to 2-chloro-2'-arabino-fluoro-2'-deoxyadenosine, a novel analogue of cladribine in human leukemic cells. Clin Cancer Res. 1999; 5:2438–44. PMID: 10499616

28. Qin T, Castoro R, El Ahdab S, Jelinek J, Wang X, Si J, et al. Mechanisms of resistance to decitabine in the myelodysplastic syndrome. PLoS One 2011; 6:e23372. doi: 10.1371/journal.pone.0023372 PMID: 21858090

29. Klanova M, Lorkova L, Vit O, Maswabi B, Molinsky J, Pospisilova J, et al. Downregulation of deoxycytidine kinase in cytarabine-resistant mantle cell lymphoma cells confers cross-resistance to nucleoside analogs gemcitabine, fludarabine and cladribine, but not to other classes of anti-lymphoma agents. Mol Cancer 2014; 13:159. doi: 10.1186/1476-4598-13-159 PMID: 24972933

30. Natsumeda Y, Prajda N, Donohue JP, Glover JL, Weber G: Enzymic capacities of purine de novo and salvage pathways for nucleotide synthesis in normal and neoplastic tissues. Cancer Res. 1984; 44:2475–9. PMID: 6327016

31. Austin WR, Armijo AL, Campbell DO, Singh AS, Hsieh T, Nathanson D, et al. Nucleoside salvage pathway kinases regulate hematopoiesis by linking nucleotide metabolism with replication stress. J Exp Med. 2012; 209:2215–28. doi: 10.1084/jem.20121061 PMID: 23148236

32. Heale JT, Ball AR Jr, Schmiesing JA, Kim JS, Kong X, Zhou S, et al. Condensin I interacts with the PARP-1-XRCC1 complex and functions in DNA single-strand break repair. Mol Cell. 2006; 21:837–48. PMID: 16543152

33. Li P, Jin H, Yu HG. Condensin suppresses recombination and regulates double-strand break processing at the repetitive ribosomal DNA array to ensure proper chromosome segregation during meiosis in budding yeast. Mol Biol Cell. 2014; 25:2934–47. doi: 10.1091/mbc.E14-05-0957 PMID: 25103240

34. Constantinou A. Rescue of replication failure by Fanconi anaemia proteins. Chromosoma 2012; 121:21–36. doi: 10.1007/s00412-011-0349-2 PMID: 22057367

35. Smith SC, Petrova AV, Madden MZ, Wang H, Pan Y, Warren MD, et al. A gemcitabine sensitivity screen identifies a role for NEK9 in the replication stress response. Nucleic Acids Res. 2014; 42:11517–27. doi: 10.1093/nar/gku840 PMID: 25217585

36. Oltvai ZN, Milliman CL, Korsmeyer SJ. Bcl-2 heterodimerizes in vivo with a conserved homolog, Bax, that accelerates programmed cell death. Cell 1993; 74:609–19. PMID: 8358790

37. Reed JC. Balancing cell life and death: bax, apoptosis, and breast cancer. J Clin Invest. 1996; 97:2403–4. PMID: 8647929

38. Reed JC. Bcl-2 family proteins: regulators of apoptosis and chemoresistance in hematologic malignancies. Semin Hematol. 1997; 34:9–19.

39. Souers AJ, Leverson JD, Boghaert ER, Ackler SL, Catron ND, Chen J, et al. ABT-199, a potent and selective BCL-2 inhibitor, achieves antitumor activity while sparing platelets. Nat Med. 2013; 19:202–8. doi: 10.1038/nm.3048 PMID: 23291630

40. Saba N, Wiestner A. Do mantle cell lymphomas have an 'Achilles heel'? Curr Opin Hematol. 2014; 21:350–7. doi: 10.1097/MOH.0000000000000057 PMID: 24857884

41. Wang ML, Rule S, Martin P, Goy A, Auer R, Kahl BS, et al. Targeting BTK with ibrutinib in relapsed or refractory mantle-cell lymphoma. N Engl J Med. 2013; 369:507–16. doi: 10.1056/NEJMoa1306220 PMID: 23782157

42. Satterthwaite AB, Witte ON. The role of Bruton's tyrosine kinase in B-cell development and function: a genetic perspective. Immunol Rev. 2000; 175:120–7. PMID: 10933597

43. Cinar M, Hamedani F, Mo Z, Cinar B, Amin HM, Alkan S. Bruton tyrosine kinase is commonly overexpressed in mantle cell lymphoma and its attenuation by Ibrutinib induces apoptosis. Leuk Res. 2013; 37:1271–7. doi: 10.1016/j.leukres.2013.07.028 PMID: 23962569

44. Seda V, Mraz M. B-cell receptor signalling and its crosstalk with other pathways in normal and malignant cells. Eur J Haematol. 2015.

45. Cyster JG, Goodnow CC. Protein tyrosine phosphatase 1C negatively regulates antigen receptor signaling in B lymphocytes and determines thresholds for negative selection. Immunity 1995; 2:13–24. PMID: 7600299

46. Vié N, Copois V, Bascoul-Mollevi C, Denis V, Bec N, Robert B, et al. Overexpression of phosphoserine aminotransferase PSAT1 stimulates cell growth and increases chemoresistance of colon cancer cells. Mol Cancer 2008; 7:14. doi: 10.1186/1476-4598-7-14 PMID: 18221502

47. Florczyk U, Golda S, Zieba A, Cisowski J, Jozkowicz A, Dulak J. Overexpression of biliverdin reductase enhances resistance to chemotherapeutics. Cancer Lett. 2011; 300:40–7. doi: 10.1016/j.canlet.2010.09.003 PMID: 20934804

48. Kim SS, Seong S, Lim SH, Kim SY. Biliverdin reductase plays a crucial role in hypoxia-induced chemoresistance in human glioblastoma. Biochem Biophys Res Commun. 2013; 440:658–63. doi: 10.1016/j.bbrc.2013.09.120 PMID: 24113378

49. Tew KD. Glutathione-associated enzymes in anticancer drug resistance. Cancer Res. 1994; 54:4313–20. PMID: 8044778

50. Yao P, Fox PL. Aminoacyl-tRNA synthetases in medicine and disease. EMBO Mol Med. 2013; 5:332–43. doi: 10.1002/emmm.201100626 PMID: 23427196

7.4 Appendix 4

Integral membrane proteins in proteomics: How to break open the black box? Vit O, Petrak J. *Journal of Proteomics.* 2017;153:8-20. (IF 2015: 3.867).

Journal of Proteomics 153 (2017) 8–20

Contents lists available at ScienceDirect

Journal of Proteomics

journal homepage: www.elsevier.com/locate/jprot

Review

Integral membrane proteins in proteomics. How to break open the black box?

O. Vit *, J. Petrak

BIOCEV, First Faculty of Medicine, Charles University in Prague, Czech Republic

ARTICLE INFO

Article history:
Received 6 April 2016
Received in revised form 30 June 2016
Accepted 9 August 2016
Available online 13 August 2016

Keywords:
Integral membrane proteins
Detergent removal
Transmembrane
Surfaceomics
Alternative proteases
Cyanogen bromide

ABSTRACT

Integral membrane proteins (IMPs) are coded by 20–30% of human genes and execute important functions – transmembrane transport, signal transduction, cell-cell communication, cell adhesion to the extracellular matrix, and many other processes. Due to their hydrophobicity, low expression and lack of trypsin cleavage sites in their transmembrane segments, IMPs have been generally under-represented in routine proteomic analyses. However, the field of membrane proteomics has changed markedly in the past decade, namely due to the introduction of filter assisted sample preparation (FASP), the establishment of cell surface capture (CSC) protocols, and the development of methods that enable analysis of the hydrophobic transmembrane segments. This review will summarize the recent developments in the field and outline the most successful strategies for the analysis of integral membrane proteins.

Significance: Integral membrane proteins (IMPs) are attractive therapeutic targets mostly due to their many important functions. However, our knowledge of the membrane proteome is severely limited to effectively exploit their potential. This is mostly due to the lack of appropriate techniques or methods compatible with the typical features of IMPs, namely hydrophobicity, low expression and lack of trypsin cleavage sites. This review summarizes the most recent development in membrane proteomics and outlines the most successful strategies for their large-scale analysis.

Contents

* Corresponding author.
E-mail address: ondrvit@gmail.com (O. Vit).

http://dx.doi.org/10.1016/j.jprot.2016.08.006
1874-3919/

1. Introduction

Cellular membranes provide an essential physical interface between individual subcellular compartments, and between the cell and its environment. Composed of proteins, phospholipids and glycolipids, cellular membranes play a critical role in cell function and survival by spatially restricting chemical and biochemical processes and defining cell borders. Integral membrane proteins, i.e. proteins that cross the phospholipid bilayer, are coded by roughly 25% of human genes [1] while representing circa 7–8% of the overall cellular protein mass in human cells [2].

Integral membrane proteins (IMPs) function as important transporters, channels, receptors, and enzymes, responsible for signal transduction, regulatory processes and cell-cell and cell-environment interactions. These roles make IMPs enormously attractive targets for therapeutic interventions. In fact, approximately half of the currently approved drugs in human medicine target IMPs [3]. The recent revolution in the development of therapeutic antibodies against surface plasma membrane proteins further augmented the wide interest in IMPs. However, our knowledge of the structure, function and expression dynamics of IMPs is still limited, mostly because of their adverse physico-chemical properties and low expression levels. Based on their structure, IMPs can be characterized as alpha-helical or beta-barrel proteins. Since beta-barrels are a minor component of mammalian genomes, restricted to several proteins of bacterial origin present in the mitochondrial membrane and can be studied by conventional approaches, this review will further discuss only the hydrophobic alpha-helical proteins. Similarly, monotopic membrane proteins, i.e. molecules that are attached or anchored to the membrane but do not traverse the bilayer, will not be discussed here.

Alpha-helical IMPs are amphipathic – composed of hydrophilic extramembrane segments and one or more hydrophobic alpha-helical segments of 20–30 amino acids spanning the phospholipid bilayer. It is this amphipathy that renders IMPs difficult to solubilize and makes membrane proteomics so challenging. Due to their "split personality" and low expression levels, IMPs are underrepresented in conventional bottom-up proteomic analyses, which generally favor soluble, abundant and easy-to-digest proteins and peptides. [4,5]. In addition to their low abundance and relative hydrophobicity, a third adverse feature of IMPs exists – low digestibility with trypsin– since the hydrophobic alpha-helical segments are poor in the charged lysines (K) and arginines (R) that are the targets for trypsin. Furthermore, the exposed hydrophilic extra-membrane segments are often of limited length and may not provide enough tryptic peptides for identification, despite being adequately rich in tryptic cleavage sites (see Fig. 1). For more information on IMP structure and their alpha helices, several high quality reviews can be recommended [6–8].

This review will summarize recent developments in the proteomics of mammalian IMPs, namely the progress in sample preparation steps preceding LC-MS analysis, and outline the most successful strategies to date regarding the number of identified IMPs and their enrichment. We will therefore deal mostly with the different strategies of solubilization and digestion of membrane samples. We also do not address the conventional 2-DE technology, as it has been largely abandoned and demonstrated to be unsuitable for the analysis of mammalian hydrophobic IMPs in complex mixtures. This incompatibility has several reasons, the major one being the low solubility of IMPs during isoelectric focusing (IEF). For detailed information on 2-DE applications in membrane proteomics, two excellent reviews can be highly recommended [9,10].

In proteomic publications, the numbers of identified IMPs are usually reported either according to their proper Gene Ontology (G.O.) annotation or, more stringently, as numbers of proteins containing at least one predicted transmembrane segment. Experimental evidence on the topology of IMPs is quite limited, but topology prediction algorithms provide fast, though potentially inaccurate information on probable IMP topology. Early methods for topology prediction were based solely on the identification of hydrophobic stretches of 15–25 amino acid residues in the protein sequence. Later, with the discovery of the "positive-inside" rule [11], predictions were further refined by enabling the correct orientation of TM segments. Current prediction methods use various algorithms ranging from the "sliding window across the sequence" to more advanced artificial neural networks, support vector machines, hidden Markov models and dynamic Bayesian networks (for review see [1,12–15]). Among the difficulties in topology prediction are hydrophobic signal sequences that are similar to N-terminal TM segments, kinks in the TM segments, and short re-entrant segments. Some of prediction methods are, however, capable of dealing even with these obstacles. Several of the algorithms also use evolutionary information by introducing multiple sequence alignments, or refine the prediction with incorporation of preexisting knowledge of the topology of some regions of the sequence. The very recently introduced CCTOP prediction web server integrates 10 different topology prediction methods [16]. In this review, we have made an effort to report the numbers of IMPs identified in the referenced publications based on the prediction of TM segments. In several cases, where such information was not available in the publication, we used the original published data and recalculated the proportion of IMPs with the TMHMM algorithm based on the hidden Markov models [17].

The field of membrane proteomics has changed dramatically in the last decade. Aside from the massive improvement in mass spectrometry (MS) instrumentation, the advent of MS-compatible detergents, filter assisted sample preparation (FASP) and surface capture protocols have markedly diversified our proteomic tool-box and opened the way toward understanding the proverbial black box of the membrane proteome.

2. Enrichment of membrane material

In general, two basic strategies in membrane proteomics exist. Membrane proteins can be either targeted as whole molecules, or alternatively, a "divide and conquer" approach can be used, aiming separately or exclusively at their hydrophilic (extramembrane) or hydrophobic (transmembrane) segments. Regardless of the strategy, membrane enrichment is an essential, and usually the first, step in both workflows. The enrichment of membrane material is almost always performed by centrifugation, ranging from one-step medium-speed crude membrane sedimentation to multistep isolation involving a density gradient or

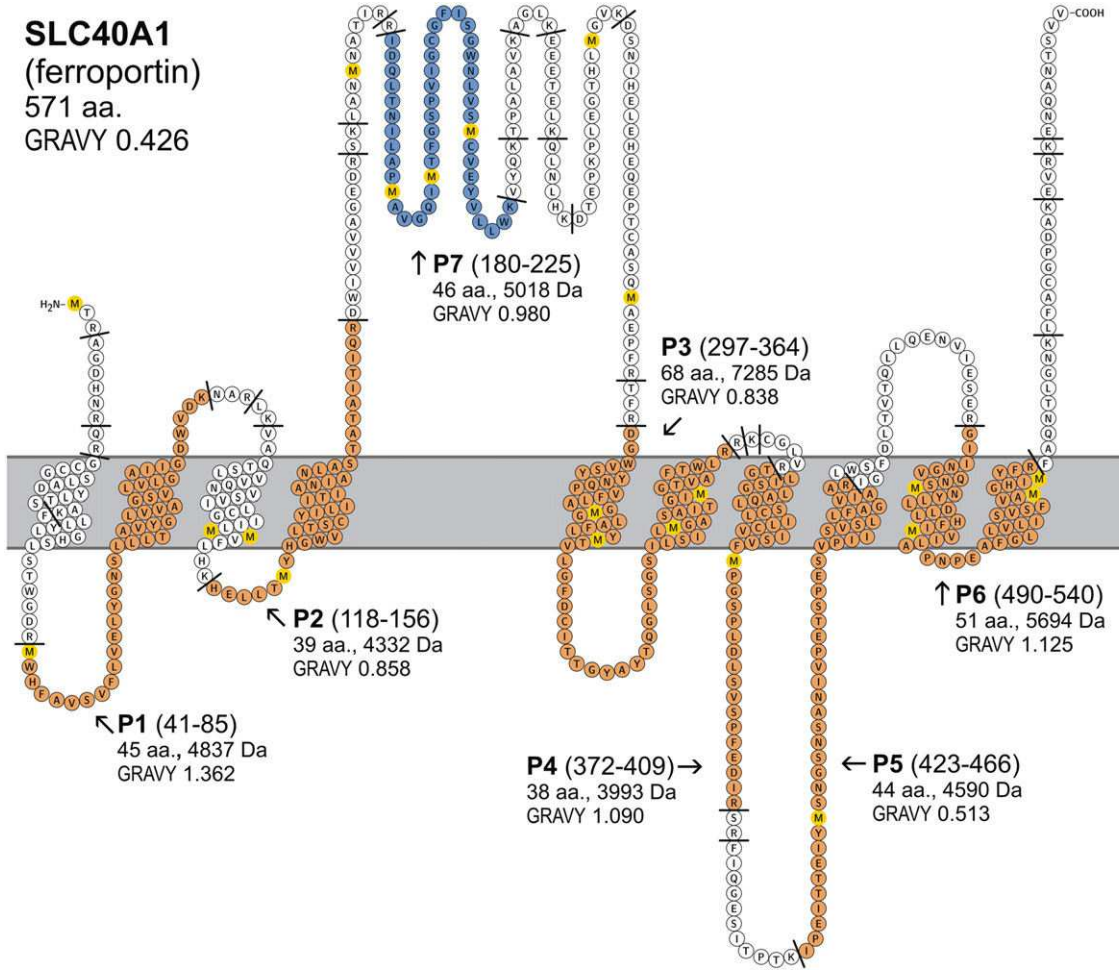

Fig. 1. The problematic digestion of IMPs with trypsin. An example of an integral membrane protein with multiple transmembrane domains – the membrane iron exporter ferroportin (10 transmembrane segments, 571 amino acids, GRAVY score 0,426). Without solubilization of the protein, a theoretical digestion with trypsin would produce 11 peptides of length between 5 and 25 amino acids. A theoretical tryptic digestion of completely solubilized ferroportin (no missed cleavages) would generate only 2 additional peptides shorter than 35 amino acids. However, an entire 49% of the molecule sequence will be represented by 6 long transmembrane hydrophobic peptides (P1-P6, orange) ranging in length from 38 to 68 amino acids (MW from 3990 to over 7290) and high hydrophobicity (GRAVY scores from 0.51 up to 1.36). Such peptides may easily get lost during sample preparation and analysis. In addition to the critical transmembrane α-helices, even the extra-membrane (soluble) portion of the ferroprotin molecule contributes one long and hydrophobic segment (P7, blue, 5018 Da, GRAVY 0.98), further increasing the proportion of the ferroprotin sequence that could possibly escape detection. Graphics: http://wlab.ethz.ch/protter/

cushion ultra-centrifugation (reviewed in [18]) based on protocols established several decades ago. Plasma membrane enrichment via peeling by a cationic silica pellicle is a methodically interesting approach, which has not, however, found wider application [19].

No matter how complex the sedimentation strategies are, due to subcellular complexity and the large hydrophobic surface of membrane vesicles, isolated "membrane enriched" fractions are inevitably heavily contaminated by major cellular proteins, ribosomes, components of the cytoskeleton, proteins attached to membranes, and other molecules. In fact, these contaminants dominate MS spectra and hamper the analysis of underrepresented IMPs. To further enrich IMPs and strip the soluble contaminants and peripheral membrane proteins, isolated membrane fractions can be washed with aqueous high ionic strength buffers, typically using high pH sodium carbonate washes originally introduced by Fujiki in the 1980s [20]. In addition to the striping of peripheral proteins, the alkaline pH and high ionic strength of sodium carbonate stimulate opening of the membrane vesicles and releasing the entrapped contents, and alkaline carbonate washing is now routinely employed in membrane proteomics [21–23 and others]. In addition, high salt washes with 1–5 M NaCl, KCl or NaBr are sometimes added to the carbonate washes [19,24–28]. As an alternative to sodium carbonate treatment, membrane washes with an organic solvent, namely trifluoroethanol (TFE), have been also successfully tested [29]. It is evident, though, that no matter how vigorous and intensive such washing steps are, they only partially reduce the presence of non-membrane proteins in the sample, as the percentage of IMPs identified in isolated and carbonate-washed membrane fractions ranges from 20 to 60% of all identified proteins even after multi-step fractionation procedures. [21,25,30–32].

No significant developments in the membrane enrichment, in the classical sense, have been made in the last decade. However, a strategy for analysis of the plasma membrane proteome based on the affinity enrichment of surface proteins, known as Cell Surface Capture (CSC), has been developed and successfully applied in numerous studies. This method will be discussed in Section 5.1.

3. Solubilization and digestion

An enriched membrane fraction is the starting material in most proteomic workflows focusing on IMPs. Extracellular segments of IMPs with large extramembrane segments may, and often do, provide several peptides sufficient for protein identification even without membrane solubilization [21,33–35]. However, a significant proportion of an IMP molecule (and in some cases most of it) is safely buried in the phospholipid bilayer, and inaccessible to protease activity. The lack of solubility of IMPs not only prevents their complete digestion but also accounts

Table 1
The most common detergents, organic solvents and chaotropes in membrane proteomics.

Compound	Advantages for membrane proteomics	Disadvantages
Detergents		
Sodium dodecyl sulfate (SDS)	-Efficiently solubilizes cell membranes and denatures all types of proteins -Can be removed using the FASP procedure	-Proteases do not tolerate concentrations of SDS higher than 0.1% -Even very low concentrations of SDS impair liquid chromatography and mass spectrometry -Removal procedures are either relatively laborious, inefficient or cause partial loss of the sample
Sodium dodecyl cholate (SDC)	-Compatible with trypsin in the concentration necessary for membrane solubilization (5% SDC) -Efficient removal by phase transfer or acid precipitation	-Lower solubilizing and denaturing ability compared to SDS
Acid-labile surfactants	-Rapid detergent removal by acid cleavage	-Expensive -Loss of hydrophobic peptides after acid cleavage and precipitation (RapiGest)
Organic solvents		
Methanol, trifluoroethanol	-60% methanol (or 50% TFE) solubilizes membranes and IMPs -Trypsin remains partially active in 60% methanol (or 25% TFE) -5–15% TFE can be used for removal of membrane-associated proteins from membrane surfaces -Easy evaporation prior to LC	-Trypsin activity and specificity are severely lowered in 60% methanol
Formic acid	-Effectively solubilizes membranes, hydrophobic proteins and peptides -Compatible with chemical cleavage using cyanogen bromide	-Incompatible with most proteases -May cause formylation and hydrolysis of proteins and peptides
Chaotropes		
Urea, guanidine hydrochloride	-6–8 M urea can be used to denature extra-membrane parts of IMPs in combination with certain proteases (Lys-C, Glu-C) -Efficient removal of both guanidine and urea prior to LC/MS using common desalting methods	-Does not solubilize membranes nor IMPs -Incompatible with trypsin at concentrations needed for protein denaturation (6 M guanidine, 6–8 M urea) -Urea may cause protein modifications at elevated temperatures

for protein precipitation, aggregation and non-specific adhesion to laboratory plastic. Therefore, solubilization of the membrane material is the cornerstone of success in membrane proteomics. The solubilization step is particularly important for the release of peptides resulting from a cleavage in extramembrane loops of IMPs with multiple transmembrane segments. Chaotropes, organic solvents and especially detergents may assist in this task to various extents (Table 1).

3.1. Detergents

Detergents are amphipathic molecules mimicking the properties of the membrane phospholipids, including the assembly of micelles. That makes them enormously useful in membrane disintegration and protein solubilization. However, detergents differ greatly in their solubilization power and denaturing effects. Also, depending on their characteristics, detergents may inactivate trypsin and other proteases, stick to hydrophobic surfaces, interfere with chromatographic separation and/or suppress peptide ionization and contaminate mass spectrometers. Therefore, significant effort has been invested into the advancement of methods for detergent removal prior to digestion or LC-MS analysis, and into the development of new detergents without such adverse effects.

3.1.1. SDS

Sodium dodecyl sulfate (SDS), a linear chain strong ionic detergent, is highly effective in the solubilization of membranes and membrane proteins as well as in protein denaturation [36]. Trypsin activity is limited in even 0.1% SDS, however, and much lower SDS concentrations can cause a reduction in the separation power of liquid chromatography (LC) and hamper peptide ionization during MS analysis [37–41]. Therefore, SDS must be removed prior to protein digestion or LC-MS/MS. To remove SDS from a membrane sample, ion-pair extraction using a mixture of triethylamine, acetone, acetic acid and water can be used [42]. Precipitation of SDS by potassium chloride is also effective and possibly more convenient [43]. Alternatively, protein precipitation with organic solvents, namely TCA [44,45], acetone, or chloroform/methanol/water [46] is an effective, simple and inexpensive way to deplete SDS with sufficient protein recovery.

Similarly to traditional in-gel protein digestion, a complex membrane sample containing SDS can be briefly electrophoresed on conventional SDS-PAGE, SDS extracted from the gel slice, and then proteins in the gel digested and peptides extracted [19,22,47–50]. In a less laborious alternative, the SDS-solubilized sample is simply mixed with a small amount of the acrylamide solution prior to its polymerization [32,51,52]. The in-gel digestion trypsin-based approach solves the problem of SDS; unfortunately, however, its applicability for the analysis of IMPs, especially IMPs with multiple transmembrane segments, is limited, since long hydrophobic peptides resist extraction from acrylamide gels [22].

Another methodically distinct way of SDS depletion from a complex sample is based on the covalent capture of proteins. Magnetic nanobeads coated with tresyl-functioned PEG covalently bind free amino groups of proteins from SDS-solubilized membranes. The captured proteins can then be washed and digested. A recent application of this approach in the analysis of a liver microsomal fraction enabled the identification of >1500 IMPs, representing roughly a quarter of all proteins identified in the study [53]. SDS depletion using SCX chromatography has also been explored [54] and found efficient in samples where SDS concentrations exceed its critical micellar concentration [55]. More importantly, a successful detergent removal on a desalting size-exclusion column with the assistance of 8 M urea [27] led to the introduction of filter assisted sample preparation (FASP) - an elegant method of sample clean-up and digestion [56].

FASP allows the depletion of detergents (or generally any low molecular weight soluble compounds) including SDS from a complex sample by centrifugation through an ultrafilter with a 10–30 kDa cut-off combined with washes with 8 M urea buffer. Further buffer exchange and a direct on-filter sample digestion may follow the washing step. This was demonstrated to be superior to the in-solution digestion approach in terms of protein sequence coverage, number of protein identifications and the absence of bias against hydrophobic proteins [56]. The applicability of the FASP workflow to membrane proteomics was clearly demonstrated in an analysis of a mouse hippocampal membrane fraction using a double on-filter digestion with Lys-C followed by trypsin that allowed the identification of over 1600 IMPs [30]. In combination with a complex multi-step sample processing procedure, GELFrEE (gel eluted liquid fraction entrapment electrophoresis), the application of FASP later enabled the identification of 2090 IMPs from a membrane fraction of human leukemia cells [57]. Recently, FASP facilitated the identification of over 300 IMPs in an analysis of technically-challenging membrane microdomains of a human renal carcinoma [58].

A modification of the FASP method with lectin-affinity capture led to development of glyco-FASP [59], enabling the selective enrichment of

glycosylated peptides from IMP extramembrane domains of the plasmatic membrane, lysosomes and endosomes (see more in Section 5.3.).

Being widely adopted and incorporated into various workflows, the elegantly simple FASP has changed the methodological repertoire of current proteomics. As evidenced above, FASP combined with a strong detergent, namely SDS, has enabled the identification of up to 1000–2000 IMPs in a single study.

3.1.2. Sodium deoxycholate

Although SDS has been the detergent of choice for the solubilization of membrane proteins, alternatives have been sought and evaluated. Sodium deoxycholate (SDC) is an ionic detergent with a steroidal hydrophobic part and a charged carboxyl group. SDC facilitates the digestion of hydrophobic proteins through efficient denaturation, although compared to SDS, cholates possess lower denaturing and solubilizing ability [60,61]. One clear advantage of SDC is its high compatibility with trypsin, which tolerates SDC concentrations up to 5–10% [61,62].

Similarly to SDS, SDC must be removed from the peptide sample before MS analysis. It can be effectively depleted by phase transfer into a water-immiscible solvent, namely ethyl acetate [61]. SDC has been successfully applied to the analysis of membranes of human HeLa cells, resulting in the identification of a total of 1450 proteins, of which 512 (35%) were IMPs [61]. Later, an analysis of membrane samples from human breast tumors solubilized by SDC led to the identification of 7095 proteins including 1977 (28%) IMPs, with at least one transmembrane alpha helix predicted by TMHMM [63]. SDC also enabled the identification of 5556 proteins including 1567 (28%) IMPs in human colorectal cancer samples [64]. SDC can be alternatively removed by acid precipitation in aqueous buffer using 0.1–2% trifluoroacetic acid or formic acid followed by centrifugation [62,65]. Side-by-side comparisons of the phase transfer and acid precipitation of SDC have produced several conflicting reports. Lin et al. [66] showed that both strategies of SDC removal led to a loss of peptides, and this loss was more pronounced in the phase transfer method. Others have demonstrated that acid precipitation is more reproducible [67,68], as it does not require the potentially problematic removal of the aqueous phase. On the other hand, León et al. [69] documented higher sequence coverage in samples undergoing phase transfer compared to acid precipitation.

SDC has also been repeatedly evaluated side-by-side with other detergents including SDS and acid-cleavable RapiGest (see below), with SDC found to be superior for the solubilization and digestion of IMPs with trypsin [69,70]. In general, enabling the identification of 500–2000 IMPs, SDC has firmly established its potential for membrane analysis along with the traditional SDS.

3.1.3. Acid-labile surfactants

Acid-labile surfactants (ALS) have been developed relatively recently to avoid or simplify the detergent removal prior to LC-MS. As the name suggests, these detergents are cleaved by a low-pH environment at elevated temperature. Their hydrophobic part becomes water-immiscible, and forms an easily-removable precipitate, while the remaining part of the molecule is LC- and MS-compatible. RapiGest™ was the first ALS to reach wider attention [71]. It structurally mimics SDS by having an ionic sulfonate moiety and hydrophobic undecyl chain, and effectively solubilizes membranes. Another important advantage of RapiGest is that it does not limit trypsin activity in concentrations up to 1% [71–74]. RapiGest was shown to be more powerful compared to urea in the solubilization of organelle-enriched fractions [72]. It was initially found to be slightly more efficient in comparison with SDS in regard to the number of identified proteins in the human MCF-7 cell line. [54] In the same study, analysis of an *E. coli* membrane fraction using RapiGest resulted in the identification of 1626 proteins, with about half being predicted IMPs. When an improved method for SDS removal was applied, both SDS and RapiGest allowed a comparable number of protein identifications in MCF-7 cells, with around 400 IMPs [55]. Several other ALSs have been developed and tested, such as 3-[3-(1,1-bisalkyloxyethyl)pyridin-1-yl]propane-1-sulfonate (PPS) [75], and more recently Progenta Anionic Acid Labile Surfactants I and II were found to be a good alternative to RapiGest [76].

The advantage of RapiGest, i.e. simplified detergent removal is, nevertheless, counterbalanced by its high price. In addition, a major complication of the RapiGest application in membrane proteomics can be the loss of the most hydrophobic peptides due to co-precipitation with the hydrophobic RapiGest fragment during its removal [61,71,77]. With the advent of FASP, which enables effective detergent removal, traditional, effective and cheap SDS, SDC or other detergents may prevail over their expensive acid-cleavable alternatives.

Several excellent reviews are available that give more detail and wider information on the available detergents and their application in the analysis of membrane proteins [60,78,79].

3.2. Organic solvents

Organic solvents have mainly been tested as an alternative to detergents. After the advent of FASP, which enables easy detergent removal, however, their importance as single agents for membrane protein solubilization and digestion will probably fade. Despite this, here we review the most commonly used.

3.2.1. Methanol and trifluoroethanol

To completely avoid the troubles with detergents interfering with LC separation or MS analysis, methanol has been exploited as an alternative for IMP solubilization and digestion. Trypsin has been shown to retain most of its activity in up to 20% methanol [80]; however, higher concentrations are needed to solubilize membranes. Trypsin activity is reduced to one-fifth in 60% methanol compared to aqueous buffer [81] and its specificity may also decrease [82]. Nevertheless, a detergent-free solubilization of an isolated membrane fraction in 60% methanol (assisted by sonication) followed by tryptic digestion in the same solvent enabled the identification of over 700 IMPs (including peptides from their transmembrane segments) in murine macrophages [83] and almost 500 membrane proteins (according to their GO annotation) in human epithelial cells [84].

Recently, however, a side-by-side comparison by Moore demonstrated that solubilization and digestion in 60% methanol is markedly inferior compared to 0.15% RapiGest or 1% SDC in a yeast membrane fraction. The use of detergents increased the total number of identified proteins and IMPs several-fold compared to methanol. [70] As an alternative to methanol, 50% trifluoroethanol (TFE) has been evaluated as membrane-solubilizing agent for erythrocyte membranes. Despite the fact that TFE-solubilized membranes provided a lower number of identified IMPs compared to 60% methanol, the proteins and peptides released by TFE had markedly higher hydrophobicity, suggesting some potential of TFE as a complementary solvent for IMP analysis. [85]. TFE has also been employed in a methodically different setting – first, to release peripheral membrane proteins from isolated membranes (5% and 15% TFE wash) and then to solubilize delipidated membrane samples and assist trypsin digestion (25% TFE) in the analysis of a human NK-like cell line microsomal fraction. In this complex multi-step study including sample delipidation, 681 IMPs were identified. [29].

Although organic solvents may assist membrane solubilization, an extensive comparison of various solvents, detergents and chaotropes in the protein extraction and digestion of mouse brain samples demonstrated that detergent-based protocols including detergent removal by FASP significantly outperform organic solvents and chaotropes in the number of identified membrane proteins. The best detergent-based protocol enabled the identification of over 500 proteins, of which 29% were IMPs [86]. More recently, a similar side-by-side comparison of several detergents, two organic solvents, and chaotropes and their combinations confirmed the superiority of detergents over organic solvents and chaotropes in membrane analysis. The same study, however,

pointed out the advantage of the additive effect of an organic solvent (acetonitrile), a chaotrope (guanidine) and an MS-compatible detergent used in combination. [76].

3.2.2. Formic acid

Concentrated formic acid (FA) is an excellent solvent for the solubilization of membranes and hydrophobic proteins and peptides. Significant downsides to FA, however, are its incompatibility with trypsin activity and tendency to generate uncontrolled damage to protein samples, like D-P bond cleavage [87] and protein formylation [88]. However, these modifications can be prevented by working at low temperatures [46].

Despite being incompatible with trypsin, FA has found its use as an alternative to SDS in the solubilization of membrane samples [89] and precipitated protein pellets [46], as a solvent for the extraction and MS-analysis of long hydrophobic peptides from acrylamide gels following their in-gel digestion [44], as well as a solvent for the digestion of membrane material with pepsin [90]. Most importantly, FA can be used for chemical cleavage of hydrophobic peptides with cyanogen bromide (CNBr) [24,91]. This will be further discussed in Sections 4.1.6. and 5.2.

3.3. Chaotropes

Although less potent in membrane protein solubilization compared to detergents and organic solvents, chaotropes are sometimes used in proteomics for the disruption of protein-protein interactions, denaturation, and maintaining the unfolded state of proteins. Urea and guanidine hydrochloride are used most often. In contrast to detergents, these small molecules do not interfere significantly with LC/MS. If desired, urea and guanidine can be removed prior to MS by common desalting techniques. The optimal concentrations of guanidine hydrochloride or urea needed for denaturation of proteins are 6 M and 8 M, respectively, both far too high to be compatible with sufficient trypsin activity. Dilution to 1 M (guanidine) and 2 M (urea) concentrations before digestion of a protein sample with trypsin is needed. However, such a dilution may lead to protein refolding [74].

Although chaotropes do not fully extract IMPs from the membrane, urea has been reported to facilitate the digestion of their extramembrane parts [91–93]. However, a side-by-side evaluation of trypsin digestion efficiency in isolated membrane fractions showed no benefit of 2 M urea over ammonium bicarbonate buffer in terms of the number of the identified membrane proteins [25]. Similarly, 1 M guanidine hydrochloride enhances the digestion efficiency of trypsin compared to ammonium bicarbonate buffer without additives [45,74] and its advantage compared to urea is also its chemical inertness [94]. Compared to detergents including ALS, the effect of chaotropes in membrane sample solubilization and digestion has been shown to be lower in terms of the number of identified proteins and peptides [25,74,76].

However, the role of chaotropes in membrane proteomics cannot be dismissed. The use of urea is inseparable from the use of endoproteases Lys-C and Glu-C, unique enzymes that tolerate up to 8 M urea. Digestion of a membrane sample with Lys-C in 6–8 M urea before dilution of the chaotrope and sample re-digestion with trypsin has been shown to improve IMP identification [25] and has become one of new standards in sample preparation (see more in Section 4.1.1).

4. Digestion of integral membrane proteins

Even the best solubilization strategy cannot increase the number of identified IMPs, nor improve their sequence coverage, without the production of peptides of a size and hydrophobicity compatible with current bottom-up technologies. Trypsin is undoubtedly the optimal protease for standard soluble protein sequences containing advantageous distributions of arginine and lysine residues [95]. However, traditional trypsin-centric strategies may not be sufficient for unlocking the secrets of the phospholipid bilayer, and the analysis of IMPs may require other strategies. Arginines and lysines, although sufficiently frequent in extracellular soluble segments of plasma membrane, may be sterically inaccessible to trypsin due to extensive glycosylation. [25,96]. Moreover, the size of trypsin-cleavable hydrophilic extramembrane portions of IMPs varies from conveniently large extracellular domains down to very short terminal or loop segments that may not provide enough sequence information for unequivocal protein identification. Most importantly, the well-established scarcity of charged lysine and arginine in hydrophobic transmembrane segments, formed preferentially by nonpolar and polar uncharged amino acids, is the most critical obstacle to effective trypsin use in membrane proteomics [97,98]. Trypsin-generated peptides including one or more transmembrane alpha-helical segments are inevitably large (30 + amino acids) and highly hydrophobic, as peptide hydrophobicity seems to be to some extent a function of their length [97]. Such peptides may readily adhere to plastic surfaces and get lost during sample preparation, may be retained on LC columns, or may not be detected by current MS instrumentation. The problem of long hydrophobic peptides resulting from trypsin cleavage is demonstrated in Fig. 1. A theoretical and complete (no missed cleavages) digestion of the fully solubilized IMP ferroportin demonstrates that half of the protein sequence is represented by 6 problematic transmembrane hydrophobic peptides with MW up to 7290 and high hydrophobicity as determined by their GRAVY score [99].

Some of the abovementioned complications of trypsin use in the analysis of IMPs may be overcome or at least limited: for instance, inclusion of a deglycosylation step prior to proteolytic digestion can lead to an increase in the number of identified IMPs [25]. Similarly, detectability of shorter trypsin-generated hydrophobic peptides by MS can be enhanced by chemical modifications leading to their increased solubility, such as the modification of methionines by oxidation [97]. However, such improvements are largely negligible, and a better solution may be to look for an alternative cleavage strategy. Such as strategy may be sought among other proteases, including specific, semi- and non-specific proteases, or among chemicals enabling peptide cleavage. Alternatively, hydrophilic and hydrophobic segments of IMPs can be targeted separately, with each requiring different strategies and tools.

4.1. The neglected world beyond trypsin

Trypsin has long been the gold standard in proteomics. Its clear dominance can be reflected in the number of available tryptic peptide datasets in databases. Enzymes other than trypsin account for only 4% of the data available in the Global Proteome Machine Database (GPM DB). Of the non-tryptic data, Lys-C has been the most significant contributor [100]. In the next paragraph, we will review the application of proteases other than trypsin in the analysis of IMPs, including the specific proteases Lys-C and Glu-C but also several semi-specific or nonspecific proteases (see also Table 2).

4.1.1. Lys-C and Glu-C

The major advantage of the bacterial serine endoprotease Lys-C (which is specific for the C-terminal peptide bond after lysine) is that it retains its activity in urea concentrations up to 8 M and enables the specific pre-digestion of hydrophobic samples in the presence of a chaotrope. This facilitates a partial solubilization and digestion of membrane proteins before urea removal and a final re-digestion with trypsin. This sequential strategy has been employed and shown to be beneficial in several membrane proteomics analyses, either in solution [34,35,52, 92,101,102 and others] or in a FASP-based arrangement [30,103]. In both cases, the advantage is that urea-denatured proteins are more prone to digestion, and after necessary dilution of the sample, this pre-digestion limits sample aggregation and facilitates the final digestion with trypsin.

The combination of detergent removal, pre-digestion with Lys-C in urea followed by final digestion with trypsin has established a workflow

Table 2
Summary of proteases and chemicals with high potential for analysis of IMPs.

Enzyme/compound	Properties	Strengths	Weaknesses
Trypsin	-Cleaves C-terminally to Arg and Lys	-Generates doubly positively charged peptides -Efficient ionization of peptides, compatibility with SILAC -Tolerance to some organic solvents	-Arg and Lys in hydrophobic segments are rare – long hydrophobic peptides escape identification -Low tolerance to detergents and chaotropes
Lys-C	-Cleaves C-terminally to Lys	-Active in high concentrations of urea – allows efficient denaturation, suitable for "shaving-off" approaches	-Lys in hydrophobic segments is rare – long hydrophobic peptides escape identification -Incubation in sub-optimal temperature in the presence of urea to prevent carbamoylation
Glu-C (V8 protease)	-Cleaves C-terminally to Asp and Glu	-Active in high concentrations of urea – allows efficient denaturation, suitable for "shaving-off" approaches	-Asp and Glu in hydrophobic segments are rare – long hydrophobic peptides escape identification -Incubation in sub-optimal temperature in the presence of urea to prevent carbamoylation
Chymotrypsin	-Cleaves C-terminal to Phe, Tyr and Trp, to a lesser extent to Leu and Met	-Cleavage sites present in hydrophobic segments	-Not an entirely specific protease -Generates long hydrophilic peptides that escape identification
Elastase	-Cleaves preferably C-terminally to small uncharged amino acids, and to a lesser extent to other amino acids	-Allows cleavage in hydrophobic transmembrane segments	-Nonspecific: generates a complex mix of multiply-overlapping peptides
Pepsin	-Cleaves preferably C-terminally to Tyr, Phe, Trp, Leu, and to a lesser extent Ala, Gly.	-Active in the presence of formic acid, which is a good solvent for hydrophobic proteins	-Nonspecific: generates a complex mix of multiply-overlapping peptides
Proteinase K	-Nonspecific, but preferentially C-terminal to aliphatic and aromatic hydrophobic amino acids	-Attenuated at high pH – generates favorable lengths of peptides -In combination with sodium carbonate buffer good for "shaving-off" approaches	-Nonspecific: generates a complex mix of multiply-overlapping peptides
Cyanogen bromide	-Cleaves C-terminally to met, converts to homoserine or homoserine lactone	-Sequentially specific to hydrophobic amino acid occurring in transmembrane segments -No sterical hindrance, does not produce missed cleavages	-High toxicity

that has become almost a standard in membrane proteomics. Lys-C has been included in the most successful membrane proteomics studies. Among those certainly deserving mention are an analysis of mouse hippocampal membranes resulting in the identification of over 1600 IMPs [30], a study of human breast tumors that resulted in the identification of 7095 proteins including 1977 (28%) IMPs [63], and an analysis of a liver microsomal fraction with >1500 identified IMPs [53].

It should be kept in mind, however, that high concentrations of urea can lead to the carbamoylation of primary amino groups in the sample when exposed to temperatures above 30–40 °C for prolonged periods of time [104]. For this reason, urea-assisted Lys-C digestions are usually carried out at 30 °C or below. Although the inclusion of Lys-C in urea facilitates the solubilization and digestion of membrane proteins, especially of their extramembrane domains, it does not solve the existing problem of long transmembrane lysine- and arginine-less segments.

Glu-C (alias V8 protease) from *Staphylococcus aureus* also retains its activity in 8 M urea but cleaves peptide bonds on the COOH terminal side of either Glu or Asp. Since these charged amino acids are not frequent in transmembrane segments, Glu-C offers only limited advantages over Lys-C. Dormeyer et al. compared the performance of Glu-C with Lys-C in a sequential digestion in 8 M urea, followed by trypsin digestion. Both enzymes produced a similar percentage of IMPs among the identified proteins, but the use of Glu-C resulted in a lower overall number of identified proteins [25].

4.1.2. Chymotrypsin

Chymotrypsin cleaves at C-terminal peptide bonds following the large aromatic amino acids phenylalanine (F), tyrosine (Y) and tryptophan (W), and also with lower efficiency after leucine (L) and methionine (M). These amino acids occur relatively frequently in the hydrophobic transmembrane segments of IMPs. Its specificity for F, W and Y was reported to increase in the presence of organic solvents [80]. An in silico proteome analysis assessing optimal cleavage conditions for IMPs of eukaryote origin suggested that chymotrypsin in combination with trypsin would radically (100-fold) lower the occurrence of large peptides (>4 kDa), while the use of chymotrypsin alone was predicted to result in higher sequence coverage of IMPs by peptides of appropriate MWs between 0.6 and 4 kDa compared to trypsin [105].

Despite its theoretical advantages, chymotrypsin has been used in only a limited number of studies. Simultaneous chymotrypsin plus trypsin digestion in 60% methanol was tested on *Corynebacterium glutamicum* membranes and resulted in the identification of 267 IMPs. [24]. The number of identified IMPs was later increased to 297 when this procedure was modified by the addition of high salt washes and dextran-PEG phase partitioning [106]. For such a simple prokaryotic organism, three hundred IMPs represent a substantial fraction of its membrane proteome.

Recently, sequential digestion of yeast membrane fractions with trypsin-chymotrypsin in tandem was shown to be inferior compared to trypsin alone [70]. While Dormeyer et al. confirmed the suitability of the chymotrypsin-trypsin combination for mammalian IMPs, they also reported that in comparison with sequential Lys-C-trypsin digestion in urea, chymotrypsin with trypsin allowed fewer overall identifications of IMPs [25].

4.1.3. Elastase

Elastase has received only limited attention in proteomics. This semi-specific protease cleaves at the C-terminal side of small neutral amino acids. Rietschel et al. compared the performance of porcine pancreatic elastase with trypsin on methanol-solubilized bacterial membranes. The two enzymes showed only a very limited overlap of identified proteins and a different representation of identified peptides: while trypsin covered over-loop segments of IMPs, elastase allowed the identification of a high number of transmembrane peptides [82]. Elastase's relative specificity was found to be 70% for the peptide bond following five amino acids (I, V, A, T, L, S) and 30% for the rest [82]. In general, the use of a protease with low specificity leads to the generation of short multiply-overlapping peptides of which only a fraction is positively charged. To address this drawback, TMT tags were used to label membrane samples digested by elastase in 60% methanol, allowing increased identifications of hydrophobic neutral and acidic cleavage products of elastase by MALDI-MS. [107].

4.1.4. Pepsin

As a gastric enzyme, pepsin has its highest activity between pH 2–4, and has been shown to preferentially cleave C-terminally to the aromatic and hydrophobic residues Y, F, W and L and to a lesser extent after A and G, its specificity being pH dependent [108–110].

So far, this protease has been employed in only a limited number of studies. Pepsin was used for the analysis of rat liver microsome membranes solubilized with 90% FA and digested with immobilized pepsin after FA dilution. Out of 235 identified proteins, 39% were IMPs [90]. Golizeh et al. compared several strategies for the digestion of microsomal membrane samples, and demonstrated the advantage of sequential pepsin and trypsin digestion in markedly increasing the sequence coverage of IMPs compared to cleavage with trypsin only [45].

4.1.5. Proteinase K

Nonspecific proteinase K (which can digest proteins down to dipeptides) was used by Wu et al. to digest or "shave" the extramembrane domains of IMPs in a protocol named "high pH-proteinase K" (hppK). The use of an alkaline carbonate buffer during agitation enabled the removal of membrane-adhered proteins and promoted the opening of membrane vesicles, enabling digestion at both membranes surfaces. The "shaved-off" soluble extramembrane peptides generated by proteinase K were analyzed by LC-MS, and 454 proteins (representing 28% of 1600 total identifications) were predicted to be IMPs. [21] More importantly, the hppK method was later extended to also include analysis of the hydrophobic transmembrane segments that remain safely protected from the protease activity by the phospholipid bilayer [91]. To make the long transmembrane segments amenable to MS analysis, the authors used chemical cleavage of the peptides with CNBr. This approach introduced a unique method for analysis of the neglected hydrophobic transmembrane segments and will be covered in detail in Section 5.2.

The potential of semi- or nonspecific proteases for the analysis of IMPs, and namely of their hydrophobic segments, may seem obvious. However, it should be kept in mind that non-tryptic non-specific peptides are usually more difficult to identify than tryptic peptides. This can be attributed to their poorer ionization and fragmentation and to the fact the lack of defined termini markedly increases database search space, as more possible peptides fall within the precursor mass tolerance and increase the false positive rates [111]. The handful of endoproteases reviewed here and summarized in Table 2 represents only a minor fraction of the proteolytic enzymes currently available for protein digestion in proteomics. More information on the current protease repertoire can be found in a recent review by Tsiatsiani et al. [100].

4.1.6. Chemical cleavage with cyanogen bromide

In addition to the rich protease palette, non-enzymatic protein cleavage further diversifies our proteomic toolbox, as exemplified by cyanogen bromide. In acidic environments (originally 0.1 N HCl [112], but more efficiently in 70% trifluoroacetic acid [113] or formic acid [114]) CNBr selectively reacts with methionine residues and yields peptidyl homoserine or homoserine lactone and an aminoacyl peptide fragment. Reduced cysteine residues may also be subject to cleavage under these conditions, although this reaction is very slow and can be avoided by cysteine alkylation [112]. Compared to any endoprotease, CNBr treatment is very robust, with yields reaching 90–100% cleaved methionine sites. The exceptions are oxidized methionines, which remain uncleaved [115], and methionines followed by serine or threonine residues, where the cleavage efficiency is reduced [116].

CNBr has been proposed as an optimal complementary tool for the MS analysis of hydrophobic IMPs, because of its specificity for the methionine C-terminal peptide bond and the fact that methionine occurs at relatively convenient intervals, mainly in TM helices [97]. Results of an in silico proteomic analysis of the yeast membrane proteome suggested a combination of CNBr and trypsin as one of the methods of choice, as it lowers the occurrence of large (>4 kDa) peptides compared to trypsin used alone, and leads to one of the highest sequence coverages in the given 0.6–4 kDa window for the yeast membrane proteome of all tested combinations of proteolytic agents [105]. As can be demonstrated by a model IMP – ferroportin – methionines are present in 5 of its 10 transmembrane segments, and the theoretical application of CNBr would generate shorter peptides from the trypsin-generated hydrophobic segments P1–6 (Fig. 1).

Van Montfort et al. demonstrated that following standard in-gel trypsin digestion, in-gel cleavage with CNBr roughly doubled the sequence coverage of hydrophobic transmembrane segments, while the coverage of non-membrane segments of IMPs did not change [117, 118]. Similar results were also reported for CNBr-only or a sequential CNBr/trypsin in-gel digestion of bacteriorhodopsin compared to trypsin alone [42]. A sequential CNBr–Lys-C–trypsin digestion was employed by Washburn et al. on a yeast crude membrane fraction [119], and CNBr–trypsin sequential digestion was applied to *C. glutamicum* membranes by Fischer et al. [24], In both studies, the inclusion of CNBr led to the identification of satisfactory numbers of IMPs (with regard to the MS instrumentation then available).

CNBr requires an acidic environment for specific protein digestion [120]. The use of formic or acetic acid as solvents at high temperature enables the simultaneous cleavage with CNBr and acid hydrolysis of the protein, which preferentially leads to cleavage on both the N- and C-termini of Asp residues. This dual chemical cleavage was employed by Lee et al. in an analysis of a rat kidney membrane fraction. Dual digestion increased the number of identified membrane proteins compared to CNBr or acid cleavage alone. A combination of dual cleavage and subsequent re-digestion with trypsin further increased the number of identified membrane proteins [114]. However, the presence of acetic or formic acid at increased temperature may cause extensive protein acetylation or formylation, respectively.

The great potential of CNBr is partly counterbalanced by its toxicity, which must always be considered though not exaggerated. Since only minor amounts (typically <10 mg) are used for a typical cleavage reaction, working in a fume hood and properly disposing the toxic waste (including precipitated vapors from sample evaporation) should be sufficient to ensure safe work.

Despite the large potential for IMP analysis due to its specificity, compatibility with organic acids and the relative high occurrence of methionine in hydrophobic transmembrane segments, CNBr has been rather neglected. More recently, however, CNBr in combination with proteinase K [91] or trypsin [121] has paved the way toward more comprehensive analyses of integral membrane proteins including their transmembrane segments, as will be discussed in Section 5.2.

5. "Divide and Conquer" strategies

5.1. Hydrophilic extramembrane segments

The difficult-to-overcome obstacles of membrane proteomics mentioned above, arising namely from the amphipathic nature of IMPs, have led inevitably to the development of "divide and conquer" strategies that aim separately or exclusively at either hydrophilic (extramembrane) or hydrophobic (transmembrane) segments. The hydrophilic extra-membrane segments of IMPs provide the easier target. Here, membrane proteomics intersects with glycoproteomics.

5.1.1. Cell-surface-capture (CSC)

Exposed extracellular segments of plasma membrane (glyco)proteins are attractive targets for labeling and affinity capture. Using biotin (or other) labels with different protein-reactive groups, different peptide moieties can be targeted. Using primary amine-reactive labels such as sulfo-NHS-SS-biotin (containing a disulfide bridge for simple reductive elution) and sulfo-NHS-LC-biotin (containing a long chain linker), the N-termini and primary amine groups of accessible lysines are

labeled [122]. More importantly, periodate-oxidated sugar moieties of surface glycoproteins can be labeled using hydrazide chemistry [123, 124]. After solubilization and digestion, biotinylated (glyco)peptides from hydrophilic segments of exposed molecules can be affinity-isolated using streptavidin-coated beads. Isolated glyco-peptides can then be eluted using peptide-N-glycosidase F (PNGase F) and subjected to MS/MS analysis.

The initial use of sulfo-NHS-SS-biotin [125] and sulfo-NHS-LC-biotin [126] in analyses of cell surface proteins led to only moderate numbers of identifications and relatively low IMP enrichment. Wollscheid et al. enhanced the protocol for glycopeptide capture and established the use of these labels, namely biocytin hydrazide in an optimized procedure termed Cell Surface Capture (CSC) [127]. This method has been applied to the analysis of the plasma membrane proteome in cell cultures or primary cells to study various biological processes such as T-cell activation [127], the cell surface response to the induction of selected signaling pathways [128], and the response to retinoic acid stimulation in human leukemia cells [129], as well as to characterize induced pluripotent stem cells [130], study the druggability of glioblastoma cells [131], the physiology of primary adipocytes [132], surfaceome changes during the development of neural cells [133,134] and others. Some of these studies used the CSC method in a quantitative arrangement combined with SILAC [127], or label-free analysis [128, 129,131–134].

Besides the biomedical reach of these works, from the technical perspective of membrane proteomics, this method has allowed an unprecedented enrichment of predicted IMPs reaching up to 90% [130] and up to 600 identified proteins with predicted transmembrane segments. The success of this method and the extensive number of plasma membrane proteome publications has given rise to a new term: surfaceomics or surfomics. The recently assembled "Cell Surface Protein Atlas" is a database of the surfaceomes of over seventy human and mouse cell types, containing 1500 human and 1300 mouse surface glycoproteins [135]. Despite the unprecedented IMP enrichment and high numbers of plasma membrane proteins identified, one should be aware of two limitations of the CSC method: it requires live cells, and preferentially targets the N-glycoproteins of the plasma membrane. One less obvious drawback may be the laboriousness of the method, which may explain the relatively limited number of laboratories currently adopting this promising technique.

5.1.2. SPEG

The requirement for live cells in the CSC protocol arises from the imperative for amine-reactive labels, where prevention of their penetration into the cell is essential [129]. In the more common cell surface (glyco)capture, the labeling of live cells enables a high enrichment of IMPs. However, glycosylation-targeted labeling is more or less specific for membrane and secreted proteins (soluble cytosolic proteins are only very rarely glycosylated) and can be modified for fresh or frozen tissues, as recently demonstrated by Liu et al. [136]. Solid Phase Extraction of formerly N-glycosylated Glycoproteins method (SPEG) uses the conjugation of oxidized sugars to hydrazide-coated beads [137,138] and has been used to identify glycoproteins associated with tumor aggressiveness in prostate cancer samples [136,139,140]. After extensive washing, glycopeptides were eluted from the hydrazide beads with PNGase F and subjected to SWATH-MS. This led to the identification of almost 900 glycoproteins, with 220 differentially expressed, of which 56% were predicted to be IMPs. [136].

5.1.3. Glyco-FASP

An alternative surface-oriented approach that combines the FASP method with lectin-affinity capture was introduced by Zielinska et al. [59]. Enrichment of glycosylated plasma membrane proteins from a whole cell lysate was achieved by the capture of SDS-solubilized glycoproteins on a lectin layer in an ultrafilter. After on-filter digestion, glycopetides remained captured by the lectin filter and were later released by PNGase. This strategy enabled the identification of 2352 glycoproteins in mouse tissues [59]. In a more recent study, Han et al. combined three FASP-based approaches including glyco-FASP, and identified 2360 IMPs in mouse tissue [141]. Deeb et al. used glyco-FASP in the analysis of human lymphoma cells, resulting in IMP enrichment (70%) and the identification of 925 IMPs [142]. Despite the impressively high numbers of identified IMPs, both N-glyco-FASP and SPEG have an identical limitation, namely exclusively targeting N-glycosylated peptides. Such peptides can be found not only in IMPs but also in secreted and potentially other non-membrane proteins. Other peptides and proteins are omitted by these methods, limiting complete descriptions of membrane proteomes.

5.2. Hydrophobic transmembrane segments

The attractivity of the accessible cell surface, advantageous specificity of glycosylation for membrane proteins and friendly nature of soluble domains are obvious. However, a significant portion of each IMP (in some cases most of the molecule) remains hidden deep in the phospholipid bilayer, inaccessible to most conventional methods and resistant to trypsin digestion. How can we effectively tap the treasure trove of information hidden in the phospholipid bilayer?

5.2.1. hppK-CNBr

A pioneering step in the analysis of the overlooked hydrophobic membrane-embedded segments of IMPs was taken by Blackler et al. [91], taking advantage of the important observation that the phospholipid bilayer effectively protects the transmembrane segments of IMPs from enzymatic proteolysis. In their hppK-CNBr (high pH, proteinase K) method, isolated membrane vesicles were "opened" by a sodium carbonate wash at high pH and low temperature, and treated with nonspecific proteinase K. The use of an alkaline carbonate buffer during agitation enabled the removal of membrane-adhered proteins and promoted the opening of membrane vesicles [20], enabling digestion at both membrane surfaces along with the unprotected extramembrane segments of IMPs [21]. The protease-treated lipid bilayer with the embedded protease-protected hydrophobic peptides was then further processed. As the membrane-embedded segments of IMPs are rather large and highly hydrophobic for optimal LC-MS analysis, they had to be re-digested. Shaved membranes were therefore solubilized in concentrated formic acid, and effectively re-digested with CNBr (which cleaves at methionine, see Section 4.1.6). The CNBr-cleaved samples were then delipidated by lipid precipitation in a diluted organic solvent and analyzed by LC-MS. Using this method, they identified 670 proteins in human HeLa cells. Of the 670 proteins 479 (72%) were IMPs. Importantly, two thirds of the identified IMPs were identified by peptides that overlapped with predicted transmembrane segments.

The pioneering hppK-CNBr method is not limited to plasma membrane proteins and can also be applied to frozen samples or tissue biopsies. Despite its high enrichment and the obvious potential for tapping the valuable information hidden in the phospholipid bilayer, the strategy has not attracted many followers. This is possibly because of the laborious multi-step workflow and application of less common cleavage strategies (non-specific proteinase K and CNBr), and potentially also the safety issues when working with toxic CNBr. Recently, our group has followed the original hppK-CNBr philosophy and introduced several modifications to the method, and applied it to the analysis of human lymphoma cells (see below).

5.2.2. hpTC

The use of non-specific proteinase K in the original hppK-CNBr protocol enables the efficient shaving of extramembrane protein material from both sides of membrane vesicles. However, the low specificity of proteinase K produces numerous overlapping peptides, leading to increased sample complexity and potentially decreasing the number of identified proteins. Moreover, the use of proteinase K precludes

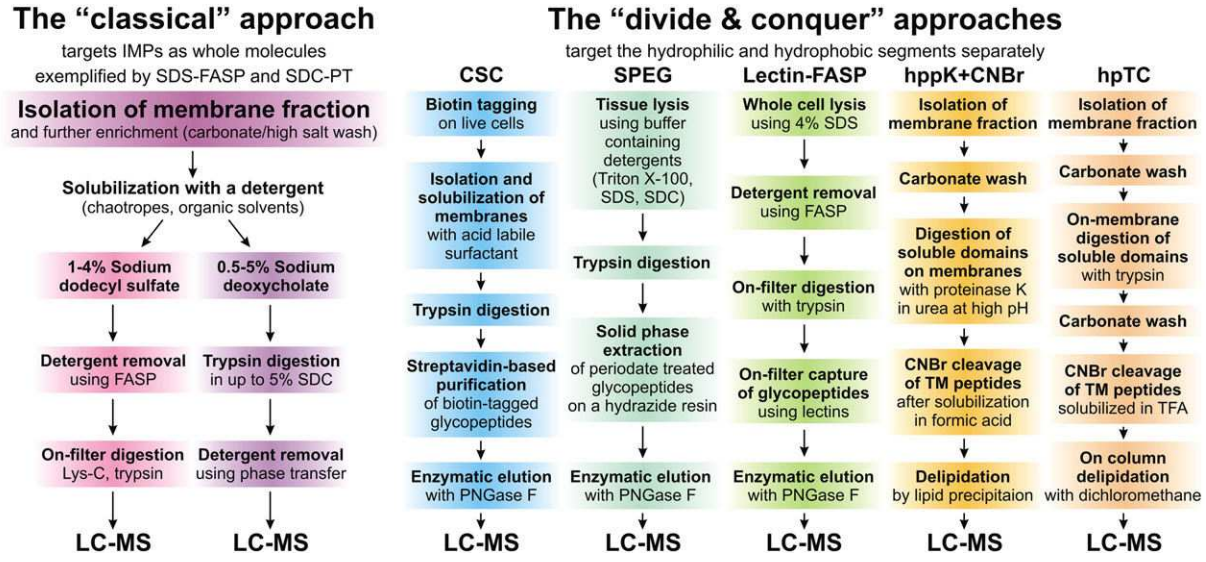

Fig. 2. The most successful strategies for proteomic analysis of IMPs. Two basic strategies in membrane proteomics can be defined. Membrane proteins are targeted either as whole molecules, or the "divide and conquer" approach can be used, aiming separately or exclusively at their hydrophilic (extramembrane) or hydrophobic (transmembrane) segments. The "classical" approach (left) is represented here by two most successful protocols, SDS-FASP and SDC–phase transfer removal (PTC). The "divide and conquer" approaches (right) target either hydrophilic domains of IMPs, as in the cases of CSC, SPEG and Lectin-FASP or hydrophobic transmembrane segments in the cases of hppK + CNBr and hpTC.

quantitative analysis using SILAC and potentially complicates label-free quantitation. Our group has modified the original method [121], in particular excluding an unnecessary ultracentrifugation step, replacing proteinase K with trypsin, and employing on-column sample delipidation with dichloromethane (a method originally devised for detergent removal [143]) instead of lipid precipitation in the aqueous-organic solvent used by Blackler et al. [91]. In reference to the original hppK method, we use the abbreviation hpTC (high pH, trypsin, CNBr).

This altered strategy enabled us to identify 1224 proteins in human lymphoma cells, including 802 (65.5%) IMPs with 1 to 16 transmembrane domains. Roughly half of the unique peptides belonging to IMPs overlapped with predicted transmembrane segments. Among the proteins identified were thirteen so-called "missing proteins", i.e. proteins with no previous evidence at the protein level. The introduction of trypsin instead of proteinase K eliminates the production of multiple overlapping peptides and increases the method's sensitivity and, most importantly, opens a new way toward combining this method with SILAC or label-free quantitation.

6. Conclusions

Aside from the rapid development of MS instrumentation, several methodical innovations and novel strategies have enabled marked progress in deciphering the membrane proteome over the last decade. In particular, the introduction of the FASP method for detergent removal, the establishment of SDC and its removal, and the application of Lys-C in the pre-digestion step are the most important methodical improvements, which have markedly increased the numbers of identified IMPs using the "classical strategy" that targets IMPs as whole molecules. The novel "divide and conquer" strategies oriented toward soluble glycosylated peptides (CSC, SPEG and glycol-FASP) or targeting hydrophobic segments using CNBr (hppK-CNBr and hpTC) have also significantly improved our knowledge of the membrane proteome. The most successful approaches in the current membrane proteome analyses addressed here are briefly summarized in Fig. 2. However, none of these workflows has the potential to completely decipher the membrane proteome in its vast complexity. Despite the high numbers of identified proteins, the classical trypsin-based strategies will inevitably neglect proteins that offer an insufficient number of (reasonably short and soluble) tryptic peptides. Similarly, glycopeptide-oriented analyses provide only a limited glyco-centric view of the membrane proteome, omitting non-glycosylated proteins. The analyses targeting the hydrophobic transmembrane alpha-helices also provide only an incomplete view of the membrane realm. However, the information provided by these three main approaches are complementary, and the combined forces of all three will probably be needed to obtain more comprehensive insights into the black box of the membrane proteome. For instance, a combination of glyco-capture with complementary analysis of the hydrophobic segments in one biological sample can be envisioned. If combined with SILAC labeling, such a combined analysis should provide a thorough and more complete snapshot. If further complemented by a classical detergent-(Lys-C)-trypsin strategy, such a "3-D" analysis would certainly provide unprecedented coverage of the membrane proteome.

Transparency document

The Transparency document associated with this article can be found in online version.

Acknowledgement

This review was supported by the Ministry of Health of the Czech Republic (www.mzcr.cz) via grant 15-32961A, by the Czech Science Foundation (www.gacr.cz) via grant 15-14200S, by ERDF via grant CZ.1.05/1.1.00/02.0109 BIOCEV and by the Ministry of Education, Youth and Sports of the Czech Republic (www.msmt.cz) via PRVOUK P24/LF1/3 and SVV 260 265/2016. The authors would like to thank Petr Man and Alan Kadek for their valuable comments. Special thanks to Mrtva Ryba.

References

[1] L. Fagerberg, K. Jonasson, G. von Heijne, M. Uhlén, L. Berglund, Prediction of the human membrane proteome, Proteomics 10 (2010) 1141–1149.
[2] N. Nagaraj, J.R. Wisniewski, T. Geiger, J. Cox, M. Kircher, J. Kelso, S. Pääbo, M. Mann, Deep proteome and transcriptome mapping of a human cancer cell line, Mol. Syst. Biol. 7 (2011) 548.
[3] M.A. Yildirim, K.I. Goh, M.E. Cusick, A.L. Barabási, M. Vidal, Drug-target network, Nat. Biotechnol. 25 (2007) 1119–1126.
[4] D. Vuckovic, L.F. Dagley, A.W. Purcell, A. Emili, Membrane proteomics by high performance liquid chromatography-tandem mass spectrometry: analytical approaches and challenges, Proteomics 13 (2013) 404–423.

[5] F. Zhou, Y. Lu, S.B. Ficarro, G. Adelmant, W. Jiang, C.J. Luckey, J.A. Marto, Genome-scale proteome quantification by DEEP SEQ mass spectrometry, Nat. Commun. 4 (2013) 2171.
[6] P.W. Hildebrand, R. Preissner, C. Frömmel, Structural features of transmembrane helices, FEBS Lett. 559 (2004) 145–151.
[7] N. Bordag, S. Keller, Alpha-helical transmembrane peptides: a "divide and conquer" approach to membrane proteins, Chem. Phys. Lipids 163 (2010) 1–26.
[8] L.E. Hedin, K. Illergård, A. Elofsson, An introduction to membrane proteins, J. Proteome Res. 10 (2011) 3324–3331.
[9] T. Rabilloud, M. Chevallet, S. Luche, C. Lelong, Fully denaturing two-dimensional electrophoresis of membrane proteins: a critical update, Proteomics 8 (2008) 3965–3973.
[10] T. Rabilloud, Membrane proteins and proteomics: love is possible, but so difficult, Electrophoresis 30 (Suppl 1) (2009) S174–S180.
[11] G. Heijne, The distribution of positively charged residues in bacterial inner membrane proteins correlates with the trans-membrane topology, EMBO J. 5 (1986) 3021–3027.
[12] G.E. Tusnády, I. Simon, Topology prediction of helical transmembrane proteins: how far have we reached? Curr. Protein Pept. Sci. 11 (2010) 550–561.
[13] K.D. Tsirigos, A. Hennerdal, L. Käll, A. Elofsson, A guideline to proteome-wide α-helical membrane protein topology predictions, Proteomics 12 (2012) 2282–2294.
[14] L. Dobson, I. Reményi, G.E. Tusnády, The human transmembrane proteome, Biol. Direct 10 (2015) 31.
[15] K.D. Tsirigos, C. Peters, N. Shu, L. Käll, A. Elofsson, The TOPCONS web server for consensus prediction of membrane protein topology and signal peptides, Nucleic Acids Res. 43 (2015) W401–W407.
[16] L. Dobson, I. Reményi, G.E. Tusnády, CCTOP: a consensus constrained TOPology prediction web server, Nucleic Acids Res. 43 (2015) W408–W412.
[17] A. Krogh, B. Larsson, G. von Heijne, E.L. Sonnhammer, Predicting transmembrane protein topology with a hidden Markov model: application to complete genomes, J. Mol. Biol. 305 (2001) 567–580.
[18] Y.H. Lee, H.T. Tan, M.C. Chung, Subcellular fractionation methods and strategies for proteomics, Proteomics 10 (2010) 3935–3956.
[19] A.M. Rahbar, C. Fenselau, Unbiased examination of changes in plasma membrane proteins in drug resistant cancer cells, J. Proteome Res. 4 (2005) 2148–2153.
[20] Y. Fujiki, A.L. Hubbard, S. Fowler, P.B. Lazarow, Isolation of intracellular membranes by means of sodium carbonate treatment: application to endoplasmic reticulum, J. Cell Biol. 93 (1982) 97–102.
[21] C.C. Wu, M.J. MacCoss, K.E. Howell, J.R. Yates 3rd., A method for the comprehensive proteomic analysis of membrane proteins, Nat. Biotechnol. 21 (2003) 532–538.
[22] Y. Zhao, W. Zhang, Y. Kho, Y. Zhao, Proteomic analysis of integral plasma membrane proteins, Anal. Chem. 76 (2004) 1817–1823.
[23] E.M. Pasini, M. Kirkegaard, P. Mortensen, H.U. Lutz, A.W. Thomas, M. Mann, In-depth analysis of the membrane and cytosolic proteome of red blood cells, Blood 108 (2006) 791–801.
[24] F. Fischer, D. Wolters, M. Rögner, A. Poetsch, Toward the complete membrane proteome: high coverage of integral membrane proteins through transmembrane peptide detection, Mol. Cell. Proteomics 5 (2006) 444–453.
[25] W. Dormeyer, D. van Hoof, C.L. Mummery, J. Krijgsveld, A.J. Heck, A practical guide for the identification of membrane and plasma membrane proteins in human embryonic stem cells and human embryonal carcinoma cells, Proteomics 8 (2008) 4036–4053.
[26] A. Lu, J.R. Wiśniewski, M. Mann, Comparative proteomic profiling of membrane proteins in rat cerebellum, spinal cord, and sciatic nerve, J. Proteome Res. 8 (2009) 2418–2425.
[27] N. Nagaraj, A. Lu, M. Mann, J.R. Wiśniewski, Detergent-based but gel-free method allows identification of several hundred membrane proteins in single LC-MS runs, J. Proteome Res. 7 (2008) 5028–5032.
[28] F.Y. Che, C. Madrid-Aliste, B. Burd, H. Zhang, E. Nieves, K. Kim, A. Fiser, R.H. Angeletti, L.M. Weiss, Comprehensive proteomic analysis of membrane proteins in *Toxoplasma gondii*, Mol. Cell. Proteomics 10 (2011) (M110.000745).
[29] D. Ghosh, D. Lippert, O. Krokhin, J.P. Cortens, J.A. Wilkins, Defining the membrane proteome of NK cells, J. Mass Spectrom. 45 (2010) 1–25.
[30] J.R. Wiśniewski, A. Zougman, M. Mann, Combination of FASP and StageTip-based fractionation allows in-depth analysis of the hippocampal membrane proteome, J. Proteome Res. 8 (2009) 5674–5678.
[31] R.A. Mathias, Y.S. Chen, E.A. Kapp, D.W. Greening, S. Mathivanan, R.J. Simpson, Triton X-114 phase separation in the isolation and purification of mouse liver microsomal membrane proteins, Methods 54 (2011) 396–406.
[32] L. Cao, J.G. Clifton, W. Reutter, D. Josic, Mass spectrometry-based analysis of rat liver and hepatocellular carcinoma Morris hepatoma 7777 plasma membrane proteome, Anal. Chem. 85 (2013) 8112–8120.
[33] J.V. Olsen, J.R. Andersen, P.A. Nielsen, M.L. Nielsen, D. Figeys, M. Mann, J.R. Wisniewski, HysTag-a novel proteomic quantification tool applied to differential display analysis of membrane proteins from distinct areas of mouse brain, Mol. Cell. Proteomics 3 (2004) 82–92.
[34] P.A. Nielsen, J.V. Olsen, A.V. Podtelejnikov, J.R. Andersen, M. Mann, J.R. Wisniewski, Proteomic mapping of brain plasma membrane proteins, Mol. Cell. Proteomics 4 (2005) 402–408.
[35] R. Lund, R. Leth-Larsen, O.N. Jensen, H.J. Ditzel, Efficient isolation and quantitative proteomic analysis of cancer cell plasma membrane proteins for identification of metastasis-associated cell surface markers, J. Proteome Res. 8 (2009) 3078–3090.
[36] J.A. Reynolds, C. Tanford, Binding of dodecyl sulfate to proteins at high binding ratios. Possible implications for the state of proteins in biological membranes, Proc. Natl. Acad. Sci. U. S. A. 66 (1970) 1002–1007.
[37] A. Bosserhoff, J. Wallach, R.W. Frank, Micropreparative separation of peptides derived from sodium dodecyl sulphate-solubilized proteins, J. Chromatogr. 473 (1989) 71–77.
[38] R.R. Loo, N. Dales, P.C. Andrews, The effect of detergents on proteins analyzed by electrospray ionization, Methods Mol. Biol. 61 (1996) 141–160.
[39] J. Funk, X. Li, T. Franz, Threshold values for detergents in protein and peptide samples for mass spectrometry, Rapid Commun. Mass Spectrom. 19 (2005) 2986–2988.
[40] N. Zhang, R. Chen, N. Young, D. Wishart, P. Winter, J.H. Weiner, L. Li, Comparison of SDS- and methanol-assisted protein solubilization and digestion methods for *Escherichia coli* membrane proteome analysis by 2-D LC-MS/MS, Proteomics 7 (2007) 484–493.
[41] D. Botelho, M.J. Wall, D.B. Vieira, S. Fitzsimmons, F. Liu, A. Doucette, Top–down and bottom-up proteomics of SDS-containing solutions following mass-based separation, J. Proteome Res. 9 (2010) 2863–2870.
[42] H. Zischka, C.J. Gloeckner, C. Klein, S. Willmann, M. Swiatek-de Lange, M. Ueffing, Improved mass spectrometric identification of gel-separated hydrophobic membrane proteins after sodium dodecyl sulfate removal by ion-pair extraction, Proteomics 4 (2004) 3776–3782.
[43] J.Y. Zhou, G.P. Dann, T. Shi, L. Wang, X. Gao, D. Su, C.D. Nicora, A.K. Shukla, R.J. Moore, T. Liu, D.G. Camp 2nd, R.D. Smith, W.J. Qian, Simple sodium dodecyl sulfate-assisted sample preparation method for LC–MS-based proteomics applications, Anal. Chem. 84 (2012) 2862–2867.
[44] H.D. Cox, C.K. Chao, S.A. Patel, C.M. Thompson, Efficient digestion and mass spectral analysis of vesicular glutamate transporter 1: a recombinant membrane protein expressed in yeast, J. Proteome Res. 7 (2008) 570–578.
[45] M. Golizeh, L. Sleno, Optimized proteomic analysis of rat liver microsomes using dual enzyme digestion with 2D-LC–MS/MS, J. Proteome 82 (2013) 166–178.
[46] A.A. Doucette, D.B. Vieira, D.J. Orton, M.J. Wall, Resolubilization of precipitated intact membrane proteins with cold formic acid for analysis by mass spectrometry, J. Proteome Res. 13 (2014) 6001–6012.
[47] X. Liang, J. Zhao, M. Hajivandi, R. Wu, J. Tao, J.W. Amshey, R.M. Pope, Quantification of membrane and membrane-bound proteins in normal and malignant breast cancer cells isolated from the same patient with primary breast carcinoma, J. Proteome Res. 5 (2006) 2632–2641.
[48] R. Shi, C. Kumar, A. Zougman, Y. Zhang, A. Podtelejnikov, J. Cox, J.R. Wiśniewski, M. Mann, Analysis of the mouse liver proteome using advanced mass spectrometry, J. Proteome Res. 6 (2007) 2963–2972.
[49] L. Peng, E.A. Kapp, D. McLauchlan, T.W. Jordan, Characterization of the Asia Oceania human proteome organisation membrane proteomics initiative standard using SDS-PAGE shotgun proteomics, Proteomics 11 (2011) 4376–4384.
[50] Kuhlmann K, Tschapek A, Wiese H, Eisenacher M, Meyer HE, Hatt HH, Oeljeklaus S, Warscheid B. The membrane proteome of sensory cilia to the depth of olfactory receptors. Mol. Cell. Proteomics;13:1828–43.
[51] X. Lu, H. Zhu, Tube-gel digestion: a novel proteomic approach for high throughput analysis of membrane proteins, Mol. Cell. Proteomics 4 (2005) 1948–1958.
[52] W. Dormeyer, D. van Hoof, S.R. Braam, A.J. Heck, C.L. Mummery, J. Krijgsveld, Plasma membrane proteomics of human embryonic stem cells and human embryonal carcinoma cells, J. Proteome Res. 7 (2008) 2936–2951.
[53] Y. Liu, G. Yan, M. Gao, C. Deng, X. Zhang, Membrane protein isolation and identification by covalent binding for proteome research, Proteomics 15 (2015) 3892–3900.
[54] F. Wu, D. Sun, N. Wang, Y. Gong, L. Li, Comparison of surfactant-assisted shotgun methods using acid-labile surfactants and sodium dodecyl sulfate for membrane proteome analysis, Anal. Chim. Acta 698 (2011) 36–43.
[55] Sun D, Wang N, Li L. Integrated SDS removal and peptide separation by strong-cation exchange liquid chromatography for SDS-assisted shotgun proteome analysis. J Proteome Res 201;11:818–28.
[56] J.R. Wiśniewski, A. Zougman, N. Nagaraj, M. Mann, Universal sample preparation method for proteome analysis, Nat. Methods 6 (2009) 359–362.
[57] Y. Yu, L. Xie, H.P. Gunawardena, J. Khatun, C. Maier, W. Spitzer, M. Leerkes, M.C. Giddings, X. Chen, GOFAST: an integrated approach for efficient and comprehensive membrane proteome analysis, Anal. Chem. 84 (2012) 9008–9014.
[58] F. Raimondo, S. Corbetta, A. Savoia, C. Chinello, M. Cazzaniga, F. Rocco, S. Bosari, M. Grasso, G. Bovo, F. Magni, M. Pitto, Comparative membrane proteomics: a technical advancement in the search of renal cell carcinoma biomarkers, Mol. BioSyst. 11 (2015) 1708–1716.
[59] D.F. Zielinska, F. Gnad, J.R. Wiśniewski, M. Mann, Precision mapping of an in vivo N-glycoproteome reveals rigid topological and sequence constraints, Cell 141 (2010) 897–907.
[60] A.M. Seddon, P. Curnow, P.J. Booth, Membrane proteins, lipids and detergents: not just a soap opera, Biochim. Biophys. Acta 1666 (2004) 105–117.
[61] T. Masuda, M. Tomita, Y. Ishihama, Phase transfer surfactant-aided trypsin digestion for membrane proteome analysis, J. Proteome Res. 7 (2008) 731–740.
[62] Y. Lin, J. Zhou, D. Bi, P. Chen, X. Wang, S. Liang, Sodium-deoxycholate-assisted tryptic digestion and identification of proteolytically resistant proteins, Anal. Biochem. 377 (2008) 259–266.
[63] S. Muraoka, H. Kume, J. Adachi, T. Shiromizu, S. Watanabe, T. Masuda, Y. Ishihama, T. Tomonaga, In-depth membrane proteomic study of breast cancer tissues for the generation of a chromosome-based protein list, J. Proteome Res. 12 (2013) 208–213.
[64] H. Kume, S. Muraoka, T. Kuga, J. Adachi, R. Narumi, S. Watanabe, M. Kuwano, Y. Kodera, K. Matsushita, J. Fukuoka, T. Masuda, Y. Ishihama, H. Matsubara, F. Nomura, T. Tomonaga, Discovery of colorectal cancer biomarker candidates by membrane proteomic analysis and subsequent verification using selected reaction monitoring (SRM) and tissue microarray (TMA) analysis, Mol. Cell. Proteomics 13 (2014) 1471–1484.
[65] J. Zhou, T. Zhou, R. Cao, Z. Liu, J. Shen, P. Chen, X. Wang, S. Liang, Evaluation of the application of sodium deoxycholate to proteomic analysis of rat hippocampal plasma membrane, J. Proteome Res. 5 (2006) 2547–2553.
[66] Y. Lin, Y. Liu, J. Li, Y. Zhao, Q. He, W. Han, P. Chen, X. Wang, S. Liang, Evaluation and optimization of removal of an acid-insoluble surfactant for shotgun analysis of membrane proteome, Electrophoresis 31 (2010) 2705–2713.
[67] A.J. Nel, S. Garnett, J.M. Blackburn, N.C. Soares, Comparative reevaluation of FASP and enhanced FASP methods by LC–MS/MS, J. Proteome Res. 14 (2015) 1637–1642.

[68] E. Scheerlinck, M. Dhaenens, A. Van Soom, L. Peelman, P. De Sutter, K. Van Steendam, D. Deforce, Minimizing technical variation during sample preparation prior to label-free quantitative mass spectrometry, Anal. Biochem. 490 (2015) 14–19.
[69] I.R. León, V. Schwämmle, O.N. Jensen, R.R. Sprenger, Quantitative assessment of in-solution digestion efficiency identifies optimal protocols for unbiased protein analysis, Mol. Cell. Proteomics 12 (2013) 2992–3005.
[70] S.M. Moore, S.M. Hess, J.W. Jorgenson, Extraction, enrichment, solubilization, and digestion techniques for membrane proteomics, J. Proteome Res. 15 (4) (2016) 1243–1252.
[71] Y.Q. Yu, M. Gilar, P.J. Lee, E.S. Bouvier, J.C. Gebler, Enzyme-friendly, mass spectrometry-compatible surfactant for in-solution enzymatic digestion of proteins, Anal. Chem. 75 (2003) 6023–6028.
[72] R.J. Arnold, P. Hrncirova, K. Annaiah, M.V. Novotny, Fast proteolytic digestion coupled with organelle enrichment for proteomic analysis of rat liver, J. Proteome Res. 3 (2004) 653–657.
[73] E.I. Chen, D. Cociorva, J.L. Norris, J.R. Yates 3rd., Optimization of mass spectrometry-compatible surfactants for shotgun proteomics, J. Proteome Res. 6 (2007) 2529–2538.
[74] F. Mbeunkui, M.B. Goshe, Investigation of solubilization and digestion methods for microsomal membrane proteome analysis using data-independent LC-MSE, Proteomics 11 (2011) 898–911.
[75] J.L. Norris, N.A. Porter, R.M. Caprioli, Mass spectrometry of intracellular and membrane proteins using cleavable detergents, Anal. Chem. 75 (2003) 6642–6647.
[76] M. Waas, S. Bhattacharya, S. Chuppa, X. Wu, D.R. Jensen, U. Omasits, B. Wollscheid, B.F. Volkman, K.R. Noon, R.L. Gundry, Combine and conquer: surfactants, solvents, and chaotropes for robust mass spectrometry based analyses of membrane proteins, Anal. Chem. 86 (2014) 1551–1559.
[77] Y.Q. Yu, M. Gilar, J.C. Gebler, A complete peptide mapping of membrane proteins: a novel surfactant aiding the enzymatic digestion of bacteriorhodopsin, Rapid Commun. Mass Spectrom. 18 (2004) 711–715.
[78] T. Arnold, D. Linke, Phase separation in the isolation and purification of membrane proteins, Biotechniques 43 (2007) 427–440.
[79] M. Orwick-Rydmark, T. Arnold, D. Linke, The use of detergents to purify membrane proteins, Curr. Protoc. Protein Sci. 84 (2016) 4.8.1–4.8.35.
[80] K.G. Welinder, Generation of peptides suitable for sequence analysis by proteolytic cleavage in reversed-phase high-performance liquid chromatography solvents, Anal. Biochem. 174 (1988) 54–64.
[81] J. Blonder, T.P. Conrads, L.R. Yu, A. Terunuma, G.M. Janini, H.J. Issaq, J.C. Vogel, T.D. Veenstra, A detergent- and cyanogen bromide-free method for integral membrane proteomics: application to Halobacterium purple membranes and the human epidermal membrane proteome, Proteomics 4 (2004) 31–45.
[82] B. Rietschel, T.N. Arrey, B. Meyer, S. Bornemann, M. Schuerken, M. Karas, A. Poetsch, Elastase digests: new ammunition for shotgun membrane proteomics, Mol. Cell. Proteomics 8 (2009) 1029–1043.
[83] J. Blonder, M.C. Rodriguez-Galan, K.C. Chan, D.A. Lucas, L.R. Yu, T.P. Conrads, H.J. Issaq, H.A. Young, T.D. Veenstra, Analysis of murine natural killer cell microsomal proteins using two-dimensional liquid chromatography coupled to tandem electrospray ionization mass spectrometry, J. Proteome Res. 3 (2004) 862–870.
[84] J. Blonder, A. Terunuma, T.P. Conrads, K.C. Chan, C. Yee, D.A. Lucas, C.F. Schaefer, L.R. Yu, H.J. Issaq, T.D. Veenstra, J.C. Vogel, A proteomic characterization of the plasma membrane of human epidermis by high-throughput mass spectrometry, J. Invest. Dermatol. 123 (2004) 691–699.
[85] H. Zhang, Q. Lin, S. Ponnusamy, N. Kothandaraman, T.K. Lim, C. Zhao, H.S. Kit, B. Arijit, M. Rauff, C.L. Hew, M.C. Chung, S.B. Joshi, M. Choolani, Differential recovery of membrane proteins after extraction by aqueous methanol and trifluoroethanol, Proteomics 7 (2007) 1654–1663.
[86] G. Shevchenko, S. Musunuri, M. Wetterhall, J. Bergquist, Comparison of extraction methods for the comprehensive analysis of mouse brain proteome using shotgun-based mass spectrometry, J. Proteome Res. 11 (2012) 2441–2451.
[87] D. Piszkiewicz, M. Landon, E.L. Smith, Anomalous cleavage of aspartyl-proline peptide bonds during amino acid sequence determinations, Biochem. Biophys. Res. Commun. 40 (1970) 1173–1178.
[88] R.R. Loo, J.A. Loo, Matrix-assisted laser desorption/ionization-mass spectrometry of hydrophobic proteins in mixtures using formic acid, perfluorooctanoic acid, and sorbitol, Anal. Chem. 79 (2007) 1115–1125.
[89] Q. Zhao, Y. Liang, H. Yuan, Z. Sui, Q. Wu, Z. Liang, L. Zhang, Y. Zhang, Biphasic microreactor for efficient membrane protein pretreatment with a combination of formic acid assisted solubilization, on-column pH adjustment, reduction, alkylation, and tryptic digestion, Anal. Chem. 85 (2013) 8507–8512.
[90] J. Ma, C. Hou, L. Sun, D. Tao, Y. Zhang, Y. Shan, Z. Liang, L. Zhang, L. Yang, Y. Zhang, Coupling formic acid assisted solubilization and online immobilized pepsin digestion with strong cation exchange and microflow reversed-phase liquid chromatography with electrospray ionization tandem mass spectrometry for integral membrane proteome analysis, Anal. Chem. 82 (2010) 9622–9625.
[91] A.R. Blackler, A.E. Speers, M.S. Ladinsky, C.C. Wu, A shotgun proteomic method for the identification of membrane-embedded proteins and peptides, J. Proteome Res. 7 (2008) 3028–3034.
[92] J. Wei, J. Sun, W. Yu, A. Jones, P. Oeller, M. Keller, G. Woodnutt, J.M. Short, Global proteome discovery using an online three-dimensional LC–MS/MS, J. Proteome Res. 4 (2005) 801–808.
[93] A.E. Speers, C.C. Wu, Proteomics of integral membrane proteins - theory and application, Chem. Rev. 107 (2007) 3687–3714.
[94] J.W. Poulsen, C.T. Madsen, C. Young, F.M. Poulsen, M.L. Nielsen, Using guanidine-hydrochloride for fast and efficient protein digestion and single-step affinity-purification mass spectrometry, J. Proteome Res. 12 (2013) 1020–1030.
[95] M.B. Ulmschneider, M.S. Sansom, A. Di Nola, Properties of integral membrane protein structures: derivation of an implicit membrane potential, Proteins 59 (2005) 252–265.
[96] M. Molinari, N-Glycan structure dictates extension of protein folding or onset of disposal, Nat. Chem. Biol. 3 (2007) 313–320.
[97] L.A. Eichacker, B. Granvogl, O. Mirus, B.C. Müller, C. Miess, E. Schleiff, Hiding behind hydrophobicity. Transmembrane segments in mass spectrometry, J. Biol. Chem. 279 (2004) 50915–50922.
[98] H.J. Sharpe, T.J. Stevens, S. Munro, A comprehensive comparison of transmembrane domains reveals organelle-specific properties, Cell 142 (2010) 158–169.
[99] J. Kyte, R.F. Doolittle, A simple method for displaying the hydropathic character of a protein, J. Mol. Biol. 157 (1) (1982 May 5) 105–132.
[100] L. Tsiatsiani, A.J. Heck, Proteomics beyond trypsin, FEBS J 282 (2015) 2612–2626.
[101] T. Le Bihan, T. Goh, I.I. Stewart, A.M. Salter, Y.V. Bukhman, M. Dharsee, R. Ewing, J.R. Wiśniewski, Differential analysis of membrane proteins in mouse fore- and hind-brain using a label-free approach, J. Proteome Res. 5 (2006) 2701–2710.
[102] J.V. Olsen, P.A. Nielsen, J.R. Andersen, M. Mann, J.R. Wiśniewski, Quantitative proteomic profiling of membrane proteins from the mouse brain cortex, hippocampus, and cerebellum using the HysTag reagent: mapping of neurotransmitter receptors and ion channels, Brain Res. 1134 (2007) 95–106.
[103] J.R. Wiśniewski, M. Mann, Consecutive proteolytic digestion in an enzyme reactor increases depth of proteomic and phosphoproteomic analysis, Anal. Chem. 84 (2012) 2631–2637.
[104] A. Görg, W. Weiss, M.J. Dunn, Current two-dimensional electrophoresis technology for proteomics, Proteomics 4 (2004) 3665–3685.
[105] F. Fischer, A. Poetsch, Protein cleavage strategies for an improved analysis of the membrane proteome, Proteome Sci. 4 (2006) 2.
[106] B. Fränzel, F. Fischer, C. Trötschel, A. Poetsch, D. Wolters, The two-phase partitioning system–a powerful technique to purify integral membrane proteins of Corynebacterium glutamicum for quantitative shotgun analysis, Proteomics 9 (2009) 2263–2272.
[107] D. Baeumlisberger, T.N. Arrey, B. Rietschel, M. Rohmer, D.G. Papasotiriou, B. Mueller, T. Beckhaus, M. Karas, Labeling elastase digests with TMT: informational gain by identification of poorly detectable peptides with MALDI-TOF/TOF mass spectrometry, Proteomics 10 (2010) 3905–3909.
[108] J. Han, K.L. Schey, Proteolysis and mass spectrometric analysis of an integral membrane: aquaporin 0, J. Proteome Res. 3 (2004) 807–812.
[109] B. Rietschel, S. Bornemann, T.N. Arrey, D. Baeumlisberger, M. Karas, B. Meyer, Membrane protein analysis using an improved peptic in-solution digestion protocol, Proteomics 9 (2009) 5553–5557.
[110] D. López-Ferrer, K. Petritis, E.W. Robinson, K.K. Hixson, Z. Tian, J.H. Lee, S.W. Lee, N. Tolić, K.K. Weitz, M.E. Belov, R.D. Smith, L. Pasa-Tolić, Pressurized pepsin digestion in proteomics: an automatable alternative to trypsin for integrated top-down bottom-up proteomics, Mol. Cell. Proteomics 10 (2011) (M110.001479).
[111] N. Gupta, N. Bandeira, U. Keich, P.A. Pevzner, Target-decoy approach and false discovery rate: when things may go wrong, J. Am. Soc. Mass Spectrom. 22 (2011) 1111–1120.
[112] E. Gross, B. Witkop, Nonenzymatic cleavage of peptide bonds: the methionine residues in bovine pancreatic ribonuclease, J. Biol. Chem. 237 (1962) 1856–1860.
[113] J.P. Bargetzi, E.O. Thompson, K.S. Sampathkumar, K.A. Walsh, H. Neurath, The amino- and carboxyl-terminal residues and the self-digestion of bovine pancreatic carboxypeptidase A, J. Biol. Chem. 239 (1964) 3767–3774.
[114] J.E. Lee, J. Kwon, M.C. Baek, A combination method of chemical with enzyme reactions for identification of membrane proteins, Biochim. Biophys. Acta 1814 (3) (2011 Mar) 397–404.
[115] E. Gross, The cyanogen bromide reaction, in: H. CHW (Ed.), Methods in Enzymology, Vol. 11: Enzyme Structure, Academic Press 1967, pp. 238–255.
[116] R. Kaiser, L. Metzka, Enhancement of cyanogen bromide cleavage yields for methionyl–serine and methionyl–threonine peptide bonds, Anal. Biochem. 266 (1999) 1–8.
[117] B.A. van Montfort, B. Canas, R. Duurkens, J. Godovac-Zimmermann, G.T. Robillard, Improved in-gel approaches to generate peptide maps of integral membrane proteins with matrix-assisted laser desorption/ionization time-of-flight mass spectrometry, J. Mass Spectrom. 37 (2002) 322–330.
[118] B.A. van Montfort, M.K. Doeven, B. Canas, L.M. Veenhoff, B. Poolman, G.T. Robillard, Combined in-gel tryptic digestion and CNBr cleavage for the generation of peptide maps of an integral membrane protein with MALDI-TOF mass spectrometry, Biochim. Biophys. Acta 1555 (2002) 111–115.
[119] M.P. Washburn, D. Wolters, J.R. Yates 3rd., Large-scale analysis of the yeast proteome by multidimensional protein identification technology, Nat. Biotechnol. 19 (2001) 242–247.
[120] W.A. Schroeder, J.B. Shelton, J.R. Shelton, An examination of conditions for the cleavage of polypeptide chains with cyanogen bromide: application to catalase, Arch. Biochem. Biophys. 130 (1969) 551–556.
[121] O. Vit, P. Man, A. Kadek, J. Hausner, J. Sklenar, K. Harant, P. Novak, M. Scigelova, G. Woffendin, J. Petrak, Large-scale identification of membrane proteins based on analysis of trypsin-protected transmembrane segments, J. Proteome (2016), http://dx.doi.org/10.1016/j.jprot.2016.03.016 in press.
[122] G. Elia, Biotinylation reagents for the study of cell surface proteins, Proteomics 8 (2008) 4012–4024.
[123] C.G. Gahmberg, L.C. Andersson, Selective radioactive labeling of cell surface sialoglycoproteins by periodate-tritiated borohydride, J. Biol. Chem. 252 (1977) 5888–5894.
[124] E.A. Bayer, H. Ben-Hur, M. Wilchek, Biocytin hydrazide-a selective label for sialic acids, galactose, and other sugars in glycoconjugates using avidin-biotin technology, Anal. Biochem. 170 (1988) 271–281.
[125] Y. Zhao, W. Zhang, M.A. White, Y. Zhao, Capillary high-performance liquid chromatography/mass spectrometric analysis of proteins from affinity-purified plasma membrane, Anal. Chem. 75 (2003) 3751–3757.
[126] H. Qiu, Y. Wang, Quantitative analysis of surface plasma membrane proteins of primary and metastatic melanoma cells, J. Proteome Res. 7 (2008) 1904–1915.
[127] B. Wollscheid, D. Bausch-Fluck, C. Henderson, R. O'Brien, M. Bibel, R. Schiess, R. Aebersold, J.D. Watts, Mass-spectrometric identification and relative quantification of N-linked cell surface glycoproteins, Nat. Biotechnol. 27 (2009) 378–386.

[128] R. Schiess, L.N. Mueller, A. Schmidt, M. Mueller, B. Wollscheid, R. Aebersold, Analysis of cell surface proteome changes via label-free, quantitative mass spectrometry, Mol. Cell. Proteomics 8 (2009) 624–638.
[129] A. Hofmann, B. Gerrits, A. Schmidt, T. Bock, D. Bausch-Fluck, R. Aebersold, B. Wollscheid, Proteomic cell surface phenotyping of differentiating acute myeloid leukemia cells, Blood 116 (2010) e26–e34.
[130] R.L. Gundry, D.R. Riordon, Y. Tarasova, S. Chuppa, S. Bhattacharya, O. Juhasz, O. Wiedemeier, S. Milanovich, F.K. Noto, I. Tchernyshyov, K. Raginski, D. Bausch-Fluck, H.J. Tae, S. Marshall, S.A. Duncan, B. Wollscheid, R.P. Wersto, S. Rao, J.E. Van Eyk, K.R. Boheler, A cell surfaceome map for immunophenotyping and sorting pluripotent stem cells, Mol. Cell. Proteomics 11 (2012) 303–316.
[131] T. Bock, H. Moest, U. Omasits, S. Dolski, E. Lundberg, A. Frei, A. Hofmann, D. Bausch-Fluck, A. Jacobs, N. Krayenbuehl, M. Uhlen, R. Aebersold, K. Frei, B. Wollscheid, Proteomic analysis reveals drug accessible cell surface N-glycoproteins of primary and established glioblastoma cell lines, J. Proteome Res. 11 (2012) 4885–4893.
[132] H. Moest, A.P. Frei, I. Bhattacharya, M. Geiger, B. Wollscheid, C. Wolfrum, Malfunctioning of adipocytes in obesity is linked to quantitative surfaceome changes, Biochim. Biophys. Acta 1831 (2013) 1208–1216.
[133] B. DeVeale, D. Bausch-Fluck, R. Seaberg, S. Runciman, V. Akbarian, P. Karpowicz, C. Yoon, H. Song, R. Leeder, P.W. Zandstra, B. Wollscheid, D. van der Kooy, Surfaceome profiling reveals regulators of neural stem cell function, Stem Cells 32 (2014) 258–268.
[134] J. Tyleckova, I. Valekova, M. Zizkova, M. Rakocyova, S. Marsala, M. Marsala, S.J. Gadher, H. Kovarova, Surface N-glycoproteome patterns reveal key proteins of neuronal differentiation, J. Proteome 132 (2016) 13–20.
[135] D. Bausch-Fluck, A. Hofmann, T. Bock, A.P. Frei, F. Cerciello, A. Jacobs, H. Moest, U. Omasits, R.L. Gundry, C. Yoon, R. Schiess, A. Schmidt, P. Mirkowska, A. Härtlová, J.E. Van Eyk, J.P. Bourquin, R. Aebersold, K.R. Boheler, P. Zandstra, B. Wollscheid, A mass spectrometric-derived cell surface protein atlas, PLoS One 10 (2015), e0121314.
[136] Y. Liu, J. Chen, A. Sethi, Q.K. Li, L. Chen, B. Collins, L.C. Gillet, B. Wollscheid, H. Zhang, R. Aebersold, Glycoproteomic analysis of prostate cancer tissues by SWATH mass spectrometry discovers N-acylethanolamine acid amidase and protein tyrosine kinase 7 as signatures for tumor aggressiveness, Mol. Cell. Proteomics 13 (2014) 1753–1768.
[137] H. Zhang, X.J. Li, D.B. Martin, R. Aebersold, Identification and quantification of N-linked glycoproteins using hydrazide chemistry, stable isotope labeling and mass spectrometry, Nat. Biotechnol. 21 (2003) 660–666.
[138] Y. Tian, Y. Zhou, S. Elliott, R. Aebersold, H. Zhang, Solid-phase extraction of N-linked glycopeptides, Nat. Protoc. 2 (2007) 334–339.
[139] Y. Tian, G.S. Bova, H. Zhang, Quantitative glycoproteomic analysis of optimal cutting temperature-embedded frozen tissues identifying glycoproteins associated with aggressive prostate cancer, Anal. Chem. 83 (2011) 7013–7019.
[140] J. Chen, J. Xi, Y. Tian, G.S. Bova, H. Zhang, Identification, prioritization, and evaluation of glycoproteins for aggressive prostate cancer using quantitative glycoproteomics and antibody-based assays on tissue specimens, Proteomics 13 (2013) 2268–2277.
[141] D. Han, S. Moon, Y. Kim, H. Min, Y. Kim, Characterization of the membrane proteome and N-glycoproteome in BV-2 mouse microglia by liquid chromatography-tandem mass spectrometry, BMC Genomics 15 (2014) 95.
[142] S.J. Deeb, J. Cox, M. Schmidt-Supprian, M. Mann, N-linked glycosylation enrichment for in-depth cell surface proteomics of diffuse large B-cell lymphoma subtypes, Mol. Cell. Proteomics 13 (2014 Jan) 240–251.
[143] M. Rey, H. Mrázek, P. Pompach, P. Novák, L. Pelosi, G. Brandolin, E. Forest, V. Havlícek, P. Man, Effective removal of nonionic detergents in protein mass spectrometry, hydrogen/deuterium exchange, and proteomics, Anal. Chem. 82 (2010) 5107–5116.

7.5 Appendix 5

Large-scale identification of membrane proteins based onanalysis of trypsin-protected transmembrane segments. Vit O, Man P, Kadek A, Hausner J, Sklenar J, Harant K, Novak P, Scigelova M,Woffendin G, Petrak J. *Journal of Proteomics* 2016;149:15-22. (IF 2015: 3.867).

Journal of Proteomics 149 (2016) 15–22

Contents lists available at ScienceDirect

Journal of Proteomics

journal homepage: www.elsevier.com/locate/jprot

Large-scale identification of membrane proteins based on analysis of trypsin-protected transmembrane segments

O. Vit [a], P. Man [b,c], A. Kadek [b,c], J. Hausner [b,c], J. Sklenar [d], K. Harant [e], P. Novak [b,c], M. Scigelova [f], G. Woffendin [g], J. Petrak [a]

[a] BIOCEV, First Faculty of Medicine, Charles University in Prague, Czech Republic
[b] Institute of Microbiology, Czech Academy of Sciences, Prague, Czech Republic
[c] Department of Biochemistry, Faculty of Science, Charles University in Prague, Czech Republic
[d] The Sainsbury Laboratory, Norwich Research Park, Norwich, UK
[e] Protemics Core Facility, Faculty of Science, Charles University in Prague, Czech Republic
[f] Thermo Fisher Scientific, Bremen, Germany
[g] Thermo Fisher Scientific, Hemel Hempstead, UK

ARTICLE INFO

Article history:
Received 30 November 2015
Received in revised form 3 February 2016
Accepted 4 March 2016
Available online 11 March 2016

Keywords:
Integral membrane proteins
CNBr
Transmembrane
Missing proteins
Hydrophobicity
Lymphoma

ABSTRACT

Integral membrane proteins are generally under-represented in routine proteomic analyses, mostly because of their relatively low abundance, hydrophobicity and lack of trypsin-cleavage sites. To increase the coverage of membrane proteomes, various strategies have been developed, targeting mostly the extra-membrane segments of membrane proteins. We focused our attention to the rather overlooked hydrophobic transmembrane segments. Such peptides can be isolated after carbonate stripping and protease "shaving" of membranes isolated by simple centrifugation procedure. The treated membranes with embedded hydrophobic peptides can then be solubilized in organic solvents, re-digested with CNBr, delipidated and subjected to LC-MS/MS analysis. We modified the original "hppK" method, and applied it for the analysis of human lymphoma cells. We identified 1224 proteins of which two-thirds were IMPs with 1–16 transmembrane segments. This method allowed us to identify 13 "missing proteins" — proteins with no previous evidence on protein level.
Biological significance: Integral membrane proteins execute numerous essential functions and represent substantial part of eukaryotic proteomes. Our knowledge of their function and expression is, however, limited. Novel approaches extending our knowledge of membrane proteome are therefore highly desired. As we demonstrate here, a non-conventional method which targets rather overlooked hydrophobic transmembrane segments of integral membrane proteins has wide potential to provide the missing information on the membrane proteome. We show that it can deliver identification and potentially also quantification of hundreds of integral membrane proteins including the so called "missing proteins".

1. Introduction

Approximately one third of eukaryotic genes code for integral membrane proteins (IMPs). These molecules execute important functions — namely signal transduction, transmembrane transport, cell-cell communication, cell adhesion to extracellular matrix and many other processes [1]. Their roles make IMPs ideal pharmacological targets. In fact, membrane proteins are the targets of 50–60% of all currently approved drugs [2]. Yet, because of relatively low expression and, above all, their hydrophobicity, IMPs are generally under-represented in routine proteomic analyses [3]. Isolation of membrane-enriched fractions is often inefficient, being plagued by extensive contamination with major cytosolic proteins, components of cytoskeleton and other proteins. Carbonate washing only partially reduces the problem of nonspecific adhesion, as the percentage of IMPs of all identified proteins in isolated membrane fractions is typically only up to 40–50% [4–6]. Presence of both hydrophilic and hydrophobic domains makes IMPs amphipathic and therefore difficult to solubilize. Use of harsh conditions including high concentration of organic solvents or inclusion of detergents may interfere with protease digestion and/or MS analysis and often requires laborious removal [7,8]. Analysis is further complicated by the fact, that the hydrophobic (mostly alpha-helical) transmembrane domains of IMPs are resistant to digestion by conventional proteases due to inherently low solubility and the absence of specific cleavage sites.

To overcome some of these obstacles, methods targeting selectively either the hydrophilic (extra-membrane) or the hydrophobic (transmembrane, TM) sections of IMPs have been introduced. Extracellular hydrophilic sections of plasma membrane proteins can be targeted by surface biotinylation of amine residues or glycosylated aminoacids, followed by protease digestion and affinity purification of labeled extracellular peptides [9,10]. This strategy of "surfaceome" analysis has been applied to human leukemia cells [11,12], adipocytes [13], glioblastoma

http://dx.doi.org/10.1016/j.jprot.2016.03.016
1874-3919/

[14], stem cells [15,16] and other cell types. The surface capture method provides very high enrichment of IMPs, 45–90% of identified proteins in these analyses contain at least one predicted TM segment. The strategy is, however, limited to intact live cells and does not allow analysis of frozen samples, biopsies or post-mortem tissues, unless lectin-based glycocapture is used instead of surface biotinylation as recently demonstrated [17].

Alternative or rather complementary approach targets the overlooked "dark side" of IMPs — hydrophobic membrane-embedded segments. This unique approach has been developed by Adele Blackler and Christine Wu [18] and takes advantage of the fact, that the phosholipid bilayer protects the transmembrane peptides from enzymatic proteolysis. Isolated membrane vesicles can thus be opened at high pH and all non-protected non-membrane proteins can be "shaved" by a protease from both surfaces of the membranes. The treated membranes with embedded hydrophobic peptides can then be solubilized in organic solvents, re-digested with CNBr, delipidated and subjected to LC-MS. The method is not limited to plasma membrane and can also be applied to frozen samples or tissue biopsies. Despite its obvious potential to tap the valuable information hidden in the phospholipid bilayer, the strategy has not attracted many followers, possibly because of the laborious multi-step workflow and application of less common cleavage strategies (non-specific proteinase K and CNBr).

We followed the directions set up by Blackler and Wu [18], modified the method and applied it for a large-scale analysis of membrane proteins in human lymphoma cells. Our modification avoids ultracentrifugation step, includes on-column sample delipidation and, most importantly, replaces the non-specific proteinase K employed in the original method with trypsin. This critical modification prevents the analysis of numerous overlapping peptides generated by the non-specific proteinase K and thus makes the technique more sensitive and makes it compatible with quantitative analysis using SILAC labeling. Using this modified version of the technique, we identified 1224 proteins in the lymphoma cell line sample, of which two-thirds (802 proteins) were IMPs with 1–16 transmembrane segments according to the Tied Mixture Hidden Markov Model (TMHMM) prediction [19].

2. Methods

2.1. Isolation of membranes, carbonate stripping and trypsin digestion

Human mantle cell lymphoma Mino cells (CRL-3000, purchased from ATTC) were grown in 75 cm^2 cultivation flasks in Iscove's Modified Dulbecco's Medium (Lonza) and upon harvesting were washed in chilled Dulbecco's Phosphate Buffered Saline (Sigma). The harvested cells were stored at −80 °C until further processing. The cell pellets were resuspended in hypotonic lysis buffer (10 mM NaCl, 10 mM HEPES pH 7.5), kept on ice for 20 min, and homogenized by passing 20 times through a gauge 25 hypodermic needle. The homogenate was centrifuged (500 ×*g*, 5 min, 4 °C) to pellet unbroken cells and nuclei. The supernatant was treated with bovine deoxyribonuclease I (Sigma) (120 Kunitz units, 60 min incubation at 37 °C with 25 mM $MgCl_2$ and 5 mM $CaCl_2$ added) and centrifuged in a benchtop centrifuge (18,000 ×*g*, 30 min, 4 °C). The pellet was solubilized in ice-cold 100 mM Na_2CO_3, agitated for 30 min on ice and centrifuged again (18,000 ×*g*, 30 min, 4 °C). Resulting pellet was solubilized in 25 mM $(NH_4)HCO_3$ with sequencing grade modified porcine trypsin (Promega) and incubated at 37 °C overnight. After the tryptic digestion the suspension was again centrifuged at 18,000 ×*g*, the resulting pellet was solubilized in ice-cold 100 mM Na_2CO_3, agitated for 30 min on ice, and the suspension was frozen and thawed 3 times, before being finally centrifuged at 18,000 ×*g*.

2.2. Electron microscopy

Three aliquots were taken during the process of membrane isolation: A) after the first centrifugation at 18,000 ×*g*, B) after the first incubation in Na_2CO_3 and C) after digestion with trypsin. Upon centrifugation at 18,000 ×*g*, all four aliquots were resuspended in 250 mM sucrose at 1:1 v/v ratio. Fixation was done by overlaying samples with 2.5% glutaraldehyde in 0.1 M cacodylate buffer (pH 7.2), incubation for 30 min on ice and centrifugation at 18,000 ×*g*, 20 min, 0 °C. Postfixation was done in 2% OsO_4 in the same buffer. Fixed tissue was dehydrated through an ascending ethanol series and embedded in Araldite – Poly/Bed® 812 mixture (Polysciences). Thin sections were cut on a Reichert–Jung Ultracut E ultramicrotome and stained using uranyl acetate and lead citrate. Sections were examined and photographed using a JEOL JEM-1011 transmission electron microscope.

2.3. Preparation of standard membrane protein sample

Proton coupled chloride transporter from *Escherichia coli* (CLC-EC1, UniProt accession number P37019) was expressed and purified as described previously [20]. Protein was precipitated using acetone in the presence or absence of a model lipid, 1,2-dimyristoyl-*sn*-glycero-3-phosphocholine (DMPC, Avanti Polar Lipids).

2.3.1. Cyanogen bromide digestion

The pellet of isolated membranes (approx. 60 μl) was resuspended in 100 μl 70% trifluoroacetic acid (TFA) with 20 mg/ml cyanogen bromide (CNBr) and digested in dark at room temperature overnight. Digested peptides were then dried in speedvac and twice solubilized in 70% methanol and dried again to remove the remaining CNBr.

Standard protein was digested by CNBr according to the same protocol. Five micrograms of pure or DMPC-spiked CLC-EC1 were subjected to digestion overnight. DMPC alone was processed in the same manner as well. For method comparison purposes, CLC-EC1 was also digested by the original procedure as described previously by [18], where the samples were digested in 90% FA and no CNBr removal step followed the reaction.

2.3.2. Standard sample preparation for LC-MS analysis

To optimize the sample preparation method, the standard samples containing CLC-EC1, DMPC or their mixture were processed by three different protocols. In two of those, dried sample was reconstituted in 80% acetonitrile/10% H_2O/10% formic acid, sonicated and diluted with solvent A (0.5% formic acid in H_2O) to 10% acetonitrile concentration. The sample was then loaded on a peptide Macrotrap in an off-line holder (Optimize Technologies) and desalted using solvent A. Next, the trap was either subjected to direct elution with 150 μl solvent B (90% acetonitrile/5% water/5% formic acid) or to a modification of lipid removal procedure described previously [21,22]. In the latter, the trap was washed (sample delipidated) with dichloromethane/0.5% FA (up to 2500 μl). After delipidation the elution was done with 150 μl solvent B. In all cases the trap was finally cleaned by 40% acetonitrile/20% methanol/10% isopropanol/10% formic acid/10% water. Alternatively the sample was also processed by the procedure described by Blackler et al., where the supernatant as well as the pellet after lipid precipitation was desalted [18]. In all the three protocols, aliquots collected at every step of the preparation were analyzed by mass spectrometry.

Following the method optimization, the cyanogen bromide digested transmembrane peptides isolated from Mino cells were processed according to the procedure with dichloromethane delipidation on a peptide trap. Desalted and delipidated peptides were dried in speedvac and stored at −80 °C.

2.3.3. MS analysis of the standard sample

Development of the sample preparation procedure was monitored by MALDI-FT-ICR and ESI-FT-ICR on a 12T SolariX XR (Bruker Daltonics). Samples from the individual steps of offline clean-up and delipidation were either directly infused via an ESI source or spotted on a MALDI plate and overlaid with α-cyano-4-hydroxycinnamic acid. MALDI

spectra were recorded with mass range from 400 to 6000 and ESI spectra from 200 to 3000.

2.4. LC-MS/MS analysis

For the trans-membrane peptide sample, the material was dissolved in 5 μl of 10% aqueous formic acid containing 80% (v/v) acetonitrile. The sample was further diluted by the addition of 4 volumes (20 μl) of water, and 5 μl of that solution were loaded onto a Thermo Scientific PepMap peptide trap (internal diameter 100 μm, length 2 cm, 5 μm particle size) using 0.05% aqueous formic acid containing 2% acetonitrile at flow rate 8 μl/min. Peptides were further separated on Thermo Scientific Acclaim EasySpray PepMap C18 RSLC column (internal diameter 75 μm, length 50 cm, 2 μm particle size, 100 Å pore size) maintained at a constant temperature (40 °C) and equilibrated with 2.4% (v/v) acetonitrile in 0.1% (v/v) aqueous formic acid (FA). Pumping was done by nano UHPLC (Easy-nLC 1000; Thermo Fisher Scientific) with a 90 min linear gradient of solvent B (80% acetonitrile in 0.1% aqueous formic acid) in solvent A (0.1% aqueous formic acid), according to the following profile: 0–5 min 10% B; 5–10 min ramping to 15% B; 10–95 min ramping to 55% B; 95–100 min ramping to 100% B; 100–104 min hold at 100% B; 104–105 min return to 10% B; 105–120 min equilibration at 10% B; flow rate of 300 μl/min. Total run time was 120 min.

Separated peptides were detected with the quadrupole-Orbitrap mass analyzer (Q Exactive; Thermo Fisher Scientific) using a data dependent acquisition in positive mode. Peptide parent ions were detected in a high resolution full scan (mass range 350–1500 m/z, 70,000 resolving power setting at m/z 200). The instrument was set so that 10 most intense ions of every full scan spectrum, meeting specific threshold criteria (minimum intensity 1.7×10^4 , charge state >1), were selected for MS/MS. Peptides were isolated with an isolation window of 3 Da, fragmented (HCD fragmentation with NCE 27 collision energy setting), and the resulting fragment ions were detected (17,500 resolving power setting). Other settings: target value 3×10^6 and 1×10^5 for full scan and MS/MS scan, respectively; maximum ion time 50 ms and 120 ms for full scan and MS/MS scan, respectively. Following their fragmentation the precursors were put on an exclusion mass list for 30 s (exclusion width ±10 ppm from the parent ion).

Data processing: Proteome Discoverer v. 1.4 (Thermo Fisher Scientific) software package was used for protein identification. The spectra were searched using Thermo Fisher Scientific Sequest HT search engine against the human subset of Swiss-Prot database with added contaminant protein sequences (20,249 sequences in total). The search settings differed between the standard and membrane sample in the cleavage specificity, trypsin with 3 missed cleavage sites and cyanogen bromide (semi-specific) with 2 missed cleavage sites, respectively. Also, there was an extra dynamic modification, Met changing to homoserine lactone (Met −48.003) on any peptide C-terminus, defined for the membrane sample search. The other settings were the same for both samples: precursor mass tolerance 10 ppm; fragment mass tolerance 60 mDa; oxidation of Met residues (+15.995) set as dynamic modification; maximum 3 equal dynamic modifications per peptide allowed. The search results were validated with decoy database search strategy using Percolator [23] with target FDR 0.01 and validation based on q-value.

3. Results and discussion

The pioneering work of Adele Blackler and Christine Wu [18] tapped the previously unexplored information on transmembrane segments of membrane proteins buried in the lipid bilayer — it enabled identification of almost 500 IMPs. The use of proteinase K at high pH facilitates membrane stripping of associated proteins and promotes membrane vesicle opening resulting in efficient shaving of extramembrane protein material from both sides of membrane vesicles [18].

However, the low specificity of proteinase K produces numerous overlapping peptides leading to increased complexity of sample and potentially decreases the number of identified proteins. In our modified approach we used trypsin instead of proteinase K and verified its efficacy for the membrane shaving and analysis of integral membrane peptides. In the course of our experiments we also introduced several other modifications. We avoided the relatively laborious purification of membrane vesicles by ultracentrifugation steps, used different CNBr digestion protocol and performed on-column delipidation of solubilized membranes instead of lipid precipitation. In reference to the original hppK (high pH, proteinase K) strategy [18,24], we propose an acronym hpTC (high-pH-Trypsin-CNBr) for this modified method.

3.1. Isolation of membrane-enriched fraction

Instead of ultracentrifugation steps used in the original protocol we homogenized the lymphoma cells simply by passing through a hypodermic needle in a hypotonic buffer and isolated the crude membrane fraction as described previously [25] (Fig. 1A).

To cope with the viscous clump of DNA released from residual nuclear fragments during the subsequent steps, we treated the crude membrane sample with DNAse prior to the digestion. The crucial step – opening of membrane vesicles in 100 mM Na_2CO_3 at high pH – was performed essentially as described in the original protocol [18] (Fig. 1B). For the digestion of all non-membrane proteins and extramembrane sections of membrane proteins we chose trypsin instead of proteinase K employed by Blackler *et al.*

Since the peptides produced by non-specific proteinase K are highly overlapping, the resulting sample would be unnecessarily complex, compared to identical digest resulting from specific cleavage with trypsin. Also, since current state-of-the-art MS instrumentation provides better fragmentation spectra and also higher resolution and mass precision, it is no longer necessary to increase the protein identification confidence by fragmenting several overlapping peptides covering the same protein sequence. This in turn leads to higher individual signal intensities as the amount of each analyte protein is not split into several overlapping peptides concurrently occurring in the sample. Further, C-terminal arginine or lysine in each peptide generated by trypsin cleavage facilitate ionization and confident protein identification and validation. Last but not least, trypsin is compatible with SILAC labeling, enabling convenient semi-quantitative expression analysis of IMPs.

The successful digestion with trypsin in the re-formed membrane vesicles is visible in Fig. 1C as the vesicles are more sharply defined. To release the cleaved extramembrane peptide content from the vesicles we re-opened the vesicles again in 100 mM Na_2CO_3 at high pH and washed and pelleted the trypsin-treated membranes. To remove all potential soluble peptides, the vesicles were repeatedly freeze-thawed in the carbonate buffer.

3.2. Re-digestion of membrane peptides

Membrane-embedded peptides produced by the treatment of membranes with trypsin alone are rather large and hydrophobic for optimal LC-MS analysis. A typical vertebrate transmembrane alpha-helix consists of 20–30 amino acids depending on particular membrane type (ER, Golgi or plasma membrane) [18,26]. Furthermore a variable number of amino acid residues to the nearest trypsin cleavage site(s) or protein terminus must be added to such a theoretical calculation as well. In order to reduce the size of the peptides and lower their hydrophobicity, solubilization of the trypsin-treated membranes in strong acid (preferably FA or TFA) followed by chemical cleavage of hydrophobic peptides with CNBr can be used [27]. CNBr cleaves proteins or long peptides C-terminal to methionine residues and generates peptides with homoserine lactone at their C-termini. Also, as the cleavage is mediated only by a small chemical agent, it is well suited to digesting samples even in the membrane bilayer environment, where enzymatic digestion suffers from the very limited accessibility of large protein-based enzymes to the substrate. High toxicity of CNBr and its byproducts, however, needs to be considered and all

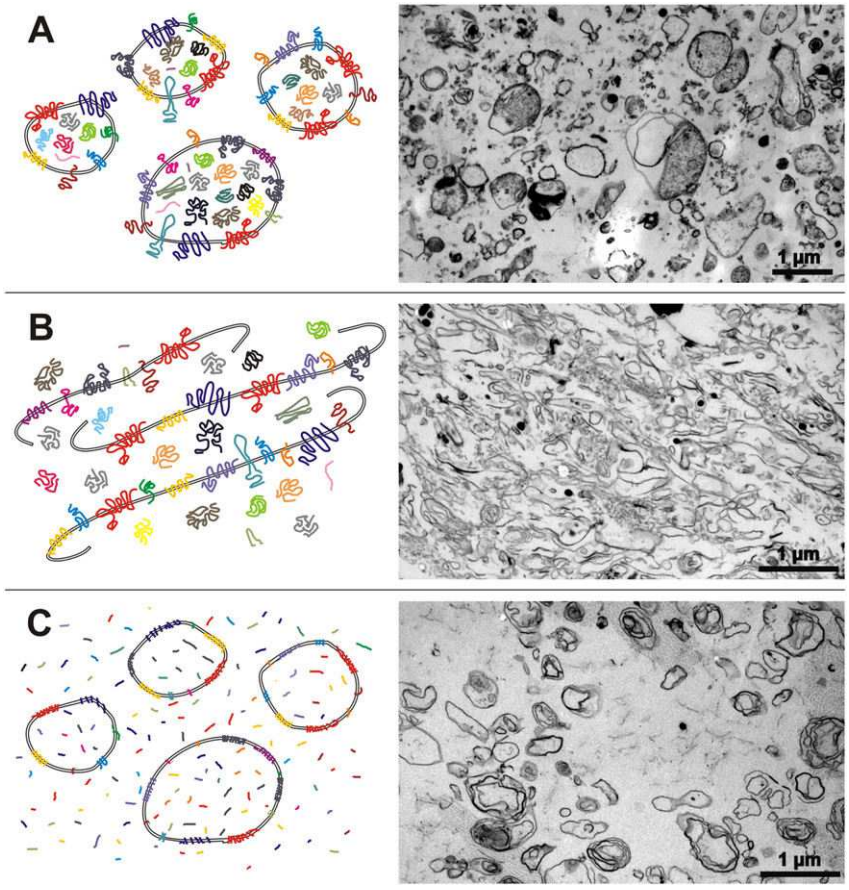

Fig. 1. Isolation, carbonate stripping and proteolytic shaving of membranes steps visualized by transmission electron microscopy (TEM). A) Upon homogenization and centrifugation steps, the isolated crude membrane fraction consists of variously sized membrane vesicles containing trapped proteins and other material. B) Carbonate stripping allows opening of the vesicles and release of trapped content. Due to the use of centrifugation during fixation for TEM, the opened membranes appear to be stacked. C) After tryptic digestion, the membrane outlines are more sharply defined and the vesicles appear empty compared to 1A. Due to previous opening and stacking, some of the resulting vesicles are multilayered.

work involving CNBr must be strictly performed in a fume hood. It should be mentioned that a combined cleavage with CNBr/trypsin has been used in membrane proteomics previously to analyze bacterial membrane, however, in a reverse order – i.e. CNBr cleavage followed by trypsin digestion and in different experimental design [28].

Initially, we performed a pilot experiment with a standard sample – membrane protein CLC-EC1. We performed the digestion according to the hppK-CNBr protocol which used solubilization and CNBr digestion in 90% formic acid. When applied to our model protein, CLC-EC1, substantial portion of the digestion products was found to be modified by formylation (Supplementary Fig. 1A). We therefore replaced the formic acid by TFA and despite the fact that formic acid was used for subsequent sample desalting, virtually no formyl adducts were found (Supplementary Fig. 1B).

3.3. Sample delipidation

After the chemical cleavage, the phospholipid-rich sample must be delipidated prior to the LC-MS/MS analysis. The original protocol employed lipid precipitation in aqueous-organic buffer [18]. Since we observed quite substantial amount of lipids in the supernatant of the precipitated and centrifuged sample, we replaced the precipitation step with on-column delipidation using dichloromethane [21,22]. The method was originally designed for non-ionic detergent removal from peptide digests but when applied to a detergent solubilized mitochondrial membrane protein ANT1, removal of the lipids was observed as well [22]. In a pilot experiment we tested the lipid removal procedure on pure CLC-EC1 digest and observed no peptide loss. In addition, even very hydrophobic peptides were detected in the final acetonitrile eluate from the trap column. Next we verified that CNBr treated lipid (DMPC) can be efficiently removed. As expected, the lipid eluted from the trap when dichloromethane was applied and no signal for the intact lipid or the acid-generated degradation product, lysoDMPC was found

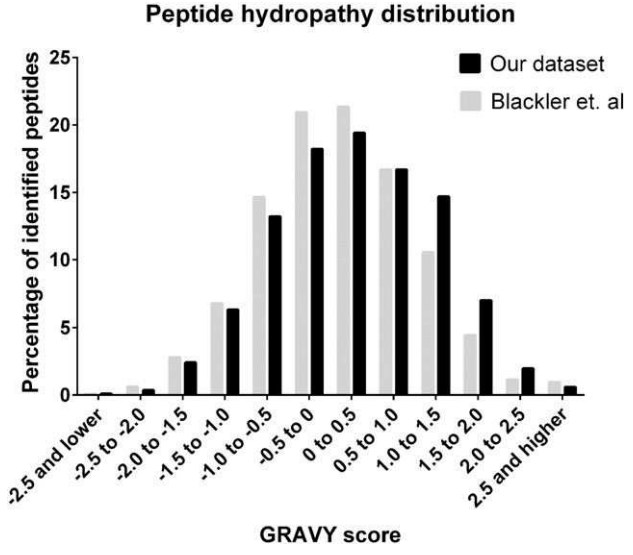

Fig. 2. Peptide hydrophobicity. Comparison of the distribution of peptide GRAVY score in our hpTC dataset with the original hppK-CNBr method. Distribution of peptides in our dataset is shifted toward higher GRAVY score (more hydrophobic peptides), presumably due to different method of sample delipidation.

in the acetonitrile elution. Finally, we used DMPC-spiked CLC-EC1 for digestion and performed the purification procedure on this sample. The result is shown in Supplementary Fig. 2 and confirms that the on-column delipidation approach represents a feasible sample preparation for membrane proteomics samples. This is further supported by the hydrophobicity calculation (GRAVY score) [29] of the peptides identified in our dataset and those from the original dataset of Blackler et al. [18] obtained after lipid precipitation. The distribution can be seen in Fig. 2. Our dataset contained more peptides with high hydrophobicity (peptides with positive GRAVY score) probably due to their preferential capture on the hydrophobic stationary phase.

3.4. LC-MS/MS analysis

In the original paper, authors analyzed the delipidated membrane sample using MudPit approach [30] consisting of twelve 2-hour steps [18]. Our 1D LC-MS/MS analysis using a 90 min gradient on a 50 cm heated column connected to Orbitrap Q Exactive mass spectrometer resulted in identification of 1224 proteins with average sequence coverage 12.2%. Of the 1224 proteins 802 molecules (65.5%) were predicted to have at least one transmembrane domain by TMHMM [19]. For the complete list of the identified proteins see Supplementary Table 1.

3.5. Integral membrane proteins, transmembrane segments

Using the hpTC method we identified 802 IMPs with up to 16 transmembrane segments (except one outlying protein with 31 predicted transmembrane segments, Piezo1, Q92508) in the human lymphoma Mino cell sample, of which proteins with two or more TM segments represented roughly two thirds. (Fig. 3) The observed distribution is in agreement with genome-wide predictions for human proteins [1] suggesting that the hpTC method is not biased toward a specific group of transmembrane proteins. Furthermore a closer analysis showed that approximately half (1274/2561) of the unique peptides used for the identification of the IMPs overlapped with predicted transmembrane regions.

To illustrate the contribution of transmembrane peptides in the hPTC analysis several topological maps generated by Protter software [31] are shown in Fig. 4. Also, to determine the relative contribution of trypsin digestion and CNBr cleavage among the identified peptides, we calculated the distribution of terminal arginines and lysines and methionines converted by CNBr to homoserine lactones (Supplementary Fig. 3). Roughly 75% of all the peptides identified in our analysis were produced by CNBr or combined action of trypsin and CNBr. However, this proportion is significantly higher (97%) for the peptides which overlapped with predicted transmembrane segments. This underlines the benefit of CNBr use in the analysis of membrane proteins.

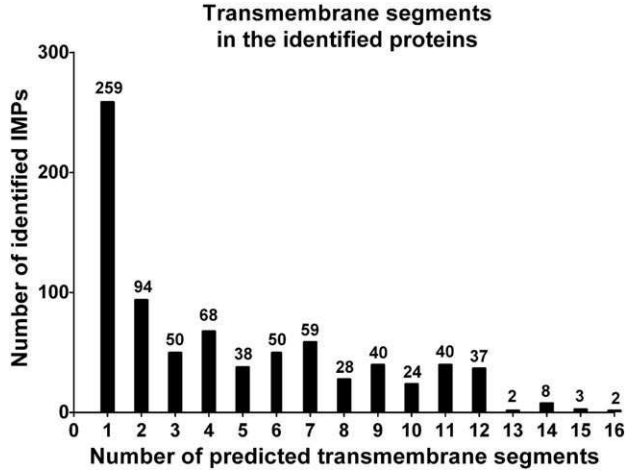

Fig. 3. Number of transmembrane segments in the identified IMPs. Number of predicted transmembrane regions (based on TMHMM prediction) in the 802 IMPs identified in our study.

3.6. Access to all cellular membrane compartments

Among the IMPs identified in the human lymphoma cells, there were numerous transporters, membrane enzymes, receptors, signal transduction proteins, and proteins with immunity-related activities and other functions. According to gene ontology annotations, the identified membrane proteins originate from various organelles, confirming the ability of the method to access not only plasmatic but all cellular membranes. Due to dynamic nature of cellular membranes (and according to their multiple G.O. annotations), many membrane proteins are associated with two or more cellular compartments. This complicates the evaluation and prevents any clear-cut calculation of protein distribution among the various membrane compartments. Nevertheless, we also observed proteins annotated exclusively to mitochondrial membrane (e.g. ADP/ATP translocases 1–3, numerous components of respiratory chain), to membranes of endoplasmic reticulum (e.g. GlcNAc-1-P transferase, UDP-glucuronic acid/UDP-*N*-acetylgalactosamine transporter) and Golgi (e.g. Alpha-(1,6)-fucosyltransferase, Beta-1,4-galactosyltransferase 3), proteins localized to nuclear envelope (e.g. lamin-B receptor, nucleoporin NDC1) and proteins known for their typical plasma membrane localization such as proteins belonging among the CD (cluster of differentiation) molecules. CD proteins expressed on the cell surface represent promising targets of modern anti-cancer drugs including therapeutic antibodies, as exemplified by rituximab targeting CD20 in B-cell lymphomas, trastuzumab targeting-HER2 in breast cancer patients or ipilimumab targeting CTLA-4 in patients with melanoma [32]. The information on expression of CD markers in cancer cells is therefore of tremendous importance. We identified 48 CD molecules in our analysis of human lymphoma cells (Table 1.)

3.7. Opening the black box

IMPs with large extra-membrane domains can provide several tryptic peptides and can be therefore identified in the conventional large scale proteomic analyses or using the surface-capture strategy. However, some membrane proteins possess only small extra-membrane segments offering no tryptic peptides of reasonable size. Such proteins thus inevitably escape detection by both surface capture methods and routine proteomic analyses. Here we show, that the CNBr cleavage of intra-membrane segments of such proteins may enable their identification as demonstrated by several proteins identified in our hpTC analysis. Such a typical difficulty to identify proteins with no extramembrane tryptic peptide can be exemplified by the identified Dolichyl-diphosphooligosaccharide-protein glycosyltransferase subunit 4 (OST4_HUMAN) or NADH-ubiquinone oxidoreductase chain 4L (NU4LM_HUMAN) in Fig. 4.

Recently, the Human Proteome Project sparked an interest in identification of "missing proteins" i.e. proteins having no evidence of existence on protein level [33]. The latest release of the neXtProt database (www.nextprot.org, September 2015) contains 3243 "missing proteins" [34]. In our dataset we identified 13 of such "previously unseen" proteins, namely O15342, O60478, Q14330, Q14656, Q5SWH9, Q6UWH6 (evidence on transcript level), A8MWL7, A2A368, C9J798, P69849 (based on homology) and O60361, Q5T1J5, Q92928 (classified as uncertain). Seven out of the thirteen proteins (O15342, O60478, Q14330, Q14656, Q5SWH9, Q6UWH6, A8MWL7) are IMPs with 2–7 transmembrane segments.

3.8. Proteins with no transmembrane domain. Contaminants?

The treatment of membranes with carbonate washing at high pH followed by trypsin digestion was in our study effective for removal of most but not all non-membrane contaminants. Among the 1224

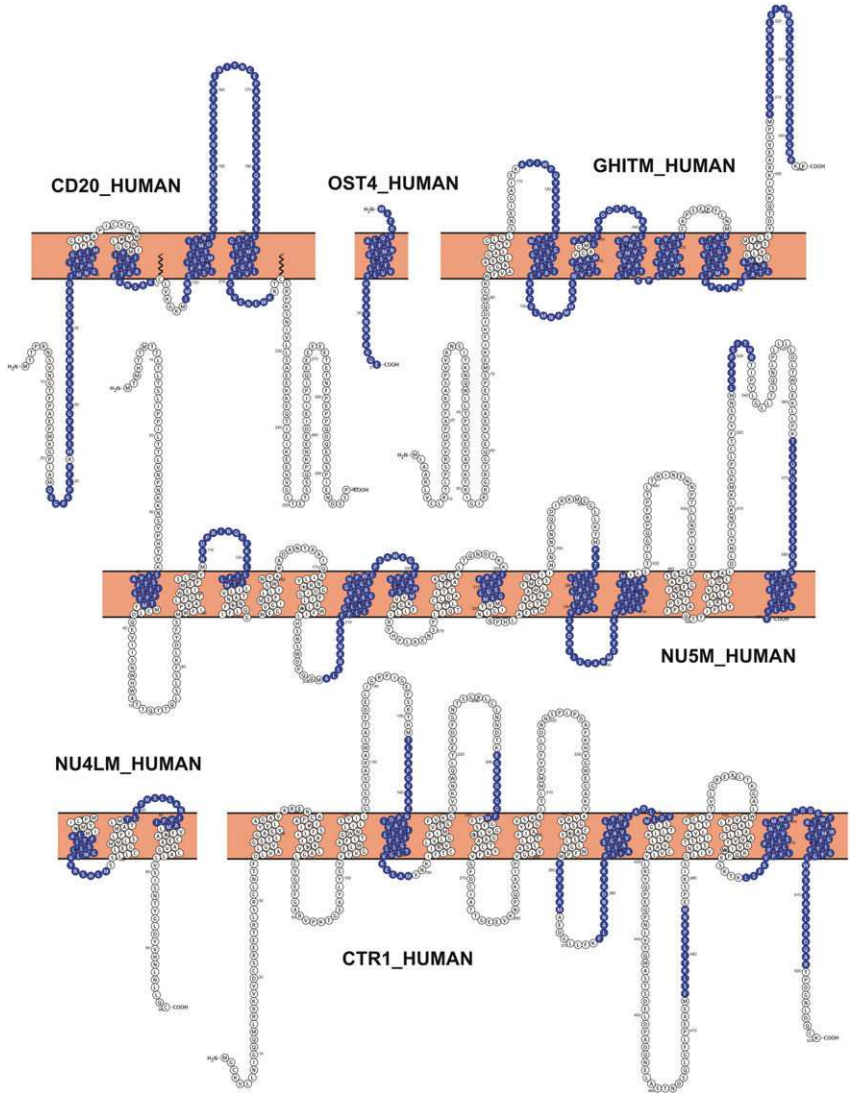

Fig. 4. Examples of sequence coverage of identified IMPs on topological prediction maps. Sequences of identified peptides used for the identification are labeled blue. Topology maps were generated using Protter (http://wlab.ethz.ch/protter). These examples illustrate that peptides overlapping with transmembrane segments significantly contribute to the protein identification. As demonstrated by OST4_HUMAN and NU4LM_HUMAN this method allows proteomic identification of small, highly hydrophobic IMPs with limited presence of trypsin cleavage sites.

identified proteins, 422 were predicted to have no transmembrane segment. Presence of these proteins in the hpTC isolate may be explained by their tight specific association with membrane lipids or proteins. For instance, we identified non-membrane protein beta-2-microglobulin, which is known to exist as a component of a large membrane-bound MHC class I complex and may be therefore shielded by the α1/α2 MHC heterodimer (also identified in our study) from the trypsin activity. Similarly, the presence of hydrophobic segments in the structure of non-membrane proteins may cause their non-specific sticking to the phospholipid bilayer during the sample preparation and may thus prevent their complete removal. In our lymphoma cell study we observed contamination by major cytosolic (alpha enolase, GAPDH, glucose-6-phosphate isomerase), cytoskeletal (actin, tubulin) and also nuclear (histones, small nuclear ribonucleoproteins) high-abundance proteins. However, as exemplified by histones, which may also be extra-nuclear and have been shown to directly interact with membrane [35,36], it is not always easy to decide where precisely to draw the line between proteins of interest and contaminants. Overall, despite the presence of some contaminating proteins in the results of our analyses, integral membrane proteins represented over 65% of all identified proteins, thus demonstrating high efficacy of the hpTC method.

3.9. Quantitative analysis of membrane proteome?

Analysis of membrane-embedded peptides clearly taps the invaluable information on membrane proteome. However, mere cataloguing of membrane proteome is not sufficient. Can we make such an analysis (semi)quantitative?

Implementation of trypsin instead of proteinase K to the method workflow potentially opens the door to quantitative membrane analysis using SILAC labeling [37]. To evaluate the theoretical potential of SILAC labeling for the hpTC method, we queried the content of canonic SILAC-compatible amino acids – arginine (R) and lysine (K) in the unique peptides identified in our lymphoma cell line analysis (Fig. 5). Out of the total number of 3884 peptides, 2055 (53%) contained at least one lysine, while arginine was present in 1965 (51%). Almost 83% of the peptides contained either K or R. Theoretically, an application of "double" (K and R) SILAC could provide semi-quantitative information on a significant

Table 1
The list of identified CD molecules.

List of identified lymphoma membrane CD proteins			
CD No.	Accession	Entry name	Protein name
CD10	P08473	NEP_HUMAN	Neprilysin
CD11a	P20701	ITAL_HUMAN	Integrin alpha-L
CD18	P05107	ITB2_HUMAN	Integrin beta-2
CD19	P15391	CD19_HUMAN	B-lymphocyte antigen CD19
CD20	P11836	CD20_HUMAN	B-lymphocyte antigen CD20
CD21	P41597	CCR2_HUMAN	C-C chemokine receptor type 2
CD27	P26842	CD27_HUMAN	CD27 antigen
CD32	P31994	FCG2B_HUMAN	Low affinity immunoglobulin gamma Fc region receptor II-b
CD39	P49961	ENTP1_HUMAN	Ectonucleoside triphosphate diphosphohydrolase 1
CD40	P25942	TNR5_HUMAN	Tumor necrosis factor receptor superfamily member 5
CD43	P16150	LEUK_HUMAN	Leukosialin
CD45	P08575	PTPRC_HUMAN	Receptor-type tyrosine-protein phosphatase C
CD47	Q08722	CD47_HUMAN	Leukocyte surface antigen CD47
CD48	P09326	CD48_HUMAN	CD48 antigen
CD50	P32942	ICAM3_HUMAN	Intercellular adhesion molecule 3
CD53	P19397	CD53_HUMAN	Leukocyte surface antigen CD53
CD54	P05362	ICAM1_HUMAN	Intercellular adhesion molecule 1
CD63	P08962	CD63_HUMAN	CD63 antigen
CD70	P32970	CD70_HUMAN	CD70 antigen
CD71	P02786	TFR1_HUMAN	Transferrin receptor protein 1
CD72	P21854	CD72_HUMAN	B-cell differentiation antigen CD72
CD74	P04233	HG2A_HUMAN	HLA class II histocompatibility antigen gamma chain
CD79a	P11912	CD79A_HUMAN	B-cell antigen receptor complex-associated protein alpha chain
CD79b	P40259	CD79B_HUMAN	B-cell antigen receptor complex-associated protein beta chain
CD81	P60033	CD81_HUMAN	CD81 antigen
CD82	P27701	CD82_HUMAN	CD82 antigen
CD84	Q9UIB8	SLAF5_HUMAN	SLAM family member 5
CD92	Q8WWI5	CTL1_HUMAN	Choline transporter-like protein 1
CD97	P48960	CD97_HUMAN	CD97 antigen
CD98	P08195	4F2_HUMAN	4F2 cell-surface antigen heavy chain
CD99	P14209	CD99_HUMAN	CD99 antigen
CD102	P13598	ICAM2_HUMAN	Intercellular adhesion molecule 2
CD107a	P11279	LAMP1_HUMAN	Lysosome-associated membrane glycoprotein 1
CD132	P31785	IL2RG_HUMAN	Cytokine receptor common subunit gamma
CD147	P35613	BASI_HUMAN	Basigin
CD159a	P26715	NKG2A_HUMAN	NKG2-A/NKG2-B type II integral membrane protein
CD184	P61073	CXCR4_HUMAN	C-X-C chemokine receptor type 4
CD185	P32302	CXCR5_HUMAN	C-X-C chemokine receptor type 5
CD192	P41597	CCR2_HUMAN	C-C chemokine receptor type 2
CD197	P32248	CCR7_HUMAN	C-C chemokine receptor type 7
CD205	O60449	LY75_HUMAN	Lymphocyte antigen 75
CD217	Q96F46	I17RA_HUMAN	Interleukin-17 receptor A
CD222	P11717	MPRI_HUMAN	Cation-independent mannose-6-phosphate receptor
CD225	P13164	IFM1_HUMAN	Interferon-induced transmembrane protein 1
CD230	P04156	PRIO_HUMAN	Major prion protein
CD289	Q9NR96	TLR9_HUMAN	Toll-like receptor 9
CD298	P54709	AT1B3_HUMAN	Sodium/potassium-transporting ATPase subunit beta-3
CD361	P34910	EVI2B_HUMAN	Protein EVI2B

portion of proteins identified in our current hpTC analysis. However, we further evaluated the content of leucine, another essential amino acid compatible with SILAC labeling, which also occurs frequently in hydrophobic transmembrane segments. Leucine was found in 3213 (83%) of all the unique peptides. Taken together, vast majority of all identified peptides (97%) contained at least one lysine, arginine or leucine, suggesting that using a triple (K, R and L) SILAC labeling of the cells could provide semi-quantitative information on most proteins identified in our current hpTC analysis (Fig. 5).

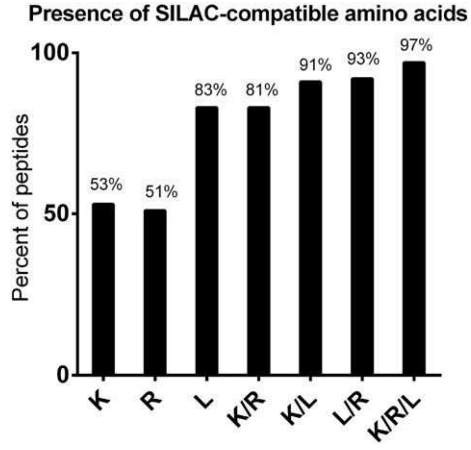

Fig. 5. Compatibility with SILAC. Percentage of unique peptides identified in our analysis containing SILAC-compatible amino acids.

4. Conclusions

In this study we demonstrate that the analysis of membrane-embedded peptides using the hpTC method enables very high enrichment of membrane proteins from all cellular compartments, including proteins with numerous transmembrane segments.

Identification of hundreds of integral membrane proteins in mammalian cells can be easily achieved in a single analysis and the whole experiment, including LC-MS/MS analysis, can be accomplished in approximately 50 h. The modified method avoids ultracentrifugation steps, employs more effective delipidation step and does not require any specialized instrumentation. Another important novelty of our modification to the original hppK method is the introduction of trypsin instead of non-specific proteinase K. This makes the method more sensitive and better suited for quantitative approaches, namely SILAC labeling and potentially opens the way toward a detailed semi-quantitative membrane proteome analysis using SILAC or super-SILAC strategy [37, 38]. However, the amphipathic nature of integral membrane proteins clearly calls for a combination of two complementary approaches. Joining forces of hydrophobic peptide-oriented hpTC approach with a soluble-peptide oriented method should provide the best results and enable deep expression analysis of membrane proteomes.

Supplementary data to this article can be found online at http://dx.doi.org/10.1016/j.jprot.2016.03.016.

Transparency document

The Transparency document associated with this article can be found, in online version.

Acknowledgements

The work was supported by the Ministry of Health of the Czech Republic (www.mzcr.cz) via grants 15-32961A, NT12248-5, by the Czech Science Foundation (www.gacr.cz) via grant 15-14200S and by the Ministry of Education, Youth and Sports of the Czech Republic (www.msmt.cz) via the institutional grants PRVOUK P24/LF1/3 and SVV-2013-260033. Support from the Grant Agency of Charles University (389115) and European Regional Development Funds (CZ.1.05/1.1.00/02.0109 - BIOCEV) is gratefully acknowledged. Authors would like to thank Miroslav Hyliš for his guidance and assistance with electron microscopy.

References

[1] L. Fagerberg, K. Jonasson, G. von Heijne, M. Uhlén, L. Berglund, Prediction of the human membrane proteome, Proteomics 10 (2010) 1141–1149.
[2] M.A. Yildirim, K.I. Goh, M.E. Cusick, A.L. Barabási, M. Vidal, Drug-target network, Nat. Biotechnol. 25 (2007) 1119–1126.
[3] D. Vuckovic, L.F. Dagley, A.W. Purcell, A. Emili, Membrane proteomics by high performance liquid chromatography-tandem mass spectrometry: analytical approaches and challenges, Proteomics 13 (2013) 404–423.
[4] J.R. Wiśniewski, A. Zougman, M. Mann, Combination of FASP and StageTip-based fractionation allows in-depth analysis of the hippocampal membrane proteome, J. Proteome Res. 8 (2009) 5674–5678.
[5] R.A. Mathias, Y.S. Chen, E.A. Kapp, D.W. Greening, S. Mathivanan, R.J. Simpson, Triton X-114 phase separation in the isolation and purification of mouse liver microsomal membrane proteins, Methods 54 (2011) 396–406.
[6] L. Cao, J.G. Clifton, W. Reutter, D. Josic, Mass spectrometry-based analysis of rat liver and hepatocellular carcinoma Morris hepatoma 7777 plasma membrane proteome, Anal. Chem. 85 (2013) 8112–8120.
[7] R.R. Loo, N. Dales, P.C. Andrews, The effect of detergents on proteins analyzed by electrospray ionization, Methods Mol. Biol. 61 (1996) 141–160.
[8] A.E. Speers, C.C. Wu, Proteomics of integral membrane proteins—theory and application, Chem. Rev. 107 (2007) 3687–3714.
[9] Y. Zhao, W. Zhang, Y. Kho, Y. Zhao, Proteomic analysis of integral plasma membrane proteins, Anal. Chem. 76 (2004) 1817–1823.
[10] B. Wollscheid, D. Bausch-Fluck, C. Henderson, R. O'Brien, M. Bibel, R. Schiess, R. Aebersold, J.D. Watts, Mass-spectrometric identification and relative quantification of N-linked cell surface glycoproteins, Nat. Biotechnol. 27 (2009) 378–386.
[11] P. Mirkowska, A. Hofmann, L. Sedek, L. Slamova, E. Mejstrikova, T. Szczepanski, M. Schmitz, G. Cario, M. Stanulla, M. Schrappe, V.H. van der Velden, B.C. Bornhauser, B. Wollscheid, J.P. Bourquin, Leukemia surfaceome analysis reveals new disease-associated features, Blood 121 (2013) e149–e159.
[12] A. Hofmann, B. Gerrits, A. Schmidt, T. Bock, D. Bausch-Fluck, R. Aebersold, B. Wollscheid, Proteomic cell surface phenotyping of differentiating acute myeloid leukemia cells, Blood 116 (2010) e26–e34.
[13] H. Moest, A.P. Frei, I. Bhattacharya, M. Geiger, B. Wollscheid, C. Wolfrum, Malfunctioning of adipocytes in obesity is linked to quantitative surfaceome changes, Biochim. Biophys. Acta 2013 (1831) 1208–1216.
[14] T. Bock, H. Moest, U. Omasits, S. Dolski, E. Lundberg, A. Frei, A. Hofmann, D. Bausch-Fluck, A. Jacobs, N. Krayenbuehl, M. Uhlen, R. Aebersold, K. Frei, B. Wollscheid, Proteomic analysis reveals drug accessible cell surface N-glycoproteins of primary and established glioblastoma cell lines, J. Proteome Res. 11 (2012) 4885–4893.
[15] R.L. Gundry, D.R. Riordon, Y. Tarasova, S. Chuppa, S. Bhattacharya, O. Juhasz, O. Wiedemeier, S. Milanovich, F.K. Noto, I. Tchernyshyov, K. Raginski, Tae H.J. Bausch-FluckD, S. Marshall, S.A. Duncan, B. Wollscheid, R.P. Wersto, S. Rao, J.E. Van Eyk, K.R. Boheler, A cell surfaceome map for immunophenotyping and sorting pluripotent stem cells, Mol. Cell. Proteomics 11 (2012) 303–316.
[16] B. DeVeale, D. Bausch-Fluck, R. Seaberg, S. Runciman, V. Akbarian, P. Karpowicz, C. Yoon, H. Song, R. Leeder, P.W. Zandstra, B. Wollscheid, D. van der Kooy, Surfaceome profiling reveals regulators of neural stem cell function, Stem Cells 32 (2014) 258–268.
[17] S.J. Deeb, J. Cox, M. Schmidt-Supprian, M. Mann, N-linked glycosylation enrichment for in-depth cell surface proteomics of diffuse large B-cell lymphoma subtypes, Mol. Cell. Proteomics 13 (2014) 240–251.
[18] A.R. Blackler, A.E. Speers, M.S. Ladinsky, C.C. Wu, A shotgun proteomic method for the identification of membrane-embedded proteins and peptides, J. Proteome Res. 7 (2008) 3028–3034.
[19] A. Krogh, B. Larsson, G. von Heijne, E.L. Sonnhammer, Predicting transmembrane protein topology with a hidden Markov model: application to complete genomes, J. Mol. Biol. 305 (2001) 567–580.
[20] M. Maduke, D.J. Pheasant, C. Miller, High-level expression, functional reconstitution, and quaternary structure of a prokaryotic ClC-type chloride channel, J. Gen. Physiol. 114 (1999) 713–722.
[21] M. Rey, H. Mrázek, P. Pompach, P. Novák, L. Pelosi, G. Brandolin, E. Forest, V. Havlícek, P. Man, Effective removal of nonionic detergents in protein mass spectrometry, hydrogen/deuterium exchange, and proteomics, Anal. Chem. 82 (2010) 5107–5116.
[22] M. Rey, P. Man, B. Clémençon, V. Trézéguet, G. Brandolin, E. Forest, L. Pelosi, Conformational dynamics of the bovine mitochondrial ADP/ATP carrier isoform 1 revealed by hydrogen/deuterium exchange coupled to mass spectrometry, J. Biol. Chem. 285 (2010) 34981–34990.
[23] L. Käll, J.D. Canterbury, J. Weston, W.S. Noble, M.J. MacCoss, Semi-supervised learning for peptide identification from shotgun proteomics datasets, Nat. Methods 4 (2007) 923–925.
[24] C.C. Wu, M.J. MacCoss, K.E. Howell, J.R. Yates III, A method for the comprehensive proteomic analysis of membrane proteins, Nat. Biotechnol. 21 (2003) 532–538.
[25] Y.J. Jin, M.W. Albers, W.S. Lane, B.E. Bierer, S.L. Schreiber, S.J. Burakoff, Molecular cloning of a membrane-associated human FK506- and rapamycin-binding protein, FKBP-13, Proc. Natl. Acad. Sci. U. S. A. 88 (1991) 6677–6681.
[26] H.J. Sharpe, T.J. Stevens, S. Munro, A comprehensive comparison of transmembrane domains reveals organelle-specific properties, Cell 142 (2010) 158–169.
[27] W.A. Schroeder, J.B. Shelton, J.R. Shelton, An examination of conditions for the cleavage of polypeptide chains with cyanogen bromide: application to catalase, Arch. Biochem. Biophys. 130 (1969) 551–556.
[28] F. Fischer, D. Wolters, M. Rögner, A. Poetsch, Toward the complete membrane proteome: high coverage of integral membrane proteins through transmembrane peptide detection, Mol. Cell. Proteomics 5 (2006) 444–453.
[29] J. Kyte, R.F. Doolittle, A simple method for displaying the hydropathic character of a protein, J. Mol. Biol. 157 (1982) 105–132.
[30] M.P. Washburn, D. Wolters, J.R. Yates III, Large-scale analysis of the yeast proteome by multidimensional protein identification technology, Nat. Biotechnol. 19 (2001) 242–247.
[31] U. Omasits, C.H. Ahrens, S. Müller, B. Wollscheid, Protter: interactive protein feature visualization and integration with experimental proteomic data, Bioinformatics 30 (2014) 884–886.
[32] Y. Zhu, S.H. Choi, K. Shah, Multifunctional receptor-targeting antibodies for cancer therapy, Lancet Oncol. 16 (2015) e543–e554.
[33] L. Lane, A. Bairoch, R.C. Beavis, E.W. Deutsch, P. Gaudet, E. Lundberg, G.S. Omenn, Metrics for the Human Proteome Project 2013-2014 and strategies for finding missing proteins, J. Proteome Res. 13 (2014) 15–20.
[34] P. Gaudet, P.A. Michel, M. Zahn-Zabal, I. Cusin, P.D. Duek, O. Evalet, A. Gateau, A. Gleizes, M. Pereira, D. Teixeira, Y. Zhang, L. Lane, A. Bairoch, The neXtProt knowledgebase on human proteins: current status, Nucleic Acids Res. 43 (2015) D764–D770.
[35] E. Hariton-Gazal, J. Rosenbluh, A. Graessmann, C. Gilon, A. Loyter, Direct translocation of histone molecules across cell membranes, J. Cell Sci. 116 (2003) 4577–4586.
[36] K. Watson, N.J. Gooderham, D.S. Davies, R.J. Edwards, Nucleosomes bind to cell surface proteoglycans, J. Biol. Chem. 274 (1999) 21707–21713.
[37] S.E. Ong, B. Blagoev, I. Kratchmarova, D.B. Kristensen, H. Steen, A. Pandey, M. Mann, Stable isotope labeling by amino acids in cell culture, SILAC, as a simple and accurate approach to expression proteomics, Mol. Cell. Proteomics 1 (2002) 376–386.
[38] T. Geiger, J. Cox, P. Ostasiewicz, J.R. Wisniewski, M. Mann, Super-SILAC mix for quantitative proteomics of human tumor tissue, Nat. Methods 7 (2010) 383–385.